ATKINS

Flood Loss Avoidance Benefits of Green Infrastructure for Stormwater Management

Prepared for:

U.S. Environmental Protection Agency
Office of Wetlands, Oceans and Watersheds
Nonpoint Source Control Branch (4503T)
1200 Pennsylvania Avenue NW
Washington, DC 20460

Prepared by:

Atkins
3901 Calverton Boulevard
Suite 400
Calverton, Maryland 20705

December 2015

Flood Loss Avoidance Benefits of Green Infrastructure for Stormwater Management

Prepared for:

U.S. Environmental Protection Agency
Office of Wetlands, Oceans and Watersheds
Nonpoint Source Control Branch (4503T)
1200 Pennsylvania Ave., NW
Washington, DC 20460

Prepared by:

Atkins
3901 Calverton Boulevard
Suite 400
Calverton, Maryland

December 2015

Acknowledgments

This document was prepared by Atkins and with support provided by the U.S. Environmental Protection Agency under contract EP-BPA-13-C-003.

The Atkins project team and the U.S. EPA wish to acknowledge those who provided assistance by reviewing the proposed methodologies, obtaining data or providing data, or by reviewing and commenting on specific issues or the report drafts. Several suggestions for improvement that were beyond the scope of this document are included in the report as recommendations for future studies. Acknowledgement of these individuals should not be construed as an endorsement for the study methodology or findings, as their role was only advisory. Sole responsibility for the work is with the project team.

The EPA staff included Lisa Hair, Project Manager, with support from Mike Borst, Thomas O'Connor, Robert Goo, Jason Berner, Alisha Goldstein (ORISE Fellow), Chris Kloss, Dennis Guignet, Matt Massey, David Simpson, Ashley Allen, and Todd Doley.

Additional assistance was provided by the San Antonio River Authority and Forsyth County, Georgia, in providing watershed data for some of the modeling exercises.

Review of the methodology, a specific issue, or a draft report was also provided by Eric Berman, FEMA; Robert Traver, Villanova University; Thomas Debo, University of Illinois; Glenn Moglen, Virginia Tech; Michael Scott, Salisbury University; Francisco Olivera, Texas A&M University; Chris Konrad, USGS; Sam Brody, Texas A&M University; Stephanie Bray, USACE; Lynn Martin, USACE; Chris Dunn, USACE; Shawn Komlos, USACE; Randall Behm, USACE, Craig Fischenich, USACE; Kevin Mickey, The Polis Center at Indiana University; Thomas Ballestero, University of New Hampshire; Jane Branson, Aither; and Jonathan Remo, Southern Illinois University.

Table of Contents

Appendices:

Tables

Page

Figures

Page

Figures, cont'd

Page

Figures, cont'd

Page

Exhibits

Acronyms and Abbreviations

AAL	Average annualized losses
AALA	Average annualized losses avoided
CN	Curve number
COOP	Cooperative observer program
DWR	California Department of Water Resources
FEMA	Federal Emergency Management Agency
FIA	Flood Insurance Administration
FIMA	Federal Insurance & Mitigation Administration
FIRM	Flood Insurance Rate Map
FIS	Flood insurance study
GBS	General building stock
GI	Green infrastructure
GIS	Geographic Information System
HUC	Hydrologic Unit Code
ICLUS	Integrated Climate and Land Use Scenario tool
LID	Low impact development
LiDAR	Light distancing and ranging
MMSD	Milwaukee Metropolitan Sewer District
NAIP	National Agricultural Inventory Project
NED	National Elevation Dataset
NFIP	National Flood Insurance Program
NID	National Inventory of Dams
NLD	National Levee Database
NHD	National Hydrographic Dataset
NLCD	National Land Cover Database
NOAA	National Oceanic and Atmospheric Administration
NRC	National Research Council
NRCS	Natural Resource Conservation Service
NRDC	Natural Resources Defense Council
OW	EPA Office of Water
PFDS	Precipitation frequency data server
PV	Present value
RFD	Rapid Floodplain Delineation
RoI	Region-of-influence

SARA	San Antonio River Authority
STATSGO2	Digital General Soil Map of the United States (formerly, State Soil Geographic database)
UDF	User-defined facility
USACE	U.S. Army Corps of Engineers
USDA	U.S. Department of Agriculture
EPA	U.S. Environmental Protection Agency
USGS	U.S. Geological Survey

Executive Summary

To address the impacts of excess stormwater, the U.S. Environmental Protection Agency (EPA) evaluated potential scenarios for managing stormwater from new development and redevelopment. The purpose of this study is to examine one of these impacts: flood loss avoidance. This study generated an estimate of the monetary value of flood loss avoidance that could be achieved by using distributed stormwater controls to capture a specified volume of runoff. This stormwater management approach retains on-site small storm events in an attempt to simulate predevelopment runoff conditions. This approach is referred to as Low Impact Development (LID) or Green Infrastructure (GI) for stormwater management and is an integrated approach that uses site planning and small engineered stormwater controls spatially distributed throughout a development site to capture runoff as close as possible to where it is generated. In this document, the term Green Infrastructure is used. Bioretention filters, landscaped roofs, rainwater cisterns, and infiltration trenches are examples of stormwater controls commonly found in GI applications. These controls infiltrate and evapotranspire runoff, or capture and store rain for beneficial uses like landscape irrigation and other non-potable uses. The approach in this study considered the application of GI only to new development and redevelopment, not as retrofits to mitigate the impact of existing imperviousness. The study approach consists of estimating flood depths and the associated flood losses with and without GI. The benefits are the losses that are avoided by watershed-wide implementation of GI. In this report, the terms "damages" and "flood losses" are used interchangeably.

The timeframe of analysis is from 2020 to 2040. The extent of GI application assumed for this study is small initially, because the assumption in this study is that GI would be implemented only on new development and redevelopment starting in 2020. The extent of GI application, and the associated benefits, would increase with development over time. Therefore, maximum benefits are realized in 2040, the last year of this study period. At the time of this report, several states have already adopted on-site retention practices; therefore, benefits of wider adoption nationwide are the focus of this study (i.e. the study focuses on areas that have not adopted retention policies to date).

Generating an estimate of the flood loss avoidance benefit from the use of small storm retention practices is problematic because data does not exist on damages from small, frequent storm events. For example, there is limited information on damages such as stream scouring that exposes buried utilities, bridges, and other assets to flood hazards. In addition, there are no national datasets of at-risk assets, flood control works, topography, and bathymetry detailed enough to generate accurate estimates, much less projections of national losses. Nevertheless, this study uses publicly available datasets and the Federal Emergency Management Agency's (FEMA) flood loss estimation model Hazus on a limited number of watersheds to obtain a conceptual quantification of the effect of stormwater retention on reducing potential riverine flood losses.

While this study relied on many assumptions to generate estimates of flood damages, it is important to keep in mind that the focus is on the "difference" between two conditions, with and without GI, given the same set of assumptions for both scenarios. Therefore, the absolute value of flood losses is less important than the relative differences between the scenarios.

Background and Context of Study: GI-based stormwater management has the primary benefit of water quality and stream protection; flood loss reduction is only one of many co-benefits. Estimation of the monetary value of these flood loss reduction co-benefits is important for decision-making because of the challenges in assigning monetary value to improved water quality and stream health. Unlike monetizing stream health, estimation of flood loss avoidance can be accomplished using established data and models that, while based on many simplifying assumptions, generate a dollar value based on defensible, systematic approaches that can be fine-tuned as appropriate, albeit with additional study costs.

The costs of GI implementation are not included in this document. Nevertheless, new development and redevelopment already require stormwater management expenditures, either on-site or downstream; therefore, GI could be used to meet those requirements fully or partially for little or no additional cost compared to overall construction costs. This study does not assume retrofitting of existing imperviousness. Retrofitting, in addition to implementation on new development and redevelopment, would be expected to generate more flood loss avoidance benefits but would incur additional costs.

The flood loss avoidance benefits estimated in this study should not be contrasted directly with GI implementation cost for a benefit-cost comparison because, as noted previously, flood loss avoidance is not the only, and certainly not the primary, benefit of GI. Comparisons of benefits to costs should be made using the full suite of benefits that include improved water quality, reduced stream erosion and scouring, healthier aquatic and benthic ecosystems, greener and cooler cities, more stable stream baseflow during droughts, groundwater recharge, reduced potable water use, and other benefits.

Retention Scenarios: In this study, the term "retention" is used to indicate capture of rainfall on site so that it does not become direct runoff. Presumably, the greater the volume of runoff captured, the greater the overall benefits. The study examines three scenarios, "high", "medium," and "low" shown in Table ES–1. The scenarios are defined by storm percentiles; for example, the 95th percentile is the storm depth such that 95% of all storms in an average year have a rainfall depth that is smaller than or equal to the percentile depth. The current analysis concentrates largely on the medium scenario; the other two are used to assess the sensitivity of the results to the volume of capture. Chapter 2 presents additional details.

Table ES–1. Retention scenarios in the study as defined by the percentile of the storm retained.

	Percentile storm retained	
Scenario	**New development**	**Redevelopment**
High	95th	90th
Medium	90th	85th
Low	85th	80th

Sample watersheds: A sample of 20 Hydrologic Unit Code 8 (HUC8) watersheds was selected to estimate the effect of GI on flood damages. The watersheds were chosen to represent the range of climate and value of assets potentially exposed to floods, within areas of the lower 48 states that currently do not have a retention standard. States that already have such standards would not accrue additional benefits from wider adoption of GI and thus were not the focus of the study; however, they were included in a national estimate. This process is described in Chapter 3.

Hydrology: Flooding is caused by extreme rainfall events. The volume of runoff generated depends on soil types and land cover. In particular, impervious surfaces generate large runoff volumes because they prevent the rain from soaking into the soil. GI reduces the volume of runoff by infiltrating it into the soil, releasing it to the atmosphere through evapotranspiration, or capturing it for beneficial use.

The hydrology of the 20 watersheds was characterized using the PeakFQ flood frequency analysis model (USGS, 2013) to derive probability distributions from existing streamflow records in unregulated streams, that is, streams without dams or otherwise affected by significant flow diversions and inflows. The Region of Influence (RoI) approach (Eng et al., 2005) was used to estimate peak flows at ungaged locations. A methodology was derived to estimate peak flows in the future based on growth projections and the associated increases in impervious surfaces. To simulate the effect of GI on the hydrology, a methodology was formulated to simulate the volume-reduction effect of GI on lessening peak flows. These methods are described in Chapter 4.

Flood hazard: The water surface elevations resulting from the peak flows during flood events define the flooding depths that are the cause of damages to buildings and other infrastructure. The Rapid Floodplain Delineation (RFD) model was used to create hydraulic models for the watersheds using publicly available terrain and hydrography datasets. The models were run for the 2-, 5-, 10-, 25-, 50-, and 100-year events. In this study the term "floodplain" indicates the horizontal extent of inundated land resulting from each of these flood events. The horizontal extent of flooding and flood depths were determined through post-processing of the water surface elevations with a Geographic Information System (GIS). The results were compiled as depth grids, with a depth value for each storm event for each grid cell.

Deployment of GI led to a general reduction in the total floodplain area for all of the 20 HUC8 watersheds modeled. As expected, the reduction was greater for the small, frequent events. For the 2-year event, the floodplain area decreased by as much as 8%, whereas for the 100-year event the greatest reduction was around 2.5%. Chapter 5 provides details on the determination of flood hazards.

Loss estimation: The Hazus model (FEMA, 2013) was used to estimate losses caused by the simulated flood events. Hazus applies the flood depths from the hydraulic model to various types of infrastructure to estimate damages to the structure and contents. Hazus contains extensive databases that aggregate the value of assets by Census block. A library of depth-damage curves is available to estimate the damage caused by a given flood depth inside a building of a given type. Hazus accumulates all damages and provides a total damage figure for a given watershed. The total damages with and without GI can be compared to assess the avoided losses. Approximations were formulated to consider the flood protection effects of dams and levees. Chapter 6 summarizes the damage estimation process.

Zero-damage thresholds: Flood damages are highly dependent on the location of assets at risk, horizontally and vertically, in relation to the source of flooding. By default, Hazus assumes that the value of assets is uniformly distributed in a given Census block. This approximation can overestimate damages because the uniform distribution of assets artificially places some dollar value in areas close to the stream that flood often but may not have any assets at risk. The fact that flood depths are the greatest in these areas compounds the overestimation effect.

The solution to this shortcoming of the default Hazus application is to use detailed structure information; however, this information does not exist as a nationally available public dataset. This information is only available at the local government level. Therefore, an approximate approach was formulated to address the problem. The approach, described in detail in Chapter 6, assumed that a given frequently occurring flood does not cause any damages because there are no exposed assets within that floodplain. The rationale was that areas that flood often would not be developed or would have assets with low value. This concept of a "zero-damage threshold" is plausible as a means to account for the damage overestimation. This study evaluates three threshold options:

1. No assets exist in the 2-year floodplain (2-year zero-damage threshold)
2. No assets exist in the 5-year floodplain (5-year zero-damage threshold)
3. No assets exist in the 10-year floodplain (10-year zero-damage threshold)

The purpose of each of these thresholds is to remove assets numerically by assigning zero damages within the corresponding floodplain and those for less severe events. The area within the zero-damage threshold increases in size as the return period increases; and the benefits decrease accordingly. The use of the zero-damage thresholds allows estimation of a range of benefits with the 2-year zero-damage threshold yielding the most losses avoided and the 10-year zero-damage

threshold producing the fewest losses avoided, or a conservative estimate. Avoided loss estimates are presented in this study for the 5-year and 10-year zero-damage thresholds.

It is noted that in an ideal world, FEMA flood insurance regulations would result in development in such a way that losses would not occur until the 100-year event is exceeded. Properties within the 100-year floodplain must be covered by flood insurance to obtain a mortgage from a federally-backed or insured lender. This insurance requirement results in a higher cost for building in the 100-year floodplain and may discourage some development, but does not eliminate all construction and therefore does not avoid the risk completely. In addition, many local building codes prescribe how development within the 100-year floodplain must proceed to reduce the potential flood damages. Nevertheless, in reality, there are many reasons why it is reasonable to assume that losses occur at more frequent events as explained in Chapter 6.

Validations: The public-domain datasets used in the analysis have accuracy limitations in their ability to place assets at risk with respect to the flood hazard. In addition, several assumptions had to be made in the study to enable a nationwide estimation. To understand the effects of the accuracy limitations and the assumptions, several localized tests were conducted to compare the data from the national datasets used with site-specific information provided by partners or specifically derived for the study. These tests were not intended to define correction factors but to understand the potential implications of using the national datasets employed in the study. Some of the tests indicate that the proposed methodology underestimates damages; others suggest the opposite. For example, use of a hydrologic model such as HEC-HMS predicted more benefits than using the stream gage analysis. Using LiDAR terrain data produces fewer damages than the publicly available digital elevation models that are less accurate. Finally, using site-specific asset location and value can produce either more or fewer damages depending on the watershed – although in the validations in this study fewer damages were observed using site-specific asset locations. As previously noted, in this study it is not the absolute value of the losses but the difference between the with- and without-GI scenarios that is of interest. On balance, the tests indicate that the methodology chosen is useful to estimate conceptually the flood losses avoided by adopting GI on a nationwide basis, which can inform policy decisions with an understanding of the limitations described in this report. For localized studies, the validation tests emphasize the need to use site-specific data, although the methodology would remain the same. These validations are presented in Chapter 7.

Nationwide scale-up: Regression equations developed to relate the flood losses avoided to watershed properties served as a tool to extrapolate the results for the 20 HUC8 watersheds in the sample to other watersheds. The accuracy of the regression was limited by both the small number of watersheds modeled and by the variable nature of the watershed properties and assets. The goal was to estimate a range of flood loss avoidance benefits to the nation that could be realized by adoption of stormwater management practices based on GI. The benefits were analyzed as a snapshot in 2040 in the following three regions:

- The 40 top-growth HUC4 watersheds, according to the 2040 forecast provided by EPA
- Conterminous United States, excluding jurisdictions that already have GI-based retention standards in place
- Conterminous United States

The benefits were adjusted to account for the value of added infrastructure between "existing" conditions (2006) and 2040. These estimates only include buildings, their contents, and the associated income loss. Consideration of roads, bridges, utilities, and other critical infrastructure would increase these values. In addition, the benefits were assumed not to propagate from one HUC8 watershed to the next one directly downstream. If they had, the losses avoided would increase.

The annual benefits in 2040 in millions (2011 dollars) are summarized in the following table for the "medium" scenario (90th percentile capture for new development and 85th percentile for redevelopment):

Table ES–2. Flood losses avoided in the year 2040 for various zero-damage thresholds, expressed in 2011 dollars (benefits in 2040 [in millions, 2011 dollars]).

	Zero-damage threshold	
	5-year	10-year
40 top-growth HUC4s	$94	$44
Conterminous United States, excluding jurisdictions with retention standards	$136	$63
Conterminous United States	$329	$114

Additional benefits would continue to accrue after 2040 with continued development and redevelopment. During the study period, it is assumed that the benefits vary linearly from zero in 2020 to the maximum values in 2040 given in Table ES–2. The present value of these linear series is one way to express the savings to the nation in flood losses avoided. Using a discount rate of 3%, the results of this calculation are shown in Table ES–3. This process and results are presented in Chapter 8.

Table ES–3. Present value of flood losses avoided between 2020 and 2040 for various zero-damage thresholds, expressed in 2011 dollars (present value of benefits between 2020 and 2040 using a 3% discount rate [billions, 2011 dollars]).

	Zero-damage threshold	
	5-year	10-year
40 top-growth HUC4s	$0.7	$0.3
Conterminous United States, excluding jurisdictions with retention standards	$1.0	$0.4
Conterminous United States	$2.3	$0.8

Conclusions and recommendations for methodology improvements: There are many sources of uncertainty in a study of this nature. Many improvements could be undertaken if the need for more accuracy warranted the additional study cost. For example, more accurate terrain and bathymetry data could be obtained, detailed hydrologic modeling could be performed, actual asset locations and characteristics could be used, and climate change could be considered. Conclusions and recommendations for methodology improvements are presented in Chapter 9.

Findings: GI can reduce flood losses when applied watershed-wide as a co-benefit to the primary objective of water quality protection. The methodology proposed in this study makes use of national public datasets that have accuracy limitations. In particular, the assumption of uniformly distributed assets across Census blocks in Hazus can diverge considerably from reality. The definition of the varying zero-damage threshold allows for a qualitative understanding of that divergence. Despite these limitations, the methodology is useful for this type of comparative national study. It is important to keep in mind that this study examined the "difference" between two conditions, with and without GI, given the same set of assumptions for both scenarios. Therefore, the absolute value of flood losses is less important than the relative differences between the scenarios.

This study indicates that the annual savings to the nation in terms of flood losses avoided in the year 2040 would range from $63 to $136 million (2011 dollars) if GI practices were more widely adopted on new development and redevelopment. This figure includes the conterminous United States, excluding jurisdictions (states and municipalities) that already have a GI-based retention standard in place. Assuming that the benefits start at zero in 2020, the corresponding present value of the stream of benefits in the following 20 years ranges from $0.4 and $1 billion (2011 dollars). These estimates only include buildings, their contents, and the associated income loss. Consideration of roads, bridges, utilities, and other critical infrastructure would increase these values. Avoided losses would continue to accrue after 2040, the end of this study period. In addition, the benefits were assumed not to propagate from one HUC8 watershed to the next one directly downstream. If they had, the losses avoided would have been greater.

1. Introduction

The impacts of stormwater from development have been documented extensively in peer-reviewed literature and summarized in the National Research Council's report titled *Urban Stormwater Management in the United States* (NRC, 2009). To address these impacts, the U.S. Environmental Protection Agency (EPA) Office of Water (OW) evaluated several potential scenarios for managing stormwater from new development and redevelopment. This study generated an estimate of the monetary value of riverine flood loss avoidance that could be achieved by using distributed stormwater controls on new development and redevelopment to capture a relatively small depth of rainfall, in the range of 0.5 to 2 inches, with a goal of reducing runoff volumes to those similar to undeveloped landscape conditions. This approach is known as green infrastructure (GI) for stormwater management or low impact development (LID). This report will use the term GI to refer to an integrated approach that uses site planning and small engineered stormwater controls spatially distributed throughout a development site to capture runoff as close as possible to where it is generated. Bioretention filters, landscaped roofs, rainwater cisterns, and infiltration trenches are examples of stormwater controls commonly found in GI applications. These controls infiltrate and evapotranspire runoff, or capture and store rain for beneficial uses like landscape irrigation and other non-potable uses. The timeframe selected for this study was the 20-year period between 2020 and 2040. In this report, the terms "damages" and "flood losses" are used interchangeably.

1.1. Background and Context of the Study

An assessment of benefits and costs, either quantitative or qualitative, serves to inform decisions to implement new environmental management approaches. When possible, a quantitative approach – generating monetary benefits and comparing them to costs – is preferable because it provides a consistent measure. Water quality improvement is the primary benefit that the GI approach affords but, because monetizing improved water quality is elusive, it is important to assess those co-benefits for which there is a systematic approach to estimate monetary benefits. There are numerous environmental, social, and economic benefits of GI, some of them are more amenable to monetization than others. Examples of these co-benefits include flood loss reduction, groundwater recharge, mitigation of urban heat island effects, increased property values, improved neighborhood aesthetics and quality of life, and reduced energy use for cooling. Although the full suite of potential benefits should be considered when comparing to an estimated cost of implementation, this study addresses only flood loss avoidance benefits. The following are limitations in the scope of this study:

- It does not calculate the costs of implementing or maintaining GI on new development and redevelopment.

- It only considers implementing GI as part of the construction of new development and redevelopment, where stormwater management costs are part of the project. Retrofitting existing systems to mitigate for existing impervious areas was not part of the evaluation.
- It addresses only riverine flooding at the HUC8 scale. Propagation of benefits downstream of a given HUC8 was not calculated, which underestimates the potential benefits.
- It does not consider climate change; therefore, it is assumed that historical rainfall records are representative of the conditions between now and 2040.

The analysis used the most appropriate tools and data available in the industry for this type of national-scale study; however, there are factors that introduce uncertainty such as future weather, accuracy and detail of national datasets, and urban development patterns. Not all avoided flood losses were included: nuisance flooding from deficient urban drainage systems – known to be a widespread problem – disrupt traffic, necessitate repeated clean-up, and require more frequent maintenance, repair and upgrading of drainage systems. Examples of other negative impacts that the study did not consider include loss of life, decreased property value and long-term health issues associated with mold and sewer backups. Additional information, such as more watersheds to model, and site-specific data such as bathymetry and local building stock information, would result in better estimates but this level of detail was beyond the scope and budget of this effort. An overview of the study limitations, the factors that may tend to over- or underestimate avoided losses, and recommendations for methodology improvements are provided in Chapter 9.

The findings of this study provide a general insight into a single potential benefit of mitigating the excess runoff from future new development and redevelopment. While the estimates are predictions that involve many assumptions, they aid in understanding the potential scale of flood losses avoided. The results are useful to inform national policy but should not be used for decision-making at the local level, for which site-specific studies would be needed, although the methodology presented herein would be entirely scalable to the local level.

1.2. Overview of Benefits of GI

The application of GI for stormwater management is based on the principle of source reduction; specifically, GI decreases the volume of water that enters waterways as direct runoff through a combination of planning practices and engineered devices that infiltrate, evapotranspire, or store runoff for beneficial use (Hinman, 2012). In this study, the term "retention" is used to indicate capture of rainfall on site so that it does not become direct runoff. Depending on the design specifications and geographic location for a site, a given volume is removed for all storms, large and small. The retention volume required is expressed as a high percentile of the rainfall distribution such that the majority of storms would be completely captured.

The benefits of GI have been reported in numerous publications; Taylor (2013) presents a useful literature review. Water quality benefits include load reduction of heavy metals, suspended solids,

hydrocarbons, and nutrients, as well as reductions in thermal loads. Groundwater recharge and baseflow augmentation are other benefits that result from GI devices that infiltrate runoff. Peak flow attenuation is another benefit of GI and aims to protect stream channels in the vicinity of where the GI controls discharge to receiving waters. Reduced peak flows result in reduced erosive forces and thus less streambank and streambed erosion. The benefits in lessening the impacts of large storm events have been surmised but documented only for individual development sites (e.g., NRDC, 1999, Chapter 12). If GI is implemented on a significant portion of a watershed, the overall volume reduction would have a cumulative impact on receiving streams that could reduce the magnitude of peak flows. In consequence, it is plausible that water surface elevations during floods would be lower and therefore cause fewer damages to buildings and their contents, as well as to other vulnerable infrastructure. This effect was demonstrated by Medina et al. (2011) on a relatively small watershed in the Southeastern United States. Braden and Johnston (2004) and Braden et al. (2006) modeled flood reduction benefits of on a subdivision scale. Similarly, Kousky et al. (2011) addressed the effect that land conservation would have on reducing flooding in a watershed in the Midwest.

GI capture typically ranges from 0.5 to 1.5 inches, which are small depths when compared with the storms responsible for causing flooding, for example, the 100-year storm events listed in Table 1–1Table 1–1. Flood control is not a primary objective for GI use; however, these retention depths would have more of an effect on the 2-year events shown in the table. These events are not as severe as the 100-year storm but are still considered significant.

Table 1–1. Depth of the 100-, and 2-year, 24-hour storm events in four locations.

Location	100-year storm depth (in)	2-year storm depth (in)
Fort Collins, Colorado	5.6	2.0
Washington, DC	8.4	3.2
Miami, Florida	14.7	5.4
Tacoma, Washington	4.2	2.1

Source: NOAA (2013)

In addition to the local rainfall patterns, the extent of the benefit that GI may have on flood loss reduction depends on the value of assets at risk and their location in relation with the sources of flood hazards. Flood losses are highly dependent on the position of assets on the landscape. In general, assets that are close to a stream or other low-lying areas will experience more frequent flooding and greater flood depths than assets that are located on high ground farther from the stream. However, even localized terrain features, such as a house located on fill, have major influence on the extent of flood damages. The value of assets could also be related to their location in a floodplain. High-end residential structures may tend to be located away from riverine floodprone areas or be elevated; low income neighborhoods may be located in floodplains. On the other hand, certain high value

assets such as wastewater treatment plants, water-based businesses, and recreational structures are purposefully located close to waterways.

In summary, the runoff volume reduction benefits that GI achieves are expected to result in fewer flood losses but the impact depends on site-specific factors related to climate and location of vulnerable assets in floodplains.

1.3. Overview of the Methodology

This report proposes a methodology to estimate the impact of GI on flood losses avoided nationwide. The methodology involves several components:

1. **Retention scenarios**: The study examines three scenarios, although it concentrates on one of them. It is expected that the greater the volume of runoff that is captured, the greater the overall benefits. The retention is assumed to be implemented on new development and redevelopment beginning in 2020, with the study period ending in 2040.
2. **Sample watersheds**: A sample of 20 HUC8 watersheds was selected to estimate the effect of GI on flood damages. The watersheds range in size between 500 and 3,000 square miles and were chosen based on climate and value of assets potentially exposed to floods, and within areas of the lower 48 states expected to experience significant development. The study approach consisted of estimating flood losses with and without GI. The benefits are the losses that are avoided by watershed-wide implementation of GI.
3. **Hydrology**: Flooding is caused by extreme rainfall events. The volume of runoff generated depends on soil types and land cover. In particular, impervious surfaces generate large runoff volumes because they prevent the rain from soaking into the soil. A method was derived to estimate peak flows in the future based on growth projections and the associated increases in impervious surfaces. On the other hand, GI reduces the volume of runoff by infiltrating it into the soil, releasing it to the atmosphere through evapotranspiration, or capturing it for beneficial use. A method was formulated to simulate the effect of GI's volume reduction on lessening peak flows.
4. **Flood hazard**: The water surface elevations resulting from the peak flows during flood events define the flooding depths that are the cause of damages to buildings and other infrastructure. A hydraulic model is the preferred tool to simulate these water surface elevations. A high-speed hydraulic modeling approach was developed to make use of publicly available terrain and hydrography datasets. The horizontal extent of flooding and flood depths were determined through post-processing of the water surface elevations with a Geographic Information System (GIS). In this study the term "floodplain" indicates the extent of inundated land resulting from each of the flood events in the analysis: 2-, 5-, 10-, 25-, 50-, and 100-year return periods. Therefore the 25-year floodplain refers to the horizontal extent of flooding caused by the 25-year event. For expediency, the term "return period" is used in this study to designate the flood events, although some agencies prefer probability of exceedence instead.

5. **Loss estimation**: The Federal Emergency Management Agency's (FEMA's) Hazus model (FEMA, 2013) was applied to estimate losses caused by the simulated flood events. Hazus applies the flood depths from the hydraulic model to various types of infrastructure to estimate damages to the structure and contents. Hazus contains extensive databases that aggregate the value of assets by Census block. A library of depth-damage curves is available to estimate the damage caused by a given flood depth inside a building of a given type. Hazus accumulates all damages to provide a total damage figure for a given watershed. The total damages with and without GI can be compared to assess the avoided losses. It should be noted that the analysis in this study included only buildings, their contents, and the associated income losses. Consideration of roads, bridges, utilities, and other critical infrastructure would increase the estimates of losses avoided.
6. **Validations**: Flood damages by nature depend on spatial location and elevation of assets that could be at risk. The public-domain datasets used in the analysis have accuracy limitations in their ability to place assets at risk with respect to the flood hazard. In addition, several assumptions were necessary in the study to enable a nationwide estimation. To understand the effects of the accuracy limitations and the assumptions, several localized tests were conducted to compare the data used with site-specific information provided by partners or specifically derived for the project. These tests were not intended to define correction factors but to understand the potential implications of using the national datasets in the study.
7. **Nationwide scale-up:** Regression equations developed to relate the flood losses avoided to watershed properties served as a tool to extrapolate the results for the 20 HUC8 watersheds in the sample to other watersheds in the lower 48 states. The benefits were adjusted to account for the value of infrastructure built out to the year 2040. The result was a range of savings to the nation that could be realized by adoption of stormwater management practices based on GI.

Table 1–2 summarizes the datasets and models used in the study. Other data sources were supplied by EPA, for example, rainfall percentiles to be retained and the 2040 forecast for new development and redevelopment.

The subsequent chapters provide details on the components of the study.

Table 1–2. Datasets and models used in the study.

Dataset	Source	Date
National Elevation Dataset (NED), 1/3 arcsecond resolution	USGS, http://ned.usgs.gov/	2013
National Land Cover Database (NLCD)	USGS, http://landcover.usgs.gov/	2006
National Hydrography Dataset, NHDPlus Version 2.1	EPA, http://www.horizon-systems.com/NHDPlus/NHDPlusV2_home.php	2013
Digital General Soil Map of the United States, STATSGO2	USDA, http://soils.usda.gov/survey/geography/ssurgo/description_statsgo2.html	2013
National Inventory of Dams (NID)	USACE, http://geo.usace.army.mil/pgis/f?p=397:12:	2012
National Levee Database (NLD)	USACE, http://nld.usace.army.mil/egis/f?p=471:1:	2012
Precipitation frequency data server	NOAA, http://dipper.nws.noaa.gov/hdsc/pfds/	2013
Peak Streamflow for the Nation	USGS, http://nwis.waterdata.usgs.gov/usa/nwis/peak	2012
Model	**Source**	**Date**
PeakFQ v 5.2	USGS, http://water.usgs.gov/software/PeakFQ/	2007
HEC-HMS v 3.5	USACE, http://www.hec.usace.army.mil/software/hec-hms/	2010
Rapid Floodplain Delineation (RFD)	Atkins	2012
Hazus-MH, v 2.1	FEMA, http://www.fema.gov/hazus	2012
SAS/STAT® v 9.3	SAS, www.sas.com	2011

2. Retention Scenarios

The options for post-development stormwater management under consideration assume a retention scenario expressed in terms of a percentile of the depth of a 24-hour storm to be retained on site. For example, the 80th percentile depth is defined as a rainfall depth such that, on average, 80% of all storms have a smaller depth. For a standard based on the 80th percentile event, all storms with rainfall depths less than the 80th percentile depth would be retained on site.

Figure 2–1 compares the rainfall distribution at four locations in the continental US and illustrates how capturing a relatively small volume controls the majority of the storms occurring at the given location. For example, 80% of all storms in a typical year in Arapahoe, Colorado are controlled by deploying stormwater management facilities that capture the volume generated by 0.7 inches of rain. In Miami, Florida, about 1.1 inches must be retained to achieve a similar level of stormwater management.

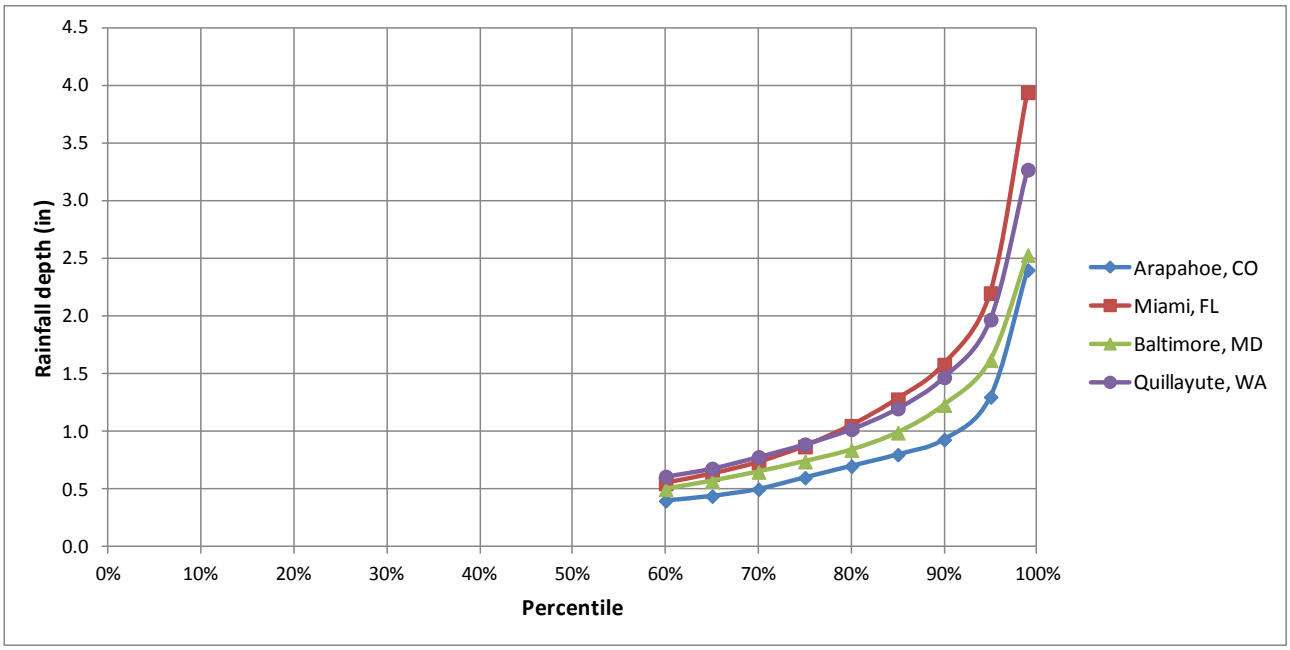

Figure 2–1. Rainfall distributions for four selected locations. The percentile is the fraction of the average annual number of storms that have depths smaller than or equal to the values in the vertical axis.

The analysis evaluated three scenarios:

- **High:** The 95th percentile depth is captured for new development projects and the 90th percentile for redevelopment projects

- **Medium:** The 90th percentile depth is captured for new development projects and the 85th percentile for redevelopment projects
- **Low:** The 85th percentile depth is captured for new development projects and the 80th percentile for redevelopment projects

It is expected that the flood avoidance benefits will decrease with lesser runoff volumes to capture.

The analysis in this study was undertaken for 20 HUC8 watersheds nationwide. However, only the "medium" scenario was evaluated for all 20 watersheds. The "high" and "low" scenarios were investigated for 9 of the watersheds, as a means of testing the sensitivity of the benefits against the magnitude of the retention scenario.

The depths for the rainfall percentiles were provided by EPA as a table for various National Oceanic and Atmospheric Administration (NOAA) Cooperative Observer Program (COOP) locations nationwide. The table is presented in Appendix A.

3. Watershed Sample Selection

The analysis unit in this study is the HUC8 watershed, selected because it is the most compatible with the national datasets available for the study. Ranging between 500 and 3,000 square miles, HUC8s encompass a variety of land uses and covers and hold low- and high-order streams. In addition, they usually contain several USGS stream gage stations. There are 2,259 HUC8s in the United States, with 2,109 of them in the contiguous 48 states.

The constraints of this study limited the number of watersheds in the analysis to 20, which may not be a statistically representative sample given the wide range of variability of factors that affect flood damages: climate, terrain slope, drainage network density, soils, land use and land cover, value of assets exposed to flood hazards, and existence of flood controls such as reservoirs, pump stations, and levees. Nevertheless, an attempt was made to distribute the 20 HUC8s to capture some of this variability.

Although several factors were considered to select watersheds, such as topography, the following major factors were evaluated in the choice of the sample:

1. **Climate:** The watersheds were classified as either dry or wet depending on whether the average annual precipitation was above or below 20 inches.
2. **Rainfall patterns:** The ability of GI controls to capture a significant amount of runoff depends on how rainfall arrives to the watershed. A series of frequent, very small events makes it easy to retain most of the storms in a year. In contrast, if a significant fraction of the annual volume of rainfall arrives in relatively few but large storm events, then the GI controls would capture the initial amount of a given storm and bypass the remainder. In the watershed sample selection, this characteristic of rainfall was represented by the mean storm depth. The rainfall records within the BASINS 4.0 model (EPA, 2007) were extracted and analyzed nationwide. All hourly records, some spanning multiple decades, were analyzed to define individual storms and find their depths. A storm was defined as a sustained period of rainfall delimited by periods of zero rain of at least 6 hours, and having a storm depth greater than 0.1 inches.
3. **Exposure:** The exposure is the total replacement value of buildings and their contents that is vulnerable to floods. The greatest benefits are expected to occur in watersheds with high exposure values. This study uses the exposure values in the Hazus software (FEMA, 2013), which tabulates the value of all assets in each Census block. Hazus contains an exposure dataset aggregated to the resolution level of Census blocks. This dataset is known as general building stock (GBS) and represents all buildings in a specified census block. The values were compiled from U.S. Census Bureau 2000 data for residential occupancies and from Dun & Bradstreet employment data for non-residential occupancies. The data were later updated to 2006 values. For the purposes of sample selection, the total replacement value of the GBS within the watersheds was used to categorize them.

These three factors resulted in the categories shown in Table 3–1 and were used to classify the watersheds as depicted in Figure 3–1. The watersheds illustrated in the figure were selected on the basis of the greatest projected increase in impervious surface throughout the period between 2010 and 2040, in jurisdictions that did not have a retention standard already. The initial selection of 20 HUC8 watersheds was further modified when one of the needed datasets was not available for a watershed or was unsuitable for the envisioned modeling approach, such as those in which extensive dams or levees modify the hydrology significantly. Figure 3–2 shows the final sample of 20 HUC8 watersheds. The names of the watersheds are indicated in this figure and Appendix B contains maps for each of the watersheds. The Northern Long Island (02030201) and Southern Long Island (02030202) HUC8s were combined into a single watershed.

Table 3–1. Categorization of watershed characteristics for sample selection.

Factor	Category 0	Category 1	Category 2
Mean storm depth	Less than 0.4 in	Between 0.4 and 0.6 in	Greater than 0.6 in
Total exposure to flood	Less than $10 million	Between $10 and $100 million	Greater than $100 million
	Dry	**Wet**	
Annual precipitation	Less than or equal to 20 in/year	Greater than 20 in/year	

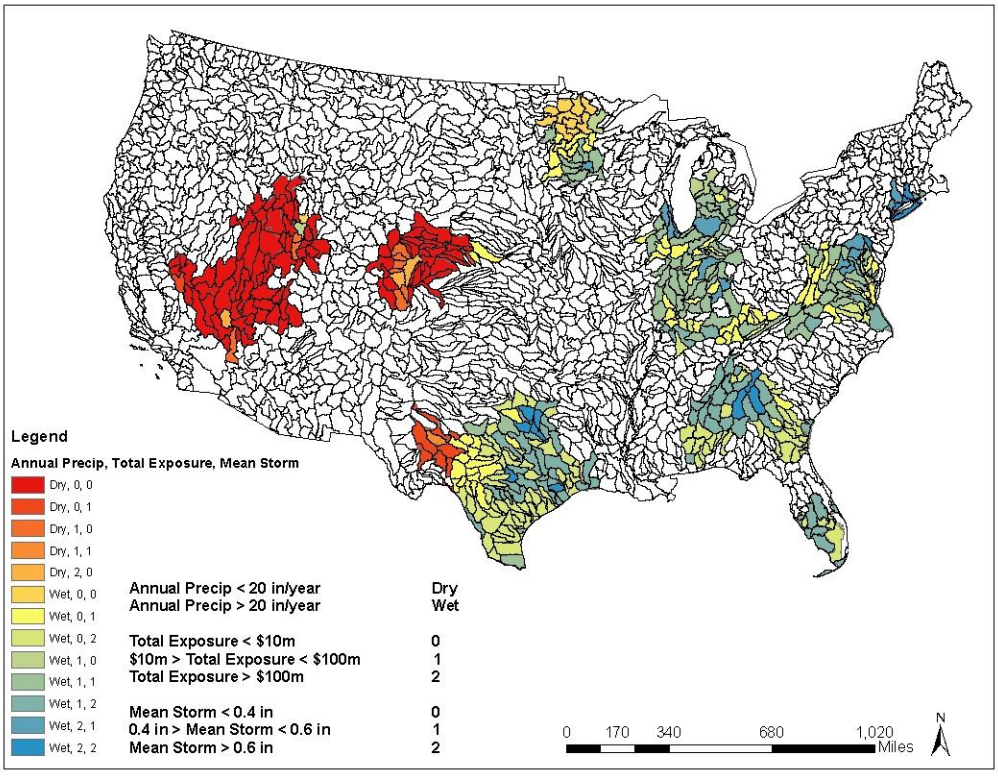

Figure 3–1. Classification of the HUC8 watersheds for sample selection according to the criteria in Table 3–1.

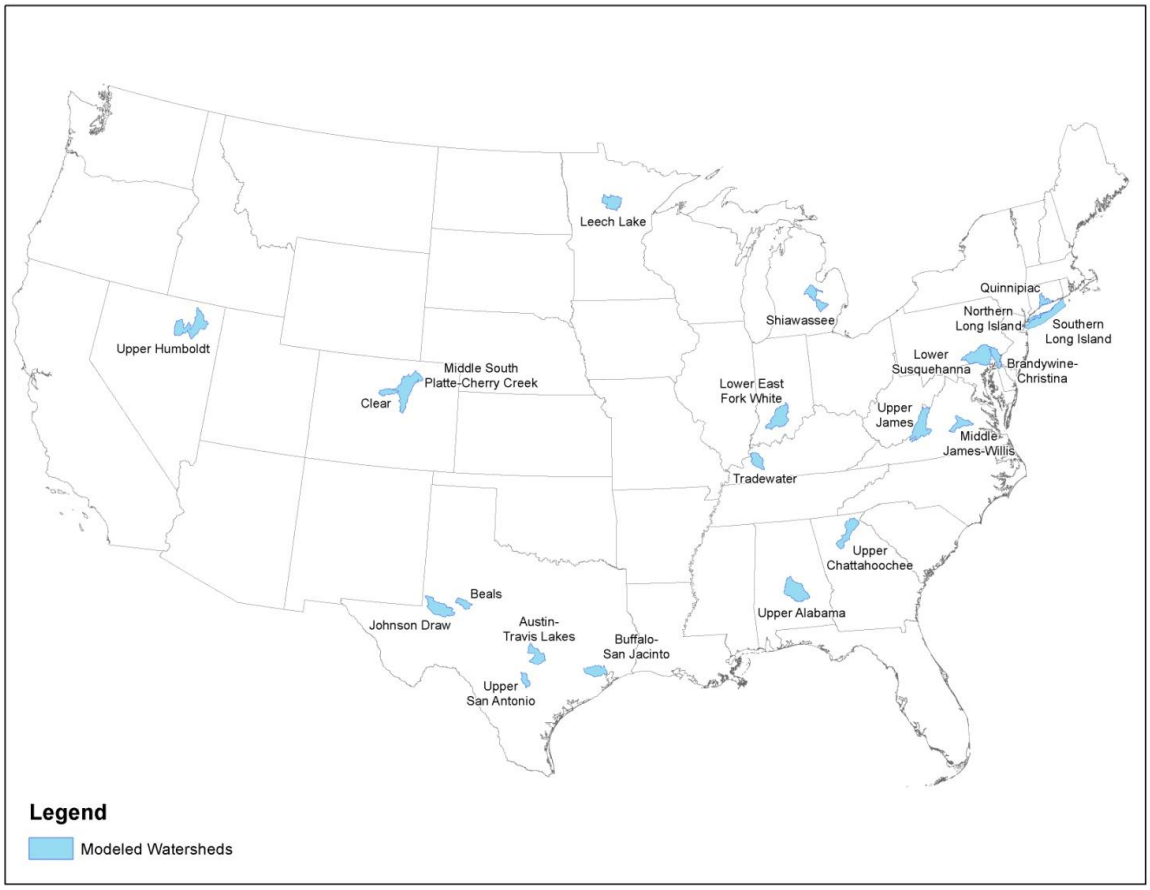

Figure 3–2. Sample 20 HUC8s selected for modeling.

EPA conducted an analysis that identified the 40 top-growth HUC4s on the basis of the greatest dollar value of construction associated with new development and redevelopment expected in 2040 (Figure 3–3). This set of watersheds became one of the study areas on which the scale-up would be performed as stated at the beginning of this section.

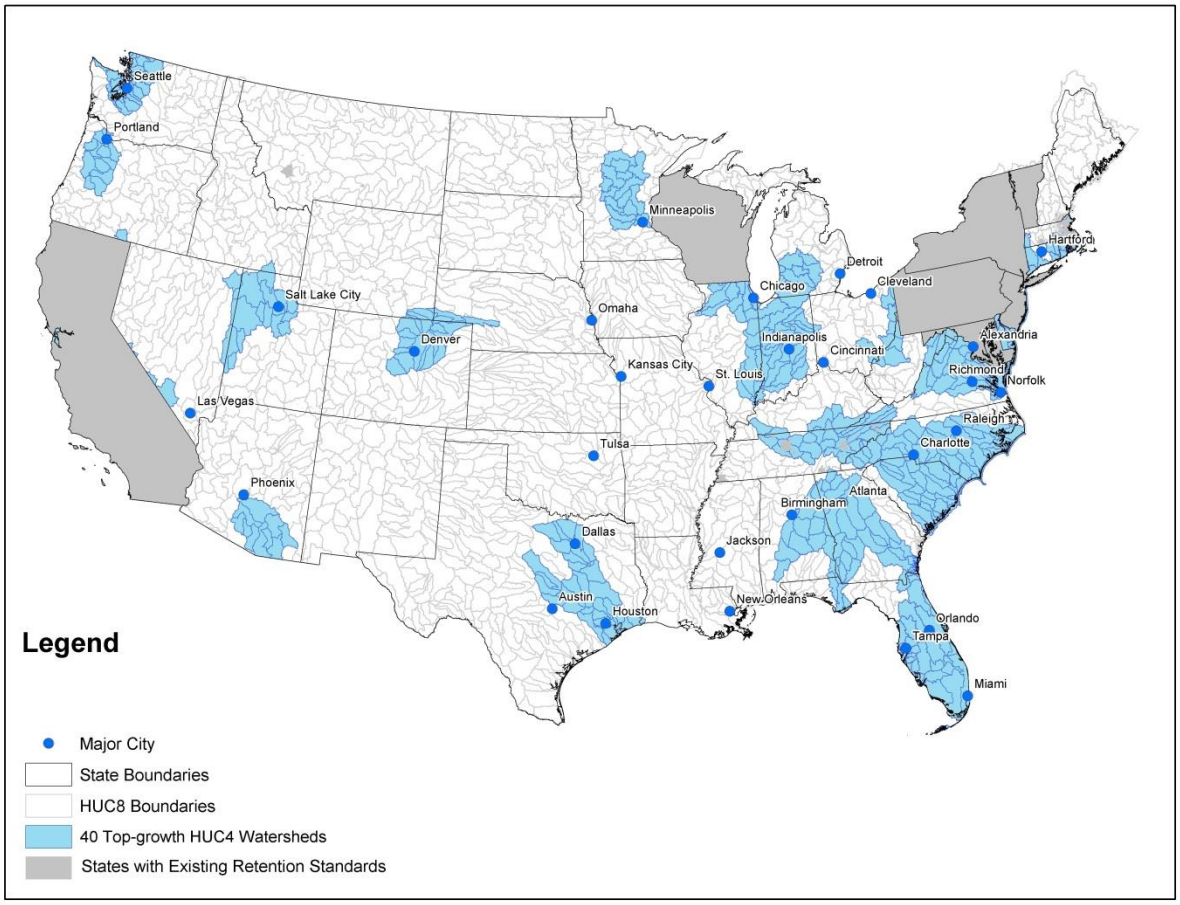

Figure 3–3. The 40 top-growth HUC4 watersheds, and states with existing retention standards.

Physical properties of the 20 HUC8s selected for modeling were extracted from the datasets listed in Table 1-2. Derivative properties such as watershed area, slope, length of stream miles, and areas protected by levees were calculated from these datasets. Growth projections up to the year 2040 were supplied by EPA in the form of total areal extents of new development and redevelopment, impervious areas, and total value of construction for residential, commercial, and industrial land uses. Table 3–2 summarizes representative properties.

Three study areas were analyzed. The first one was limited to the top 40 HUC4 watersheds expected to experience the most development activity by 2040. Several jurisdictions, ranging from municipalities to entire states, have already implemented this type of on-site retention; therefore, these jurisdictions were removed from consideration because they would not experience significant additional benefits (Appendix C). After removal of these jurisdictions, the first study area consists of the 501 HUC8s shown in Figure 3–3. The second study area includes all of the conterminous United States, excluding areas with stormwater regulations that require GI retention. The third study area is the conterminous United States without any exclusion.

Table 3–2. Properties of the 20 sample HUC8s.

01100004	Quinnipiac (CT)	50	$ 106,527,456	3.23	4.21	5.00	5.89	6.57	7.10	0.63	0.85	1.00	1.24	1.61
02030201+02030202	Northern +Southern Long Island (NY)	50	$ 778,802,733	3.40	4.43	5.15	5.97	6.87	7.36	0.64	0.83	0.98	1.22	1.64
02040205	Brandywine-Christina (DE)	46	$ 105,513,311	3.24	4.09	4.80	5.84	6.72	7.68	0.61	0.85	0.99	1.21	1.61
02050306	Lower Susquehanna (PA)	43	$ 120,824,208	3.04	3.87	4.59	5.67	6.62	7.69	0.56	0.73	0.86	1.08	1.49
02080201	Upper James (VA)	40	$ 4,548,148	2.98	3.74	4.36	5.26	6.00	6.81	0.48	0.73	0.84	1.00	1.31
02080205	Middle James (VA)	44	$ 31,386,000	3.28	4.20	4.97	6.12	7.11	8.19	0.57	0.84	0.99	1.24	1.63
03130001	Upper Chattahoochee (GA)	60	$ 214,758,979	4.27	5.34	6.23	7.32	8.14	8.62	0.73	1.06	1.27	1.50	2.01
03150201	Upper Alabama (AL)	53	$ 33,231,478	4.54	5.77	6.67	7.64	8.52	9.33	0.71	1.09	1.27	1.52	2.03
04080203	Shiawassee (MI)	32	$ 24,544,624	2.30	3.00	3.52	3.88	4.26	4.61	0.40	0.61	0.72	0.87	1.19
05120208	Lower East Fork White (IN)	46	$ 21,821,655	3.15	3.91	4.53	5.39	6.10	6.85	0.49	0.90	1.05	1.23	1.60
05140205	Tradewater (KY)	47	$ 4,627,186	3.50	4.37	5.08	6.09	6.93	7.83	0.61	0.91	1.07	1.31	1.74
07010102	Leech Lake (MN)	27	$ 2,348,558	2.41	3.16	3.69	4.22	4.76	5.33	0.38	0.60	0.71	0.86	1.18
10190003	Middle South Platte-Cherry Creek (CO)	15	$ 146,772,202	1.74	2.34	2.86	3.35	3.80	4.31	0.31	0.60	0.70	0.83	1.19
10190004	Clear (CO)	17	$ 34,434,582	1.55	2.15	2.68	3.13	3.45	4.02	0.29	0.60	0.70	0.83	1.20
12100301	Upper San Antonio River (TX)	33	$ 99,226,000	4.01	5.44	6.59	7.81	8.83	9.96	0.66	1.07	1.30	1.69	2.38
12040104	Buffalo-San Jacinto (TX)	51	$ 308,634,534	5.04	6.79	8.34	9.67	11.12	12.56	0.79	1.15	1.37	1.71	2.28
12080005	Johnson Draw (TX)	14	$ 30,312,264	2.71	3.68	4.50	5.17	5.97	6.70	0.50	0.72	0.85	1.07	1.44
12080007	Beals (TX)	20	$ 3,020,189	3.01	4.16	4.98	5.94	6.69	7.56	0.52	0.75	0.91	1.12	1.55
12090205	Austin-Travis Lakes (TX)	33	$ 101,343,163	4.05	5.46	6.62	7.79	8.82	9.92	0.66	1.01	1.21	1.49	2.01
16040101	Upper Humboldt (NV)	10	$ 2,719,561	1.22	1.54	1.80	2.16	2.44	2.73	0.26	0.39	0.47	0.56	0.72

Table 3–2, cont'd

HUC8	Watershed name (State)	Watershed area (mi^2)	Main stem stream length (mi)	Median watershed slope	2040 New development (mi^2)	2040 Redevelopment (mi^2)	Sum of new development and redevelopment areas/watershed area	Area protected by levees and diversions (mi^2)	No. of dams
01100004	Quinnipiac (CT)	512	358	3.83%	50.04	48.82	19.3%	0.030	74
02030201+02030202	Northern +Southern Long Island (NY)	2,337	729	1.23%	152.88	375.25	22.6%		23
02040205	Brandywine-Christina (DE)	756	480	4.27%	77.66	60.68	18.3%	0.47	52
02050306	Lower Susquehanna (PA)	2,486	1,835	6.17%	142.88	85.51	9.2%	2.51	71
02080201	Upper James (VA)	2,212	1,555	25.06%	3.38	4.36	0.3%		18
02080205	Middle James (VA)	945	650	5.46%	26.25	11.31	4.0%		98
03130001	Upper Chattahoochee (GA)	1,586	1,148	9.18%	113.07	73.79	11.8%		221
03150201	Upper Alabama (AL)	2,391	1,608	3.59%	20.20	13.00	1.4%	0.040	145
04080203	Shiawassee (MI)	1,266	1,037	0.63%	30.50	19.50	3.9%		27
05120208	Lower East Fork White (IN)	2,029	1,443	7.94%	10.23	7.22	0.9%		101
05140205	Tradewater (KY)	942	602	5.42%	0.51	3.32	0.4%	1.40	42
07010102	Leech Lake (MN)	1,341	863	1.13%	0.18	0.21	0.0%		3
10190003	Middle South Platte-Cherry Creek (CO)	2,879	2,058	2.27%	226.25	110.27	11.7%	0.09	143
10190004	Clear (CO)	566	389	29.22%	20.53	23.61	7.8%		45
12100301	Upper San Antonio River (TX)	507	409	2.44%	33.97	34.60	13.5%	0.54	33
12040104	Buffalo-San Jacinto (TX)	1,182	829	0.25%	81.00	149.21	19.5%		16
12080005	Johnson Draw (TX)	1,979	1,464	0.65%	22.82	13.71	1.8%		3
12080007	Beals (TX)	608	431	1.94%	0.40	0.38	0.1%		12
12090205	Austin-Travis Lakes (TX)	1,241	925	4.91%	112.00	66.17	14.4%		63
16040101	Upper Humboldt (NV)	2,754	2,345	9.34%	3.71	0.82	0.2%		37

4. Hydrology

The constraints of the project did not allow for the development of detailed hydrologic models (e.g., HEC-HMS; USACE, 2010) for each of the watersheds. Instead, USGS stream flow records and the PeakFQ software (USGS, 2007) were used to estimate peak flows of various return periods for current conditions. The resulting peak flows were adjusted to reflect the additional imperviousness projected for future conditions, with and without GI. This section describes the procedure and assumptions.

4.1. Watershed Characterization

For each HUC8 selected, USGS terrain and stream gage stations, NHDPlus hydrography, STATSGO2 soil data, and NLCD land cover data were used for watershed characterization. The NHDPlus flow direction grids were used to generate streamlines and sub-basins. A typical network of streamlines and sub-basins derived using these datasets is shown in Figure 4–1. In a typical streamline network, streamlines only go between nodes of the network. These streamlines are linked at each confluence following the largest drainage area upstream on the same flow path. The goal of the hydrologic analysis is to estimate peak flows at every point in the streamline network.

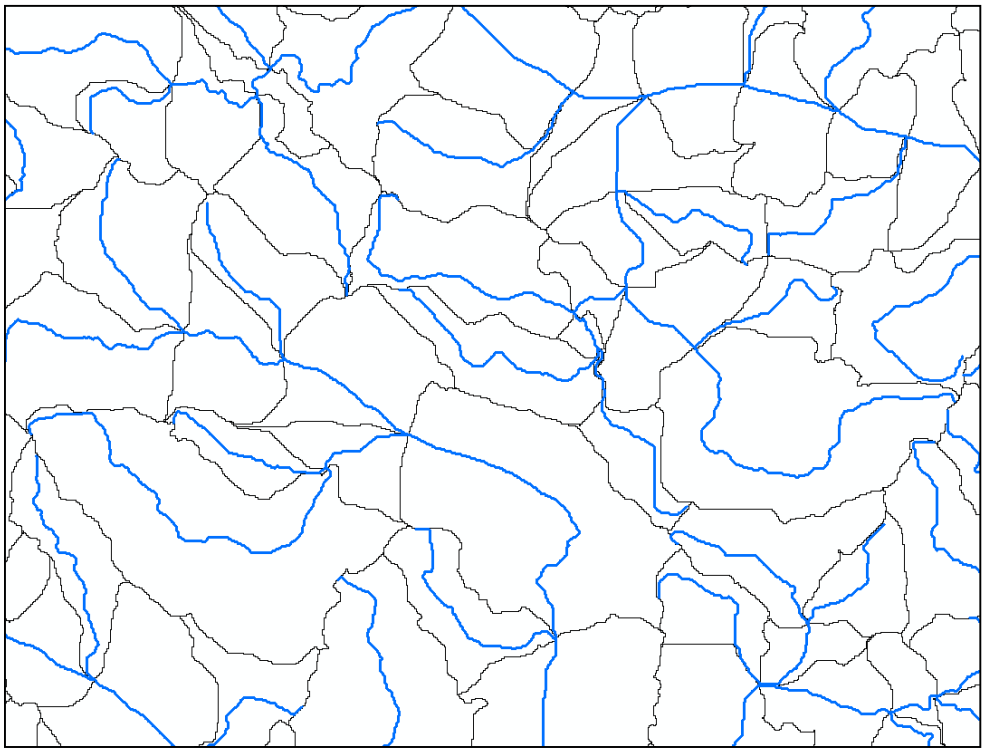

Figure 4–1. Typical sub-basins outlined in thin black and streamlines in thick blue (not to scale).

4.2. Existing Conditions

Available streamflow data from USGS gaging stations was assumed to characterize existing conditions. USGS regression equations are available for numerous locations to generate peak discharges at ungaged locations. However, these equations are complex in most cases and require numerous watershed physiographic inputs that are not amenable for geoprocessing and exceed the level of effort available for this study. Instead, given the constraints of the project, the region-of-influence (RoI) technique (similar to Eng et al., 2005) was used to assign peak flows to ungaged locations along the stream network in the HUC8. RoI is a general designation for approaches that yield a unique regression equation for ungaged sites based on proximal stream gages. The National Streamflow Statistics program (USGS, 2011) has implemented this approach for several states. It is also presented in USGS procedures for rural regression equations for Minnesota and Tennessee (Lorenz et al., 2009).

For a given ungaged site where peak flows needed to be estimated, the peak flow records for all gages within 100 miles were processed through the PeakFQ software (USGS, 2007) to determine the USGS Bulletin 17B discharges for a series of return periods: the 2-, 5-, 10-, 25-, 50-, 50-, and 100-year events. For every location in the analysis, there were on average 50 to 200 gage sites within this radius. The influence of each gage site on the ungaged location is affected by the number of years in the systematic record and the distance between the gage and the ungaged site. Gages closer to the site and with longer records provide more reliable information about the ungaged site. Using this methodology, the RoI technique was used with these flows to develop separate regression equations (one for each event), in which the drainage area is the independent variable. Weighted least-squares regression was used in which the weight for each gage station is equal to the length of the systematic record divided by the square of the distance between the gage and the ungaged site. Weighted least-squares regression reflects the behavior of the random errors in the model by associating weights with each data point into the equation-fitting criterion. The relative magnitude of the weight indicates the precision of the information contained in the observations associated with the gage and determines the contribution of each observation to the final parameter estimates (NIST/SEMATEC, 2012). The main advantage of this procedure over ordinary least-squares regression is the ability to handle datasets in which the data points are of varying quality, which is often the case with stream gages with varying lengths of record. Therefore, gage data closer to the ungaged site and with a longer record of observations are deemed more reliable. Two conditions were imposed to avoid any one gage to exert an excessively large weight in the process:

1. The weight of stations within 10 miles of the ungaged site was calculated with a distance of 10 miles, and
2. The stations with the top ten weights were assigned a weight equal to the tenth largest weight.

The overall effect of these conditions was that no station received a weight greater than 10%.

These weights were used to derive power regression equations of the form $Q = a\ (DA)^b$, where Q is the peak flow (cfs) for a given return period, DA is the drainage area (mi^2), and a and b are constants resulting from the weighted least-squares regression procedure. These equations, one for each return period, were used to estimate flows along the stream network in places where there were no stream gages.

It should be noted that the streamflow records used in the hydrologic analysis to derive peak flows are nonhomogenous, which means that flows in the earlier records are the result of different imperviousness conditions than in recent records. True existing conditions would require an estimation of flows as a result of the current amount and distribution of impervious surfaces. Nevertheless, this is the current practice in estimation of peak flow distribution because historical imperviousness records are generally not available to adjust the records accordingly.

4.3. Approaches to Simulate Future Hydrology

This study involves the large storms associated with flooding events; therefore, the Natural Resource Conservation Service's (NRCS) curve number (CN) methodology is appropriate. The runoff depth for existing conditions is a function of CN and can be calculated using the TR-55 method described in USDA (1986). The equations are

$$V = \frac{(P - 0.2S)^2}{P + 0.8S} \quad (4\text{-}1)$$

$$S = \frac{1000}{CN} - 10 \quad (4\text{-}2)$$

where:

P is the precipitation depth (in)

V is the runoff depth (in), and

S is the potential maximum retention (in)

If $P \leq 0.2S$, then the runoff depth V equals zero. The values for CN range from about 40 to 100, where greater values denote more impervious surfaces. A value of 100 indicates a completely impervious surface where all of the rainfall becomes runoff. Paved surfaces are assigned a CN value of 98. The ability of soils to infiltrate water is characterized by A, B, C, and D designations for the hydrologic soil type, where A soils are the most permeable and D the least. The CN for a given sub-basin is the area-weighted sum of the CN for individual combinations of soil types and land covers.

CN values for existing conditions were estimated using GIS data for soils and land cover. EPA provided estimated coverage of future new development and redevelopment from Integrated Climate and Land Use Scenario tool (ICLUS) modeling and EPA's Office of Science and Technology's development prediction modeling. The GIS land cover layers resulting from this prediction exercise were used to estimate *CN* values for future conditions. The two sets of *CN* values (i.e., for existing conditions and for future development) allow computation of runoff volumes everywhere in a given watershed.

Once the runoff depth is established, the peak flows can be calculated from

$$Q = q_u A V F_p \tag{4-3}$$

where:

q_u is the unit peak discharge (cfs/mi^2/in)

Q is the peak flow (cfs)

A is the watershed area (mi^2)

V is the depth of direct runoff (in), and

F_p is the pond-and-swamp adjustment factor

The Milwaukee Metropolitan Sewer District documented several approaches to adapt the TR-55 methodology to simulate runoff control using GI (MMSD, 2005):

1. Reduce the amount of rainfall by the amount of retention. As an example, if the 80th percentile is removed, the runoff depth would be

$$V = \frac{(P - 0.2S - d_{80})^2}{P + 0.8S - d_{80}} \tag{4-4}$$

   This approach assumes that a given amount of rain never reaches the ground, which seems reasonable; however, the nature of the TR-55 equations does not allow for an exact water balance[1].

2. Compute the hydrograph produced by the storm and remove the initial portion such that its volume is equal to the volume retained by GI controls. This approach assumes that the GI controls are effective only at the beginning of the storm and that the retention takes place as if an in-line storage facility exists at the downstream end of the drainage area, just before the

[1] This shortcoming is better illustrated with a numerical example. For the conditions without GI, assume that the rainfall depth is *P*=4 in and *CN*=75; therefore, Eqns. 4-1 and 4-2 yield *V*=1.7 in. If the rainfall is reduced by 0.9 in. to account for GI, that is *P*=3.1 in., and *CN* remains the same, then application of the same equations yield a runoff depth *V*=1.0 in for the conditions with GI. It follows that the captured volume is 1. 7 in – 1.0 in = 0.7 in., which is not equal to 0.9 in. The discrepancy becomes smaller as the rainfall depth increases; for instance, if *P*=9.9 in, then the captured depth is 0.8 in., which is closer to 0.9 in.

outlet. The removed volume must extend past the peak for an impact to be noticeable, which is not reasonable for two reasons. The first is that GI controls are expected to work throughout the duration of a storm, even if excess runoff bypasses the controls. The second is that the controls are spatially distributed upstream of the outlet and thus it is sensible to expect that the retention will reduce the peak flows to some degree even if relatively small runoff volumes are retained.

3. Scaling of the peak flows by the ratio of runoff depths. The approach follows the principle that peak flows are directly proportional to the depth of runoff (Eqn. 4-3), which is expressed as

$$Q_{2040} = Q_e \frac{V_{2040}}{V_e} \quad (4\text{-}5)$$

where:

Q_{2040} is the future peak flow at a given location in the watershed including the effect of new development and redevelopment in 2040,

Q_e is the existing peak flow from the stream gage record analysis,

V_{2040} is the runoff depth in 2040, and

V_e is the runoff depth for existing conditions.

As expressed in Eqn. 4-5, if the peak flows and corresponding runoff depth are known for existing conditions, and the runoff depth can be estimated for a future condition, then the future peak flows are equal to the current peak flows multiplied times the ratio of future runoff depth to current runoff depth. This option assumes that A, F_p, and q_u in Eqn. 4-3 remain constant. Appendix D discusses the applicability of this assumption.

4. Reduction of the runoff depth by the amount of retention. As an example, for the case of retaining the 80th percentile this approach is equivalent to

$$V_{GI} = \frac{(P - 0.2S)^2}{P + 0.8S} - d_{80} \quad (4\text{-}6)$$

where V_{GI} is the runoff depth with GI. This modified depth would need to be converted into a hydrograph to determine the new peak flows. This approach is the most consistent with the intent of GI and how to simulate it using hydrologic models based on the TR-55 methodology such as HEC-HMS. However, the commonly used models do not allow for this computation.

5. Adjustment of the CN so that the resulting runoff is equal to the original runoff minus the GI retention depth. This is computationally equivalent to using the depth resulting from Eqn. 4-6 to back-calculate a modified value of S from Eqn. 4-1 and subsequently an adjusted value of CN from Eqn. 4-2 (Medina et al., 2011). This approach has the effect of making the

watershed more pervious, which is the intent of GI controls. It produces an exact water balance and represents the GI controls operating throughout the duration of the storm.

The following sections describe the process selected to simulate future peak flows with and without GI.

4.4. Future Conditions Without GI

In 2040, the end of the study period, new development and redevelopment will increase the amount of impervious surfaces and thus, the depth of runoff generated as well as the peak flows. For the analysis, the future volume of runoff without GI was estimated as described in Section 4.3 and Option 3 was applied to estimate the peak flows based on the ratio of runoff depths as expressed by Eqn. 4-4, in which V_{2040} and Q_{2040} are respectively the runoff depth and the peak flow in 2040 without GI. The result is a set of modified peak flows at any point in the drainage network.

Because future development is expected to increase impervious surfaces, future runoff without GI will be greater than for existing conditions. Therefore, as expected, peak flows in 2040 without GI also will be greater than for existing conditions.

4.5. Future Conditions With GI

The effect of GI was simulated using Option 4, that is, by subtracting the depth of the retention standard from the future runoff generated by a given storm. For every storm simulated, the future runoff depth without GI was computed as described in the previous section, and the retention depth was subtracted as expressed in Eqn. 4-6 to yield the future runoff depth with GI. For the "medium" scenario, the runoff depth after GI implementation was estimated as

$$V_{GI} = V_{2040} - d_{90} \quad (4\text{-}7)$$

for new development, and

$$V_{GI} = V_{2040} - d_{85} \quad (4\text{-}8)$$

for redevelopment, where d_{90} and d_{85} are respectively the 90th and 85th percentile depths to be retained on site by the GI controls. Appendix D presents details on the runoff calculation methodology.

The assumption implies that a system of stormwater controls distributed on urban development areas in a watershed are sized and deployed to remove this amount of water from direct runoff. The controls are assumed to capture a portion of the runoff generated from the entire developed site, not just from the impervious areas. The captured runoff will be infiltrated, evapotranspired, or harvested for irrigation or other uses; the specific configuration of the stormwater controls deployed is not

germane to this study. Excess water will bypass the controls and reach the streams as direct runoff. This assumption is valid for the extreme storm events that are likely to cause flooding because the removed runoff will arrive to the stream as interflow much later than the peak of direct runoff.

After estimating the future runoff depth with GI, Option 3 was used again to modify the peak flows.

$$Q_{GI} = Q_{2040} \frac{V_{GI}}{V_{2040}} \quad (4\text{-}9)$$

where V_{GI} and Q_{GI} are the runoff depth and the peak flow with GI implementation in 2040.

Because future runoff with GI is less than without GI, Eqn. 4-9 indicates that peak flows in 2040 with GI will be smaller than without GI, as expected.

The result after application of this process is a set of peak flows at various locations along the stream network that are representative of the conditions expected in 2040 with GI; that is, with GI retention across the newly developed and redeveloped areas.

5. Flood Hazard

The flood hazard is determined through a hydraulic analysis to derive the flood elevations caused by the peak flows developed in the hydrologic analysis, for both the conditions with and without GI implementation. The hydraulic analysis uses the streamlines and drainage areas described in the previous chapter.

5.1. Hydraulic Modeling

Using the discharges estimated during the hydrologic analysis and the streamlines, hydraulic models were constructed and floodplains generated for each return period. The hydraulic model used was RFD (Rapid Floodplain Delineation), a program developed by Atkins used in numerous FEMA flood studies, which generates hydraulic backwater models and floodplains at very high speed. RFD incorporates a number of techniques to facilitate automated modeling. RFD can automatically generate cross-sections, perform a backwater calculation, and delineate a floodplain in a single step.

RFD can perform backwater calculations using its own computation engine or utilize HEC-RAS. In this study, the RFD computation engine was used rather than HEC-RAS, because the latter is too slow for the high-speed modeling required. The computed water surfaces between the two methods are nearly identical in almost all cases (Exhibit 5-1). RFD has been utilized as the sole modeling and delineation tool in well over 15,000 miles of FEMA floodplain studies (with the HEC-RAS computation engine used). All FEMA Flood Insurance Studies (FISs) must meet strict guidelines and specifications (FEMA, 2009a). The data has been provided to multiple state agencies, and Minnesota and Michigan have explicitly approved the use of RFD in their states. For example, the Minnesota FISs for Douglas County (FEMA, 2009b), Mille Lacs County (FEMA, 2013b), Rice County (FEMA, 2012), Steele County (FEMA, 2011a), and Todd County (FEMA, 2011b) were all performed with RFD.

In addition to floodplain polygons, RFD also produces depth grids, which are needed for the loss estimation phase of the analysis described in the next chapter. For the base topography for the models, the entire 1/3 arcsecond (approximately 10-meter) NED for the continental United States was employed. RFD is able to utilize this topography in native format.

The result of the hydraulic analysis was one set of RFD models and the corresponding depth grids for each return period modeled (2-, 5-, 10-, 25-, 50-, and 100-year) for both with- and without-GI conditions, for each of the 20 HUC8 watersheds. Figure 5–1 shows a typical depth grid that results from the RFD run for a given return period; the colors in the legend indicate the variation of flood depths. While the NED resolution is approximately 10 meters, the grids are not square as the dimensions vary with latitude; therefore, the depth grids were re-sampled to obtain 8-meter square cells to facilitate input into Hazus.

As part of the development of flood maps for the California Department of Water Resources (DWR, 2013), Atkins conducted a study in Calaveras County to compare the RFD backwater computational engine with HEC-RAS. The comparison involved 303 hydraulic models with a total of 48,146 cross sections. The water surface elevations from both models were compared for each cross-section. The average absolute difference in computed water surface elevation was 0.00005 feet across the 48,146 cross sections. The 99th percentile of the absolute differences was 0.026 feet, meaning that 99% of the cross-sections had water surfaces elevation differences of less than 0.026 feet. Some of this variation may not be due to computational differences, but to the removal and filtering of points that HEC-RAS performs. HEC-RAS cross-sections are limited to 500 station-elevation points; therefore, some cross-sections had points removed out to accommodate this maximum. RFD has no such restriction. (Source: California Department of Water Resources, Awareness Floodplain Maps. http://www.water.ca.gov/floodmgmt/lrafmo/fmb/fes/awareness_floodplain_maps/)

Exhibit 5-1. A test case comparing water surface elevations from RFD and HEC-RAS.

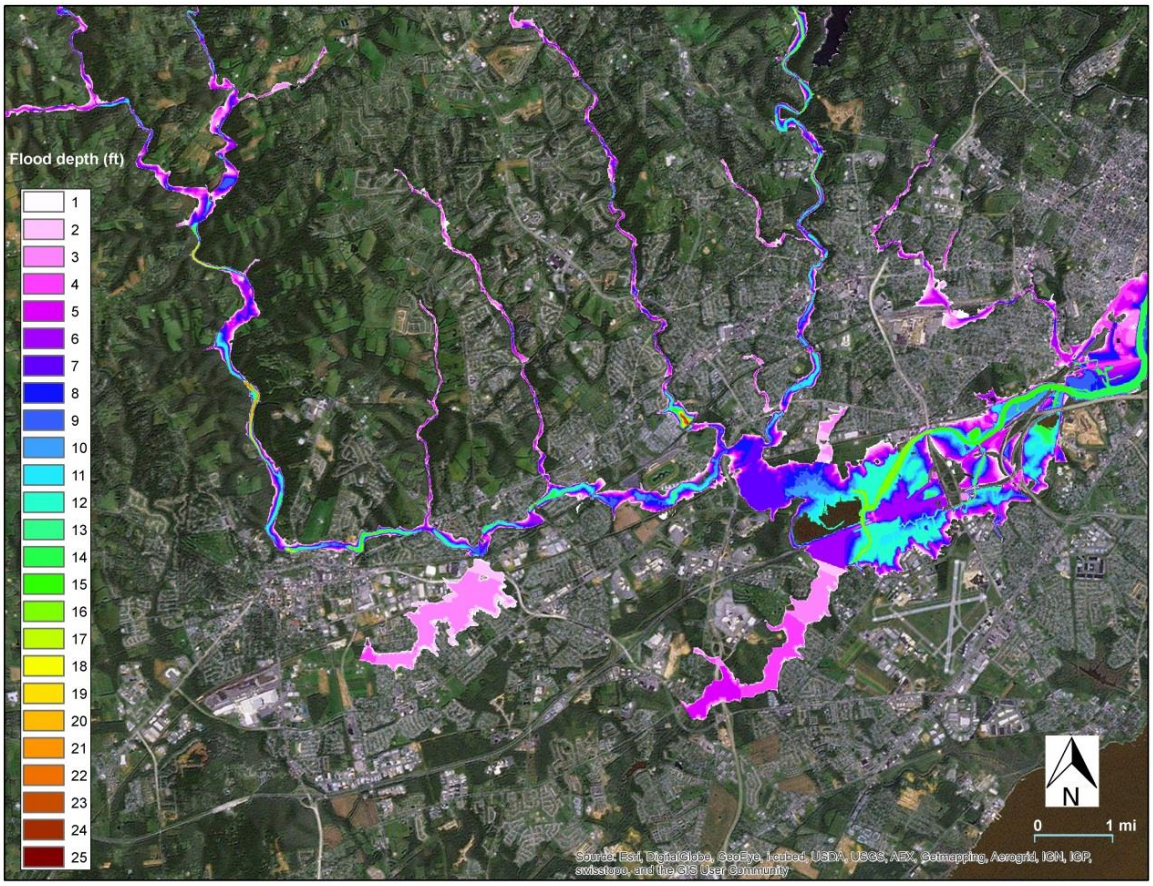

Figure 5–1. Example of a RFD depth grid, Brandywine-Christina River HUC8, Delaware.

Several assumptions were necessary to enable a study at such large scale within the constraints of the project. While the effect of these assumptions could over- or under-estimate the flood losses, it is important to keep in mind that this study looked at the "difference" between two conditions given the same set of assumptions for both the GI and non-GI scenarios. Therefore, the absolute value of flood losses is less important than the differences between the scenarios. The most salient simplifying assumptions are as follows:

- *Stream crossings:* No site-specific information was included regarding the geometry of bridges, culverts, and other stream crossings. Stream crossings can restrict flow, capture fallen trees and other debris during a flood, and worsen flooding upstream of the structure, while lessening the flood hazard downstream. Neglecting these structures underestimates flood depths upstream and overestimates them downstream of a given location.
- *Levees, dams, diversions*: While the effects of flood control structures were considered in the 20 HUCs modeled to prevent overestimation of losses, no national information was available to take into account the effect of levees, dams, diversions, and other flood control measures in the scale-up. These assumptions and their effects were considered to some degree as will be discussed in the next chapter. These structures would reduce flood hazards; therefore, the RFD-modeled flood depths can be worse than in reality.
- *Channel geometry:* The cross sections were defined using the NED, which typically does not include bathymetry; therefore, the definition of the main channel of the streams is limited to the terrain that was not underwater when the topographic data was acquired. This assumption results in less conveyance in the stream network, which forces water that otherwise would stay in the main channel to spill onto the floodplain. Therefore, the assumption may make flood hazards appear worse, especially for the less severe events such as the 2-year flood.
- *Channel roughness*: The Manning's roughness coefficient *n* was set to a uniform value of 0.05. Roughness coefficients depend on many stream characteristics including the material in the bed and banks, the type and density of vegetation in the channel and the floodplains, the sinuosity of the stream, and other factors that create resistance to flow (Chow, 1959). Usually, determination of the roughness coefficient requires a visual assessment of these factors, which is beyond the scope of this project. Instead, the photographs in Barnes (1967) suggest that a value of 0.05 applies to a wide range of stream conditions and is suitable for the scale of this study. For example, the California DWR used this value for their Awareness Floodplain Mapping program, which employed a similar level of modeling to develop flood hazard information for nearly 6,700 miles of streams (DWR, 2013).

5.2. Effect of Flood Control Structures

Most large watersheds in the United States have undergone some type of major hydraulic modification for flood control or water supply, for example, levees, dams, pump stations, and diversions. Dam data are maintained by the USACE in the NID, which has restricted access. Levee data are available in the NLD, also maintained by the USACE; most but not all levees in the United

States are included in this database. No national datasets exist for diversions, pump stations, or other flood control works. Site-specific plans or regional or state information are the only source of information for these projects. For this type of large scale analysis, it is not possible to include the detailed information associated with these structures, nor their operation rules.

The approach selected to take into account the flood protection that these hydraulic structures provide is to assume that they prevent losses for all flood events, both with and without GI. In the case of dams, this assumption means that areas below the dam do not benefit from the effects of GI applied upstream of the dam. This assumption is conservative because the reduced runoff volume upstream of the dam would result in lesser flows below the dam. In the case of levees, the approach implies that all areas behind a levee experience no damages; this assumption effectively removes all of these areas from the benefit calculation. Nevertheless, in reality damages can occur from flooding due to interior drainage on the landward side of the levees, which can results in high costs associated with pumped drainage systems; therefore, this assumption is conservative because GI would lessen the flood potential from interior drainage.

Diversions are handled similarly to levees. The protected area is entirely removed from the damage calculation. For example, the diversion tunnels in San Antonio, Texas protect the city up to the 100-year flood level. Figure 5–2 shows the layout of the tunnel system and the effect of the assumption on the floodplain. The RFD model predicts floodplains between the inlet and outlet of the tunnels because the model has no information about the conveyance of the diversion system. To take into account the flood protection afforded by the tunnels, the crosshatched areas are eliminated from the damage computation. Therefore, GI does not accrue any benefit in those areas for any of the flood events.

5.3. Downstream Effects

Runoff that is retained within a given watershed will lead to less runoff reaching downstream watersheds. However, due to modeling constraints, the effect of retaining runoff is confined to each HUC8 where the modeling is performed. Therefore, the modeling approach underestimates flood losses avoided in a given watershed because it does not consider the cumulative effects of GI applied in upstream watersheds.

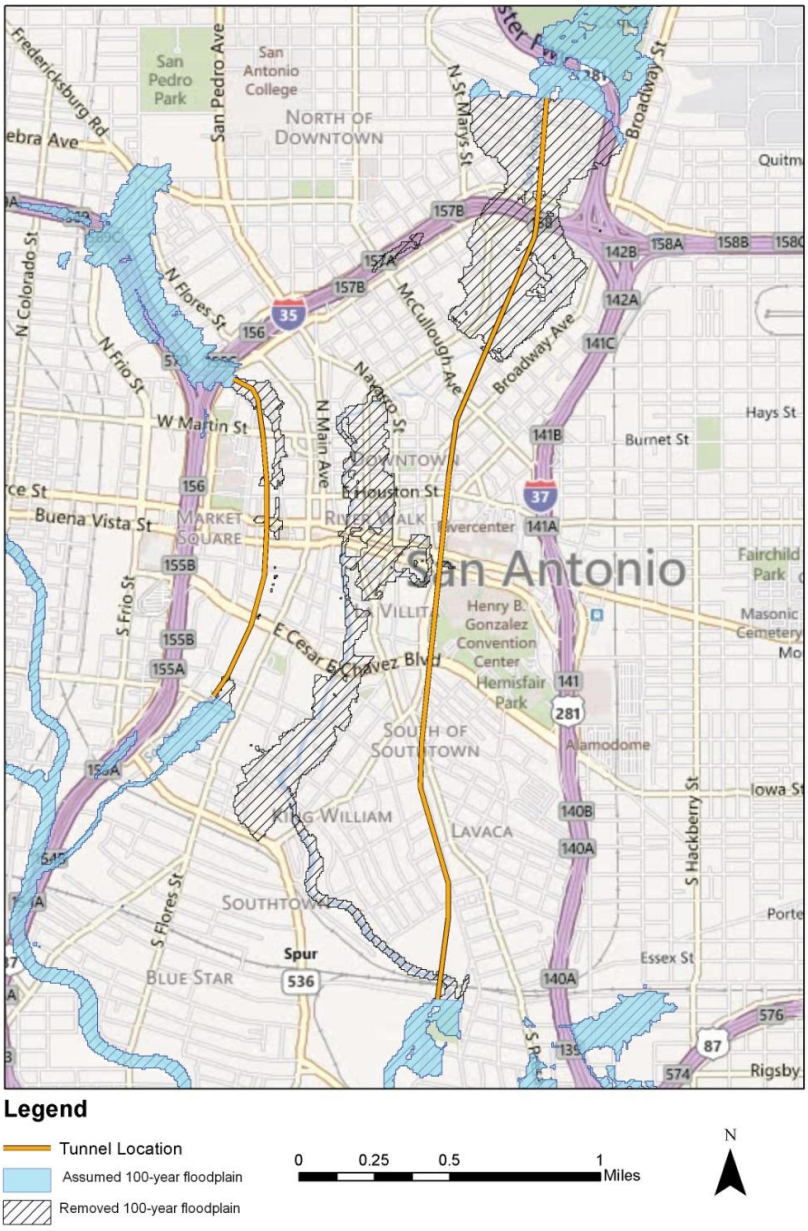

Figure 5–2. Diversion tunnels in the City of San Antonio, Texas, and effect of the flood protection assumption on the 100-year floodplain.

5.4. Floodplain Area Reduction Due to GI

The hydraulic analysis yields water surface elevations from which several derivative variables can be calculated, for example flood depths such as those illustrated in Figure 5–1. A global variable that illustrates the effect of GI is the impact on reducing the extent of floodplains. Figure 5–3 summarizes this effect for all 20 HUC8 watersheds and for various return periods. The floodplain reduction is

calculated as the difference between the total floodplain area for each HUC8 without GI, minus the floodplain area with GI, and divided by the total floodplain area without GI.

The figure shows the expected behavior that the effect of GI becomes less pronounced as the return period of the flood event increases. Because the GI retention depth is of the order of one to two inches, this amount of water represents a greater fraction of the depth of a small, frequent storm than for a severe, infrequent event.

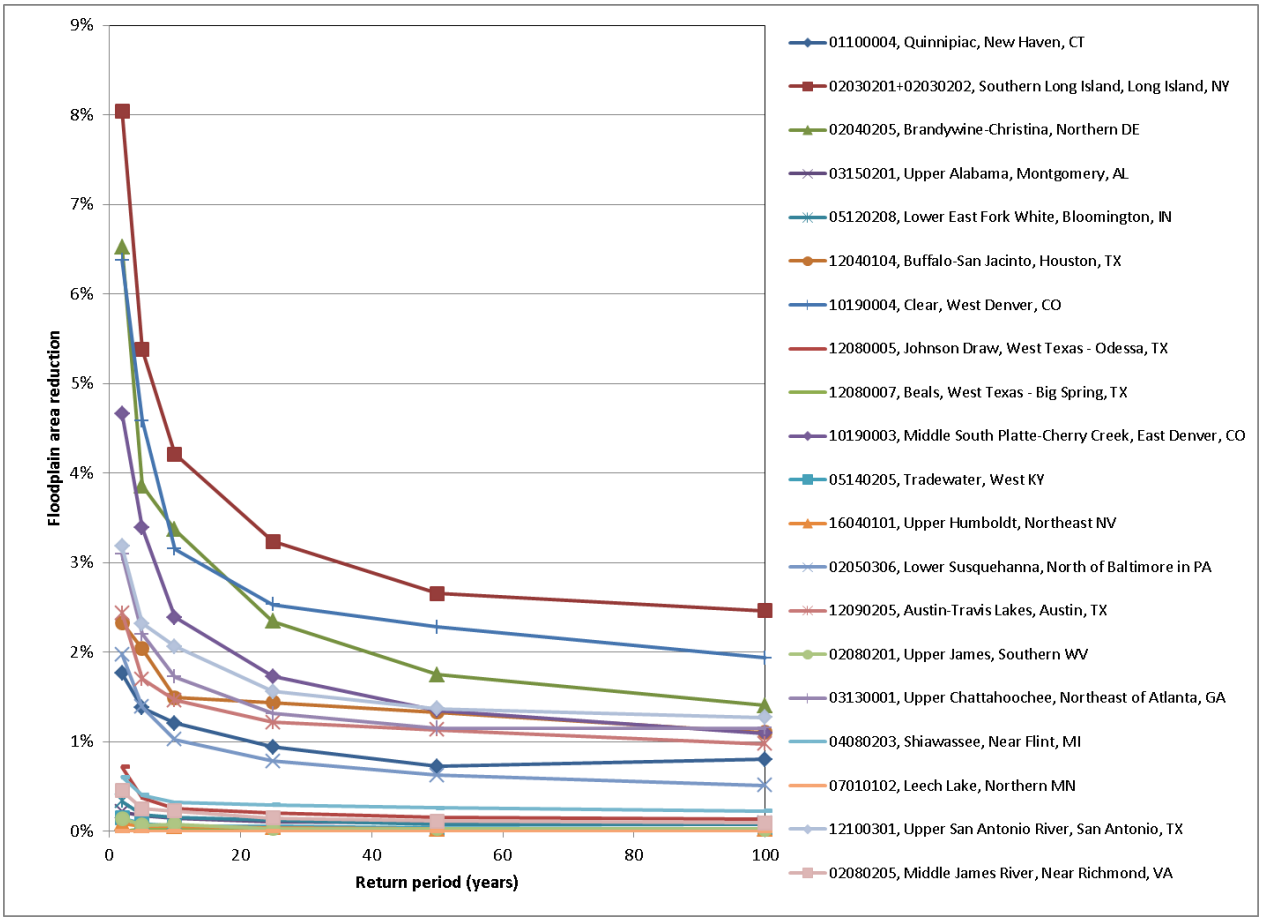

Figure 5–3. Reduction in the floodplain area due to implementation of GI for 20 HUC8 watersheds for various return periods.

6. Loss Estimation

Loss estimation was conducted using the Hazus software (FEMA, 2013a). Built on a Geographic Information System (GIS) platform, Hazus is a public domain application used by FEMA and other emergency management organizations to estimate potential losses associated with natural disasters. The methodology in Hazus enables estimates of physical, economic, and social impacts of earthquakes, hurricanes, and floods. Physical damages include the cost to replace or repair residential and commercial buildings, and other infrastructure; economic losses include lost jobs and business interruptions; while examples of social impacts include shelter needed, displaced households, and debris amounts. This study focused only on damages to buildings, to their contents, and the associated economic losses. Additional information on Hazus can be found in www.fema.gov/hazus.

Hazus can use detailed, watershed-specific inventories, or Census 2000 data to develop the value of assets within each HUC8. Census 2010 data are not yet available in Hazus. Therefore, this study used the Census 2000 datasets that contain values of residential, commercial, and industrial assets divided into structural and contents components for several types of land uses that include single-family residential, multi-family residential, commercial, and industrial. Hazus can also consider crop losses, and with supplementary data, critical facilities such as hospitals, roads, and power plants; however, this study did not include these components because there were no national databases available. Therefore, this study underestimates losses avoided on this account.

Some explanation is needed for the basis of the dollar figures to be presented subsequently. Hazus's damage output is expressed in 2006 dollars. Furthermore, this study takes a snapshot in time in 2040 and thus calculates the flood hazard based on the hydrology for the level of development expected in 2040. Therefore, the charts that follow depict monetary values in 2006 dollars resulting from 2040 hydrologic conditions. Two adjustments will be applied later in the study to resolve these date differences. In the first one, the dollar values are modified to reflect the expected additional construction value in 2040 as will be explained later in this report. In the second, all dollar figures are baselined to 2011 dollars, which is the year EPA selected for presentation of the benefits.

Hazus can calculate damages using full replacement or depreciated replacement values. For economic analyses, the common practice is valuation using depreciated replacement value, which accounts for the remaining useful life of the assets before they were damaged. However, this study used full replacement value principally because of data limitations in the new construction forecast available for the target year of 2040, which did not consider depreciation. Inclusion of depreciation is complex and uncertain because assets would be built at various times; therefore, the depreciated value in 2040 would depend on when construction took place and the useful life of assets. This type analysis was beyond the scope of this study. However, the method used allows a contrast between the with- and without-GI conditions.

Losses are calculated using depth-damage curves that relate depth of flooding, as measured from the top of the first finished floor, to damage expressed as a percent of replacement cost of the building. The replacement value includes the structure; architectural, mechanical and electrical components; and building finishes. Similar curves exist for building contents. An example of a damage curve is shown in Figure 6–1. These curves originate from several sources, including flood loss claims by the Flood Insurance Administration (FIA) (now the Federal Insurance & Mitigation Administration, FIMA) and various studies nationwide by the USACE. The vulnerability curves are coded in Hazus for the set of occupancy classes listed in Appendix E. For the general building stock used in the analysis, Hazus applies default heights above grade to the top of the first floor, for each of the foundation types associated with the standard occupancy classes (FEMA 2013a).

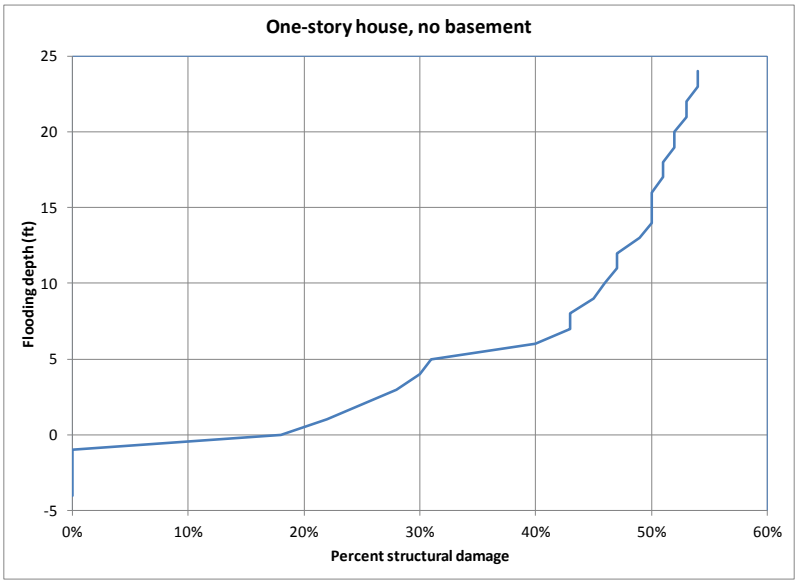

Figure 6–1. Example of a depth-damage curve.

6.1. Estimation of Avoided Flood Losses

For each watershed, loss estimation is performed for the six return periods, which produces a damage frequency curve that relates monetary damages to the return period. More severe flood events cause greater damages. For example, Figure 6–2 shows this relationship for the Upper San Antonio and Middle James HUC8 watersheds for the damages expected in 2040 without GI implementation.

Another common way to present this information is in terms of the exceedence probability, which is equal to one divided by the return period. For example, the 2-year event has a 50% probability of being equaled or exceeded on average in any given year. Figure 6–3 shows this representation, which depicts the typical behavior of increasing damages as the probability decreases. Large damages are the result of a rare severe event and therefore, have a low probability of being exceeded.

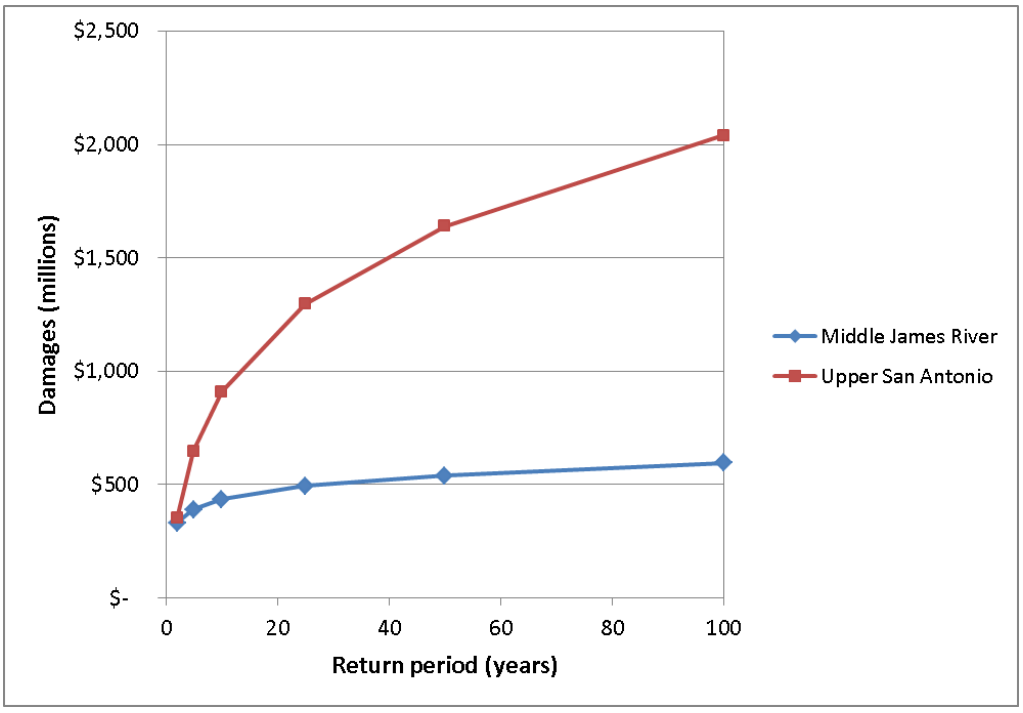

Figure 6–2. Examples of damage curves for two watersheds (2040 conditions without GI, 2006 dollars).

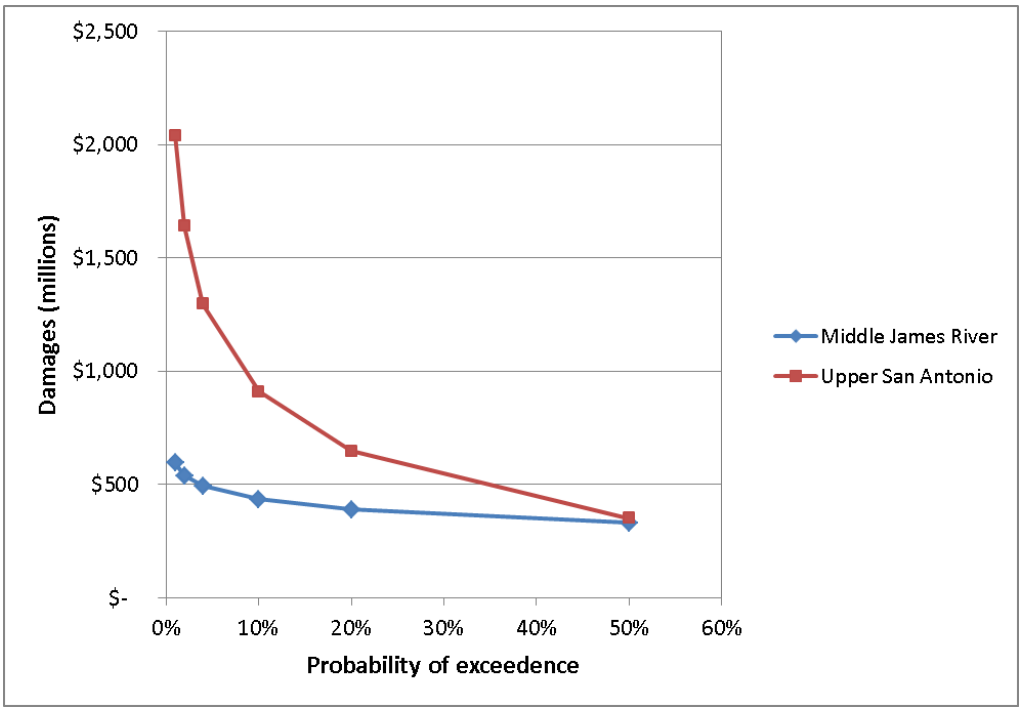

Figure 6–3. Examples of damage probability curves for two watersheds (2040 conditions without GI, 2006 dollars).

The area under each curve in Figure 6–3 is the expected value of the damages, which in this report is termed the average annualized losses (AAL). The computation of this area has the effect of weighting the damages by their probability.

Damage curves with and without GI were developed for all of the 20 HUC8s. The difference between the damages without GI and those with GI are the flood losses avoided, which are equal to the benefits of GI. These benefits can be represented by the average annualized losses avoided (AALA), which is equal to the AAL without GI minus the AAL with GI.

6.2. Zero-Damage Thresholds

Figure 6–2 and Figure 6–3 were constructed assuming that events less severe than the 2-year flood produce no damages anywhere in the watershed. In actuality, flood losses are highly dependent on the location of assets with respect to the flooding source and on measures to protect the assets against flood damage. Therefore, damages may begin to occur at different degrees of flood event severity. On a low order stream, flood waters may enter the floodplain at the 1- or 2-year event; but the damages will be nil if no assets are within those floodplains. Conversely, there could be valuable assets at risk near a river but local flood control works may prevent damages for all but the most extreme events.

The concept of a threshold where damages begin to occur is critical to this study because an important assumption in Hazus is that the value of assets is uniformly distributed in a given Census block. This approximation has a significant impact on the loss estimation. If a block includes the stream channel, the value of assets in the channel itself or the immediate vicinity should be zero because no structures exist in the middle of the stream. However, the uniform distribution of assets could place some dollar value in these areas thereby overestimating the damages. The fact that flood depths are the greatest in these areas compounds the overestimation effect.

The solution to this shortcoming is to use detailed structure information, which includes geographic coordinates, elevation of the first floor, type of structure, and replacement value of the building and contents. However, this information resides in municipal tax assessors' offices and is not available as a public dataset. Therefore, it was necessary to formulate an approximate approach to the problem. The solution used is to assume that a flood of a given return period does not cause any damages because there are no exposed assets within that floodplain. The rationale is that areas that flood often would not be developed or would have assets with low value. For some smaller streams, there may be no assets in the 2-year floodplain, whereas with larger streams and rivers land within the 10-year floodplain may have no assets exposed. In actuality, there are always some assets exposed to flood risk; for example, a minor flood event can close roads, wash out foot bridges, or cause sewer backups in homes. Therefore, some monetary damages are expected to occur. But the concept of a "zero-damage" threshold is plausible as a means to account for the damage

overestimation. This study evaluates three threshold options under which the AALA was calculated for each HUC8:

1. No assets exist in the 2-year floodplain (2-year zero-damage threshold)
2. No assets exist in the 5-year floodplain (5-year zero-damage threshold)
3. No assets exist in the 10-year floodplain (10-year zero-damage threshold)

The purpose of each of these assumptions is to assign zero damages to the corresponding flood and to less severe events. This effect was accomplished by numerically setting zero flood depths in the respective floodplains. Figure 6–4 is a representation of a hypothetical "actual" situation in which there are assets at risk within the 25-year floodplain (Building A) but not within the 5-year floodplain. Therefore, damages are zero for the 5-year event and nonzero for the 25-year event. Figure 6–5 represents the zero-damage threshold approximation under option 2 above. Building B is not actually in the 5-year floodplain but Hazus' uniform distribution assumption places some value at risk at that location. To ensure that no damages occur during the 5-year event as in the "actual" situation, the assets are redistributed so that the entire value of the block is placed on Building A, and zero flood depths are assumed within that 5-year floodplain. For the 25-year event, damages arise only from areas where the flood depth is not zero, in the fringe between the 5- and the 25-year floodplains.

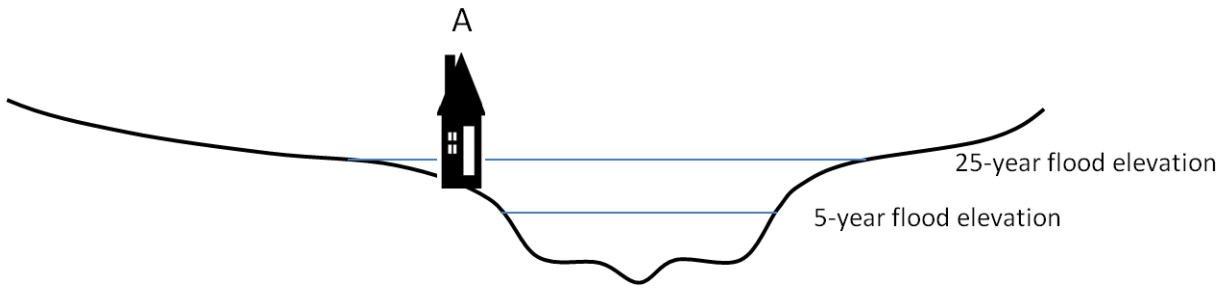

Figure 6–4. Hypothetical "actual" situation. Assets are at risk only within the 25-year floodplain.

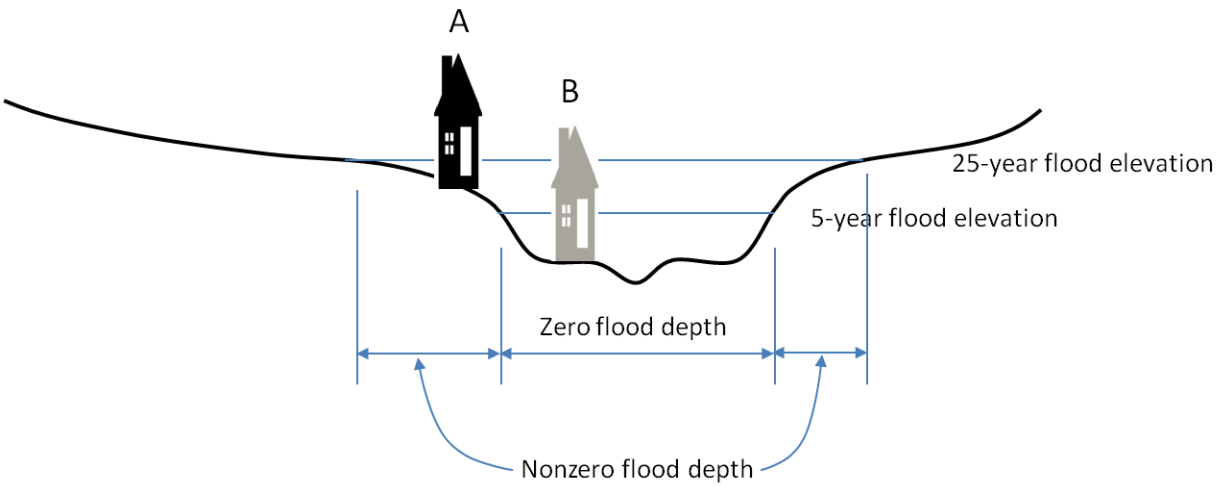

Figure 6–5. The uniform distribution in Hazus may place assets at risk in the 5- and the 25-year floodplains.

As mentioned above, the actual threshold at which damages begin to occur depends on the location within the watershed; for example, for a given flow in the river, floodwaters may enter some portions of the floodplain but not others depending on localized characteristics of the stream channel. The publicly available datasets used in this analysis do not have sufficient detail to consider this kind of variability; therefore, the three zero-damage threshold options are an approximation to account for the fact that certain areas around floodprone streams do not contain valuable assets. Chapter 7 will show that this assumption is conservative and that there can be assets exposed to relatively frequent flood events.

In the subsequent discussion the term "zero-damage threshold" will be used to denote each of the three scenarios above. For example, the "5-year zero-damage threshold" indicates that within the 5-year floodplain the original depth grids resulting from the hydraulic model are set to zero; therefore, only the flood depths outside this zero-damage threshold are nonzero. The result is that flood depths will be nonzero for the 10-, 25-, 50-, and 100-year events in the fringe between those floodplains and the 5-year floodplain. For the 2- and the 5-year events, the flood depths are zero everywhere because they are fully covered by the 5-year zero-damage threshold.

Application of the three zero-damage thresholds provides some insight into the range of possible losses, which affects calculation of the avoided losses benefits. The use of thresholds dramatically reduces the damages from the default Hazus estimates that do not assume a zero-damage area around the streams. The typical effect is shown in Figure 6–6 that depicts the losses with GI for the Upper Chattahoochee HUC8. As expected, the 10-year zero-damage threshold produces the fewest losses because it assumes the largest no-asset area. Figure 6–7 shows the comparison of losses avoided and exhibits a similar behavior in which the 2-year zero-damage threshold yields the most benefits and the 10-year the fewest. As in the case of the losses, the zero-damage thresholds markedly reduce the benefits with respect to the original Hazus estimates.

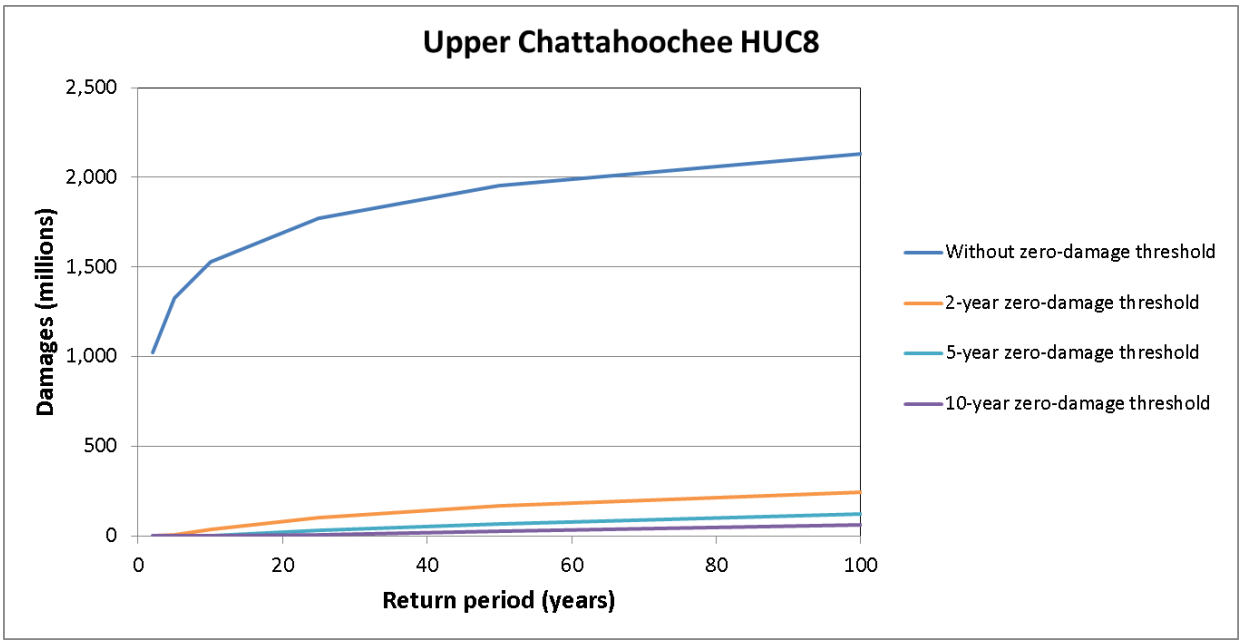

Figure 6–6. Comparison of the flood damages as a function of the return period, with and without zero-damage thresholds (2040 conditions, 2006 dollars).

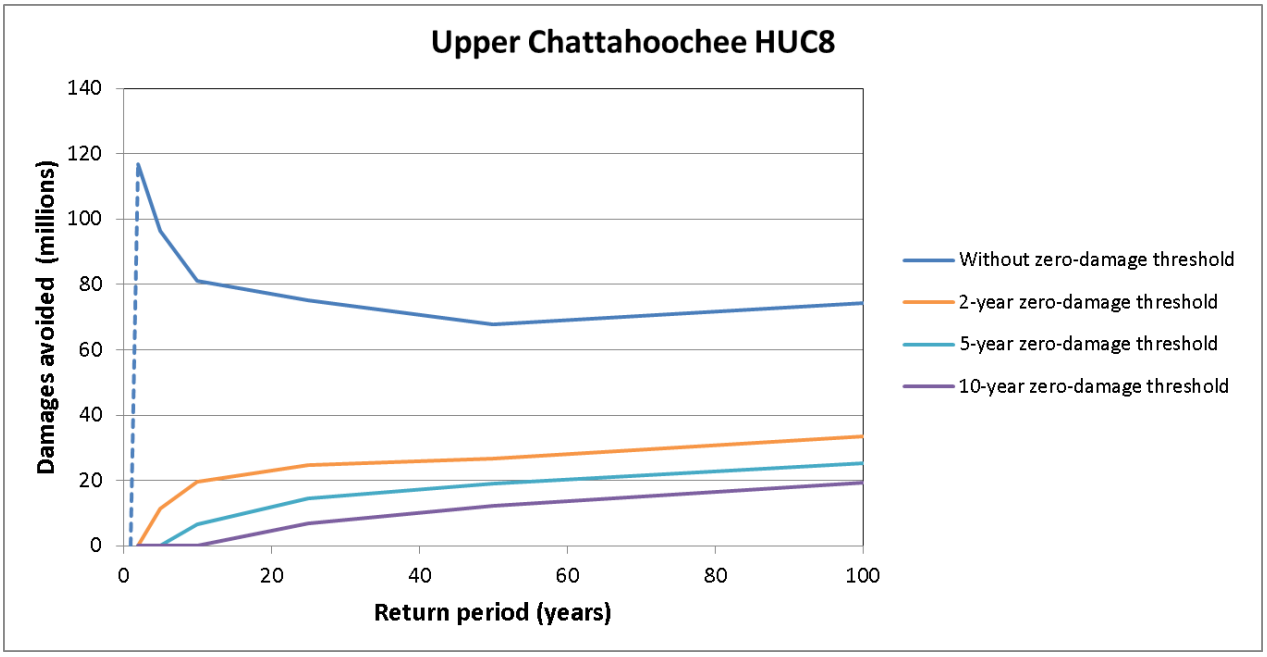

Figure 6–7. Comparison of the damages avoided as a function of the return period, with and without zero-damage thresholds (2040 conditions, 2006 dollars).

The assumption of the zero-damage threshold also affects the shape of the curves in Figure 6–7. The impact of GI in reducing damages depends on several factors. First is the volume of the retention scenario with respect to the volume of rain associated with an event. For a specified capture depth, a greater fraction of the 2-year storm is retained than of the 100-year storm. This rationale supports the expectation that GI would have the greatest benefit for the more frequent flood events and is the general behavior that Figure 6–7 exhibits for the uniformly distributed assets in the default Hazus estimate without a zero-damage threshold (blue curve).

However, a second and more influential factor is the actual value and location of the assets at risk. For a given capture depth, areas with more valuable assets will benefit more from GI than other areas in the same general vicinity but with assets of lesser value. The effect of the zero-damage thresholds is to remove the swath of assets closest to the flood hazard. Therefore the benefits of GI shift to the fringe areas outside the zero-damage thresholds. The result is that benefits increase with the return period, which seems counterintuitive in light of the previous paragraph. In reality, all curves exhibit a similar behavior in which the benefits reach a maximum and then decrease. In the case of the default Hazus estimate with no zero-damage threshold, the dashed blue line in Figure 6–7 represents the rise to the maximum that is expected between zero benefits for events so small that never leave the stream channel (and thus do not benefit from GI) and the first modeled event, the 2-year flood. For the results with the zero-damage thresholds, the largest event modeled was the 100-year flood but it is conceivable that as the magnitude of the events increases beyond this extreme event, the retained volume will be too small compared to the rainfall depth to make a difference and the benefits will be nil; therefore, all benefit curves will drop to zero for very high values of the return period.

6.3. Vulnerability of New Construction

An important consideration is the expected vulnerability of existing and new construction to floods. In an ideal world, construction would comply with local floodplain regulations that, at a minimum, follow the FEMA National Flood Insurance Program (NFIP). The regulations state that, to be eligible for flood insurance, a building within the FEMA-mapped 100-year floodplain must have the top of the first floor above the water surface elevation of the 100-year flood at that location. In principle, that building would not suffer damages during events less severe than the design standard. This expectation would imply that the value of construction, particularly new construction, should not be included in the calculations. However, other factors suggest that existing and new construction will not be free of flood risk:

- The vast majority of streams in the United States have not undergone FEMA flood studies. Out of approximately 3.5 million stream miles (EPA, 2014) only 1.1 million are part of FEMA flood insurance studies (FEMA, 2014). Therefore, building codes in unstudied streams are often not based on reliable flood hazard information.
- Building codes underestimate flood risk. In most communities, floodplain regulations are based on maps developed for flood insurance purposes that estimate the current level of risk

when the flood study is conducted. Very few communities regulate floodplain activities using future hydrology. Therefore, the elevation of structures may not be adequate for future levels of risk as imperviousness increases or other watershed characteristics change.

- Flood maps are updated on a five-year cycle but often the engineering studies (hydrology and hydraulics) that characterize the hazard data are not updated that often. If the hazard data is found to be outdated, the study still has to wait, sometimes as long as five more years, for adequate funding to redo the engineering and remap the flood hazard. Therefore, the design standards can lag behind the risk by several years.
- Even if the living space is above the 100-year flood, there are damages that accrue to properties and public infrastructure, in addition to business disruption, emergency response, basements, and post-storm cleanup.
- In many communities, regulations allow for placement of fill in the floodplain so long as it does not result in more than one foot increase in the flood water surface elevation. Thus, even if there is no increase in imperviousness in the upstream watershed, the placement of fill could raise the water surface up to one foot in the future. Structures built to be compliant at the time of construction eventually become non-compliant, even without any additional development in the upstream watershed.
- Current floodplain mapping accuracy compliant with FEMA standards is in the range of one foot to two feet, at best. Yet, exposure to flood hazard at a given structure is determined at the tenth of a foot. Therefore, even with state-of-the-art technology, flood hazard could be underestimated.
- Flood insurance studies do not consider sea level rise, changes in the local historical rainfall pattern, dam breaks, levee failure, stream channel meandering, deposition of sediment, collapsing embankments, trees or other debris that may lodge in stream crossing structures during a flood creating backwater, or localized urban flooding, all of which are expected to increase damages in many urban areas. Increased runoff may exacerbate some of these factors.
- Many damages occur outside the mapped 100-year floodplain. In particular, so-called "urban flooding" occurs largely outside mapped floodplains where runoff overwhelms the drainage system. While this is not a widely studied issue, one study in Illinois found 90% of urban flooding damage claims from 2007 to 2014 to be outside the mapped floodplains (Illinois Department of Natural Resources, 2015). The study documented in this report did not address urban flooding, which underestimates the losses and avoided losses.

For these reasons, this study assumed that existing and future construction is still exposed to flood risks. In principle, damages could decrease due to better building codes and the effect could be evaluated in a future study by assuming fewer assets exposed to flooding in the floodplains. Additional considerations for future studies are presented in Chapter 9.

6.4. Estimation of Losses Avoided

The benefit results for all 20 HUC8s are shown in Figure 6–8 through Figure 6–10. For each watershed, the three curves, one for each zero-damage threshold, provide a range of values for the benefits, given the imperfect information about where assets are located with respect to flood sources. In the presentation of results later in this report, the 2-year zero-damage threshold is not included as it is assumed to overestimate damages. Nevertheless, the results associated with this threshold are shown in this section to illustrate the effect on the losses.

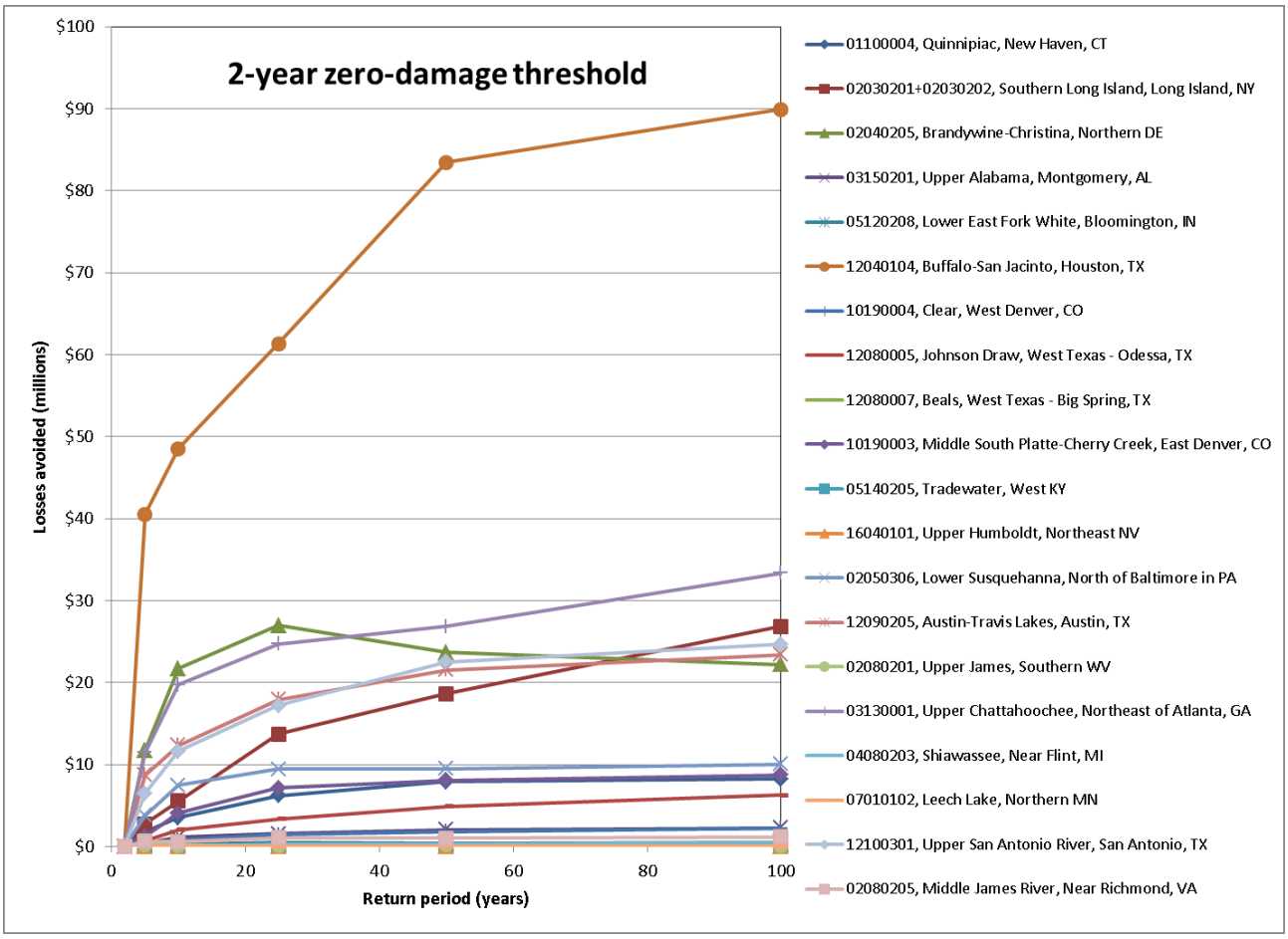

Figure 6–8. Flood losses avoided in 2040 as a function of the return period for the 20 HUC8s modeled and using the 2-year zero-damage threshold (2006 dollars).

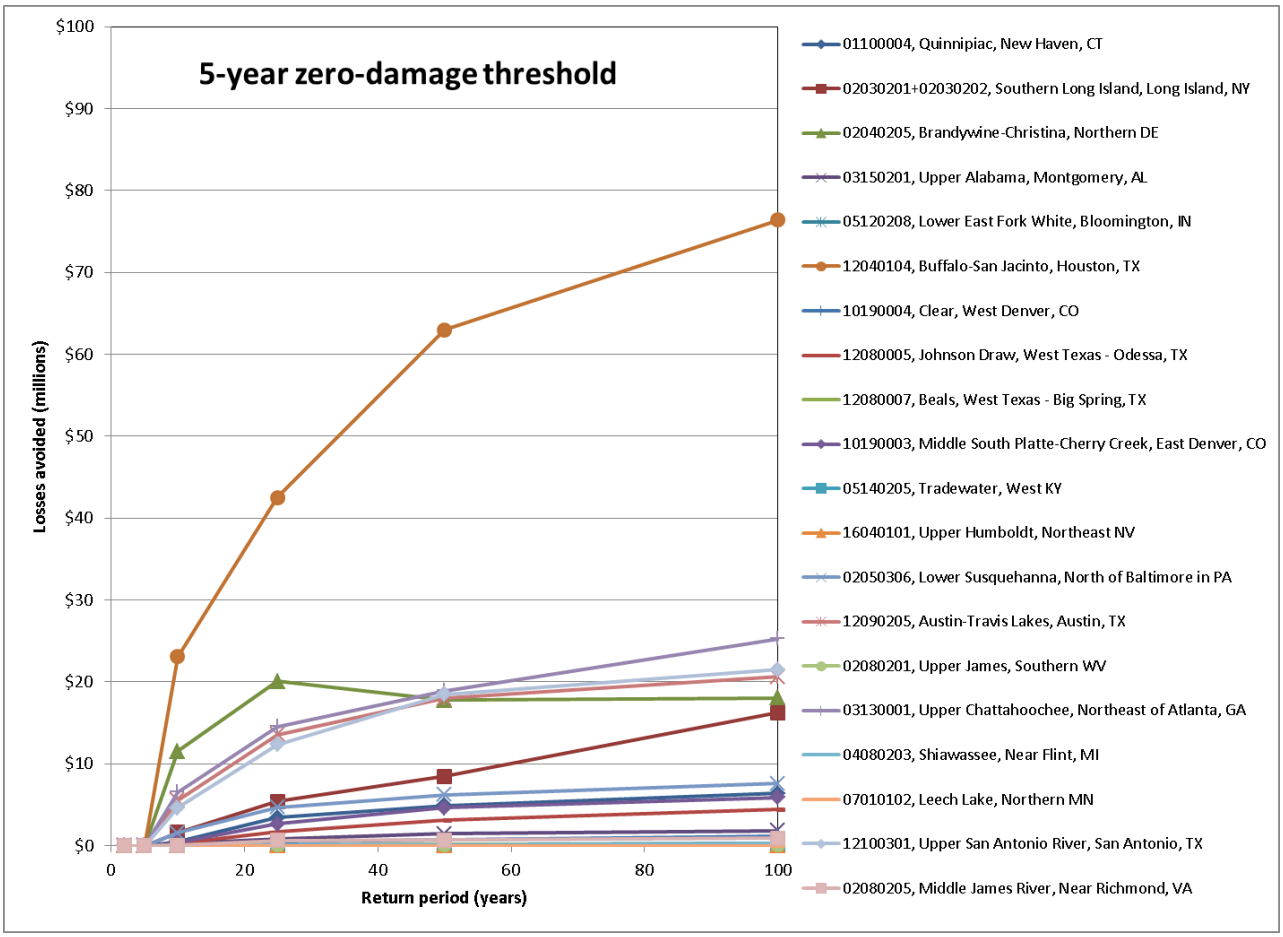

Figure 6–9. Flood losses avoided in 2040 as a function of the return period for the 20 HUC8s modeled and using the 5-year zero-damage threshold (2006 dollars).

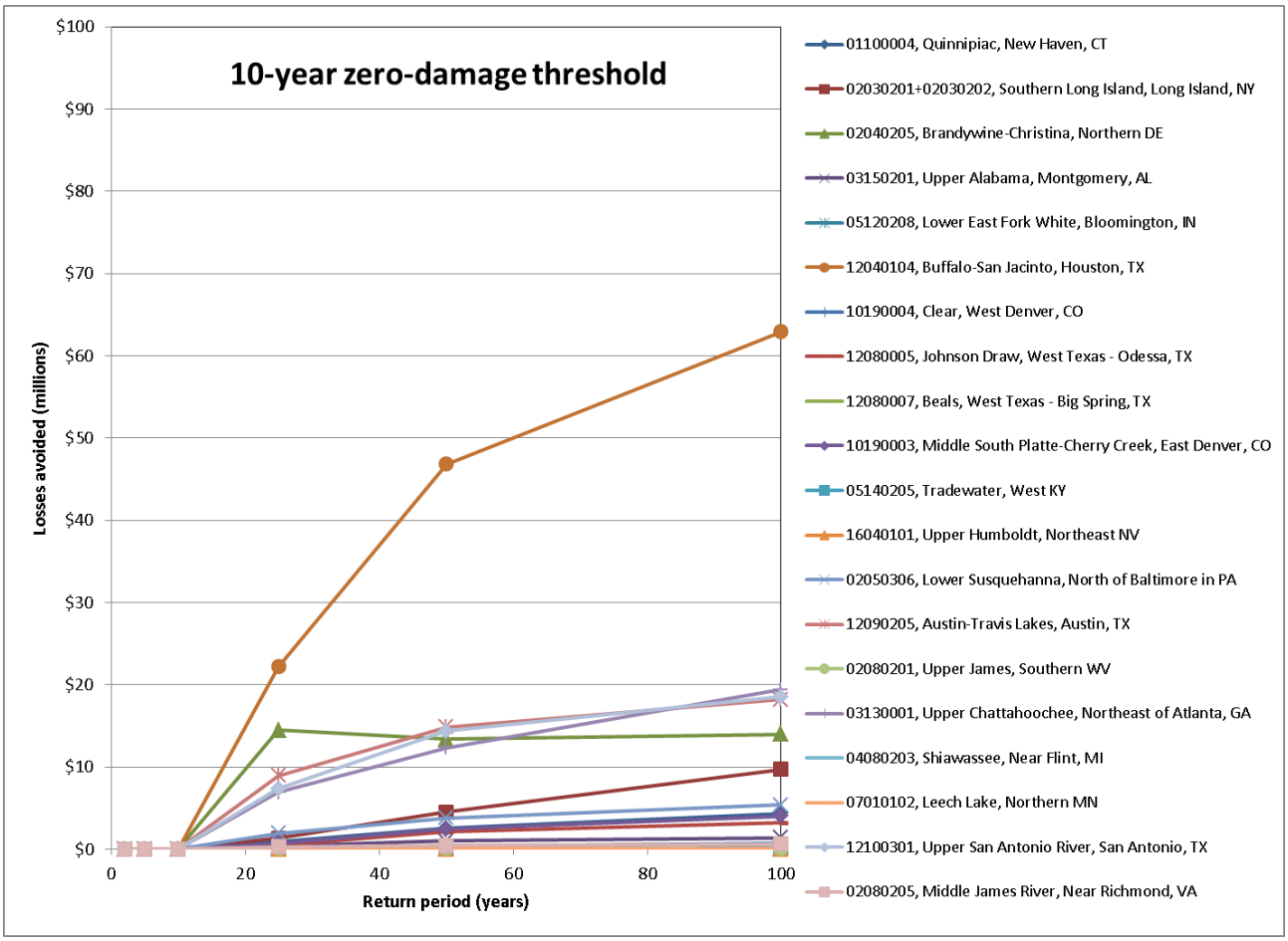

Figure 6–10. Flood losses avoided in 2040 as a function of the return period for the 20 HUC8s modeled and using the 10-year zero-damage threshold (2006 dollars).

As stated earlier, the AALA is the difference of the AAL without GI minus the AAL with GI. For each watershed, these two AAL values were calculated as the area under the damage probability curve, and subtracted to obtain the AALA. Figure 6–11 shows the values for all watersheds in the sample. The AALA has been normalized by the total value of exposed assets and is expressed in units of dollars of flood loss avoided per million dollars of exposure.

Figure 6–11 indicates that the AALA in the sample varies between zero and about $53 per million dollars of exposure, if the 2-year zero-damage threshold is used. The maximum AALA drops to approximately $20 if the 5-year zero-damage threshold is used, and to $8 for the 10-year zero-damage threshold. The AALA values in the figure integrate all watershed characteristics: exposure, expected development in 2040, climate, and the depth of the retention scenario at that location. In this sense, the figure indicates that the sample chosen covers a wide variation of the losses avoided in response to all of these factors combined.

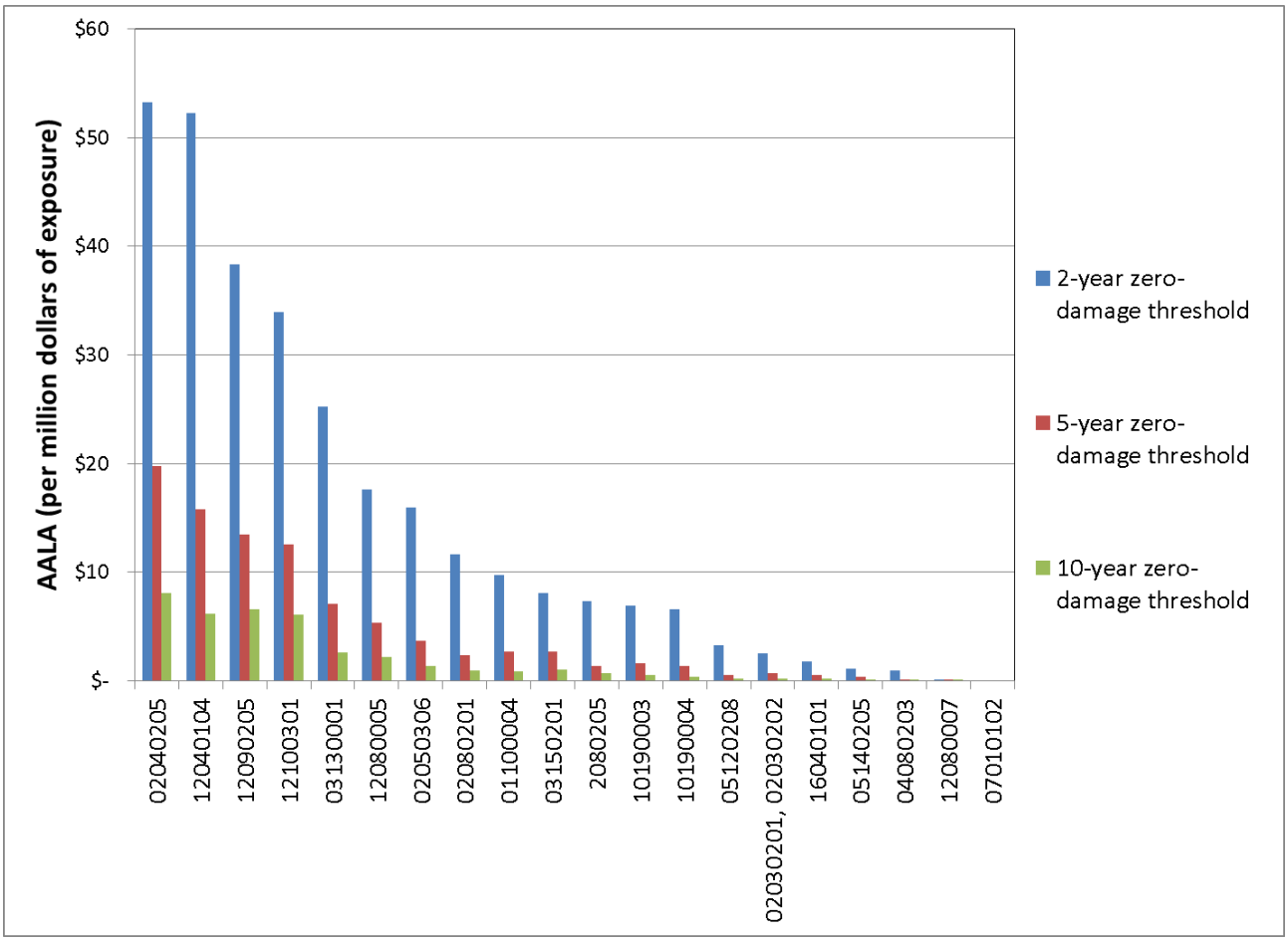

Figure 6–11. AALA for the 20 HUC8 watersheds using the three zero-damage thresholds (2040 conditions, 2006 dollars).

To test the sensitivity of the AALA results with respect to the level in the application of GI, nine of the watersheds in the sample were selected to apply the three different retention scenarios introduced in Chapter 2:

- Low: 85th percentile capture for new development and 80th percentile for redevelopment
- Medium: 90th percentile capture for new development and 85th percentile for redevelopment
- High: 95th percentile capture for new development and 90th percentile for redevelopment

The medium scenario corresponds to the analysis conducted for all 20 watersheds using the 2-year zero-damage threshold as described above. On average, the AALA increases 20% if GI implementation changes from medium to high, and decreases by about 13% if it changes from medium to low for the assumption of the 2-year damage threshold.

7. Validations

The previous chapters described the computational process as well as the assumptions that were made in obtaining the estimates of flood losses avoided. The purpose of this chapter is to explore how some of the major assumptions may affect the results. The approach is to test these assumptions against detailed, site-specific information for a small set of subwatersheds. The intent is not to derive a "correction factor" for the HUC8 results but to understand the implications of the assumptions and how the results may be different if site-specific information were available for all HUC8 watersheds in the study.

The following validation tests were conducted:

1. Comparison of the approximate hydrology based on stream gages against a hydrologic model
2. Evaluation of the effect of more accurate terrain data
3. Assessment of the extent of the zero-damage threshold when compared to visual examination of assets on the ground
4. Comparison of general building stock against actual inventory of buildings on the ground.

In each of these tests, only one factor was changed to isolate its effects on the results. The subsections below provide details on the tests.

7.1. Hydrologic Modeling

The Salado Creek subwatershed, part of the Upper San Antonio River HUC8 in Bexar County, Texas (Figure 7–1), was used as a test case to evaluate how the stream gage approach used in the study compares with one based on hydrologic modeling using the USACE's HEC-HMS model. The Upper San Antonio HUC8 covers an area of 507 square miles and has 409 streams miles. The Salado Creek subwatershed encompasses 223 square miles and has 183 stream miles. A calibrated HEC-HMS model exists for this watershed as part of a separate project sponsored by the San Antonio River Authority (SARA) to develop floodplain maps. The model follows the Guidelines and Specifications for Flood Hazard Mapping Partners published by FEMA, which is the standard to develop Flood Insurance Rate Maps (FIRMs) (FEMA, 2009a). The maps were approved and issued in 2010. Unless indicated otherwise, all other datasets are identical to those used in the stream gage procedure to ensure that the hydrologic simulation approach is the only varying factor.

For the comparison with the HEC-HMS model, a modified retention scenario of 80th percentile capture (0.9 inches) for both new development and redevelopment was selected to simplify the runoff computations needed to simulate the effect of GI using the model. The simulation was conducted for the forecast development conditions in 2040.

As with the stream gage approach, in the HEC-HMS model the effect of GI is simulated by abstracting the volume of water associated with the depth of the retention scenario from the runoff generated by a given storm. As stated earlier, this assumption is valid for the extreme storm events that are likely to cause flooding because the removed runoff will arrive to the stream as interflow later than the peak of direct runoff.

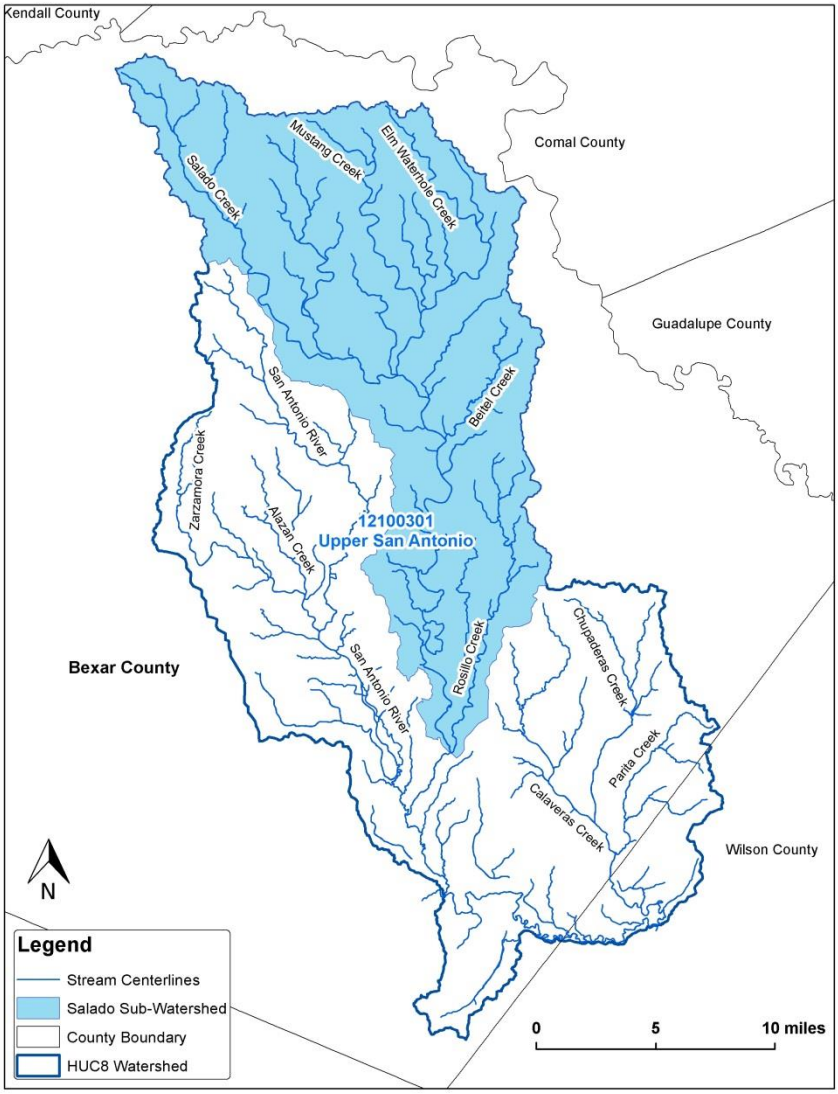

Figure 7–1. Streams in the Salado Creek subwatershed in relation to the Upper San Antonio HUC8.

HEC-HMS simulates runoff volumes and peak flows resulting from watershed and rainfall data. A HEC-RAS hydraulic model is also available but was not used in this case study because only the impact of hydrologic modeling is to be evaluated. Instead of HEC-RAS, the RFD model was used to simulate water surface elevations.

For the stream gage approach, the base topography the 1/3-arcsecond (approximately 10-meter) NED for the continental United States was utilized. Much more accurate LiDAR terrain data is also available for the subwatershed but was not used so that the only variable factor was the approach to estimate peak flows; therefore, the NED terrain dataset was used to delineate the floodplains resulting from the HEC-HMS flows.

The HMS model of the Salado Creek subwatershed consists of 121 reaches and 162 sub-basins ranging in size from 0.27 to 4.27 square miles. A map of the sub-basins and reaches is shown in Figure 7–2.

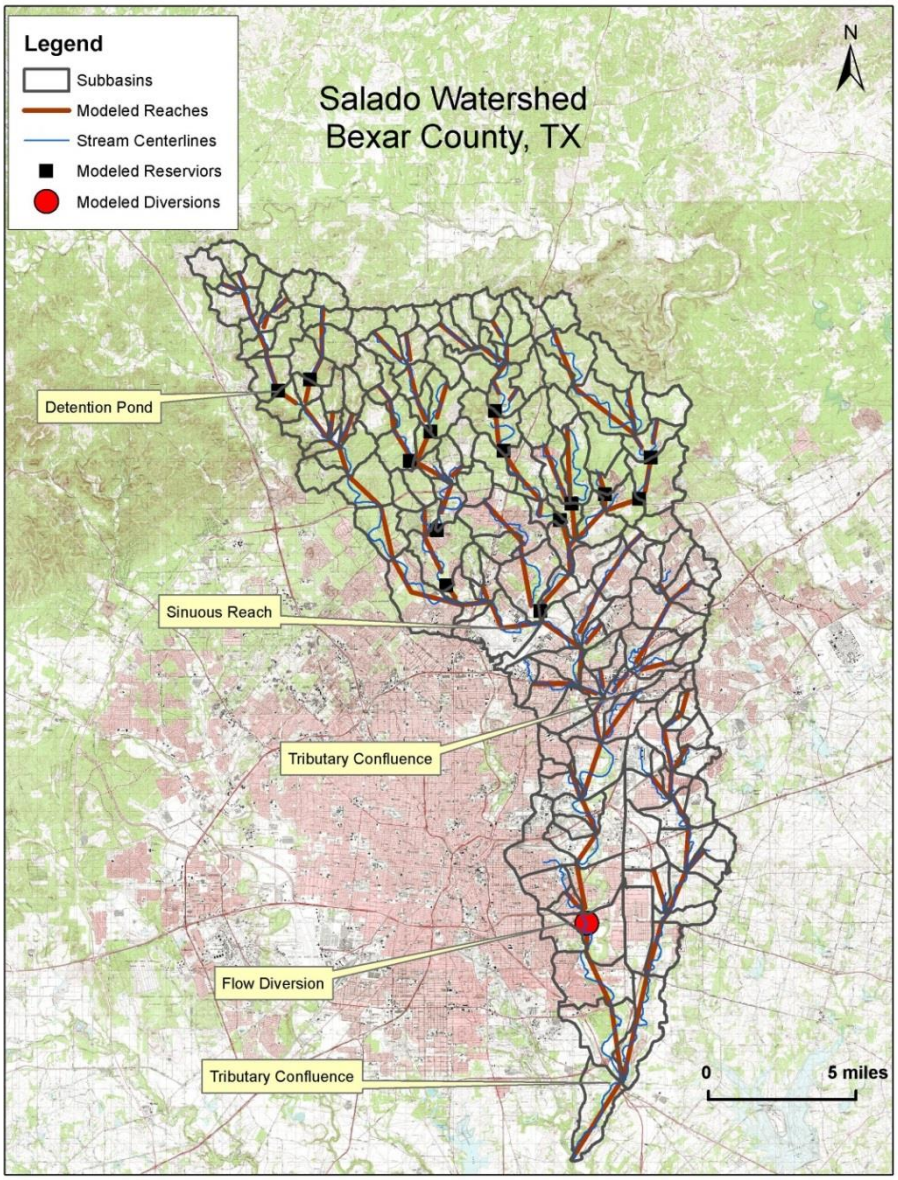

Figure 7–2. Schematic of the HEC-HMS model for the Salado Creek subwatershed.

The model includes the following major features that impact peak flows in the watershed:

- A flood-control detention basin south of Camp Bullis owned by SARA. The impoundment has a maximum storage capacity of 623 ac-ft created by a dam with a height of 80 feet.
- At the confluence of Mud and Lorence Creeks with Salado Creek, significant peak flow attenuation occurs due to the milder slope of the channel and the associated increased storage.
- An engineered diversion occurs upon entering the South Side Lions Park East. Flow splits into a channel running along the east side of the park and converges back with Salado Creek upon exiting the park to the south.
- Two major tributaries cause sudden increases in streamflow. The first one occurs at the confluence of Beitel and Salado Creeks and contributes 15 square miles of drainage area. The second is the confluence with Rosillo Creek, which drains 28 square miles for a total drainage area of 223 square miles at the confluence.

Detailed hydrologic and hydraulic data for these features was included in the model as is required for the development of flood maps (FEMA, 2009a).

HEC-HMS uses the *CN* to calculate the runoff depth produced by a given storm depth. The equations were presented in Chapter 4. The precipitation depths are given in Table 7–1 for various return periods in Bexar County.

Table 7–1. Bexar County, Texas, rainfall depths for various return periods.

Return period	Rainfall depth (in)
2	4.0
5	5.4
10	6.6
25	7.8
50	8.8
100	9.9

As part of the floodplain mapping project, the HEC-HMS model was calibrated to existing conditions. The calibration process entailed adjusting model parameters to match the simulated flows to the observed flows in the stream gages. Once a model is calibrated, watershed parameters can be varied to examine the impact of these changes on the peak flows and water surface elevations. Two changes were implemented for the present study to simulate the conditions in 2040:

1. Modification of the *CN* to reflect 2040 conditions, which include the imperviousness created by new development and redevelopment

2. Modification of the *CN* values in 2040 to simulate the effect of GI controls in removing a volume of 0.9 inches.

Modification 1 generally increases the *CN* for a given watershed because more imperviousness is expected in 2040. In consequence, the peak flows are expected to increase with respect to current conditions. This modification involves a straightforward recalculation of the *CN* based on the forecast of additional impervious surfaces.

Modification 2 follows Option 5 in Section 4.3 that assumes that GI controls can be simulated by decreasing the *CN* to account for the runoff that they retain. This adjustment of the *CN* is such that the resulting runoff depth is equal to the original runoff minus the GI retention depth. The adjusted *CN* values depend on the amount of precipitation, which appears counterintuitive because the *CN* is only a function of physical watershed properties: soils and land cover. However, because the modified *CN* is simply a numerical artifact to achieve an accurate water balance, the adjustment procedure is straightforward. Figure 7–3 shows the relationship between the original and adjusted *CN* values for the various storm depths in the watershed.

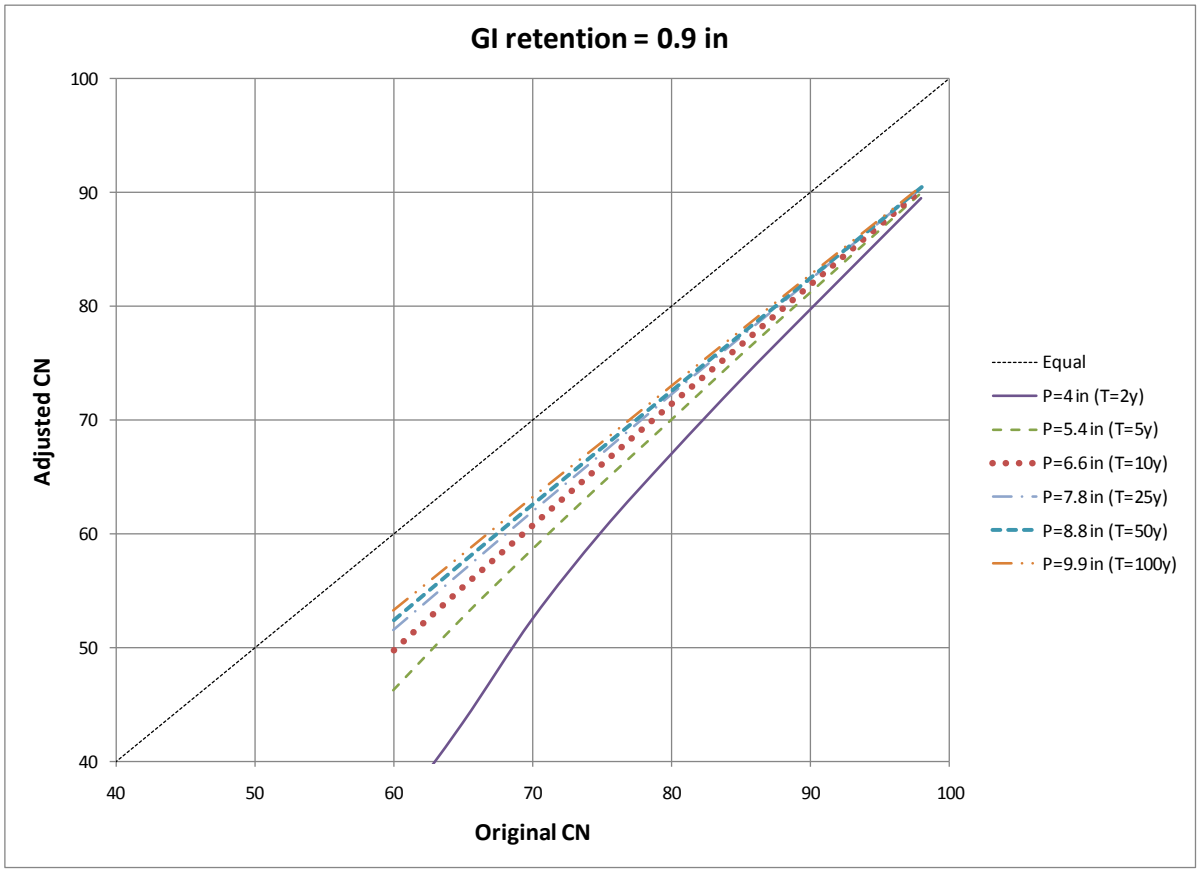

Figure 7–3. Original and adjusted CN values for the Salado Creek subwatershed for various return periods.

As noted in Chapter 4, the application of the relationships in Figure 7–3 leads to an overall decrease in *CN* as a result of the GI controls. The reduction is greater for the small storm events and decreases as the amount of rainfall increases, which is the expected behavior because the volume of GI retention is relatively larger compared to the smaller volumes of rain associated with the more frequent storms.

The HEC-HMS model was re-run with the adjusted *CN* values to arrive at the predicted peak flows for the year 2040 with GI applied to every new development and redevelopment project in the watershed.

A comparison between the results using the two approaches is shown in Figure 7–4 and Figure 7–5, which contrast the peak flows for the 2- and the 100-year flood events. The two plots show similar trends as the flow moves downstream, but they also reveal the significant impact of the hydrologic methodology. Both approaches show a response to features such as the detention pond, the sinuous channel reach, and the tributary confluences, although the effects are muted when using the stream gage approach, which by nature is less detailed. For example, the gage method does not reflect the tributary confluence but the HMS model does. The flow diversion is imperceptible using the stream gage flows; whereas the hydrologic model reflects the intended flood control function of the diversion into the park. The differences in the flows between the two approaches are more pronounced for the 2-year event, which is possibly due to the fact that the model was calibrated using records for large rain events. Also, the TR-55 methodology tends to overestimate peak flows for the less severe events.

Overall, the results appear reasonable considering two major differences in the two approaches. First, the hydrologic model has greater detail about watershed physiography and site-specific features. Second, the two approaches use different methods to simulate the effect of GI and the impact of future development. The stream gage approach uses a ratio of runoff depths to adjust the peak flows (Option 3, Section 4.3); the HEC-HMS model uses a set of modified *CN* values (Option 5, Section 4.3).

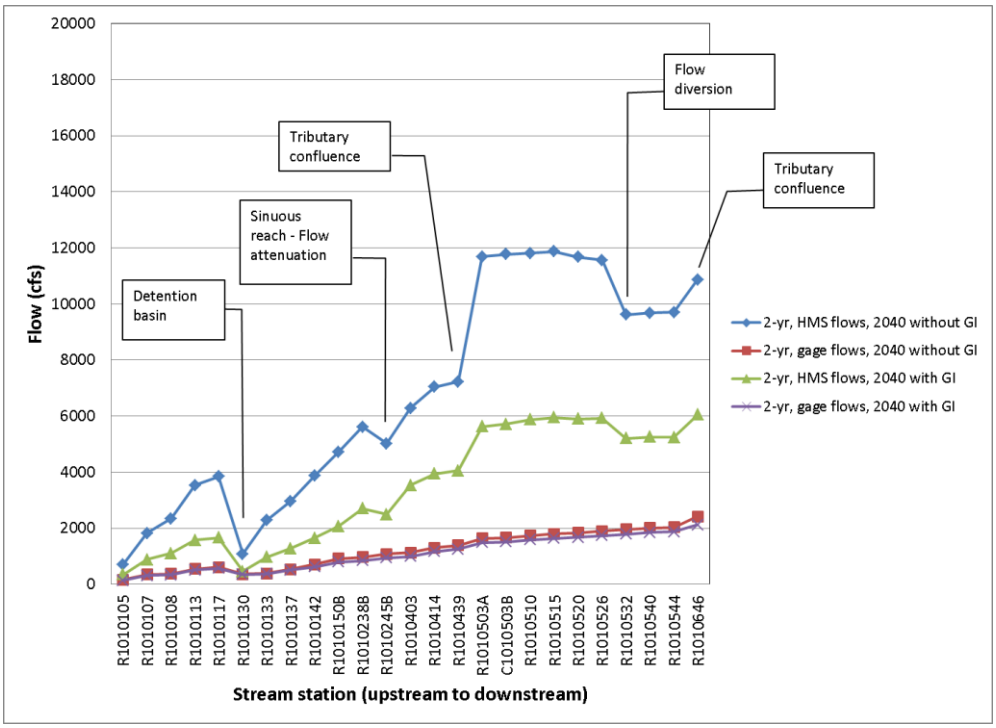

Figure 7–4. Comparison of the 2-year peak flows along Salado Creek using two modeling approaches.

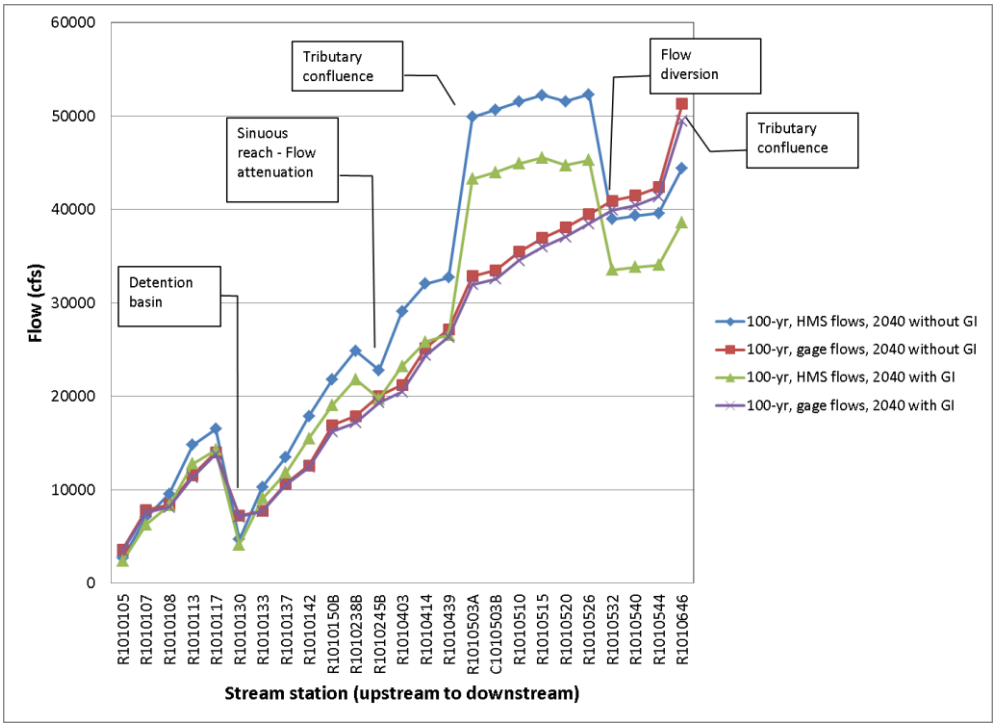

Figure 7–5. Comparison of the 100-year peak flows along Salado Creek using two modeling approaches.

Using the streamlines and the discharges estimated during the hydrologic analysis (stream gage and HEC-HMS), RFD hydraulic models were constructed and floodplains generated for each return period. The result of the hydraulic analysis was one set of RFD models and the corresponding depth grids for each return period modeled (2-, 5-, 10-, 25-, 50-, and 100-year) for conditions with and without GI, using the peak flows from the stream gage approach and the model-based approach.

The default Hazus loss estimation procedure was performed for the six return periods, which produced a damage frequency curve that relates monetary damages to the return period. The more severe the flood event is, the greater the damages. Figure 7–6 shows this relationship for the damages expected in 2040. The figure highlights the effect of the hydrologic modeling approach. The HMS model flows are greater than those from the stream gage analysis and cause more damages. In addition, HMS predicts more benefits as a result of GI; that is, the reduction in damages with GI is relatively greater using the HMS model than with the stream gage analysis.

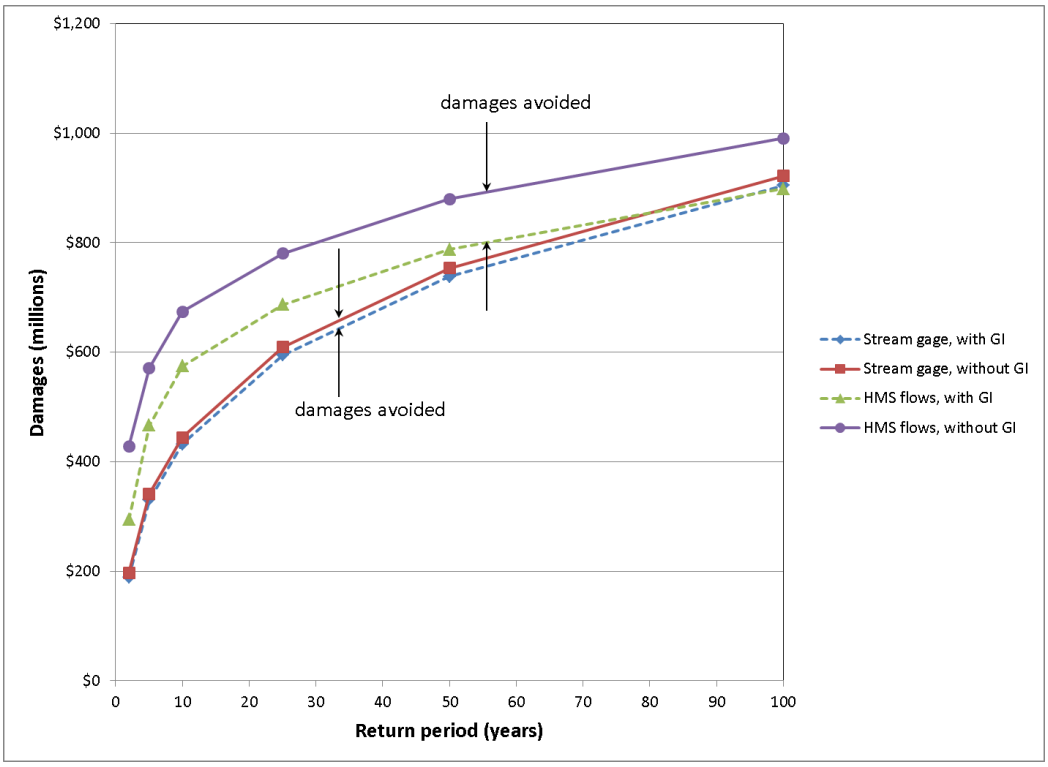

Figure 7–6. Modeled damages in Salado Creek in 2040, without GI, as a function of return period (2006 dollars).

As stated earlier, the benefits introduced by the application of GI are the flood losses avoided and are estimated as the difference between the damages without GI and those with GI. Figure 7–7 shows the damages avoided as a function of the return period for the conditions in 2040. The plot illustrates the earlier observation that the HEC-HMS model predicts greater benefits associated with application of GI.

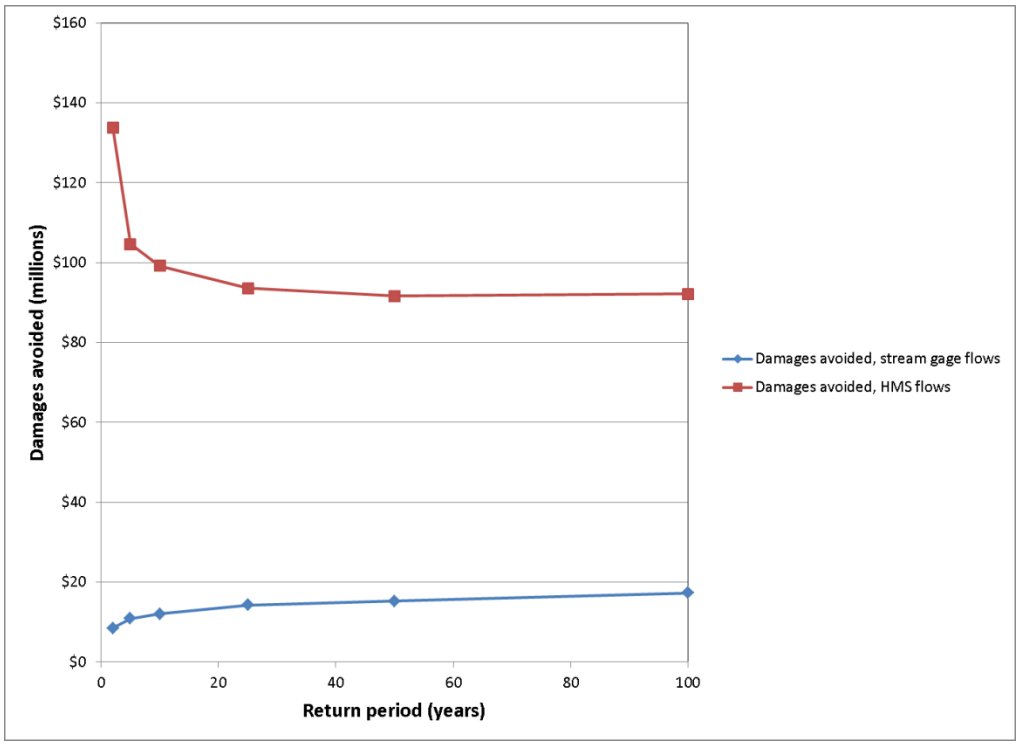

Figure 7–7. Damages avoided in 2040 for the Salado Creek subwatershed (2006 dollars).

In conclusion, a single case study is not sufficient to distinguish a general trend about the two hydrology methods but it sheds light on the potential sources of inaccuracy using the stream gage approach. Overall, for the Salado Creek subwatershed, the stream gage flows tend to be smaller than those resulting from the HEC-HMS model. The difference is greater for the more frequent events, possibly because the HEC-HMS model was calibrated for a large event and because the TR-55 methodology in HEC-HMS tends to overestimate peak flows for small rain events. Nevertheless, considering the numerous assumptions that went into the original analysis, the flow results are informative for an appropriate understanding of the level of accuracy in this study. There is no substitute for a calibrated model when available. Table 7–2 compares the differences and similarities between the approaches.

Table 7–2. Comparison between the stream gage and HEC-HMS approaches.

Element	Stream gage hydrology	HEC-HMS modeling
Different		
Peak flow estimation for existing conditions	Flood frequency analysis performed according USGS's Bulletin 17B. Region-of-influence technique applied to estimate flows at ungaged locations	HEC-HMS model was developed for floodplain mapping according to FEMA (2009) and calibrated to existing conditions for large storm events.
Peak flow estimation for future conditions, with and without GI	Peak flows for existing conditions were adjusted using the ratio of runoff depths (Option 3, Section 4.3).	*CN* values were adjusted according to Option 5, Section 4.3. Figure 7–3 shows the adjusted values.
Hydrologic features (flood control works, channel geometry, diversions)	Assumed that stream flow record reflects the effect of all features	Explicitly included in the input data
Existing land use	National Land Cover Dataset	Hybrid of City of San Antonio zoning, Bexar County parcel data, and National Land Cover Dataset
Similar		
Future land use	EPA 2040 land use forecast used to calculate future runoff volumes	EPA 2040 land use forecast used to calculate future *CN* values
Identical		
Effect of retention	To simulate the effect of GI controls, the retention volume was subtracted from the runoff from the entire site, including pervious and impervious areas. Peak flows were calculated as a function of the remaining runoff.	
Terrain	NED (10-m digital elevation model)	
Hydraulic modeling	RFD model used to develop depth grids for use in Hazus	
Exposure	Census blocks with uniformly distributed assets used in the Hazus runs	
Other		
Time of concentration	Not a variable in this approach	Left the same for existing and future conditions, with and without GI
Rainfall	Not a variable in this approach	Rainfall frequency distribution for San Antonio used as input data

7.2. Terrain Resolution

The terrain models used in modeling the 20 HUC8s were the digital elevation models in the NED, which have a resolution of 1/3 of an arcsecond, or approximately 10 meters. This resolution is the best that is available for the large scale modeling effort in the study but more accurate terrain models exist in many parts of the United States and a comparison between the two levels of resolution is useful to assess the difference in flood losses resulting from using the NED terrain. For example, LiDAR technology can yield terrain models with a resolution of 3 meters or better. LiDAR is a robust industry-standard terrain acquisition technology that FEMA accepts for flood insurance studies (FEMA, 2011c).

This validation test examines two case studies that compare the flood losses resulting from the two terrain datasets. The first is the Upper San Antonio River HUC8 in Texas (Figure 7–1), which covers an area of 507 square miles and has 409 miles of streams. The second is the Big Creek HUC12

subwatershed (Figure 7–8) in the Upper Chattahoochee River HUC8 in Georgia, which has an area of 35 square miles and a total stream length of 46 miles. In both locations LiDAR data was collected and processed according to FEMA specifications to produce FIRMs (FEMA, 2010; FEMA, 2013c).

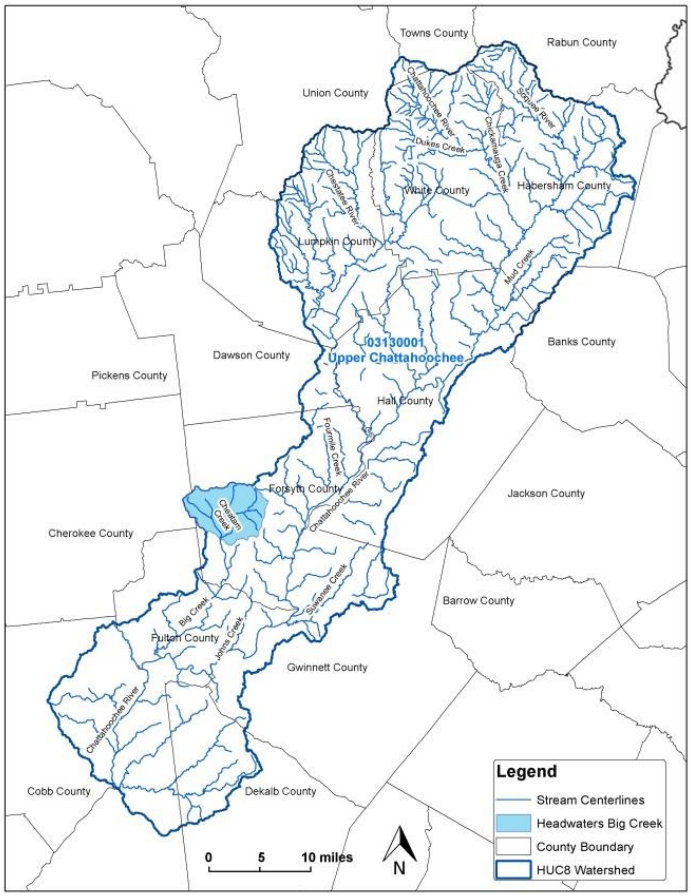

Figure 7–8. Location of the Big Creek Headwaters subwatershed in the Upper Chattahoochee HUC8, Georgia.

Because LiDAR represents conditions found now or in the recent past, the comparison in this test was performed using flood losses for existing conditions rather than avoided flood losses in 2040. All other data sources and modeling procedures (RFD and Hazus) remained the same to ensure that any differences found are due solely to the choice of the terrain model.

In general, the refining effect of LiDAR results in smaller floodplains as shown in Figure 7–9. The floodplain boundary appears pixelated because it is extracted from the depth grid. The inset in the figure shows a large area that appears inundated with the 10-meter NED terrain model but is out of the floodplain if the 3-meter LiDAR terrain is used. Figure 7–10 and Figure 7–11 compare the damages for existing conditions estimated in the two subwatersheds using the two different terrain models. In both cases, the 3-meter LiDAR terrain results in fewer losses.

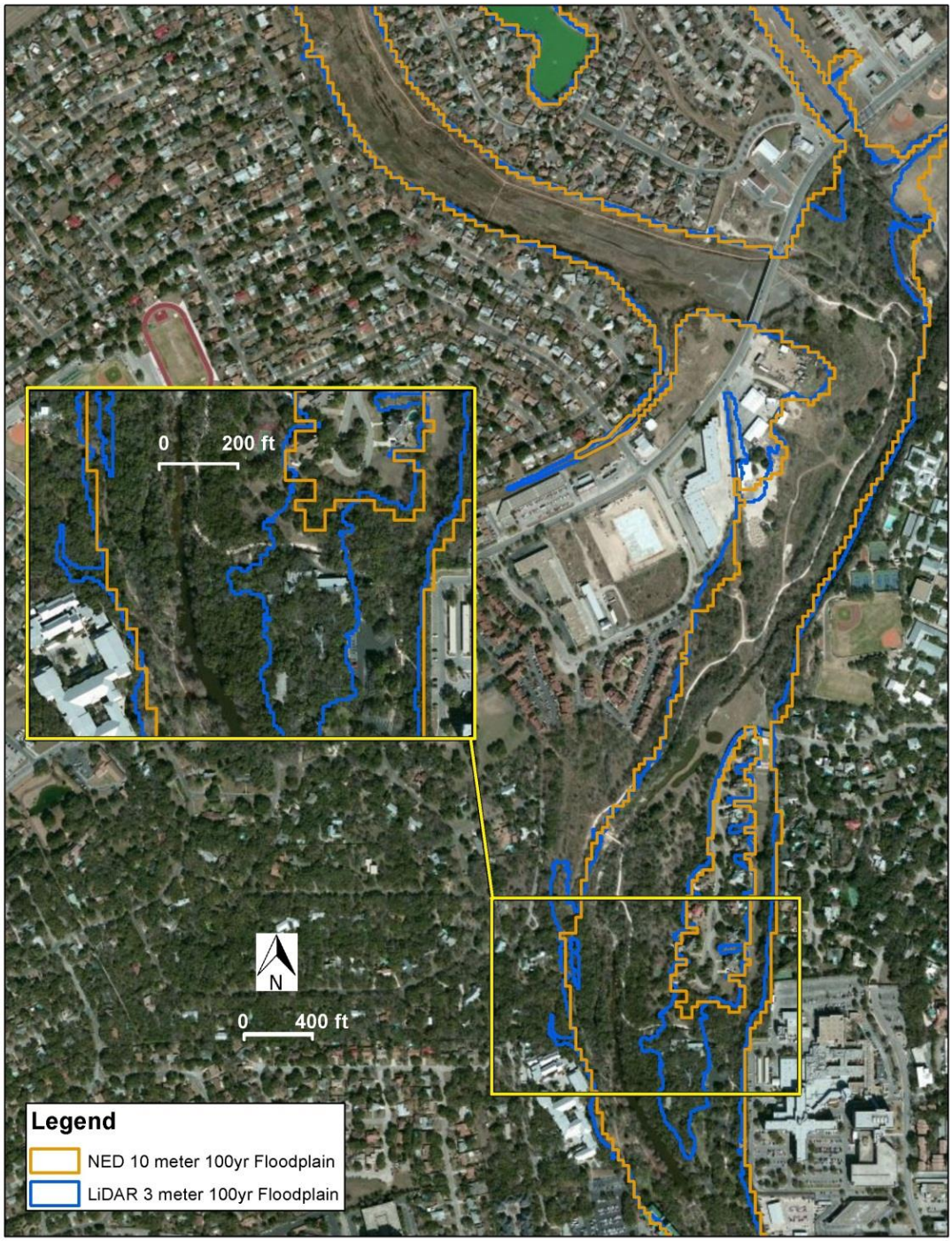

Figure 7–9. Comparison of the floodplains produced by the two terrain models in a section of the Big Creek headwaters subwatershed, Georgia.

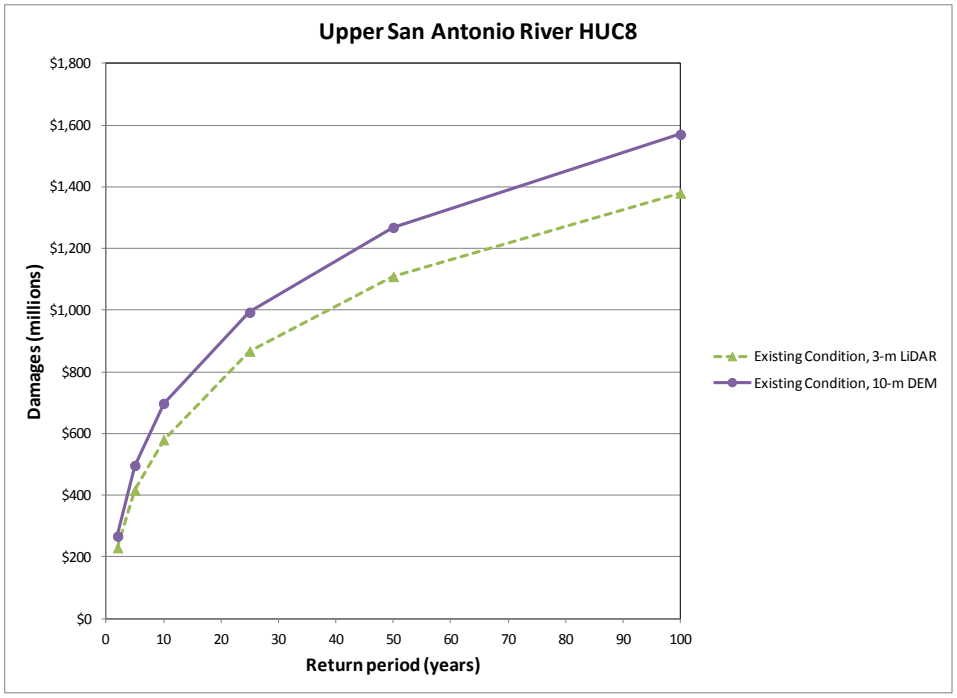

Figure 7–10. Comparison of the damages for existing conditions using two terrain models for the Upper San Antonio HUC8 (2006 dollars).

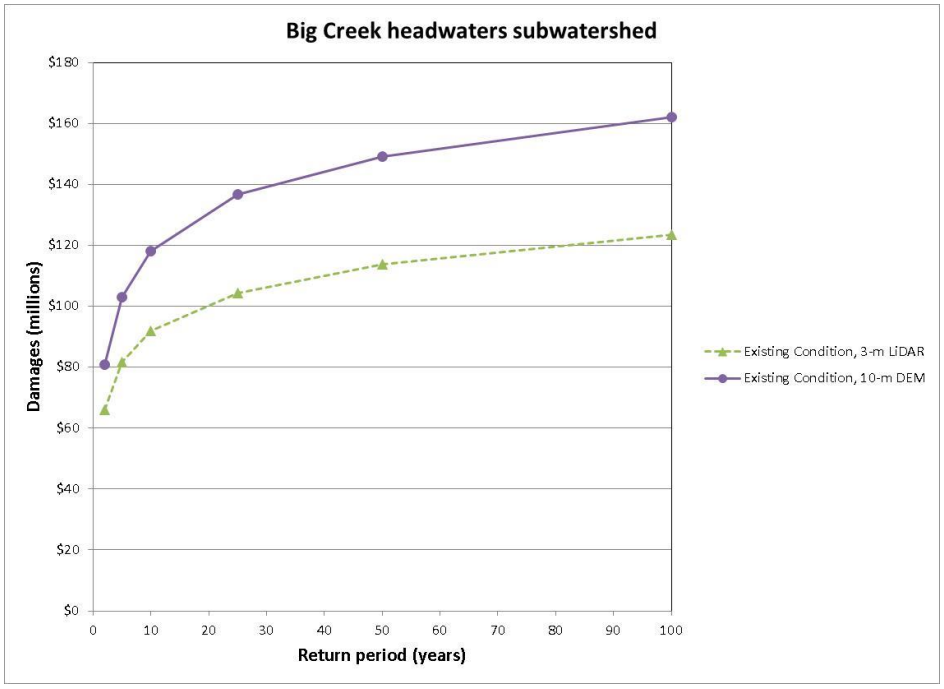

Figure 7–11. Comparison of the damages for existing conditions using two terrain models for the Big Creek headwaters subwatershed (2006 dollars).

The conclusion from this test and from experience using LiDAR data is that a more accurate terrain model results in smaller floodplains, which lead to fewer damages. Finer resolution allows definition of levees and other flood management structures where present, which would reduce damages also. Therefore, use of the NED terrain probably overestimates flood damages.

7.3. Zero-Damage Threshold Validation

Water flowing in a stream after a storm event only becomes a flood if the water reaches a given elevation that indicates flood stage. The water may enter the floodplain naturally in certain places or be contained within the channel in other places due to levees and other channel modifications. Such local features dictate when and where flooding begins to occur. Moreover, for the same storm event, water may access the floodplain in some places but not in others. Therefore, it is reasonable to surmise that there is a threshold for incipient flooding that may vary along the stream network.

As explained in Chapter 6, the actual location of assets in relation to the sources of flooding, vertically and horizontally, greatly influences the damage estimate. The GBS datasets do not allow this type of definition because the value of assets is uniformly distributed on the Census blocks. In reality, the assets are spatially arranged in response to local factors such as land availability, development ordinances, and socioeconomic conditions. It is possible that assets close to the stream, and thus in floodprone areas, are less valuable than others in places with lower flood risk. Yet, the opposite may occur as well as noted earlier; some types of high-value public infrastructure need to be close to the water, for example wastewater treatment plants. Therefore, a given Census block in the vicinity of a stream may have very different property values depending on proximity to a floodprone area.

As described in Section 0, three zero-damage thresholds were examined to arrive at a range of results:

1. No assets at risk of flooding exist within the 2-year floodplain
2. No assets at risk of flooding exist within the 5-year floodplain
3. No assets at risk of flooding exist within the 10-year floodplain

To test the validity of these assumptions, four subwatersheds were examined using aerial photographs to delineate manually an area surrounding the stream where no assets were visible. The objective was to compare this area with the three assumptions and determine which better matches the “true” spatial location of assets as they appear in the aerial photographs.

Publicly available imagery was investigated to identify orthophotos dated 2006 so that they would match the Census data in Hazus. The closest match was aerial imaging collected between 2005 and 2006. The main source of imagery was USDA’s Farm Service Agency National Agricultural Inventory Project (NAIP) found in http://datagateway.nrcs.usda.gov/, with Bing Maps imagery used as a secondary source when the USDA imagery was not sufficiently clear to identify actual locations.

"No-asset" polygons were digitized by examining the orthophotos and identifying the assets closest to the source of flooding. Lines were drawn between the locations of these assets such that the region closer to the stream would have no assets. An example of the result after digitizing the polygons is illustrated in Figure 7–12.

The assets in each block that the polygon intersected were modified to reflect the premise that there are no assets within the no-asset polygon. To accomplish this objective, the total asset value of the block was assigned to the portion of the block away from the stream, that is, outside of the no-asset polygon. This modification numerically associates the total asset value of the block with the portion of the block where assets are visible on the photos (i.e. outside the no-asset polygon), while ensuring that the total value of assets in the block remains the same as in the original block.

After the assets were removed from the no-asset polygon, Hazus was run with the depth grids from the hydraulic model applied over the modified Census blocks. Damages were calculated for the 2-, 5-, 10-, 25-, 50- and 100-year flood events using "existing" conditions (2006).

Five subwatersheds were examined:

- Salado Creek in the Upper San Antonio HUC8, Texas (Figure 7–1)
- Big Creek in the Upper Chattahoochee HUC8, Georgia (Figure 7–8)
- Lower Christina River in the Brandywine-Christina HUC8, Delaware (Figure 7–13)
- Sand River in the Middle South Platte-Cherry Creek HUC8, Colorado (Figure 7–14)
- Town Lake in the Austin-Travis Lakes HUC8, Texas (Figure 7–15)

Figure 7–12. Example of a manually digitized polygon where no assets are at risk of flooding (Big Creek subwatershed).

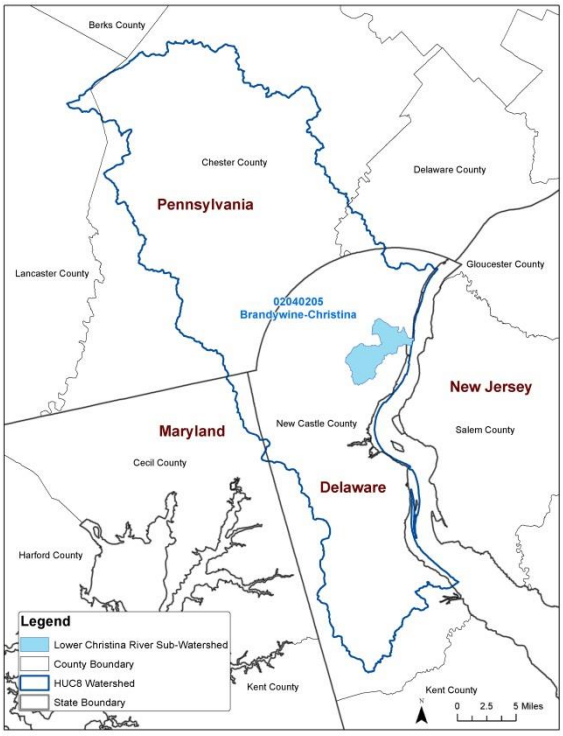

Figure 7–13. Location of the Lower Christina River subwatershed in the Brandywine-Christina HUC8, Delaware.

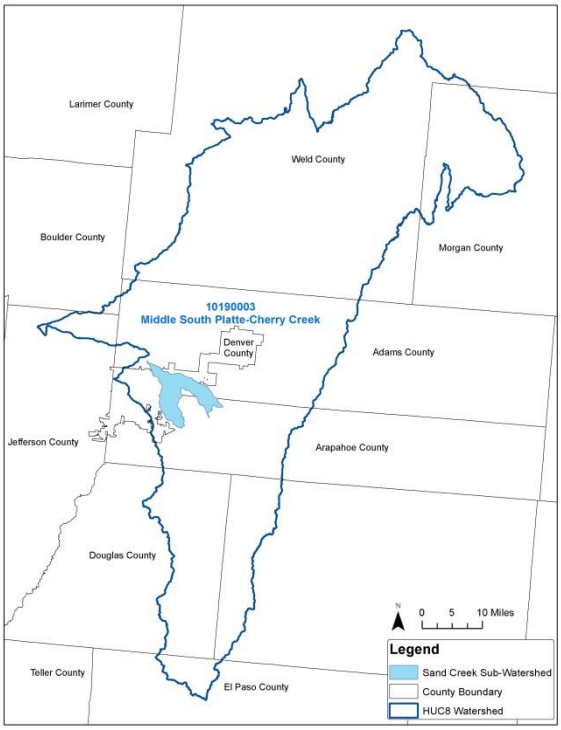

Figure 7–14. Location of the Sand River subwatershed in the Middle South Platte-Cherry Creek HUC8, Colorado.

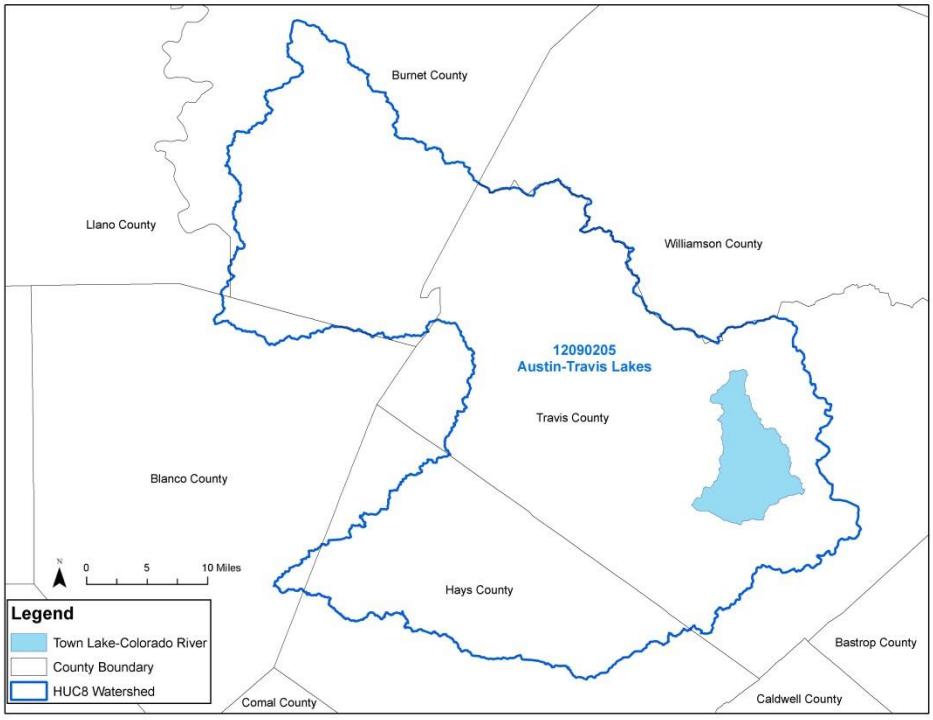

Figure 7–15. Location of the Town Lake subwatershed in the Austin-Travis Lakes HUC8, Texas.

Figure 7–16 through Figure 7–20 summarize the results. The blue curve is the default damage curve without any adjustments to account for where the assets are in relation to the stream, that is, without a zero-damage threshold. The red curve represents the damages resulting from the visual definition of a no-asset polygon; the value of assets is numerically removed from the no-asset polygon so that there is no value exposed to flooding within the polygon. As expected, the fewer damages in the red curve reflect the reduction on the value of assets exposed. The red line can be considered the modeled "true" damages because they are adjusted to what is visibly exposed to flooding. The solid yellow curve depicts the damages that would take place under the assumption that there are no assets at risk within the 2-year threshold. In this case, the value of the assets in the Census block was left as the default. The dashed yellow line represents the same situation as the solid yellow line, except that the assets were moved from the flood threshold area so that the total value of assets is assigned to the portions of the block outside of the zero-damage threshold. Comparison with the red line indicates that the assumption of no assets within the 2-year floodplain is overly conservative because the damages are much fewer than the modeled "true" damages. The light blue and purple lines depict the damages with application of the 5- and the 10-year zero-damage thresholds respectively. These two assumptions result in even greater divergence from the "true" damages. Runs with assets removed from the flood threshold using these two zero-damage thresholds were not performed because it was obvious that they would not improve the match with the modeled "true" damages.

This behavior was consistent for all test subwatersheds, insinuating that the 2-year zero-damage threshold produces the closest results to the manually defined zero-asset polygon. Removing the assets from the flood threshold introduced a minor improvement, except for the Lower Christina subwatershed where the improvement was more noticeable, even if it still could not close the gap. These observations must be placed within the context of the uncertainties caused by the 10-meter DEM and the lack of stream bathymetry that tend to overestimate flood depths.

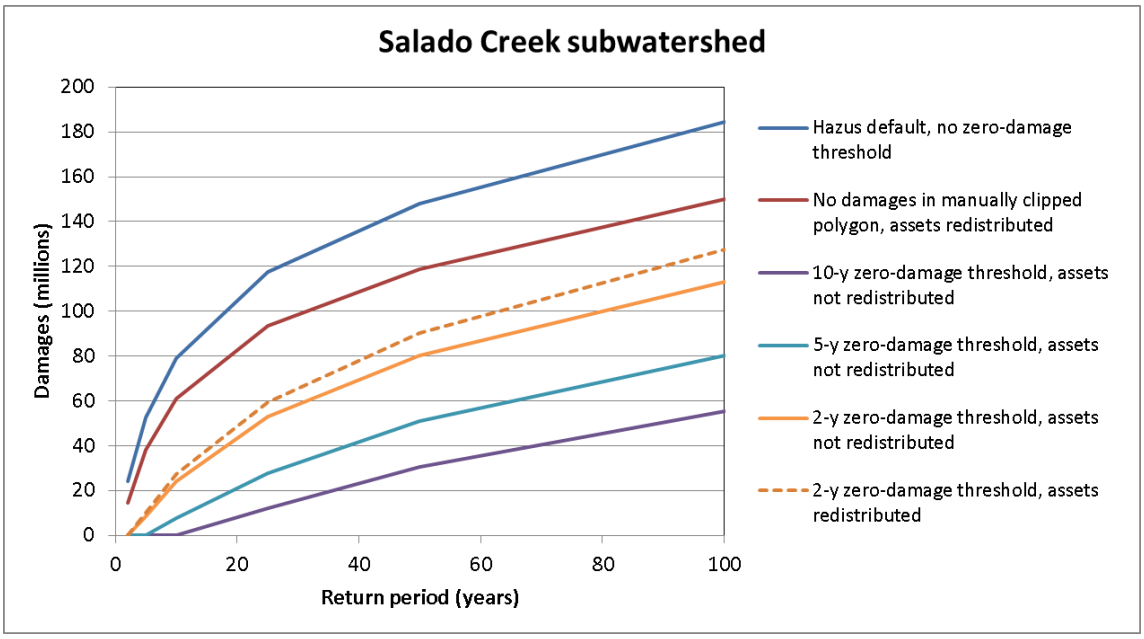

Figure 7–16. Damages for the Salado Creek subwatershed for various zero-damage assumptions (existing conditions, 2006 dollars).

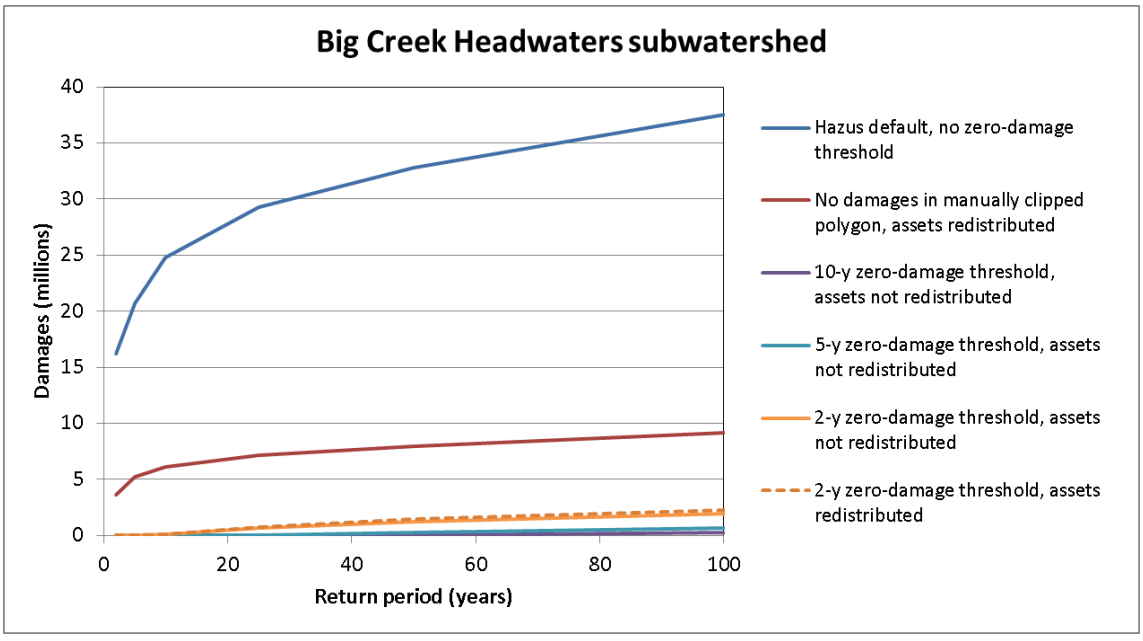

Figure 7–17. Damages for the Big Creek headwaters subwatershed for various zero-damage assumptions (existing conditions, 2006 dollars).

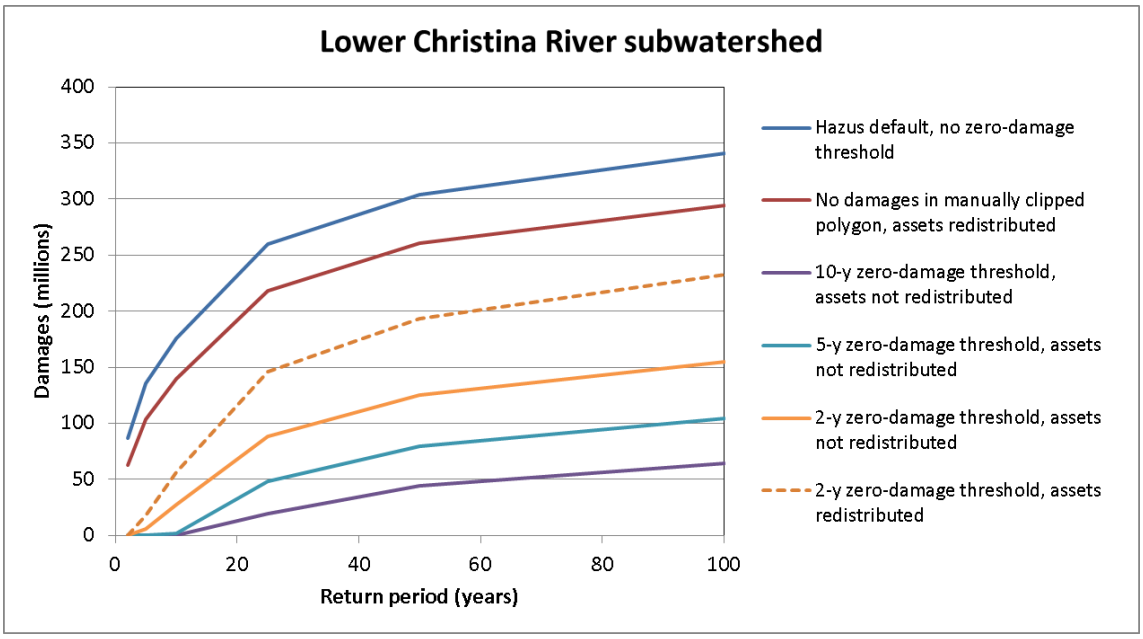

Figure 7–18. Damages for the Lower Christina River subwatershed for various zero-damage assumptions (existing conditions, 2006 dollars).

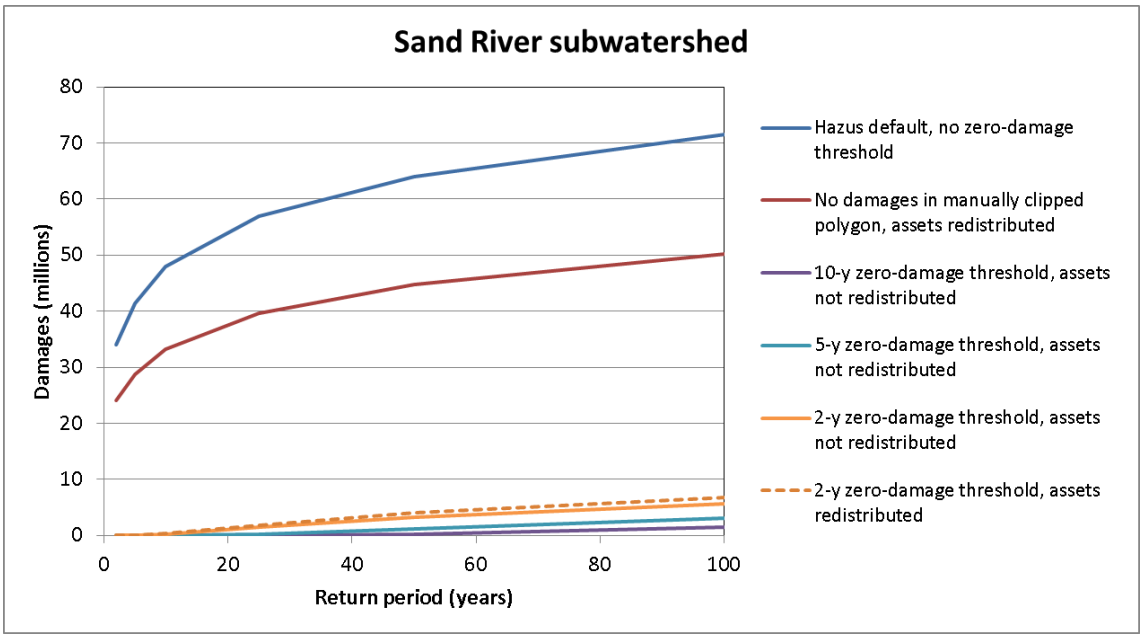

Figure 7–19. Damages for the Sand River subwatershed for various zero-damage assumptions (existing conditions, 2006 dollars).

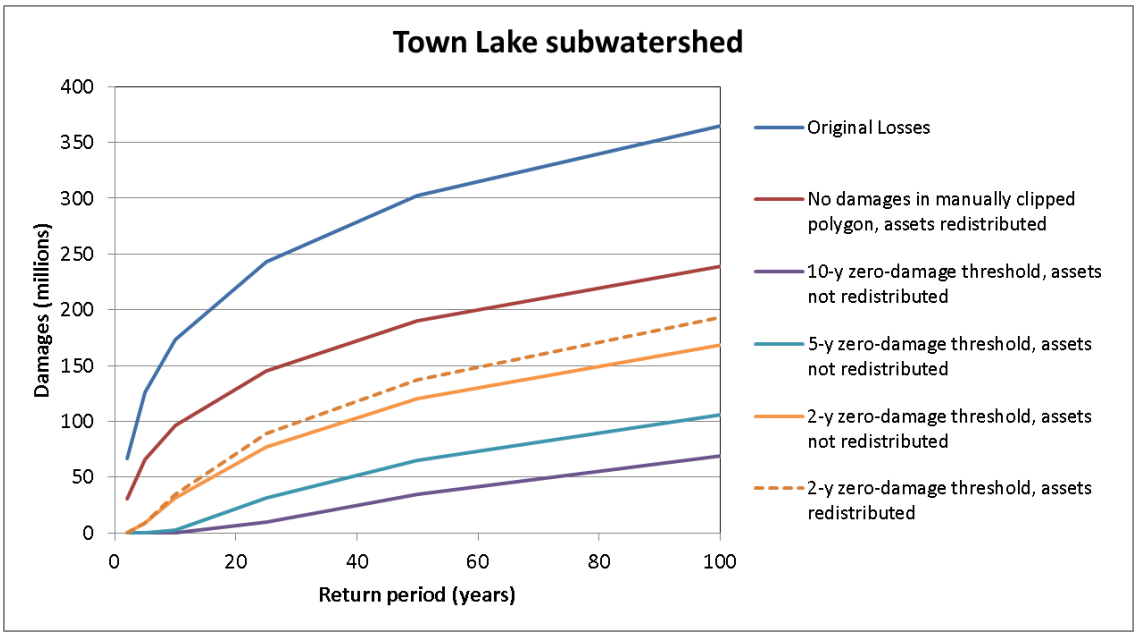

Figure 7–20. Damages for the Town Lake subwatershed for various zero-damage assumptions (existing conditions, 2006 dollars).

The results are compared side by side in Figure 7–21 using the AAL. The color convention in the previous figures carries into this figure. The "true" AAL represented by the red star is greater than the AALs resulting from all of the three zero-damage thresholds (2-, 5-, and 10-year). Of these, the 2-year zero-damage threshold appears the closest to the "true" AAL but in most cases it is noticeably smaller, suggesting that the assumption of no assets at risk within the 2-year floodplain underestimates damages and thus is overly conservative in these test cases. However, this observation needs to be tempered with important caveats.

The main caveat to consider is that the spatial resolution of the NED terrain used in the study is unable to capture the geometry of the stream channels; certainly, bathymetry is not part of the terrain model. Therefore, the hydraulic model may underestimate the conveyance capacity of the streams and "force" the water to spill onto the floodplains. It is plausible for a relatively frequent event like the 2-year flood to be entirely contained in a stream channel or nearly so, especially if it has been altered for flood control purposes. In the absence of detailed topographic and bathymetric surveys for all streams, it is not possible to consider channel conveyance more accurately in this study. Therefore, the lack of channel information likely affects the relation between the data points in Figure 7–21. Another caveat is that structures visually observed to be in the floodplain could be elevated, thus reducing the potential losses for some flood events. A third caveat is the assumption of uniform distribution of assets in Census blocks. The impact of this imperfect information is that the estimated losses can be greater than in reality, which tempers the foregoing statement that the 2-year AAL estimate is closest to the "true" losses.

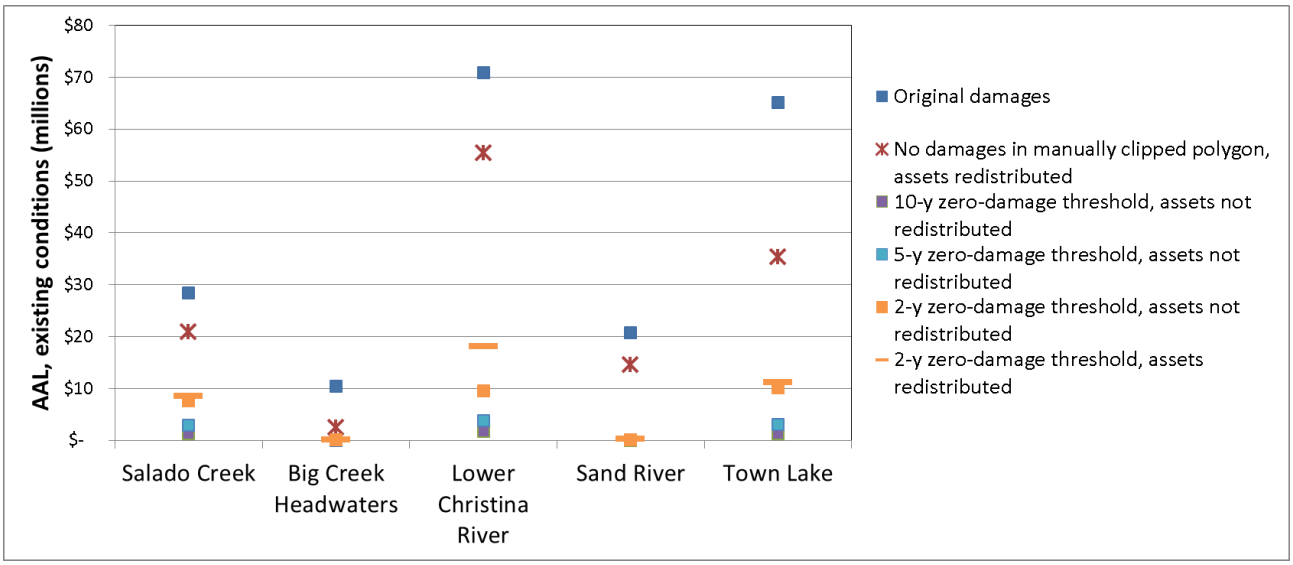

Figure 7–21. Comparison of all subwatershed AAL values for various zero-damage assumptions (existing conditions, 2006 dollars).

In conclusion, while this validation test is not intended to generalize all cases in the study, in the tested subwatersheds, the analysis shows that the assumption of zero assets within the 2-year floodplain most closely represents a situation in which assets can visually assumed not to be exposed to flooding. Because national datasets are used in the analysis, it is possible that the coarse NED terrain, the lack of specific first-floor elevation data, and the assumed uniform distribution of assets in the Census blocks will overestimate the damages, in some cases significantly. Yet site-specific testing would be needed to determine whether the choice of a particular zero-damage threshold leads to a match of damages with actual local data.

7.4. Geographic Location of Assets

The default estimation method in Hazus is based on general building stock (GBS) databases that are associated with Census blocks. The types and value of this infrastructure are uniformly distributed in each block. This section examines how this approach compares against using building-specific information entered into Hazus as user-defined facilities.

GBS is the default building inventory in Hazus and was derived from proxy data representative of the building stock in a given Census block. For all HUC8s in the analysis, the GBS tables for square footage and building count built in Hazus were used. Building counts in each occupancy class are inferred from the total square footage in the block divided by typical square footage values for individual facilities in the class.

As an improvement over the default analysis, Hazus allows entering user-defined facility (UDF) data, for example spatial location of buildings, occupancy type, foundation type, structural replacement

values, contents replacement values, and first floor elevations. The goal of the case studies in this section is to compare the damages resulting from the GBS and UDF approaches. Two subwatersheds were selected where parcel records were available to create the UDF inventories. The first one is the Salado Creek subwatershed of the Upper San Antonio River HUC8 (Figure 7–1) in Bexar County, Texas, for which SARA supplied the parcel data. The second is the HUC12 subwatershed corresponding to the headwaters of Big Creek in the Upper Chattahoochee HUC8 (Figure 7–8) in Forsyth County, Georgia. Forsyth County provided the parcel data for this subwatershed.

Except where indicated, all other datasets and procedures are identical in both the GBS and UDF approaches to ensure that the building stock inventory is the only varying factor. Nevertheless, four notable differences in the approaches impact the results significantly:

1. GBS assumes uniformly distributed assets over the area of a given Census block. UDF is based on a specific point location for each building. In the absence of building footprints, the case studies assumed that the buildings were located at the centroids of the parcels.
2. For GBS exposure, aggregate regional building inventories, representing building square footage by occupancy class, were developed from Census data for residential land uses, and from Dun & Bradstreet employment data for non-residential land uses. Exposure for UDF is inferred from the assessed value of each building in the parcel records. These values are not necessarily close to structure replacement values, which are the quantity of interest for loss calculations. The case studies assumed that the assessed value is equal to the replacement value.
3. First-floor elevations are needed to estimate flooding depths from the results of hydraulic modeling. In GBS, default assumptions based on the distribution of foundations were used to assign first-floor elevations to the various occupancy classes. In UDF, parcel records often do not include information on the type of foundation or how high it is above the ground. The case studies assumed a slab-on-grade foundation and a first floor located one foot above the ground.
4. Hazus damage curves are associated with various occupancy classes. These occupancy classes were manually matched to the land use categories in the parcel records. Given the variability of land use categories among the municipalities, judgment was necessary to match every building to the most representative curve.

These assumptions are consistent with current best practices for Hazus use for FEMA applications.

The contrast between GBS and UDF proceeded by comparing damages under existing conditions rather than in 2040. The reason is that the parcel information from the municipalities is available for existing conditions. The 2040 forecast provides acreage of new development and redevelopment but it cannot infer the actual location and type of buildings.

The term “existing conditions” requires some clarification as it is not a snapshot in time for all variables in the analysis. The following are the most salient facts:

- The exposure values that Hazus uses to calculate GBS damages are in 2006 dollars
- Municipal records are of various ages. Assessed values for property change depending on real estate transactions, new construction and re-construction, and periodic general appraisals that often reflect the local real estate market. Because this analysis employs the assessed value of structures rather than the replacement value, not all buildings have a common baseline year for their value.

Ideally all variables in the analysis would have been adjusted to the same year; however, such adjustment would have required detailed research into the properties affected to determine whether they were built and what their value was then. The schedule and budget constraints of the project did not allow for this type of research. Nevertheless, the results presented later properly reflect the order of magnitude of the difference, even without these adjustments.

As discussed earlier, Hazus calculates damages using vulnerability curves that relate a given flooding depth to a percent damage sustained by a particular type of building, for the structure and for the contents. For the GBS approach, the default Hazus loss estimation procedure was performed for the six return periods using the damage curves for the occupancy classes in Appendix E.

The UDF approach required a significant effort to align the damage curves in Appendix E with the parcel records. Virtually every municipality employs its own land use classification system but, because a particular building must be associated with a set of damage curves, the municipality's land use codes need to be matched to the Hazus occupancy classes. All of the municipal codes need to be examined individually to select the proper occupancy class. Often, there are records that do not have a land use associated with them; in such cases, a determination was made by examining other attributes of the property and visual inspection of aerial photographs. This process yielded the lookup tables for the two watersheds shown in Appendix F.

Due to their very different origins, the total value of assets in the UDF approach cannot be expected to match the GBS. Therefore, a fairer comparison between the two approaches is to create an "updated" GBS dataset by aggregating the UDF data and distributing it uniformly on the Census blocks in the study area. The total value of the updated GBS is then guaranteed to match the total value of UDF. Therefore, in the subsequent discussion, three approaches are compared:

- Default GBS as supplied in Hazus
- UDF
- Updated GBS created from UDF data

Figure 7–22 and Figure 7–23 show the damages for existing conditions calculated using these three approaches. All approaches calculate direct damages to the structure and its contents. For nonresidential properties, Hazus also estimates inventory damages and income losses. The default GBS computation includes also business disruption as indirect damages, whereas the UDF and

updated GBS computations do not. Therefore, the indirect damages were removed from the default GBS computation to obtain a consistent set of damage types among the approaches. The figures show that the "true" damages as given by the UDF approach differ from the default GBS by a factor of roughly ten for the Salado Creek case, and three for the Big Creek headwaters subwatershed. In Salado Creek, the default GBS damages are greater than the updated GBS, whereas the opposite takes place in Big Creek. The explanation is that in the former, the total value of assets in the default GBS is greater than in the UDF, which is the source of the updated GBS; in Big Creek, the total UDF value is greater than the default in the Hazus GBS database.

The main reason for the large differences is that GBS, whether default or updated, is the assumption of a uniform distribution of assets as discussed in the previous section. Figure 7–24 illustrates a particular situation in the Big Creek headwaters subwatershed that arises from this assumption. A large portion of Block A is flooded by the 100-year event but few buildings are affected. In Block B, only a small area is flooded but it contains several buildings. In both cases, the assumption of uniform distribution is unlikely to match reality. Table 7–3 summarizes the differences in the updated GBS and UDF approaches for these blocks. These two blocks illustrate the wide array of possibilities that can take place.

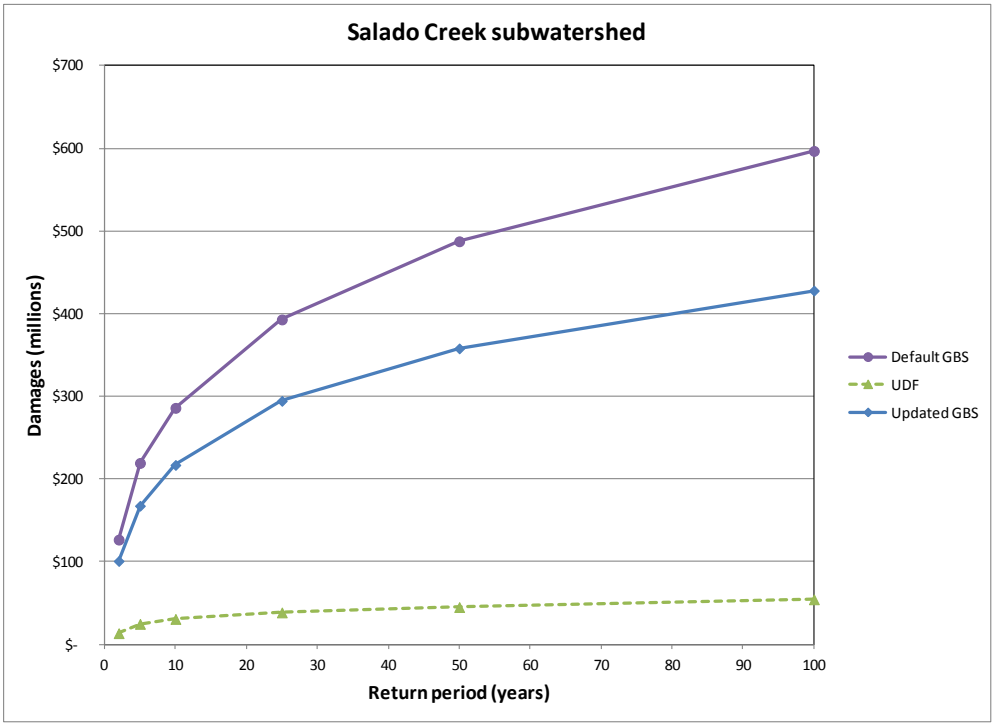

Figure 7–22. Comparison of GBS and UDF damages for existing conditions for the Salado Creek subwatershed (existing conditions, 2006 dollars).

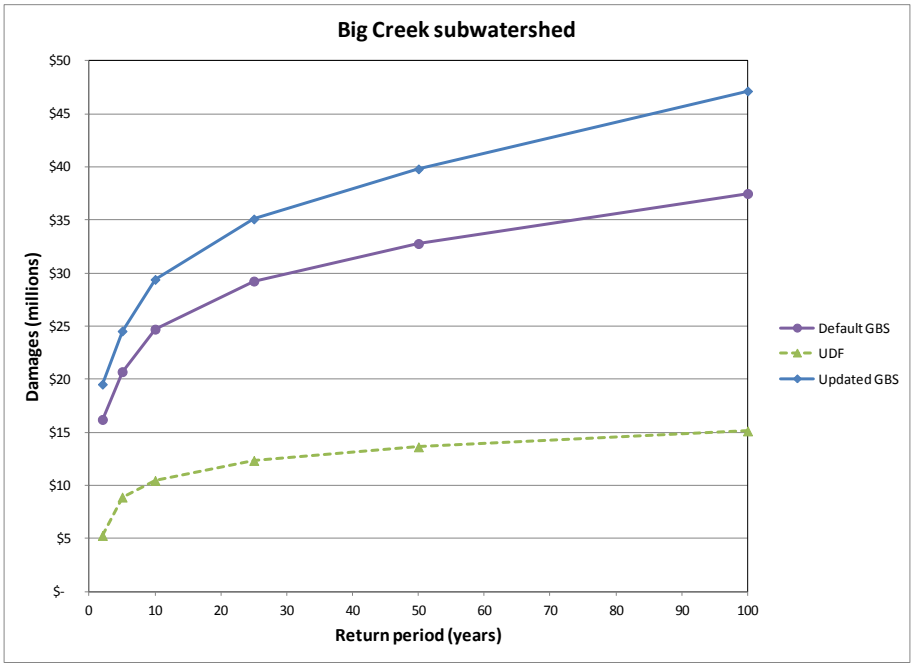

Figure 7–23. Comparison of GBS and UDF damages for existing conditions for the Big Creek headwaters subwatershed (existing conditions, 2006 dollars).

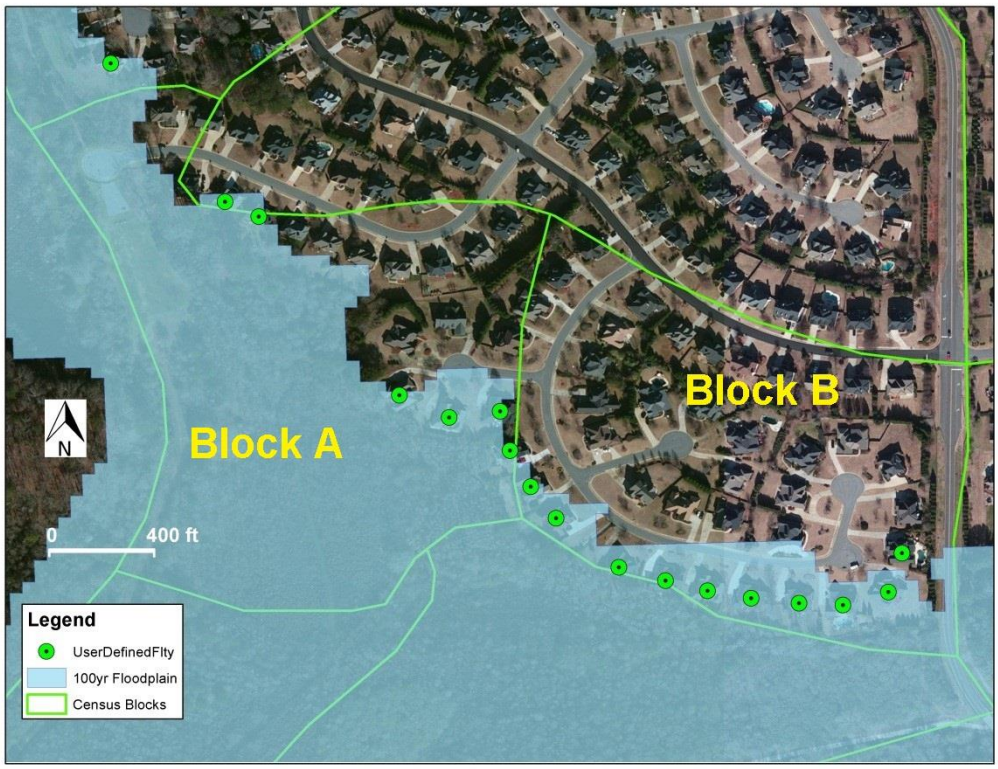

Figure 7–24. Section of the Big Creek headwaters subwatershed showing sources of discrepancies between the GBS and UDF approaches.

Table 7–3. Summary of damages for the 100-year flood for Blocks A and B in Figure 7–24 using the UDF and updated GBS inventories.

	Building count		Buildings damaged		Damages	
Block	Updated GBS	UDF	Updated GBS (inferred)	UDF (actual)	Updated GBS	UDF
A	19	19	9	5	$1,519,000	$320,000
B	37	37	6	10	$388,000	$764,000

In summary, in Block B, the updated GBS produces fewer losses than UDF because only a small portion of the block is flooded, yet it contains several buildings. In Block A, the opposite takes place: a large portion of the block is flooded but only a few buildings are affected; therefore, the updated GBS losses are greater than UDF losses. The difference between the actual number of damaged buildings and the inferred number is an artifact of the process of inferring building counts from square footage.

In conclusion, this validation test confirms and emphasizes the sensitivity of the damage computation to the location of assets in the floodplain. The actual horizontal and vertical location of buildings in a watershed is highly variable, as are other features that affect flood damages, such as foundation types. Therefore, it is not possible to generalize the results of this test to correct the values obtained for the 20 HUC8s using the default GBS approach. UDF is the preferred approach because it provides specific location of assets at risk; however, parcel data are not publicly available for all of the HUC8 watersheds in the study. In addition, it is impossible to derive a UDF inventory for the conditions in 2040. Because the current study is concerned with benefits, which are a difference between two sets of damages, it is expected that some of the inaccuracy will cancel out as the without- and with-GI damages are subtracted to arrive at the benefits. However, the inaccuracies inherent in using GBS – the only source of asset data available for a national study – should be understood when evaluating the estimate of flood losses avoided.

8. Nationwide Scale-Up

The final step of the study is to use the results for the 20 HUC8s modeled to extrapolate to other watersheds not modeled, in an effort to estimate the total flood loss avoidance benefits to the nation stemming from GI implementation on new development and redevelopment.

The approach consisted of deriving regression relationships between the AALA for the medium scenario and watershed properties. In principle, all of the properties in Table 3–2 can be considered as potential explanatory variables to predict the flood losses avoided. However, in practice, several of these variables are not readily available for all watersheds in the nation. Therefore, part of the effort was aimed at defining an appropriate set of independent variables that could be used for prediction. In addition, several of the independent variables were highly correlated; for example, the 80th and 85th percentile depths.

The SAS/STAT® software was applied to conduct the regression analyses. A number of other independent variables were investigated if they showed potential for use in the model but were highly correlated. The effects of multicollinearity among independent variables were detected using orthogonality tests in SAS/STAT. For example, the AALA is highly correlated to exposure; therefore, a normalized dependent variable was developed by dividing the AALA in 2040 by the total exposure. This normalized variable is the fraction of the exposure corresponding to the avoided losses.

The remaining independent variables were individually regressed against the dependent variable using linear stepwise least-squares regression (the GLM Procedure in SAS/STAT 9.3) to determine which were the most explanatory. Additionally, variables considered to be related to watershed size were normalized by the watershed area. Area of new development and area of redevelopment were highly correlated; therefore, these variables were added and normalized dividing the sum by the watershed area to produce a new variable that represents the fraction of a watershed that would be developed with GI. The stepwise regression procedure yielded the multivariate models described below:

2-year zero-damage threshold ($R^2 = 0.56$)

$$\frac{AALA_{2006}}{E_{2006}} = \exp\left(-0.313 + 3.944\left[\frac{A_N + A_R}{A}\right]^{0.5} + 0.2086\,HS\right) - 1 \qquad (8\text{-}1)$$

5-year zero-damage threshold ($R^2 = 0.65$)

$$\frac{AALA_{2006}}{E_{2006}} = \exp\left(-1.4353 + 3.1298\left[\frac{A_N + A_R}{A}\right]^{0.5} + 0.1865\,HS + 2.6285\,RI\right) - 1 \qquad (8\text{-}2)$$

10-year zero-damage threshold ($R^2 = 0.66$)

$$\frac{AALA_{2006}}{E_{2006}} = \exp\left(-0.7496 + 2.0992\left[\frac{A_N + A_R}{A}\right]^{0.5} + 0.2339\,HS - 0.0184\,R\right) - 1 \qquad (8\text{-}3)$$

where:

$AALA_{2006}$ is the avoided flood losses in 2006 in millions of dollars (2006 dollars)

E_{2006} is the total exposure in 2006 in millions of dollars (2006 dollars)

A_N is the area of new development in 2040 (mi^2)

A_R is the area of redevelopment in 2040 (mi^2)

A is the watershed area (mi^2)

HS is the rainfall depth of the 100-year storm (in)

R is the average annual rainfall (in)

RI is the ratio of the 100-year storm depth to annual average rainfall depth (dimensionless)

These equations can be applied to other watersheds that were not modeled to estimate the losses avoided. To evaluate the flood losses avoided in a watershed not modeled, its known values of E_{2006}, A_R, A_N, A, HS, RI, and R were used in the regression equations to estimate the value of $AALA_{2006}$. The SAS/STAT printouts for these regression equations can be found in Appendix G.

The limitations of the study did not allow modeling of more than 20 watersheds, which results in a small sample of data points to conduct regression analyses. Ideally, with a larger number of data points, a portion of the dataset could be set aside to verify the results of the regression using the remainder of the dataset. In this study it was decided that removal of some of the 20 data points would deteriorate the resulting regressions equations. However, this is an exercise that could be done if additional resources become available to model more watersheds in the future.

The following sections describe various adjustments needed to complete the analysis. The following are two terms that will be used in the subsequent discussion:

E_{2040} = Total exposure in the year 2040 (2011 dollars)

$AALA_{2040}$ = Average annualized losses avoided in the year 2040 (2011 dollars)

8.1. Economic Growth

The results from the regression equations need to be modified to make them consistent with other analyses that require the benefits to be expressed in 2011 dollars. This correction was made using the Engineering News Record construction index. In 2006, the average value of the index was 7751;

in 2011 the value was 9070. Therefore, the results need to be multiplied by 9070/7751 = 1.17 to convert the $AALA_{2006}$ to 2011 dollars

Another adjustment is needed to consider the additional value of construction. The losses from Hazus reflect the infrastructure that was built in 2006. Since the study period extends between 2020 and 2040, the additional value of construction between 2006 and 2040 needs to be considered in the calculations. EPA provided projections of new construction values added between 2016 and 2040 for four land uses: commercial, industrial, single-family residential, and multi-family residential (in 2011 dollars). Figure 8–1 shows the total value of new construction within the top 40 HUC4s expected to experience the greatest amount of growth.

An important consideration is the expected vulnerability of new construction as well as existing construction to floods. In principle, new construction will comply with floodplain regulations and will not suffer damages during events less severe than the local design standard, which often requires that the first floor be above the 100-year water surface elevation. This expectation would imply that the value of new construction should not be included in the calculations. Factors suggesting that new construction, as well as existing construction, will not be free of flood risk are presented in Section 6.3. For these reasons, this study assumed that future construction is still exposed to flood risks. In principle, damages could decrease due to better building codes and the effect could be evaluated in a future study by assuming fewer assets exposed to flooding in the floodplains.

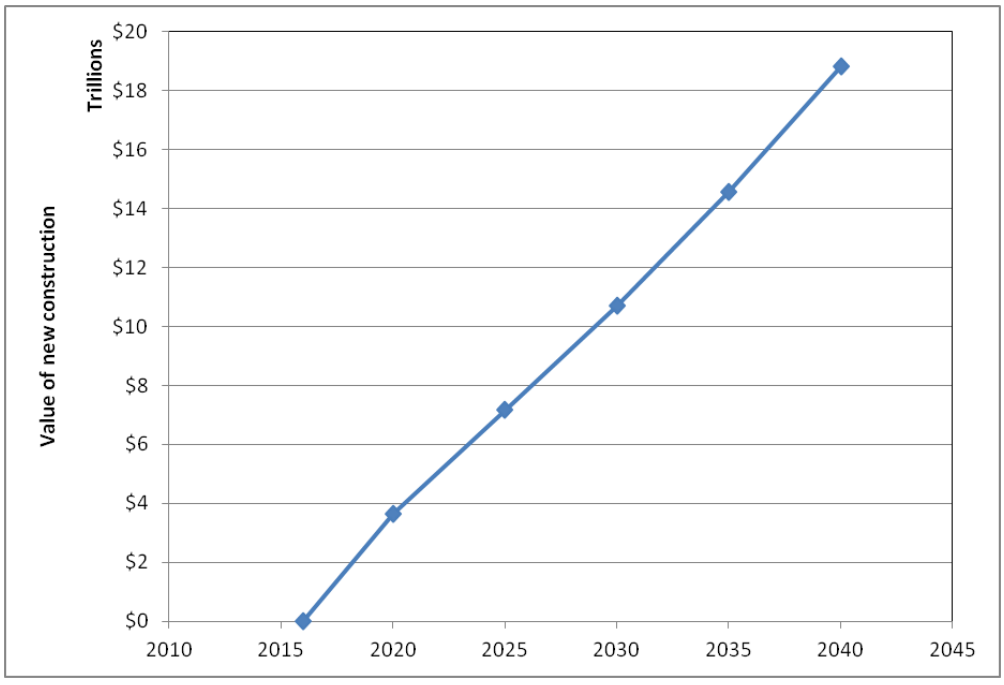

Figure 8–1. Variation of total new construction projected in the 40 top-growth HUC4s (2011 dollars).

A constant annual growth rate was assumed to determine the total value of construction between 2006 and 2040, as shown in Figure 8–1. In each watershed, the annual growth rate is calculated as the total value of construction in 2040 divided by 24, which is the number of years between 2016 and 2040. The total exposure in 2040 (in 2011 dollars) is then

$$E_{2040} = (1.17 \times 10^6)\, E_{2006} + 34 \frac{\sum C_j}{24} \tag{8-4}$$

where ΣC_j is the cumulative value of new construction between 2016 and 2040 for each of four land uses j: commercial, industrial, single-family residential, and multi-family residential (2011 dollars). The factor 1.17×10^6 accounts for the conversion to 2011 dollars and the fact that E_{2006} is expressed in millions of dollars in the regressions equations. The factor of 34 multiplying the summation is the number of years between 2006 and 2040.

Furthermore, it is assumed that the benefits are directly proportional to the exposure. Therefore, the *AALA* in 2040 (expressed in 2011 dollars) is

$$AALA_{2040} = 1.17\, AALA_{2006} \left[\frac{E_{2040}}{(1.17 \times 10^6) E_{2006}} \right] \tag{8-5}$$

where $AALA_{2040}$ is the avoided flood losses in 2040 (corrected by the 1.17 factor to obtain 2011 dollars). Using Eqn. 8-4, this expression becomes

$$AALA_{2040} = 1.17\, AALA_{2006} \left[\frac{(1.17 \times 10^6) E_{2006} + 34 \frac{\sum C_j}{24}}{(1.17 \times 10^6) E_{2006}} \right] \tag{8-6}$$

which results in

$$AALA_{2040} = 1.17\, AALA_{2006} \left[1 + 1.21 \frac{\sum C_j}{(1 \times 10^6) E_{2006}} \right] \tag{8-7}$$

8.2. Scale-Up Procedure

The scale-up was performed in three regions: 1) the 40 top-growth HUC4 watersheds, from which jurisdictions have been removed that have already implemented stormwater management policies based on GI; 2) the conterminous United States after removing jurisdictions that have already implemented stormwater management policies based on GI; and 3) the conterminous United States.

The scale-up procedure applies the regression Eqns. 8-1, 8-2, and 8-3 to each HUC8 in each scale-up region to estimate the benefits in 2040 for each assumption of the zero-damage threshold (in 2006

dollars). The results are modified using Eqn. 8-7 to account for the conversion to 2011 dollars and the additional new construction between 2006 and 2040. Because of the potential for over-estimation associated with the 2-year zero-damage threshold, results are shown only for the 5- and 10-year zero-damage thresholds.

The results of this procedure are presented in Figure 8–2 and Figure 8–3.

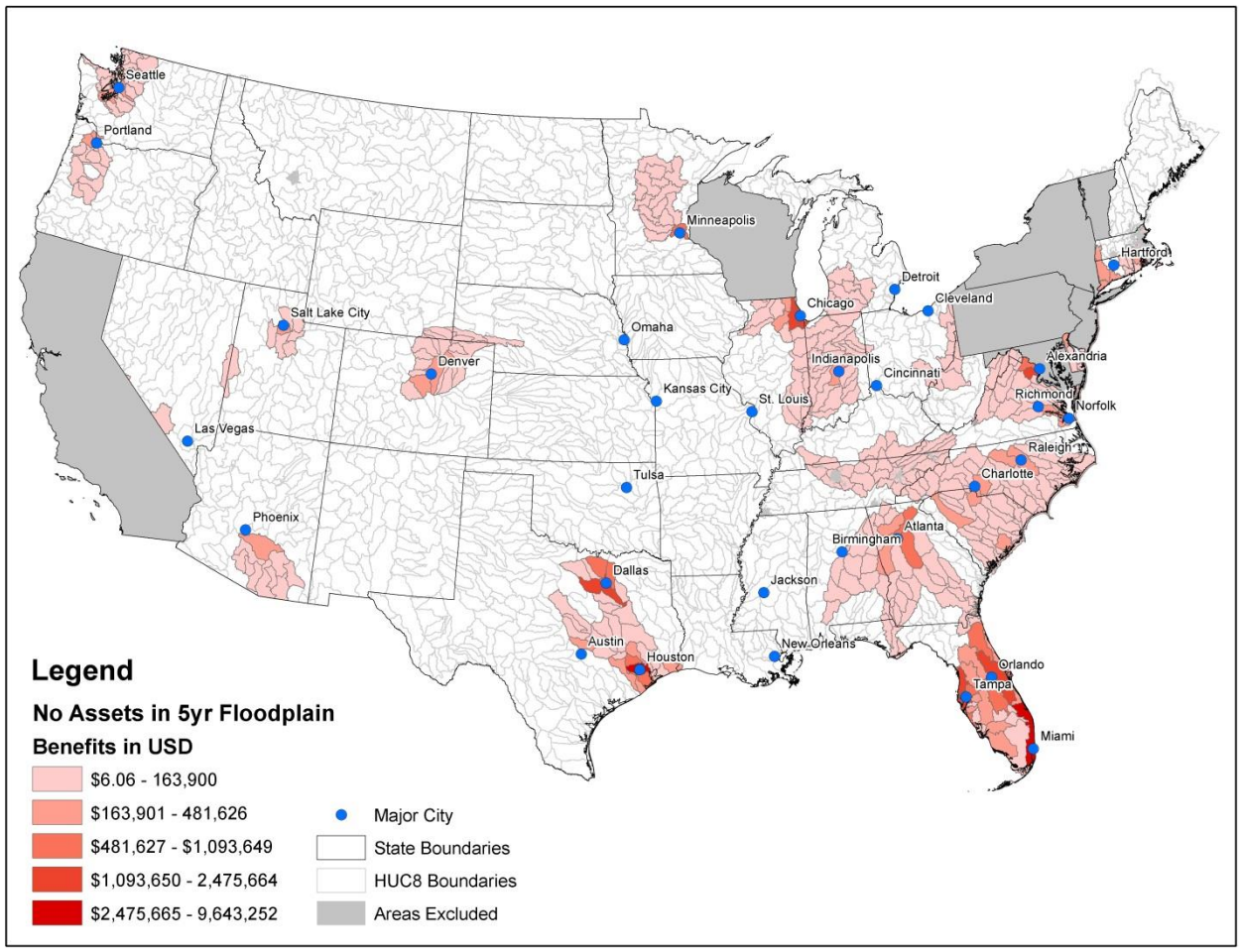

Figure 8–2. Distribution of the AALA in 2040 in the 40 top-growth HUC4s using the 5-year zero-damage threshold (2011 dollars).

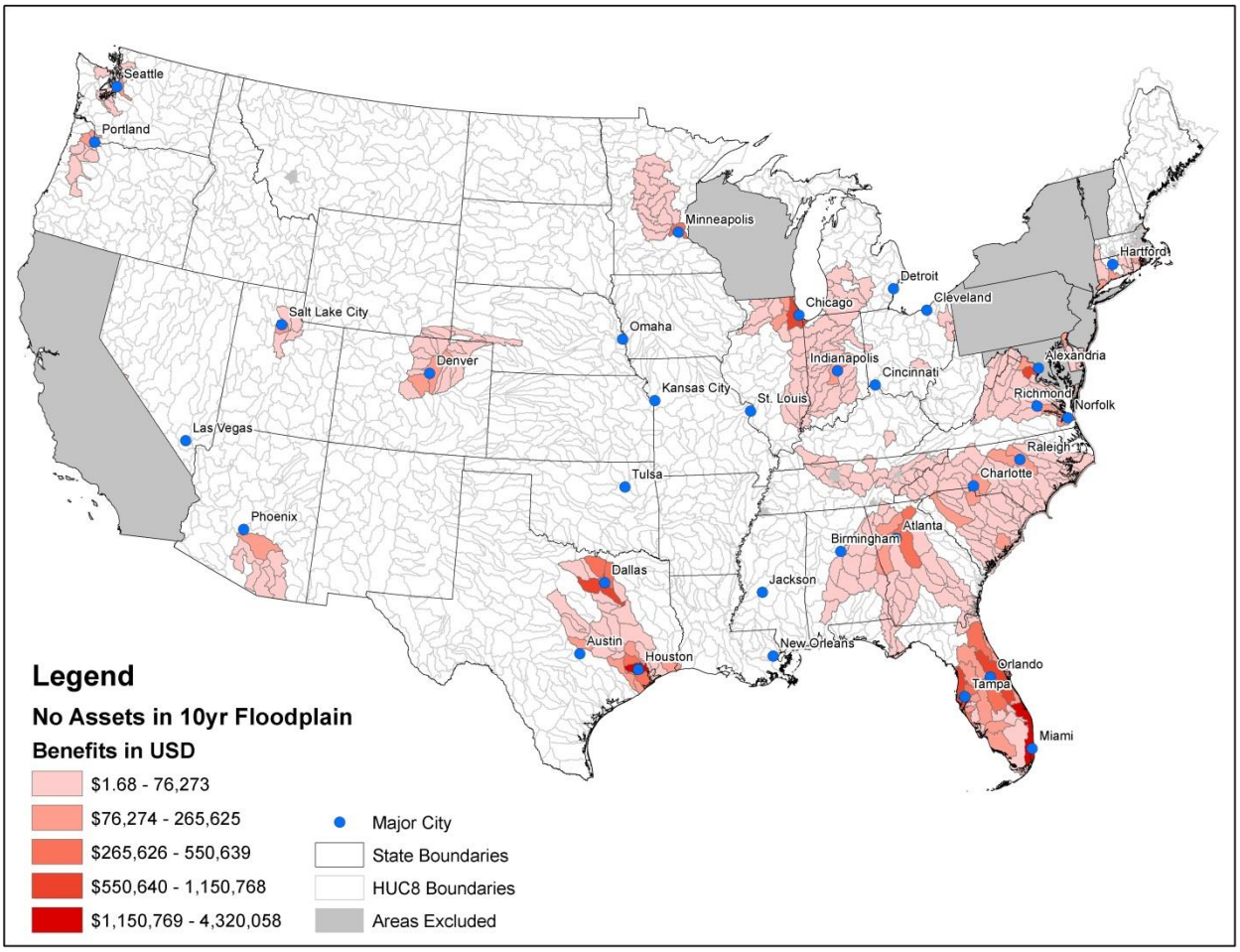

Figure 8–3. Distribution of the AALA in 2040 in the 40 top-growth HUC4s using the 10-year zero-damage threshold (2011 dollars).

The total losses avoided in the year 2040 in the 40 top-growth HUC4s are:

5-year zero-damage threshold: $94 million

10-year zero-damage threshold: $44 million

The analysis was also extended to all of the lower 48 states, excluding those jurisdictions that already have a GI-based retention in place. Figure 8–4 and Figure 8–5 illustrate the results.

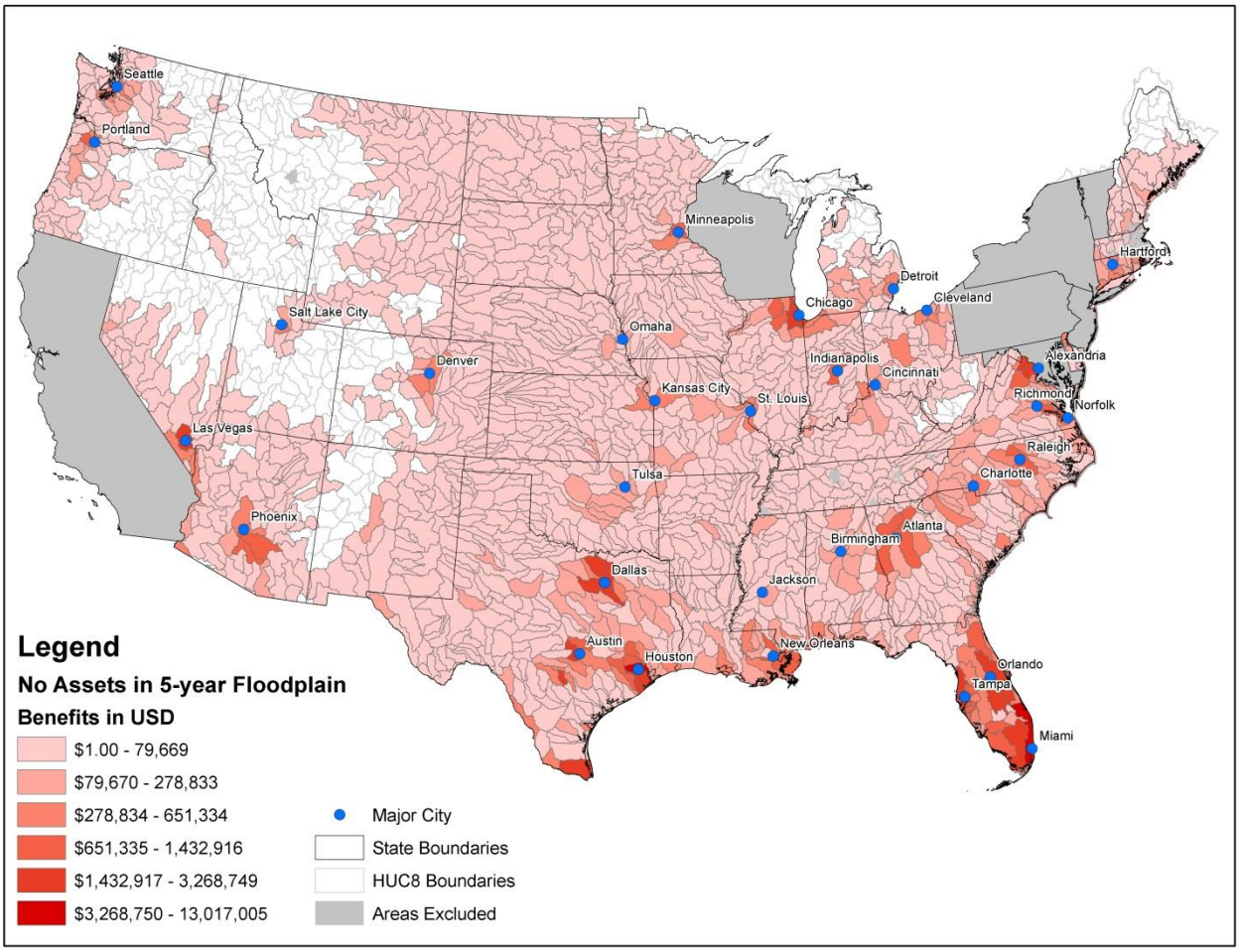

Figure 8–4. Distribution of AALA in 2040 in the conterminous United States using the 5-year zero-damage threshold, excluding jurisdictions with GI-based retention standards (2011 dollars).

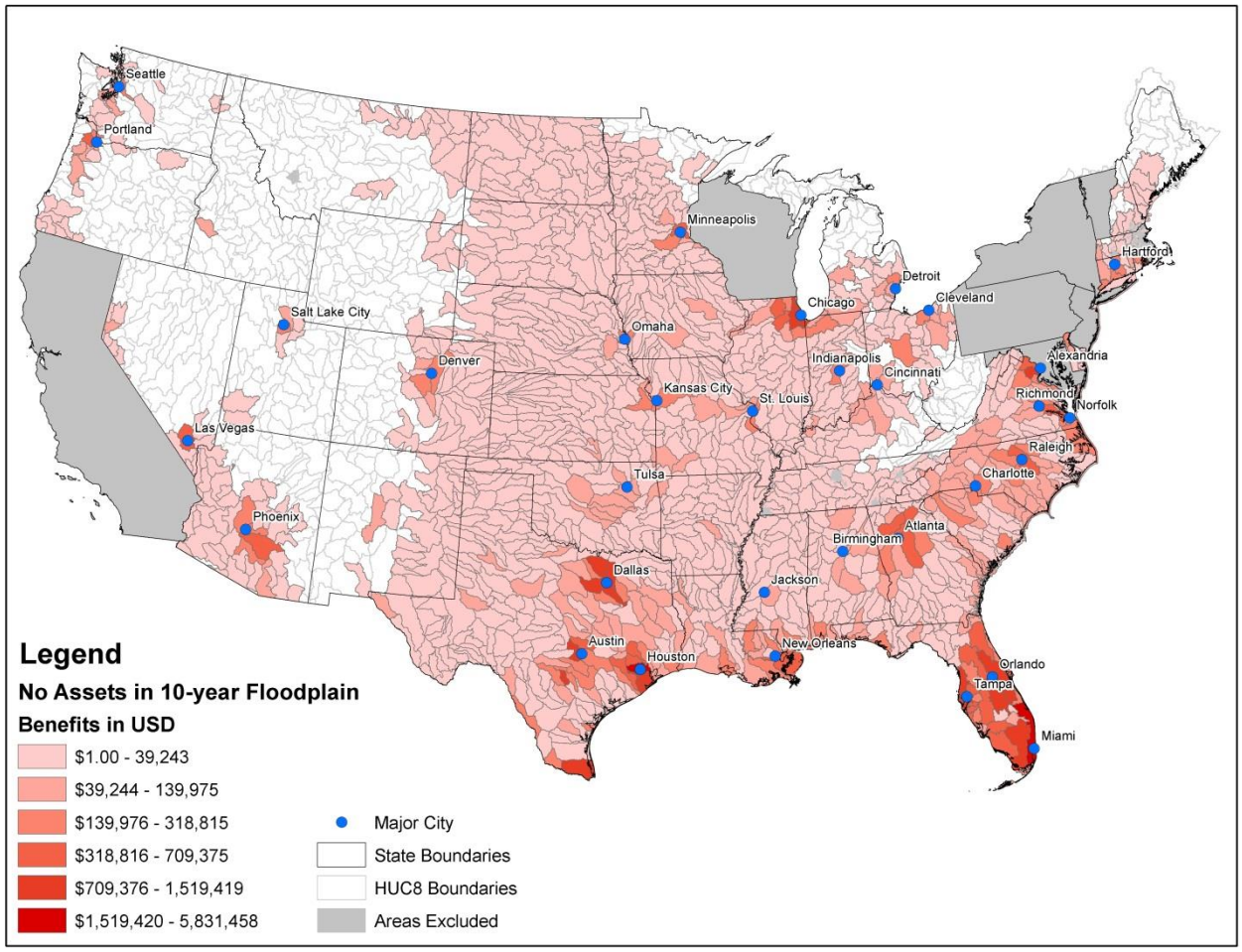

Figure 8–5. Distribution of AALA in 2040 in the conterminous United States using the 10-year zero-damage threshold, excluding jurisdictions with GI-based retention standards (2011 dollars).

The sequence of maps shows how large regions of the western states receive no benefits as more assets are assumed nonexistent in the floodplain. The total losses avoided nationwide in the year 2040 are:

5-year zero-damage threshold: $136 million

10-year zero-damage threshold: $63 million

As reference, the benefits to the nation (in the lower 48 states) of of using stormwater retention practices on new and redevelopment can also be estimated including those jurisdictions that already have retention policies in place. The results are summarized in Figure 8–6 and Figure 8–7.

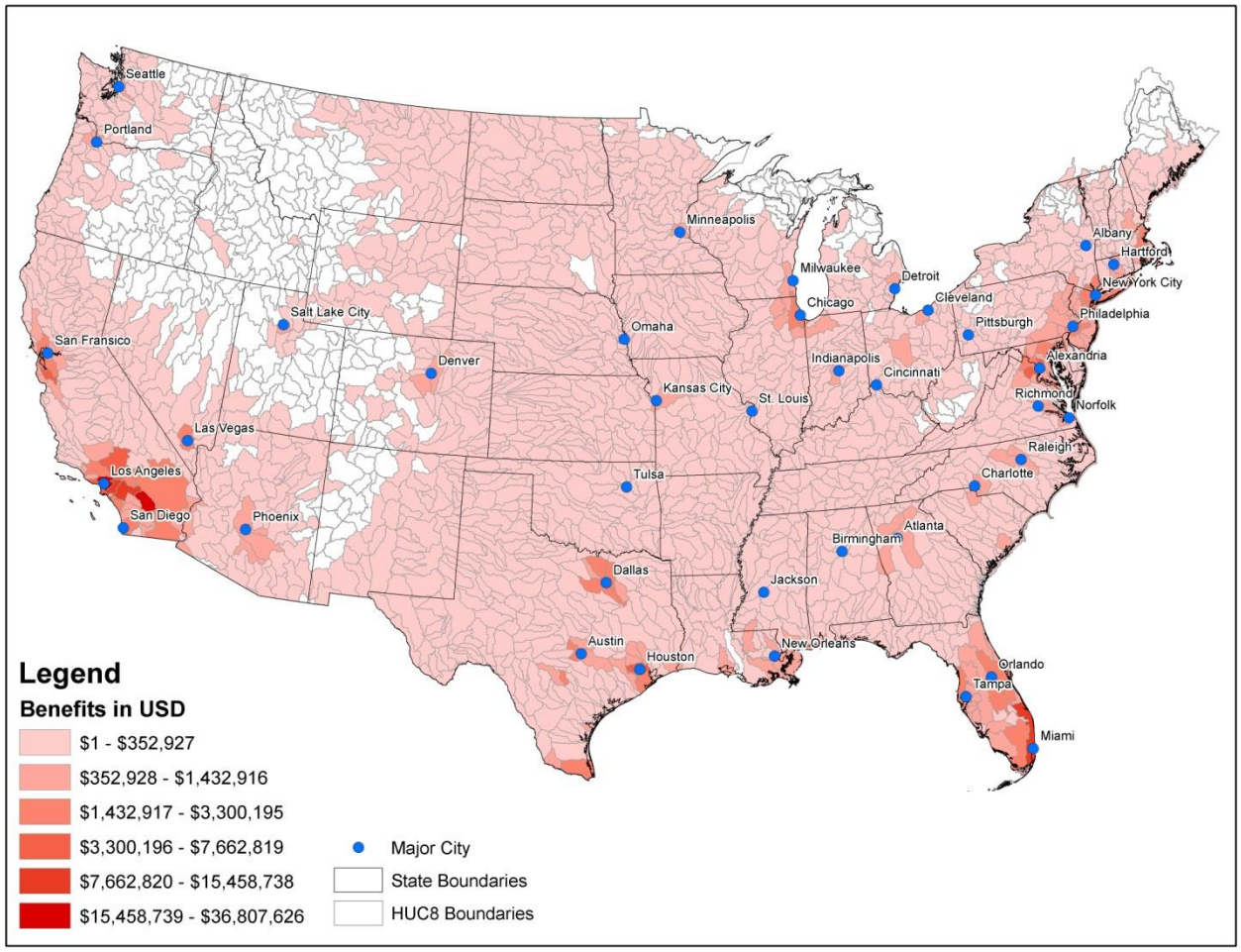

Figure 8–6. Distribution of AALA in 2040 in the conterminous United States using the 5-year zero-damage threshold (2011 dollars).

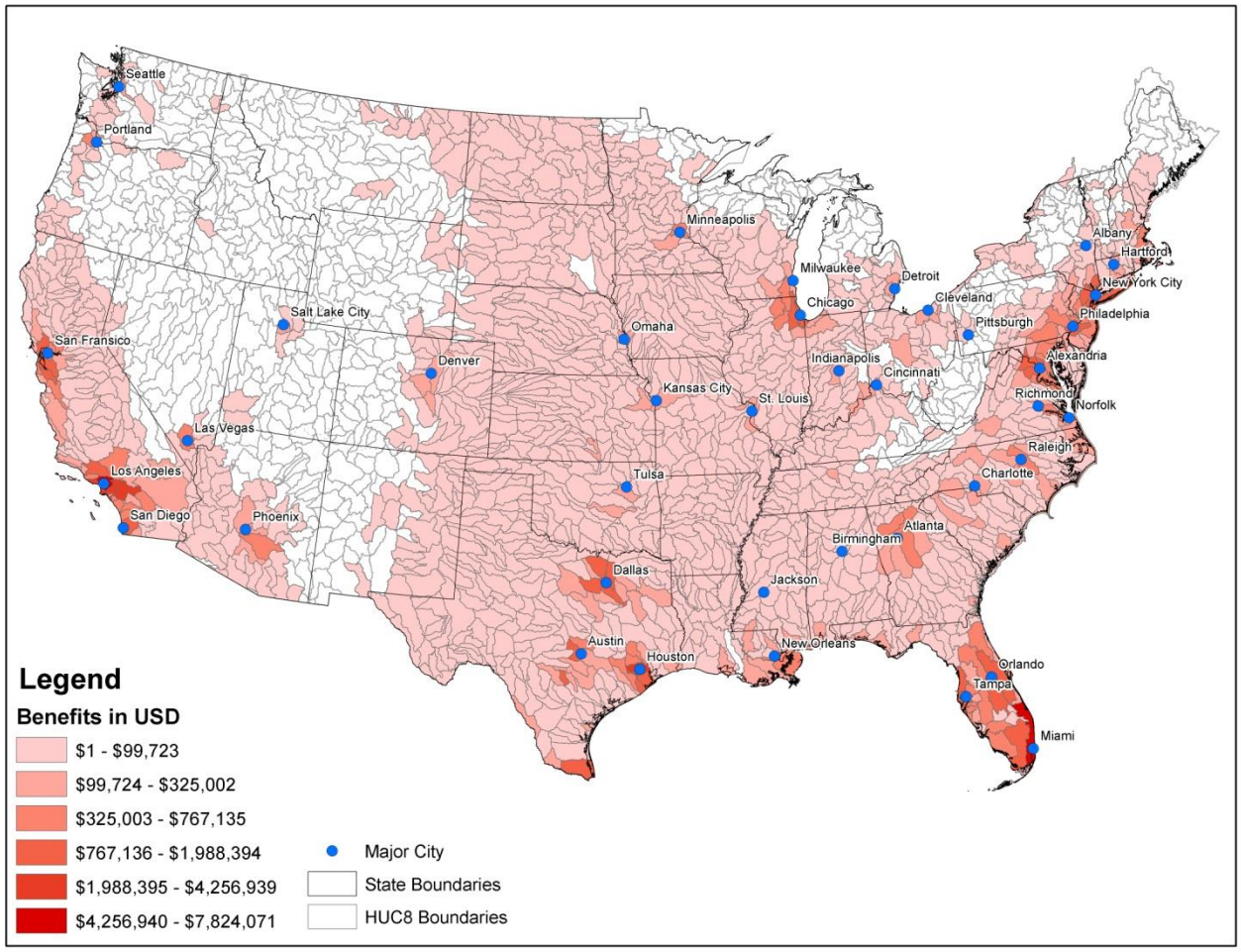

Figure 8–7. Distribution of AALA in 2040 in the conterminous United States using the 10-year zero-damage threshold (2011 dollars).

The total losses avoided nationwide in the year 2040 are:

5-year zero-damage threshold: $328 million

10-year zero-damage threshold: $114 million

8.3. Present Value Calculations

Avoided losses take place every year between 2020 and 2040. Therefore, it is useful to estimate the present value of all of these losses avoided during that period. In the subsequent discussion the following terms are used:

$AALA_t$ = Average annualized losses avoided in the year t, which varies depending on the year (2011 dollars)

PV = Present value in 2020 of the series of $AALA_t$ (2011 dollars)

$AALA_{eq}$ = Annual value of an equivalent uniform series that would yield the same present value PV (2011 dollars). In other words, $AALA_{eq}$ is a uniform series equivalent to the nonuniform series of $AALA_t$.

The procedure to derive the present value of the series of $AALA_t$ consists of the following steps:

1. Estimate the AALA for each year between 2020 and 2040 using a linear variation between zero in 2020 and the values in 2040 summarized in the previous Section. The linear variation is consistent with the assumed rate of increase in new construction shown in Figure 8–1. These linear streams of benefits are shown in Figure 8–8 through Figure 8–10 and the values for the 5-year and 10-year zero-damage thresholds are tabulated in Appendix H.

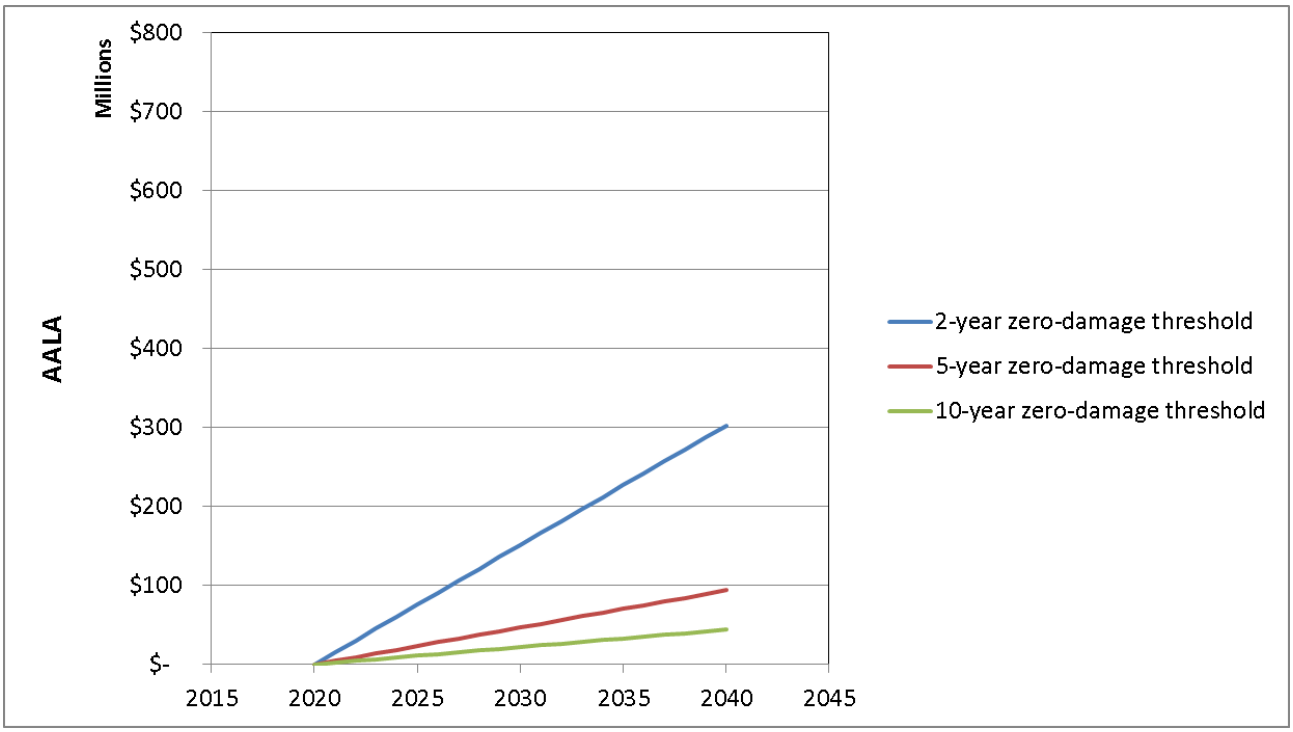

Figure 8–8. Assumed variation of the AALA in the 40 top-growth HUC4s between 2020 and 2040 (2011 dollars).

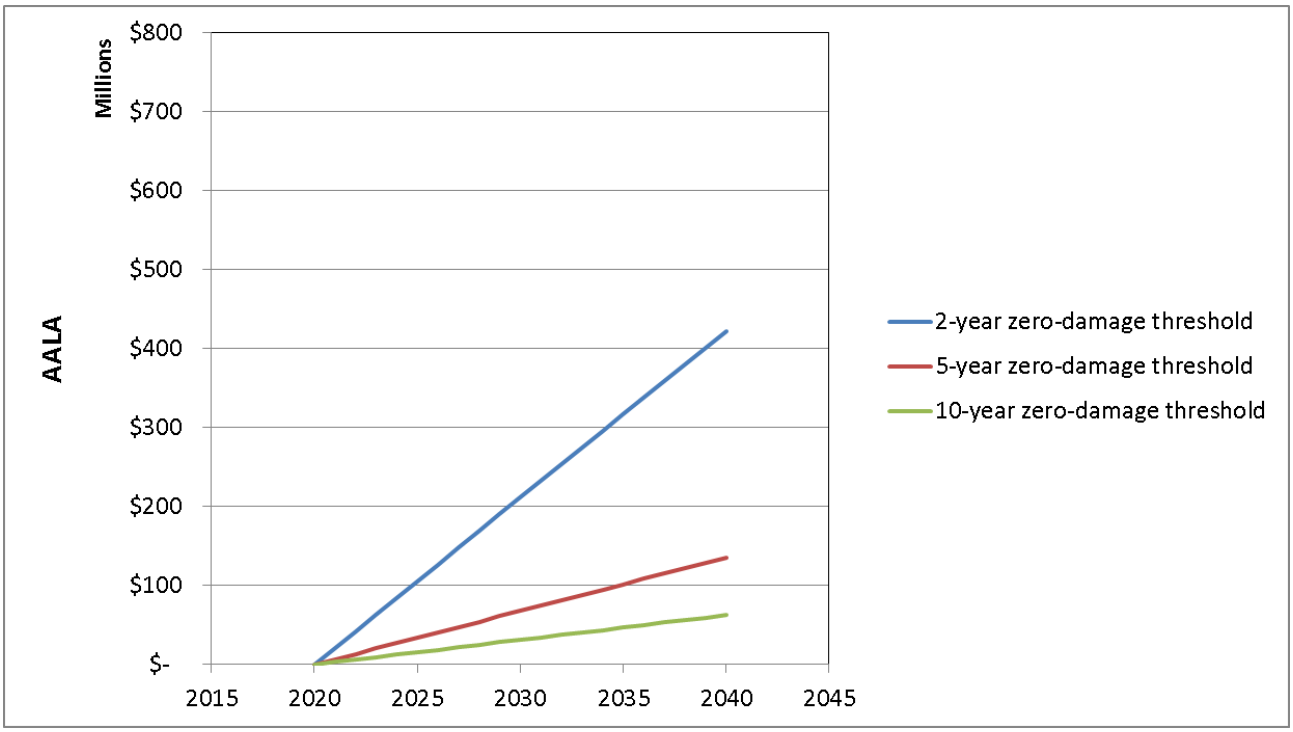

Figure 8–9. Assumed variation of the AALA in the conterminous United States between 2020 and 2040, excluding jurisdictions with GI-based retention standards (2011 dollars).

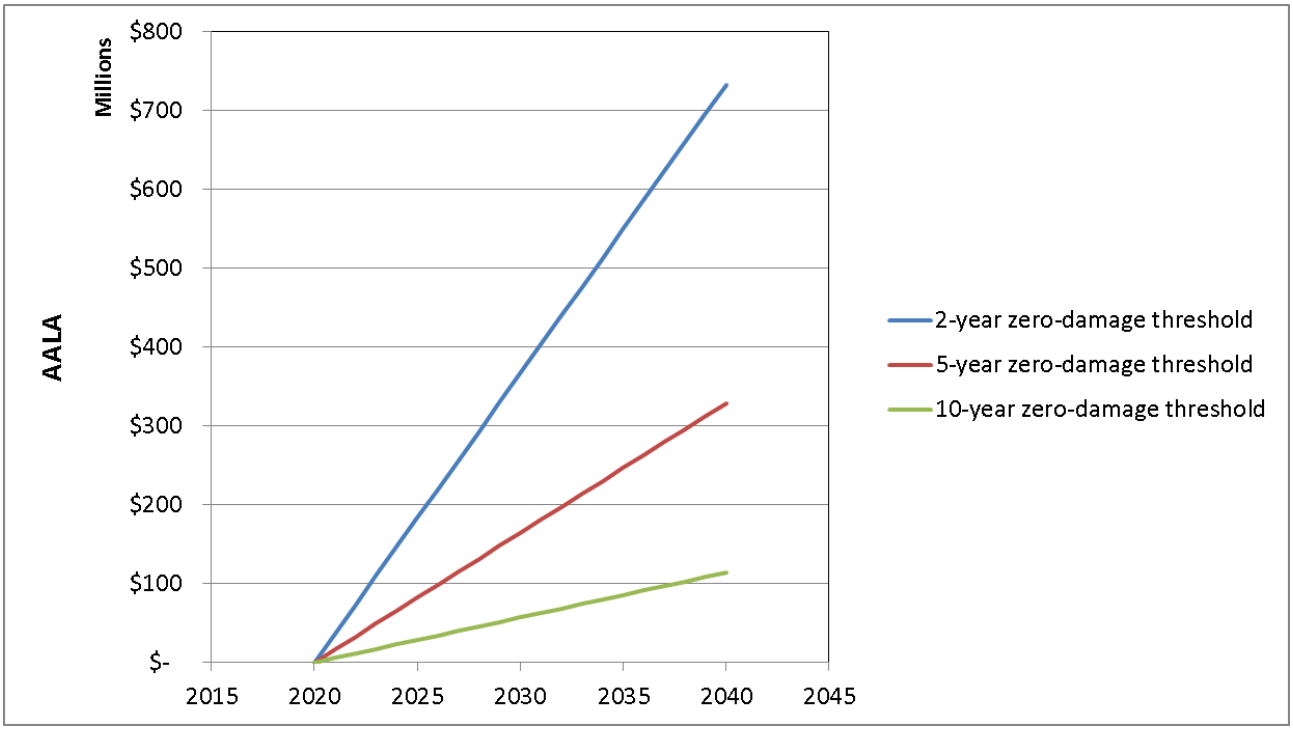

Figure 8–10. Assumed variation of the AALA in the conterminous United States between 2020 and 2040 (2011 dollars).

2. Estimate the present value of the series of AALAs in 2020

$$PV = \sum_{t=0}^{20} \frac{AALA_t}{(1+i)^t}$$

$AALA_t$ is the value interpolated for the t-th year, where 2020 is year zero and 2040 is the 20th year, and i is the annual discount rate.

3. Estimate the value of an equivalent uniform series over the 2020-2040 period

$$AALA_{eq} = PV \frac{i}{1-(1+i)^{-20}}$$

The results are summarized in Table 8–1 for the 5-year and 10-year zero damage threshold assumptions and using two discount rates.

Table 8–1. Summary of AALA for three geographic extents, expressed as present value and as an equivalent annual series using two discount rates (in 2011 dollars).

	i = 3%		*i* = 7%	
	PV in 2020 (billions)	***$AALA_{eq}$ (millions)***	***PV in 2020 (billions)***	***$AALA_{eq}$ (millions)***
40 top-growth HUC4s				
5-year zero-damage threshold	$0.7	$45	$0.4	$39
10-year zero-damage threshold	$0.3	$21	$0.2	$18
Conterminous United States, excluding jurisdictions with retention standards				
5-year zero-damage threshold	$1.0	$65	$0.6	$56
10-year zero-damage threshold	$0.4	$30	$0.3	$26
Conterminous United States, including jurisdictions with retention standards				
5-year zero-damage threshold	$2.3	$157	$1.4	$137
10-year zero-damage threshold	$0.8	$54	$0.5	$48

9. Conclusions and Recommendations for Methodology Improvements

GI can reduce flood losses when applied watershed-wide as an ancillary benefit to GI's main objective of water quality protection. Estimation of the avoided losses in dollars is problematic because tools and datasets that exist on a national scale lack the resolution to reliably predict flooding extents and asset value impacts for a change in an inch or two of rainfall. This study used Hazus to quantify conceptually the potential for avoiding flood losses through the application of GI on new development and redevelopment, although not as retrofits to existing imperviousness in urban areas. The methodology proposed in this study makes use of national public datasets that have accuracy limitations. In particular, the assumption of uniformly distribute assets across Census blocks in Hazus can diverge considerably from reality. Nevertheless, the methodology is useful for this type of comparative study in estimating changes in floodplain area and avoided losses.

Deployment of GI led to a general reduction in the total floodplain area for all of the 20 HUC8 watersheds modeled. As expected, the reduction was greater for the small, frequent events. For the 2-year event, the floodplain area decreased by as much as 8%, whereas for the 100-year event the greatest reduction was around 2.5%.

This study indicates that the annual savings to the nation in terms of flood losses avoided in 2040 for expanding stormwater retention practices range from $63 to $136 million (2011 dollars). This figure includes the conterminous United States, excluding jurisdictions that already have GI-based retention policies in place. Assuming that the benefits start at zero in 2020 and a discount rate of 3%, the corresponding present value of the stream of benefits in the following 20 years ranges from $0.4 and $1 billion (2011 dollars). Averaged over the 20 years between 2020 and 2040, the benefits range between $30 and $65 million per year.

9.1. Limitations of the Study

There are many sources of uncertainty in a study of this nature. The findings suggest that the resolution of the terrain model, the horizontal and vertical location of assets at risk, and the expected patterns of future development are the most sensitive variables. The following is a summary of the major limitations:

- A small number of watersheds were modeled. A regression model based on only 20 modeled watersheds may not be sufficiently representative for a nationwide scale-up. This is potentially the largest source of uncertainty in the study.

- The linear approach to adjust current peak flows to 2040 conditions is an approximation that needs to be validated further. There is no substitute for a properly calibrated model; therefore, any hydrologic approximation invariably introduces errors.
- The resolution of the NED dataset is not as accurate as LiDAR terrain data in defining the horizontal extent of flooding, and also leads to significant uncertainty in the flood depths affecting infrastructure.
- The lack of bathymetric data precludes adequate definition of the main channel of the streams. This shortcoming of the terrain dataset results in less conveyance in the stream network, which forces water that would stay in the main channel otherwise to spill onto the floodplain. Therefore, the assumption may make flood hazards appear worse, especially for the less severe events.
- The uniform distribution of assets in Census blocks artificially places assets at risk of flooding. Specific locations of buildings and other infrastructure yield the most accurate damage estimates. Lack of this information may overestimate the damages for frequent flood events.
- The estimates only include buildings, their contents, and the associated income loss. Consideration of roads, bridges, utilities, and other critical infrastructure would increase the estimates of losses avoided.
- Localized flooding commonly occurring in urban areas due to deficient drainage was not considered, although it may be one aspect of urban flooding that GI can address effectively. The calculation underestimates losses avoided in these circumstances.
- General building stock (GBS) datasets include default first-floor elevations that are assumed to correspond to the various occupancy classes in the software. Actual first-floor elevations can be obtained only if a UDF approach were used.
- Lack of detailed information on levees, diversions, dams, pumping stations, and other flood control works overestimates flood hazards and possibly the losses avoided.
- Forecasts of future new development and redevelopment are by nature uncertain; this uncertainty propagates to the avoided loss estimates. It is not possible to infer the effect of this uncertainty on increasing or decreasing the losses avoided.
- The benefits were assumed not to propagate from one HUC8 watershed to the next one directly downstream. If they had, the losses avoided would be greater.
- The regression analysis used some of the watershed properties in Table 3–2 as independent variables. There could be statistically significant correlations between the AALA and several of the other watershed properties in the table, for example, stream length or watershed aspect ratio. However, these properties are not readily available as a national dataset; therefore, they would not be usable for extrapolation to other watersheds.

All of the limitations listed above affect the accuracy of absolute estimates of flood losses. However, because this study compares the with- and without-GI conditions, the effect on the flood losses avoided is expected to be less.

The analysis presented herein generally informs the effect of a GI-based stormwater management policy at the national scale; however, the methodology can be readily adapted to regional and jurisdiction-specific analysis with detailed data.

The following section proposes enhancements for methodology improvements.

9.2. Recommendations for Methodology Improvements

If better accuracy were needed, future studies could address the following elements, all of which require datasets with better resolution:

- Analysis of additional watersheds to support a robust statistical analysis that validates and improves the prediction of the regression models.
- Hydrologic modeling and calibration on each subwatershed modeled to better predict the impact of infiltration and evapotranspiration from GI deployment on peak flows, as well as to validate the linear approximation to adjust current peak flows to 2040 conditions.
- Additional datasets to expand the scope of the validations in Section 7.
- Additional set of validations to evaluate the effect of roughness coefficients and more accurate topography and bathymetry to better define flow in stream channels.
- Detailed analysis of the effects of flood control works: dams, levees, pump stations, and diversions.
- Additional studies with detailed building stock information at the watershed level, and using regional depth-damage curves.
- Sensitivity analyses in individual watersheds to assess the uncertainty introduced by model variables, in addition to those considered in this study, on output quantities such as runoff volume, peak flows, water surface elevations and flood depth, and flood-loss estimates. These analyses can be used to assess the potential cumulative impact of uncertainties on the flood-loss avoidance estimates.
- Propagation of GI benefits to downstream watersheds.
- Effect of building codes on new construction as the regulations are updated with new levels of flood hazard.
- Consideration of climate change.

10. References

Barnes, H. H. 1967. *Roughness characteristics of natural channels*. USGS Water Supply Paper: 1849.

Braden, J.B., and D.M. Johnston. 2004. "Downstream economic benefits from storm-water management." *Journal of Water Resources Planning and Management*, 130(6): 498–505.

Chow, V. T. 1959. *Open Channel Hydraulics*. McGraw-Hill. 680 p.

Department of Water Resources. 2013. California Awareness Floodplain Maps. http://www.water.ca.gov/floodmgmt/lrafmo/fmb/fes/awareness_floodplain_maps/ (last accessed May 22, 2013).

Eng, K., G. D. Tasker, and P. C. D. Milly. 2005. "An analysis of region-of-influence methods for flood regionalization in the Gulf-Atlantic rolling plains." *Journal of the American Water Resources Association*. 41(1), p. 135-143.

Environmental Protection Agency. 2014. *Rivers and Streams*. http://water.epa.gov/type/rsl/ (last accessed November 5, 2014).

Federal Emergency Management Agency. 2009a. *Guidelines and Specification for Flood Hazard Mapping Partners. Appendix C: Guidance for Riverine Flooding Analyses and Mapping*. November. Washington, DC.

———. 2009b. *Flood Insurance Study, Douglas County, Minnesota, and Incorporated Areas*.

———. 2010. *Flood Insurance Study, Bexar County, Texas, and Incorporated Areas*.

———. 2011a. *Flood Insurance Study, Steele County, Minnesota, and Incorporated Areas*.

———. 2011b. *Flood Insurance Study, Todd County, Minnesota, and Incorporated Areas*.

———. 2011c. *Guidelines and Specification for Flood Hazard Mapping Partners. Appendix A: Guidance for Aerial Mapping and Surveying*. November. Washington, DC.

———. 2012. *Flood Insurance Study, Rice County, Minnesota, and Incorporated Areas*.

———. 2013a. *Hazus: The Federal Emergency Management Agency's (FEMA's) Methodology for Estimating Potential Losses from Disasters*. http://www.fema.gov/hazus (last accessed May 20, 2013).

———. 2013b. *Flood Insurance Study, Mille Lacs County, Minnesota, and Incorporated Areas*.

———. 2013c. *Flood Insurance Study, Forsyth County, Georgia, and Incorporated Areas*.

———. 2014. *CNMS: Coordinated Needs Management Strategy*. https://hazards.fema.gov/cnms/ (last accessed November 5, 2015).

Hinman, C. 2012. *Low Impact Development: Technical Guidance Manual for Puget Sound*. Prepared for the Puget Sound Partnership. Publication No. PSP–2012-3. Puyallup, Washington. 365 p.

Illinois Department of Natural Resources. 2015. Report for the Urban Flooding Awareness Act. https://www.dnr.illinois.gov/WaterResources/Documents/Final_UFAA_Report.pdf (last accessed November 13, 2015).

Johnston, D.M., J.B. Braden, and T.H. Price. (2006). "Downstream Economic Benefits of Conservation Development." *Journal of Water Resources Planning & Management*, 132(1): 35–43.

Kousky, C., S. Olmstead, M. Walls, A. Stern, and M. Macauley. 2011. *The Role of Land Use in Adaptation to Increased Precipitation and Flooding: A Case Study in Wisconsin's Lower Fox River Basin*. Resources for the Future report. Washington, DC.

Lorenz, D. L., C. A. Sanocki, and M. J. Kocian. 2009. *Techniques for Estimating the Magnitude and Frequency of Peak Flows on Small Streams in Minnesota Based on Data through Water Year 2005*. USGS Scientific Investigations Report 2009-5250.

Medina, D.E., J. Monfils, and Z. Baccala. 2011. "Green Infrastructure Benefits for Floodplain Management: A Case Study," *Stormwater Magazine*, November- December.

Milwaukee Metropolitan Sewer District. 2005. *Surface Water and Storm Water Rules Guidance Manual*. Appendix L. http://www.mmsd.com//media/MMSD/Documents/Rules%20and%20Regs/Manuals/Appendix_L.pdf (last accessed, November 6, 2014).

National Oceanic and Atmospheric Administration. 2013. *Precipitation Frequency Data Server*. http://hdsc.nws.noaa.gov/hdsc/pfds/index.html (last accessed May 150, 2013).

National Research Council. 2009. *Urban Stormwater Management in the United States.* National Academy Press. Washington, DC.

Natural Resources Defense Council. 1999. *Stormwater Strategies: Community Responses to Runoff Pollution*. http://www.nrdc.org/water/pollution/storm/stoinx.asp (last accessed May 17, 2013).

NIST/SEMATECH. 2012. *e-Handbook of Statistical Methods*, http://www.itl.nist.gov/div898/handbook/ (last accessed July 5, 2013).

Taylor W. J. 2013. *Stormwater Management Program Effectiveness Literature Review: Low Impact Development Techniques*. Prepared for Association of Washington Cities and Washington State Department of Ecology. http://www.ecy.wa.gov/programs/wq/psmonitoring/ps_monitoring_docs/SWworkgroupDOCS/LIDWhitePaperFinalApril2013.pdf (last accessed May 157, 2013).

U.S. Army Corps of Engineers. 2010. *Hydrologic Modeling System HEC-HMS*. http://www.hec.usace.army.mil/software/hec-hms/documentation.aspx (last accessed July 3, 2013).

U.S. Department of Agriculture. 1986. *Urban Hydrology for Small Watersheds*. Technical Release 55. Natural Resources Conservation Service, Conservation Engineering Division. Washington, DC.

U.S. Environmental Protection Agency. 2007. BASINS (Better Assessment Science Integrating point & Non-point Sources). http://water.epa.gov/scitech/datait/models/basins/index.cfm (last accessed May 20, 2013).

U.S. Geological Survey. 2007. PeakFQ: Flood Frequency Analysis Based on Bulletin 17B. http://water.usgs.gov/software/PeakFQ/ (last accessed May 21, 2013)

———. 2011. NSS, Version 6: National Streamflow Statistics. http://water.usgs.gov/software/NSS/ (last accessed May 21, 2013)

Zomorodi, K. 2007. "Effectiveness of time of concentration elongation on peak flow reduction." Proceedings of the 2nd National Low Impact Development Conference. North Carolina State University. March 12-14. Wilmington, NC.

Appendix A

Rain Percentiles for Selected Locations

COOP Station ID	Station Name	County	State	99%	95%	90%	85%	80%	75%	70%	65%	60%
10063	ADDISON	Winston	AL	3.70	2.10	1.60	1.30	1.10	0.97	0.85	0.75	0.67
10140	ALBERTA	Wilcox	AL	4.00	2.20	1.60	1.40	1.15	1.00	0.90	0.80	0.70
10831	BIRMINGHAM MUNI AP	Jefferson	AL	3.27	1.93	1.46	1.20	1.04	0.90	0.80	0.70	0.61
12124	DADEVILLE 2	Tallapoosa	AL	3.50	2.00	1.50	1.30	1.10	0.90	0.80	0.70	0.60
14064	HUNTSVILLE/MADISON CO., AL.	Madison	AL	3.39	2.00	1.49	1.24	1.04	0.90	0.78	0.69	0.61
14209	JACKSONVILLE	Calhoun	AL	3.10	1.92	1.46	1.20	1.00	0.90	0.80	0.70	0.60
15478	MOBILE/BATES FIELD, AL.	Mobile	AL	4.44	2.42	1.80	1.45	1.22	1.02	0.89	0.76	0.65
15550	MONTGOMERY/DANNELLY, AL.	Montgomery	AL	3.47	2.01	1.51	1.25	1.08	0.92	0.78	0.68	0.60
20487	ASH FORK	Yavapai	AZ	1.90	1.10	0.80	0.69	0.60	0.50	0.41	0.40	0.34
24645	KINGMAN NO 2	Mohave	AZ	2.10	1.20	0.90	0.80	0.60	0.60	0.50	0.50	0.40
26323	PAYSON	Gila	AZ	2.50	1.50	1.10	0.90	0.75	0.67	0.60	0.50	0.45
26481	PHOENIX/SKY HARBOR INTL, AZ.	Maricopa	AZ	1.58	1.02	0.80	0.67	0.57	0.50	0.43	0.38	0.34
28820	TUCSON/INT., AZ.	Pima	AZ	1.87	1.10	0.82	0.66	0.55	0.49	0.43	0.38	0.34
29439	WINSLOW	Navajo	AZ	1.28	0.75	0.59	0.48	0.43	0.38	0.34	0.31	0.28
29660	YUMA INTL AP	Yuma	AZ	2.17	1.11	0.70	0.58	0.52	0.45	0.39	0.35	0.31
30220	ARKADELPHIA 2 N	Clark	AR	3.70	2.30	1.80	1.44	1.20	1.03	0.90	0.80	0.70
30458	BATESVILLE LIVESTOCK	Independence	AR	3.35	2.10	1.60	1.30	1.10	0.93	0.80	0.70	0.61
32356	EUREKA SPRINGS 3 WNW	Carroll	AR	2.92	1.91	1.46	1.20	1.01	0.90	0.80	0.70	0.60
32574	FORT SMITH/MUN., AR.	Sebastian	AR	3.22	1.92	1.46	1.20	0.99	0.84	0.73	0.64	0.57
32794	GILBERT	Searcy	AR	3.21	1.95	1.45	1.18	0.99	0.87	0.75	0.68	0.60
32810	GILLHAM	Polk	AR	4.20	2.40	1.80	1.50	1.30	1.10	0.90	0.80	0.70
34248	NORTH LITTLE ROCK/MUNICIPAL	Pulaski	AR	3.57	2.10	1.58	1.28	1.08	0.92	0.79	0.69	0.61
35754	PINE BLUFF	Jefferson	AR	3.76	2.20	1.70	1.40	1.20	1.00	0.90	0.78	0.66
36920	STUTTGART 9 ESE	Arkansas	AR	3.40	2.20	1.69	1.30	1.10	0.97	0.86	0.76	0.70
40161	ALTURAS	Modoc	CA	1.26	0.72	0.59	0.50	0.40	0.40	0.32	0.30	0.30
42910	EUREKA, CA.	Humboldt	CA	2.22	1.37	1.04	0.88	0.76	0.66	0.58	0.52	0.46
43257	FRESNO/AIR TERM., CA.	Fresno	CA	1.52	0.97	0.80	0.68	0.57	0.50	0.44	0.40	0.35
44232	INDEPENDENCE	Inyo	CA	2.60	1.30	0.90	0.70	0.65	0.54	0.50	0.40	0.35

COOP Station ID	Station Name	County	State	99%	95%	90%	85%	80%	75%	70%	65%	60%
45114	LOS ANGELES/INT., CA.	Los Angeles	CA	2.73	1.60	1.26	1.02	0.82	0.72	0.65	0.56	0.49
47740	SAN DIEGO/LINDBERGH, CA.	San Diego	CA	1.96	1.25	0.96	0.78	0.65	0.57	0.51	0.44	0.39
47769	SAN FRANCISCO/INTL, CA.	San Mateo	CA	2.13	1.39	1.08	0.89	0.75	0.65	0.58	0.50	0.44
48873	TERMO 1 E	Lassen	CA	1.30	0.80	0.60	0.49	0.40	0.38	0.32	0.30	0.28
50304	ARAPAHOE	Cheyenne	CO	2.40	1.30	0.93	0.80	0.70	0.60	0.50	0.44	0.40
51179	BYERS 5 ENE	Adams	CO	2.00	1.20	0.83	0.70	0.60	0.50	0.43	0.40	0.35
53477	GRANADA	Prowers	CO	2.40	1.40	1.00	0.80	0.69	0.60	0.50	0.44	0.40
53488	GRAND JUNCTION/WALKER F.,CO.	Mesa	CO	0.92	0.61	0.50	0.42	0.36	0.31	0.28	0.26	0.24
57337	SAGUACHE	Saguache	CO	1.04	0.64	0.50	0.44	0.40	0.36	0.30	0.30	0.30
60806	BRIDGEPORT SIKORSKY	Fairfield	CT	2.77	1.60	1.19	0.96	0.81	0.70	0.60	0.53	0.47
63456	HARTFORD/BRADLEY INTL, CT.	Hartford	CT	2.72	1.60	1.25	1.01	0.85	0.74	0.63	0.56	0.49
65445	NORFOLK 2 SW	Litchfield	CT	2.81	1.69	1.26	1.04	0.89	0.77	0.66	0.58	0.51
73570	GEORGETOWN 5 SW	Sussex	DE	2.90	1.70	1.30	1.10	0.90	0.80	0.70	0.60	0.54
79595	WILMINGTON NEW CASTLE CNTY AP	New Castle	DE	2.51	1.62	1.22	0.99	0.85	0.75	0.66	0.58	0.50
80211	APALACHICOLA/MUN., FL.	Franklin	FL	4.76	2.39	1.71	1.40	1.16	0.99	0.85	0.74	0.64
80975	BRANFORD	Suwannee	FL	4.10	2.20	1.55	1.29	1.09	0.90	0.80	0.70	0.60
82158	ORLANDO/JETPORT, FL.	Volusia	FL	3.51	2.03	1.49	1.20	1.00	0.86	0.75	0.64	0.56
83186	FORT MYERS PAGE FLD	Lee	FL	3.89	2.30	1.70	1.40	1.20	1.00	0.90	0.80	0.68
84570	KEY WEST/INT., FL.	Monroe	FL	3.70	1.92	1.41	1.09	0.87	0.74	0.64	0.55	0.48
85612	MELBOURNE REGIONL AP	Brevard	FL	3.70	2.10	1.51	1.30	1.10	0.90	0.80	0.70	0.60
85663	MIAMI, FL.	Dade	FL	3.94	2.20	1.58	1.28	1.05	0.87	0.73	0.63	0.55
90435	ATHENS	Clarke	GA	3.19	1.85	1.41	1.18	1.00	0.85	0.74	0.66	0.57
90495	AUGUSTA/BUSH FIELD, GA.	Richmond	GA	2.86	1.77	1.36	1.10	0.92	0.80	0.70	0.61	0.54
91619	CARNESVILLE 4 N	Franklin	GA	3.20	1.95	1.50	1.28	1.07	0.90	0.80	0.70	0.60
92166	COLUMBUS METRO AP	Muscogee	GA	3.22	1.90	1.46	1.18	0.99	0.85	0.75	0.65	0.57
92485	DALLAS 7 NE	Paulding	GA	3.20	1.98	1.42	1.20	1.00	0.90	0.80	0.70	0.60
93028	EDISON	Calhoun	GA	3.33	2.15	1.60	1.30	1.10	0.90	0.80	0.70	0.60
95443	MACON/LEWIS B.WILSON,GA.	Bibb	GA	2.96	1.86	1.37	1.13	0.94	0.80	0.70	0.62	0.55
96879	PEARSON	Atkinson	GA	3.30	2.00	1.50	1.29	1.10	0.90	0.80	0.70	0.60
97847	SAVANNAH/MUNICIPAL, GA.	Chatham	GA	3.42	1.95	1.42	1.18	0.98	0.85	0.75	0.65	0.58

COOP Station ID	Station Name	County	State	99%	95%	90%	85%	80%	75%	70%	65%	60%
101022	BOISE/MUN., ID.	Ada	ID	0.91	0.61	0.49	0.42	0.36	0.32	0.29	0.26	0.24
101079	BONNERS FERRY	Boundary	ID	1.48	0.90	0.70	0.59	0.50	0.42	0.40	0.36	0.30
103143	FENN	Idaho	ID	1.58	1.00	0.80	0.68	0.60	0.50	0.45	0.40	0.40
103677	GOODING 1 S	Gooding	ID	1.05	0.80	0.60	0.50	0.44	0.40	0.39	0.30	0.30
103811	GRASMERE 3 S	Owyhee	ID	1.16	0.80	0.60	0.50	0.40	0.40	0.30	0.30	0.30
104456	IDAHO FALLS 16 SE	Bonneville	ID	1.10	0.70	0.60	0.50	0.40	0.40	0.33	0.30	0.30
105169	LEADORE	Lemhi	ID	1.10	0.60	0.50	0.40	0.37	0.30	0.30	0.28	0.25
105241	LEWISTON NEZ PERCE	Nez Perce	ID	1.00	0.62	0.48	0.41	0.36	0.32	0.29	0.26	0.24
107211	POCATELLO/NUM., ID.	Power	ID	0.94	0.63	0.50	0.42	0.37	0.33	0.30	0.27	0.24
107327	PRAIRIE	Elmore	ID	1.90	1.05	0.80	0.68	0.58	0.50	0.40	0.40	0.35
110082	ALEXIS 1 SW	Warren	IL	2.67	1.60	1.20	0.97	0.80	0.70	0.60	0.55	0.50
111577	CHICAGO	Cook	IL	2.59	1.50	1.10	0.90	0.78	0.66	0.60	0.50	0.45
112353	DIXON SPRINGS AGR CE	Pope	IL	3.05	1.82	1.40	1.15	0.99	0.81	0.70	0.62	0.60
114198	HOOPESTON 1 NE	Vermilion	IL	2.40	1.50	1.10	0.90	0.80	0.70	0.60	0.50	0.50
115751	MOLINE/QUAD CITY, IL.	Rock Island	IL	2.56	1.56	1.16	0.96	0.81	0.69	0.59	0.52	0.46
115983	MURPHYSBORO 2 SW	Jackson	IL	3.10	1.74	1.39	1.10	0.96	0.81	0.70	0.65	0.60
116159	NEWTON 6 SSE	Jasper	IL	2.50	1.60	1.20	1.00	0.90	0.80	0.70	0.60	0.52
116711	PEORIA/GREATER PEORIA, IL.	Peoria	IL	2.50	1.47	1.12	0.93	0.78	0.66	0.58	0.50	0.45
118179	SPRINGFIELD/CAPITAL, IL.	Sangamon	IL	2.71	1.47	1.11	0.90	0.77	0.66	0.58	0.51	0.44
120132	ALPINE 2 NE	Fayette	IN	2.35	1.46	1.12	0.92	0.80	0.70	0.60	0.53	0.50
120482	BATESVILLE WATERWORK	Ripley	IN	2.56	1.50	1.17	1.00	0.82	0.70	0.63	0.60	0.50
120922	BRAZIL	Clay	IN	2.90	1.61	1.20	1.00	0.90	0.80	0.70	0.60	0.50
122738	EVANSVILLE/REG., IN.	Vanderburgh	IN	2.70	1.70	1.26	1.03	0.87	0.77	0.67	0.60	0.52
123037	FORT WAYNE/MUN.,BAER FL.,IN.	Allen	IN	2.09	1.30	1.00	0.82	0.69	0.60	0.53	0.46	0.41
124259	INDIANAPOLIS/I.-MUN/WEI.,IN.	Marion	IN	2.45	1.47	1.11	0.91	0.78	0.67	0.58	0.52	0.46
125535	MEDARYVILLE	Pulaski	IN	2.50	1.50	1.10	0.90	0.77	0.70	0.60	0.50	0.49
126580	OOLITIC PURDUE EXP F	Lawrence	IN	2.70	1.60	1.23	1.05	0.90	0.80	0.70	0.60	0.54
128187	SOUTH BEND/ST.JOSEPH CO.,IN.	Saint Joseph	IN	2.15	1.33	1.00	0.80	0.68	0.59	0.51	0.45	0.40
130608	BELLEVUE L AND D 12	Jackson	IA	2.60	1.54	1.15	0.98	0.80	0.70	0.60	0.57	0.50
131245	CARSON	Pottawattamie	IA	3.03	1.86	1.32	1.06	0.90	0.80	0.70	0.60	0.50

COOP Station ID	Station Name	County	State	99%	95%	90%	85%	80%	75%	70%	65%	60%
132195	DERBY	Lucas	IA	2.96	1.63	1.20	1.00	0.84	0.74	0.62	0.60	0.50
132203	DES MOINES/MUN., IA.	Polk	IA	2.51	1.50	1.12	0.91	0.77	0.67	0.58	0.51	0.45
136975	REMSEN	Plymouth	IA	2.80	1.50	1.19	0.97	0.80	0.70	0.60	0.52	0.50
137602	SHELL ROCK 2 W	Butler	IA	2.60	1.50	1.10	0.92	0.80	0.70	0.60	0.50	0.47
137708	SIOUX CITY/MUN., IA.	Woodbury	IA	2.41	1.35	1.05	0.87	0.73	0.63	0.55	0.49	0.43
138009	STRAWBERRY POINT	Clayton	IA	2.57	1.52	1.15	0.93	0.80	0.70	0.60	0.53	0.48
138688	WASHINGTON	Washington	IA	2.70	1.60	1.20	1.00	0.80	0.70	0.60	0.53	0.50
141351	CASSODAY	Butler	KS	3.06	1.80	1.40	1.15	1.00	0.82	0.75	0.69	0.60
141730	COLLYER 10 S	Trego	KS	2.39	1.40	1.10	0.90	0.77	0.66	0.55	0.50	0.43
141767	CONCORDIA/BLOSSER MUN., KS.	Cloud	KS	2.47	1.60	1.19	0.97	0.80	0.68	0.60	0.53	0.47
142164	DODGE CITY/MUN., KS.	Ford	KS	2.55	1.44	1.05	0.86	0.72	0.62	0.53	0.47	0.41
143153	GOODLAND/RENNER FIELD/, KS.	Sherman	KS	2.24	1.27	0.95	0.74	0.63	0.54	0.48	0.42	0.38
143810	HORTON	Brown	KS	3.00	1.90	1.40	1.10	0.94	0.80	0.70	0.60	0.52
144178	KANOPOLIS LAKE	Ellsworth	KS	2.85	1.70	1.30	1.07	0.90	0.80	0.70	0.60	0.50
148167	TOPEKA/MUN., KS.	Shawnee	KS	2.83	1.78	1.35	1.07	0.89	0.76	0.66	0.58	0.51
148830	WICHITA, KS.	Sedgwick	KS	2.65	1.76	1.31	1.10	0.92	0.78	0.68	0.59	0.52
151080	BUCKHORN LAKE	Perry	KY	2.28	1.44	1.10	0.90	0.78	0.69	0.60	0.53	0.47
151631	CLINTON 4 S	Hickman	KY	3.30	1.90	1.43	1.20	1.00	0.90	0.79	0.70	0.60
154746	LEXINGTON/BLUE GRASS, KY.	Fayette	KY	2.60	1.50	1.15	0.94	0.80	0.69	0.61	0.55	0.49
154954	LOUISVILLE/STANDIFORD, KY.	Jefferson	KY	2.54	1.51	1.16	0.95	0.81	0.72	0.63	0.56	0.50
160549	BATON ROUGE RYAN AP	East Baton Rouge	LA	4.10	2.30	1.68	1.36	1.12	0.96	0.84	0.73	0.63
165021	LAFAYETTE	Lafayette	LA	4.50	2.70	2.00	1.50	1.28	1.10	0.94	0.80	0.70
165078	LAKE CHARLES/MUN., LA.	Calcasieu	LA	4.42	2.55	1.81	1.47	1.23	1.02	0.88	0.75	0.65
165266	LEESVILLE	Vernon	LA	4.20	2.40	1.70	1.40	1.20	1.01	0.90	0.80	0.70
166660	NEW ORLEANS/MOISANT INT., LA	Jefferson	LA	4.21	2.40	1.77	1.44	1.20	1.01	0.88	0.76	0.67
168440	SHREVEPORT/REG., LA.	Caddo	LA	3.42	2.16	1.63	1.32	1.11	0.96	0.83	0.71	0.62
169357	VIDALIA 2	Concordia	LA	4.24	2.55	1.80	1.50	1.29	1.10	0.96	0.82	0.73
169803	WINNFIELD 2 W	Winn	LA	3.90	2.30	1.80	1.40	1.20	1.10	0.90	0.80	0.70
169806	WINNSBORO 5 SSE	Franklin	LA	4.00	2.30	1.78	1.46	1.22	1.10	0.90	0.80	0.70
171175	CARIBOU/MUN., ME.	Aroostook	ME	1.80	1.06	0.83	0.70	0.61	0.53	0.46	0.41	0.36

COOP Station ID	Station Name	County	State	99%	95%	90%	85%	80%	75%	70%	65%	60%
176905	PORTLAND/INTNL. JET PORT, ME	Cumberland	ME	2.83	1.62	1.20	0.97	0.82	0.72	0.63	0.55	0.48
178641	SWANS FALLS	Oxford	ME	2.51	1.60	1.20	1.00	0.87	0.73	0.64	0.57	0.50
180465	BALTIMORE/BALTIMO-WASHINGT	Anne Arundel	MD	2.53	1.62	1.23	0.99	0.84	0.74	0.65	0.57	0.50
180470	BALTIMORE CITY	Baltimore city	MD	2.80	1.72	1.28	1.05	0.89	0.77	0.68	0.60	0.53
183090	FEDERALSBURG	Caroline	MD	3.50	1.90	1.40	1.10	1.00	0.90	0.80	0.70	0.60
184030	HANCOCK	Washington	MD	2.20	1.30	1.08	0.90	0.76	0.69	0.60	0.50	0.44
186915	PATUXENT RIVER	St. Mary's	MD	3.40	2.00	1.40	1.10	0.90	0.80	0.70	0.60	0.50
188005	SALISBURY WICOMICO	Wicomico	MD	2.37	1.86	1.14	0.92	0.78	0.68	0.57	0.52	0.48
188315	SINES DEEP CREEK	Garrett	MD	1.80	1.16	0.91	0.74	0.64	0.56	0.50	0.45	0.40
190736	BLUE HILL OBS., MA.	Norfolk	MA	2.85	1.75	1.30	1.08	0.90	0.78	0.68	0.59	0.51
190770	BOSTON/LOGAN INT., MA	Suffolk	MA	2.64	1.57	1.19	0.96	0.82	0.71	0.62	0.55	0.49
193985	KNIGHTVILLE DAM	Hampshire	MA	2.85	1.68	1.24	1.00	0.85	0.73	0.64	0.56	0.50
200164	ALPENA PHELPS COL AP	Alpena	MI	1.73	1.04	0.81	0.66	0.56	0.49	0.43	0.38	0.34
200662	BELLAIRE	Antrim	MI	1.80	1.10	0.80	0.70	0.60	0.50	0.50	0.40	0.40
202846	FLINT/BISHOP, MI.	Genesee	MI	1.95	1.16	0.85	0.71	0.60	0.53	0.46	0.41	0.36
203170	GLADWIN	Gladwin	MI	2.00	1.40	1.00	0.80	0.70	0.60	0.51	0.50	0.40
203333	GRAND RAPIDS/KENT CO., MI.	Kent	MI	2.30	1.33	1.00	0.82	0.69	0.60	0.52	0.46	0.40
203580	HARBOR BEACH	Huron	MI	2.00	1.10	0.82	0.70	0.60	0.50	0.44	0.40	0.37
204090	IRON MTN-KINGSFORD W	Dickinson	MI	2.00	1.20	0.90	0.79	0.67	0.60	0.50	0.45	0.40
204155	JACKSON 3 N	Jackson	MI	1.90	1.26	1.00	0.80	0.70	0.60	0.50	0.50	0.40
205712	MUSKEGON/COUNTY, MI.	Muskegon	MI	1.93	1.15	0.86	0.71	0.59	0.51	0.44	0.39	0.35
207366	SAULT STE. MARIE, MI.	Chippewa	MI	1.60	1.02	0.77	0.62	0.53	0.46	0.41	0.36	0.32
210112	ALEXANDRIA CHANDLER	Douglas	MN	2.11	1.31	1.01	0.83	0.70	0.60	0.52	0.46	0.40
212248	DULUTH/INT.,MN.	Saint Louis	MN	2.31	1.31	1.00	0.79	0.66	0.58	0.49	0.42	0.38
214026	INT.FALLS/FALLS INT.MN.	Koochiching	MN	2.22	1.14	0.82	0.68	0.57	0.50	0.44	0.39	0.33
215435	MINNEAPOLIS/ST.PAUL INTL,MN.	Hennepin	MN	2.24	1.33	1.00	0.80	0.69	0.57	0.50	0.44	0.38
215987	NORTHFIELD 2 NNE	Dakota	MN	2.50	1.42	1.10	0.90	0.73	0.64	0.60	0.50	0.48
217004	ROCHESTER/MUN., MN.	Olmsted	MN	2.32	1.44	1.02	0.85	0.71	0.62	0.53	0.47	0.41
217294	ST. CLOUD/WHITNEY, MN.	Sherburne	MN	2.45	1.39	1.01	0.83	0.68	0.59	0.52	0.46	0.40
218235	THIEF LAKE REFUGE	Marshall	MN	2.40	1.30	1.00	0.80	0.65	0.56	0.50	0.41	0.40

COOP Station ID	Station Name	County	State	99%	95%	90%	85%	80%	75%	70%	65%	60%
218323	TRACY	Lyon	MN	2.50	1.40	1.09	0.90	0.72	0.63	0.60	0.50	0.43
221743	CLEVELAND 3 N	Bolivar	MS	3.80	2.30	1.80	1.40	1.20	1.02	0.90	0.80	0.70
225062	LEXINGTON 2 NNW	Holmes	MS	3.80	2.23	1.70	1.40	1.18	1.00	0.90	0.78	0.69
225776	MERIDIAN/KEY, MS.	Lauderdale	MS	3.50	2.12	1.56	1.30	1.11	0.96	0.82	0.70	0.61
227220	PURVIS 2 N	Lamar	MS	3.80	2.30	1.76	1.40	1.20	1.03	0.90	0.80	0.70
227714	RUTH 1 SE	Lincoln	MS	3.90	2.35	1.77	1.43	1.20	1.05	0.90	0.80	0.70
227815	SARDIS DAM	Panola	MS	3.78	2.16	1.60	1.32	1.12	1.00	0.84	0.73	0.64
227840	SAUCIER EXP FOREST	Harrison	MS	4.40	2.50	1.85	1.50	1.28	1.06	0.90	0.80	0.70
228374	STATE UNIVERSITY	Oktibbeha	MS	3.40	2.11	1.60	1.30	1.10	1.00	0.86	0.75	0.70
228445	STONEVILLE EXP STN	Washington	MS	3.45	2.10	1.69	1.40	1.14	1.00	0.85	0.75	0.67
229003	TUPELO C D LEMONS AP	Lee	MS	3.70	2.13	1.60	1.30	1.10	0.95	0.81	0.71	0.63
233999	HORNERSVILLE	Dunklin	MO	3.64	2.07	1.55	1.25	1.07	0.91	0.80	0.70	0.61
234358	KANSAS CITY, INTL, MO.	Platte	MO	3.02	1.76	1.22	1.01	0.87	0.76	0.66	0.58	0.50
235987	NEVADA WATER PLANT	Vernon	MO	3.30	1.90	1.47	1.20	1.00	0.90	0.78	0.70	0.60
237455	ST. LOUIS/LAMBERT, ST., MO.	Saint Louis	MO	2.50	1.57	1.19	0.96	0.81	0.70	0.61	0.53	0.47
237976	SPRINGFIELD/MUN., MO.	Greene	MO	2.96	1.78	1.35	1.10	0.92	0.79	0.68	0.60	0.53
238620	VIENNA 2 WNW	Maries	MO	3.05	1.74	1.40	1.11	0.97	0.81	0.70	0.61	0.55
240807	BILLINGS/LOGAN INT., MT.	Yellowstone	MT	1.46	0.85	0.62	0.51	0.44	0.39	0.34	0.31	0.28
241088	BREDETTE	Roosevelt	MT	1.60	1.02	0.80	0.65	0.53	0.46	0.40	0.35	0.30
241309	BUTTE 8 S	Silver Bow	MT	1.20	0.80	0.60	0.50	0.40	0.40	0.40	0.30	0.30
241737	CHOTEAU	Teton	MT	1.67	1.00	0.75	0.63	0.50	0.45	0.40	0.37	0.30
244055	HELENA/COUNTY-CITY, MT.	Lewis and Clark	MT	1.15	0.73	0.55	0.45	0.39	0.35	0.31	0.28	0.26
245745	MISSOULA/JOHNSON-BELL F.,MT.	Missoula	MT	1.06	0.64	0.48	0.41	0.35	0.31	0.28	0.25	0.23
248169	TERRY 21 NNW	Prairie	MT	1.90	1.06	0.80	0.63	0.53	0.47	0.40	0.35	0.30
252560	EDISON	Furnas	NE	2.22	1.41	1.10	0.90	0.80	0.70	0.60	0.50	0.47
253395	GRAND ISLAND, NE	Hall	NE	2.57	1.45	1.09	0.88	0.74	0.64	0.55	0.49	0.43
254795	LINCOLN/MUN., NE.	Lancaster	NE	2.62	1.55	1.19	0.94	0.80	0.67	0.58	0.51	0.45
255995	NORFOLK/KARL STEFAN, NE.	Madison	NE	2.49	1.48	1.11	0.88	0.72	0.60	0.53	0.46	0.41
256065	NORTH PLATTE/LEE BIRD, NE.	Lincoln	NE	2.21	1.25	0.96	0.81	0.69	0.58	0.50	0.43	0.38
257665	SCOTTSBLUFF HEILIG	Scotts Bluff	NE	1.75	0.99	0.76	0.61	0.50	0.44	0.39	0.35	0.31

COOP Station ID	Station Name	County	State	99%	95%	90%	85%	80%	75%	70%	65%	60%
258395	SYRACUSE	Otoe	NE	3.20	1.70	1.26	1.00	0.85	0.70	0.65	0.60	0.50
258760	VALENTINE MILLER FLD	Cherry	NE	2.04	1.22	0.92	0.73	0.63	0.54	0.46	0.41	0.37
262631	ELY/YELLAND, NV.	White Pine	NV	1.02	0.63	0.51	0.44	0.38	0.33	0.30	0.27	0.25
264436	LAS VEGAS/MCCARRAN, NV.	Clark	NV	1.29	0.88	0.69	0.58	0.51	0.44	0.39	0.35	0.31
268170	TONOPAH AP	Nye	NV	1.20	0.63	0.53	0.42	0.38	0.35	0.31	0.30	0.27
269171	WINNEMUCCA/MUN., NV.	Humboldt	NV	0.88	0.58	0.45	0.39	0.35	0.31	0.29	0.26	0.24
271683	CONCORD/MUN., NH.	Merrimack	NH	2.09	1.33	1.04	0.85	0.72	0.63	0.54	0.48	0.43
275639	MOUNT WASHINGTON, NH.	Coos	NH	3.14	1.77	1.27	1.02	0.86	0.74	0.64	0.55	0.48
280311	ATLANTIC CITY, NJ.	Atlantic	NJ	2.70	1.63	1.22	1.01	0.86	0.75	0.65	0.57	0.50
281351	CAPE MAY 2 NW	Cape May	NJ	2.70	1.66	1.20	1.00	0.90	0.78	0.70	0.60	0.50
286026	NEWARK INTL ARPT	Essex	NJ	2.72	1.61	1.20	0.99	0.85	0.74	0.64	0.56	0.50
290234	ALBUQUERQUE/INT.,NM.	Bernalillo	NM	1.25	0.77	0.60	0.51	0.43	0.38	0.34	0.31	0.28
290600	ARTESIA 6 S	Eddy	NM	2.60	1.30	1.00	0.78	0.68	0.60	0.50	0.43	0.40
292030	CONCHAS DAM	San Miguel	NM	2.10	1.30	1.00	0.80	0.65	0.60	0.50	0.46	0.40
292250	CUBERO	Cibola	NM	1.50	0.90	0.70	0.60	0.50	0.50	0.40	0.40	0.30
292837	EL VADO DAM	Rio Arriba	NM	1.22	0.80	0.60	0.50	0.45	0.40	0.38	0.30	0.30
293142	FARMINGTON AG SCI CT	San Juan	NM	1.00	0.70	0.60	0.50	0.40	0.40	0.40	0.30	0.30
294426	JORNADA EXP RANGE	Dona Ana	NM	1.70	1.07	0.80	0.65	0.58	0.50	0.40	0.40	0.32
297094	PROGRESSO	Torrance	NM	1.51	1.02	0.78	0.62	0.54	0.50	0.40	0.40	0.31
300042	ALBANY COUNTY AIRPORT, NY	Albany	NY	2.02	1.27	0.96	0.80	0.68	0.60	0.53	0.46	0.42
300687	BINGHAMTON/BROOME CO., NY.	Broome	NY	1.85	1.16	0.89	0.74	0.62	0.54	0.48	0.42	0.38
301185	CANTON 4 SE	Saint Lawrence	NY	1.80	1.14	0.88	0.70	0.60	0.51	0.47	0.40	0.40
303851	HIGHMARKET	Lewis	NY	2.40	1.50	1.10	0.90	0.80	0.70	0.60	0.50	0.50
303983	HORNELL ALMOND DAM	Steuben	NY	2.08	1.20	0.90	0.70	0.60	0.50	0.50	0.40	0.40
305811	NEW YORK/LA GUARDIA, NY.	New York	NY	2.80	1.68	1.22	1.00	0.85	0.73	0.64	0.56	0.50
307167	ROCHESTER/R-MONROE CTY., NY.	Monroe	NY	1.74	1.03	0.79	0.65	0.56	0.48	0.43	0.38	0.34
308383	SYRACUSE/HANCOCK, NY.	Onondaga	NY	1.88	1.13	0.85	0.70	0.60	0.51	0.46	0.40	0.35
308586	TRIBES HILL	Montgomery	NY	2.10	1.30	1.00	0.80	0.70	0.60	0.50	0.50	0.41
309389	WHITEHALL	Washington	NY	2.40	1.35	1.07	0.87	0.72	0.64	0.60	0.50	0.47
310301	ASHEVILLE	Buncombe	NC	2.25	1.37	1.00	0.82	0.69	0.60	0.54	0.47	0.43

COOP Station ID	Station Name	County	State	99%	95%	90%	85%	80%	75%	70%	65%	60%
311458	CAPE HATTERAS, NC.	Dare	NC	3.84	2.16	1.59	1.26	1.02	0.87	0.76	0.65	0.58
311690	CHARLOTTE/DOUGLAS, NC.	Mecklenburg	NC	2.65	1.67	1.25	1.01	0.86	0.74	0.66	0.57	0.51
313630	GREENSBORO/G.-HIGH PT., NC.	Guilford	NC	2.76	1.56	1.20	0.98	0.83	0.71	0.63	0.55	0.49
317069	RALEIGH/RALEIGH-DURHAM, NC.	Wake	NC	2.68	1.57	1.20	0.99	0.85	0.75	0.65	0.58	0.52
319457	WILMINGTON INTL AP	New Hanover	NC	3.83	2.19	1.56	1.24	1.05	0.89	0.77	0.65	0.57
319476	WILSON 3 SW	Wilson	NC	2.90	1.74	1.30	1.10	0.92	0.80	0.70	0.60	0.58
319675	YADKINVILLE 6 E	Yadkin	NC	2.70	1.63	1.30	1.00	0.90	0.80	0.70	0.60	0.50
320382	ASHLEY	McIntosh	ND	2.30	1.40	1.00	0.80	0.70	0.60	0.50	0.47	0.40
320492	BALFOUR 6 SSW	McHenry	ND	2.10	1.30	0.92	0.76	0.60	0.53	0.50	0.40	0.40
320819	BISMARCK/MUN.,ND.	Burleigh	ND	1.91	1.12	0.84	0.66	0.56	0.48	0.43	0.37	0.33
321435	CAVALIER 7 NW	Pembina	ND	2.30	1.50	1.10	0.90	0.80	0.60	0.60	0.50	0.40
322018	DAWSON	Kidder	ND	2.40	1.38	0.96	0.79	0.67	0.60	0.50	0.40	0.40
322859	FARGO/HECTOR FIELD, ND.	Cass	ND	2.33	1.30	0.94	0.74	0.63	0.54	0.46	0.40	0.36
327530	RICHARDTON ABBEY	Stark	ND	2.23	1.21	0.93	0.70	0.60	0.50	0.47	0.40	0.39
327585	RIVERDALE	McLean	ND	2.20	1.35	0.96	0.80	0.70	0.60	0.50	0.40	0.40
329425	WILLISTON/SLOULIN FIELD, ND.	Williams	ND	1.72	1.02	0.75	0.57	0.48	0.42	0.37	0.32	0.29
330058	AKRON/AKRON-CANTON REG., OH.	Summit	OH	2.05	1.21	0.87	0.72	0.62	0.54	0.48	0.42	0.38
331786	COLUMBUS/PORT COLUMBUS, OH.	Franklin	OH	2.21	1.32	0.95	0.79	0.68	0.59	0.52	0.46	0.41
332075	DAYTON/. COX, OH	Montgomery	OH	2.23	1.34	0.99	0.80	0.68	0.60	0.53	0.46	0.41
334004	JACKSON	Jackson	OH	2.25	1.45	1.10	0.90	0.76	0.69	0.60	0.51	0.48
334865	MANSFIELD LAHM AP	Richland	OH	2.05	1.30	1.00	0.80	0.68	0.59	0.52	0.46	0.41
334992	MASSILLON	Stark	OH	2.00	1.40	1.10	0.90	0.80	0.70	0.60	0.50	0.50
336196	OBERLIN	Lorain	OH	2.00	1.24	0.94	0.78	0.65	0.58	0.50	0.45	0.40
337935	SPRINGFIELD NEW WW	Clark	OH	2.49	1.40	1.10	0.90	0.75	0.65	0.60	0.50	0.50
338357	TOLEDO/EXPRESS, OH.	Lucas	OH	1.95	1.22	0.91	0.76	0.64	0.56	0.49	0.43	0.38
338378	TOM JENKINS DAM-BURR	Athens	OH	2.20	1.30	1.00	0.80	0.70	0.60	0.56	0.50	0.43
340670	BENGAL	Latimer	OK	3.90	2.40	1.77	1.40	1.20	1.01	0.90	0.80	0.70
343002	EVA	Texas	OK	2.20	1.30	1.00	0.80	0.70	0.60	0.50	0.48	0.40
343281	FORT COBB	Caddo	OK	3.70	2.01	1.50	1.20	1.00	0.90	0.79	0.67	0.60
343304	FORT SUPPLY	Woodward	OK	2.74	1.71	1.23	1.00	0.86	0.75	0.66	0.59	0.50

COOP Station ID	Station Name	County	State	99%	95%	90%	85%	80%	75%	70%	65%	60%
344865	KINGSTON	Marshall	OK	3.56	2.18	1.65	1.34	1.13	0.97	0.82	0.71	0.61
345648	MAYFIELD	Beckham	OK	3.00	1.90	1.39	1.10	0.90	0.80	0.70	0.60	0.50
346661	OKLAHOMA CITY/W.R.WORLD, OK.	Oklahoma	OK	3.39	1.87	1.43	1.17	0.98	0.85	0.73	0.64	0.56
348497	STIGLER 1 SE	Haskell	OK	3.68	2.30	1.70	1.35	1.17	1.00	0.90	0.80	0.70
348992	TULSA/INTL, OK.	Tulsa	OK	3.22	1.95	1.49	1.23	1.03	0.89	0.77	0.68	0.59
350328	ASTORIA/CLATSOP, OR.	Clatsop	OR	2.36	1.42	1.08	0.88	0.76	0.66	0.58	0.52	0.47
352697	ESTACADA 24 SE	Clackamas	OR	2.30	1.40	1.00	0.88	0.70	0.63	0.60	0.50	0.45
353232	GERBER DAM	Klamath	OR	3.11	1.20	0.80	0.60	0.50	0.50	0.40	0.40	0.37
354321	JORDAN VALLEY	Malheur	OR	1.37	0.71	0.51	0.45	0.40	0.35	0.30	0.30	0.28
354670	LAKEVIEW 2 NNW	Lake	OR	1.26	0.79	0.60	0.50	0.43	0.40	0.35	0.30	0.30
355429	MEDFORD/MEDFORD- JACKSON COU	Josephine	OR	1.63	0.97	0.72	0.60	0.50	0.43	0.39	0.34	0.31
356546	PENDLETON, OR.	Umatilla	OR	0.97	0.62	0.48	0.41	0.36	0.33	0.30	0.26	0.24
356751	PORTLAND/INT., OR.	Multnomah	OR	1.61	0.98	0.76	0.63	0.53	0.47	0.42	0.38	0.34
356845	PRAIRIE CITY	Grant	OR	1.20	0.70	0.53	0.47	0.40	0.36	0.30	0.30	0.30
360106	ALLENTOWN/A.-BETHLEHEM-.,PA.	Lehigh	PA	2.62	1.57	1.19	0.99	0.83	0.72	0.62	0.55	0.49
362265	DU BOIS 7 E	Clearfield	PA	1.82	1.15	0.93	0.75	0.63	0.55	0.48	0.43	0.39
362682	ERIE INTL ARPT	Erie	PA	1.88	1.21	0.90	0.73	0.61	0.52	0.46	0.40	0.36
363699	HARRISBURG CPTL CY AIRPORT	York	PA	2.40	1.47	1.06	0.84	0.72	0.64	0.57	0.50	0.44
364001	HOLLIDAYSBURG 2 NW	Blair	PA	2.20	1.30	1.00	0.81	0.70	0.60	0.57	0.50	0.44
366889	PHILADELPHIA/INT., PA.	Philadelphia	PA	2.55	1.60	1.20	0.99	0.85	0.73	0.63	0.55	0.49
366993	PITTSBURGH/GREATER PITT.,PA.	Allegheny	PA	1.80	1.13	0.87	0.71	0.61	0.53	0.47	0.42	0.38
367931	SELINSGROVE 2 S	Snyder	PA	2.40	1.70	1.20	1.00	0.90	0.80	0.70	0.60	0.50
368905	TOWANDA 1 ESE	Bradford	PA	2.00	1.21	0.95	0.80	0.70	0.60	0.51	0.48	0.40
369705	WILKES-BARRE-SCRANTON, PA.	Luzerne	PA	2.14	1.29	0.97	0.78	0.67	0.58	0.51	0.45	0.41
376698	PROVIDENCE/GREEN STATE, RI.	Kent	RI	2.82	1.75	1.32	1.05	0.89	0.75	0.65	0.57	0.51
381544	CHARLESTON/MUN., SC.	Charleston	SC	3.69	2.00	1.47	1.20	0.99	0.85	0.74	0.64	0.56
381939	COLUMBIA, SC.	Lexington	SC	2.99	1.92	1.45	1.19	0.99	0.85	0.72	0.62	0.54
383747	GREENVILLE/SPATANBURG, SC	Spartanburg	SC	3.01	1.86	1.39	1.12	0.94	0.80	0.70	0.62	0.54
384581	JOCASSEE 8 WNW	Oconee	SC	4.94	2.80	2.01	1.60	1.33	1.10	0.98	0.85	0.75
385306	LORIS	Horry	SC	3.13	1.90	1.43	1.20	1.00	0.90	0.77	0.67	0.60

COOP Station ID	Station Name	County	State	99%	95%	90%	85%	80%	75%	70%	65%	60%
386209	NEWBERRY	Newberry	SC	3.20	1.90	1.50	1.20	1.00	0.90	0.79	0.70	0.60
389327	WINNSBORO	Fairfield	SC	2.70	1.90	1.45	1.20	1.00	0.90	0.80	0.70	0.60
390020	ABERDEEN/REG., S.D.	Brown	SD	2.32	1.32	0.95	0.79	0.66	0.55	0.49	0.43	0.38
392557	EDGEMONT	Fall River	SD	1.80	1.02	0.80	0.62	0.56	0.50	0.40	0.40	0.31
394127	HURON/HURON REGIONAL, SD.	Beadle	SD	2.17	1.28	0.98	0.78	0.66	0.56	0.50	0.43	0.38
394864	LEMMON	Perkins	SD	2.03	1.20	0.90	0.71	0.60	0.50	0.43	0.39	0.34
395620	MISSION	Todd	SD	2.50	1.41	1.10	0.90	0.70	0.60	0.57	0.50	0.40
396170	OAHE DAM	Stanley	SD	2.26	1.30	1.00	0.80	0.70	0.60	0.50	0.44	0.40
396282	ONAKA	Faulk	SD	2.30	1.40	1.00	0.80	0.70	0.60	0.50	0.50	0.40
396427	PACTOLA DAM	Pennington	SD	2.00	1.20	0.82	0.70	0.60	0.50	0.46	0.40	0.38
397667	SIOUX FALLS/FOSS FIELD, SD.	Minnehaha	SD	2.36	1.41	1.05	0.85	0.71	0.61	0.53	0.46	0.40
401656	CHATTANOOGA/LOVELL FIELD, TN	Hamilton	TN	3.02	1.79	1.35	1.12	0.96	0.83	0.73	0.64	0.56
405954	MEMPHIS INTL ARPT	Shelby	TN	3.24	2.02	1.57	1.30	1.10	0.93	0.81	0.71	0.62
406170	MONTEREY	Putnam	TN	3.30	1.82	1.40	1.19	1.00	0.90	0.80	0.70	0.60
406402	NASHVILLE/METROPOLITAN,TN.	Davidson	TN	2.82	1.75	1.30	1.05	0.90	0.77	0.67	0.59	0.53
410428	AUSTIN/ROBERT MUELLER., TX.	Travis	TX	3.65	2.01	1.49	1.21	1.01	0.85	0.73	0.63	0.54
411136	BROWNSVILLE/INT., TX.	Cameron	TX	4.22	2.28	1.54	1.17	0.97	0.80	0.68	0.57	0.49
412797	EL PASO/INT., TX.	El Paso	TX	1.70	1.04	0.76	0.60	0.51	0.44	0.38	0.34	0.31
413284	FORT WORTH MEACHAM F	Tarrant	TX	3.16	2.03	1.50	1.20	1.00	0.89	0.79	0.70	0.60
414191	HINDES	Atascosa	TX	3.89	2.38	1.69	1.30	1.07	0.90	0.78	0.66	0.58
415411	LUBBOCK/LUBBOCK INTL, TX.	Lubbock	TX	2.72	1.55	1.12	0.91	0.75	0.65	0.58	0.49	0.43
418845	TARPLEY	Bandera	TX	4.15	2.22	1.63	1.30	1.10	0.95	0.80	0.70	0.60
419364	VICTORIA/VICTORIA REG., TX.	Victoria	TX	4.22	2.30	1.64	1.32	1.08	0.92	0.78	0.67	0.59
419665	WHEELOCK	Robertson	TX	3.88	2.20	1.70	1.36	1.14	1.00	0.85	0.75	0.67
419729	WICHITA FALLS/SHEPS AFB TX	Wichita	TX	3.15	1.86	1.36	1.13	0.97	0.84	0.72	0.63	0.54
420738	BLANDING	San Juan	UT	1.39	0.90	0.70	0.58	0.50	0.43	0.40	0.35	0.30
422090	DELTA	Millard	UT	1.10	0.69	0.50	0.45	0.40	0.35	0.30	0.30	0.30
422385	ECHO DAM	Summit	UT	1.10	0.70	0.60	0.50	0.40	0.40	0.33	0.30	0.30
426135	NEPHI	Juab	UT	1.10	0.75	0.60	0.50	0.45	0.40	0.40	0.31	0.30
427395	ROOSEVELT RADIO	Uintah	UT	1.30	0.70	0.51	0.46	0.40	0.37	0.30	0.30	0.30

COOP Station ID	Station Name	County	State	99%	95%	90%	85%	80%	75%	70%	65%	60%
427516	ST GEORGE	Washington	UT	1.15	0.80	0.60	0.55	0.50	0.40	0.40	0.38	0.30
427598	SALT LAKE CITY/INTL, UT.	Salt Lake	UT	1.14	0.80	0.61	0.51	0.44	0.40	0.35	0.32	0.29
431081	BURLINGTON/INTL, VT.	Chittenden	VT	1.78	1.10	0.84	0.69	0.60	0.52	0.46	0.41	0.37
431565	CORINTH	Orange	VT	2.10	1.30	1.00	0.80	0.70	0.60	0.55	0.50	0.42
438556	UNION VILLAGE DAM	Orange	VT	2.20	1.26	0.95	0.77	0.66	0.57	0.51	0.45	0.40
442729	ELKWOOD 6 SE	Culpeper	VA	2.50	1.49	1.17	0.98	0.82	0.70	0.63	0.56	0.50
445120	LYNCHBURG RGNL AP	Campbell	VA	2.43	1.55	1.16	0.93	0.79	0.69	0.62	0.54	0.48
446139	NORFOLK/INT., VA.	Norfolk city	VA	3.12	1.76	1.26	1.01	0.84	0.73	0.64	0.56	0.50
447201	RICHMOND/BYRD, VA.	Henrico	VA	2.82	1.69	1.28	1.01	0.86	0.74	0.66	0.58	0.51
447285	ROANOKE/MUN., VA.	Roanoke	VA	2.51	1.50	1.15	0.93	0.81	0.69	0.60	0.53	0.47
448547	TROUT DALE 3 SSE	Grayson	VA	2.40	1.44	1.10	0.90	0.80	0.70	0.60	0.53	0.50
453357	GREENWATER	Pierce	WA	2.20	1.31	0.95	0.79	0.66	0.58	0.50	0.46	0.40
453515	HARRINGTON 1 NW	Lincoln	WA	0.90	0.66	0.50	0.50	0.40	0.40	0.30	0.30	0.30
454849	LUCERNE 1 N	Chelan	WA	2.10	1.16	0.86	0.68	0.57	0.50	0.43	0.39	0.34
456114	OLYMPIA, WA.	Thurston	WA	2.14	1.27	0.95	0.79	0.67	0.58	0.51	0.45	0.41
456678	PORT TOWNSEND	Jefferson	WA	1.32	0.72	0.55	0.46	0.40	0.34	0.31	0.28	0.25
456789	PULLMAN 2 NW	Whitman	WA	1.19	0.80	0.61	0.51	0.45	0.40	0.36	0.32	0.30
456858	QUILLAYUTE, WA.	Clallam	WA	3.27	1.97	1.47	1.20	1.02	0.89	0.78	0.68	0.61
457938	SPOKANE/INT.,WA.	Spokane	WA	0.95	0.66	0.53	0.45	0.39	0.35	0.32	0.28	0.26
458009	YAKIMA/YAKIMA AIR TERM.,WA.	Kittitas	WA	2.89	1.80	1.32	1.07	0.91	0.78	0.68	0.59	0.52
458207	SUNNYSIDE	Yakima	WA	0.90	0.60	0.50	0.40	0.35	0.30	0.30	0.29	0.25
461570	CHARLESTON/KANAWHA.,WV.	Kanawha	WV	2.00	1.24	0.96	0.79	0.69	0.60	0.53	0.46	0.42
462718	ELKINS RNDLPH CO AP	Randolph	WV	1.76	1.12	0.86	0.72	0.62	0.54	0.47	0.42	0.38
465002	LAKE LYNN	Monongalia	WV	1.81	1.20	0.90	0.75	0.63	0.60	0.50	0.47	0.40
465739	MATHIAS	Hardy	WV	2.37	1.30	1.00	0.80	0.70	0.60	0.50	0.48	0.40
466859	PARKERSBURG	Wood	WV	1.83	1.18	0.91	0.78	0.65	0.57	0.50	0.44	0.40
469011	UNION 3 SSE	Monroe	WV	2.00	1.20	0.92	0.80	0.70	0.60	0.50	0.50	0.40
470349	ASHLAND EXP FARM	Bayfield	WI	2.10	1.34	1.00	0.80	0.70	0.60	0.52	0.50	0.40
471676	CLINTONVILLE	Waupaca	WI	2.08	1.39	1.00	0.82	0.70	0.60	0.53	0.49	0.40
473269	GREEN BAY/A.-STRAUBEL, WI.	Brown	WI	1.89	1.18	0.92	0.74	0.63	0.53	0.46	0.41	0.36

COOP Station ID	Station Name	County	State	99%	95%	90%	85%	80%	75%	70%	65%	60%
474546	LANCASTER 4 WSW	Grant	WI	2.81	1.50	1.10	0.90	0.75	0.66	0.58	0.50	0.45
474961	MADISON/DANE COUNTY REGIONAL	Dane	WI	2.41	1.42	1.02	0.83	0.70	0.61	0.53	0.46	0.40
475479	MILWAUKEE/GEN. MITCHELL, WI.	Milwaukee	WI	2.19	1.33	0.99	0.79	0.69	0.59	0.52	0.45	0.40
475948	NEW RICHMOND	Saint Croix	WI	2.45	1.50	1.11	0.90	0.80	0.70	0.60	0.50	0.47
476510	PESHTIGO	Marinette	WI	2.10	1.30	1.00	0.80	0.70	0.60	0.50	0.49	0.40
476939	RAINBOW RSVR LAKE	Oneida	WI	2.01	1.20	0.90	0.74	0.62	0.53	0.48	0.41	0.40
481570	CASPER/NATRONA COUNTY I.,WY.	Natrona	WY	1.62	0.80	0.57	0.45	0.39	0.34	0.31	0.28	0.26
485345	LAKE YELLOWSTONE	Teton	WY	1.10	0.70	0.51	0.43	0.40	0.35	0.30	0.30	0.29
485390	LANDER/HUNT, WY.	Fremont	WY	1.56	0.97	0.74	0.60	0.52	0.46	0.41	0.36	0.32
486440	MORAN 5 WNW	Teton	WY	1.31	0.77	0.60	0.50	0.42	0.40	0.35	0.30	0.30
486660	NEWCASTLE	Weston	WY	1.55	1.00	0.80	0.60	0.50	0.48	0.40	0.40	0.30
487105	PATHFINDER DAM	Natrona	WY	1.55	0.75	0.59	0.50	0.40	0.36	0.31	0.30	0.29
487270	PINE TREE 9 NE	Campbell	WY	1.87	1.11	0.80	0.60	0.50	0.42	0.37	0.32	0.30
487845	ROCK SPRINGS AP	Sweetwater	WY	1.10	0.60	0.50	0.40	0.40	0.33	0.30	0.30	0.30
488155	SHERIDAN/COUNTY, WY.	Sheridan	WY	1.40	0.83	0.61	0.52	0.44	0.38	0.33	0.30	0.27
488852	TEN SLEEP 4 NE	Washakie	WY	1.40	0.90	0.70	0.60	0.50	0.40	0.40	0.34	0.30
500352	ANNETTE ISLAND	Prince of Wales-Outer Ketchika	AK	2.54	1.70	1.31	1.08	0.93	0.80	0.70	0.62	0.55
511492	HILO	Hawaii	HI	5.16	2.27	1.45	1.07	0.86	0.72	0.60	0.52	0.46
668812	SAN JUAN/INTL, PUERTO RICO	San Juan	PR	2.91	1.53	1.06	0.82	0.68	0.56	0.49	0.42	0.37

Appendix B

Watershed Maps

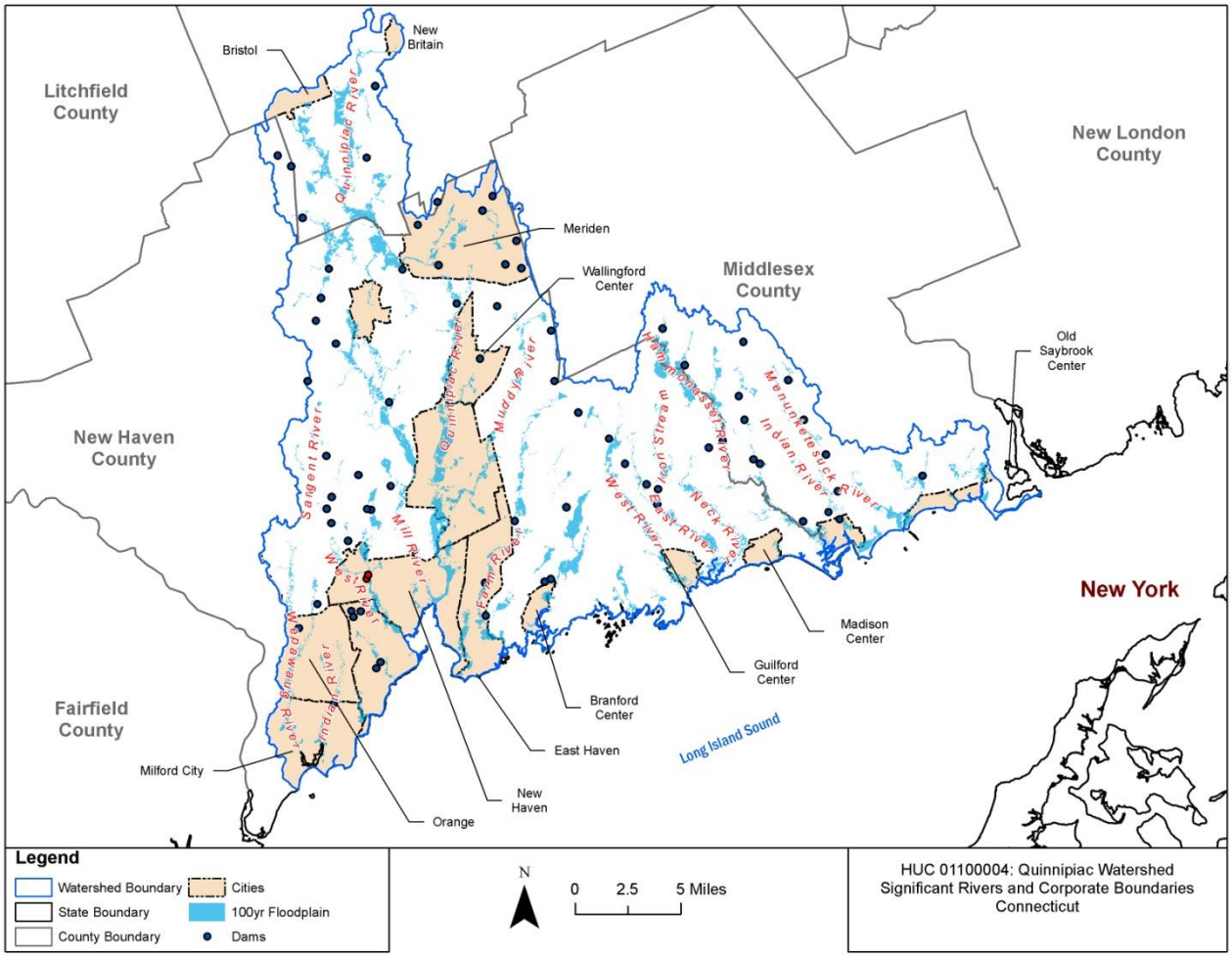

Figure B-1. HUC8 1100004, Quinnipiac.

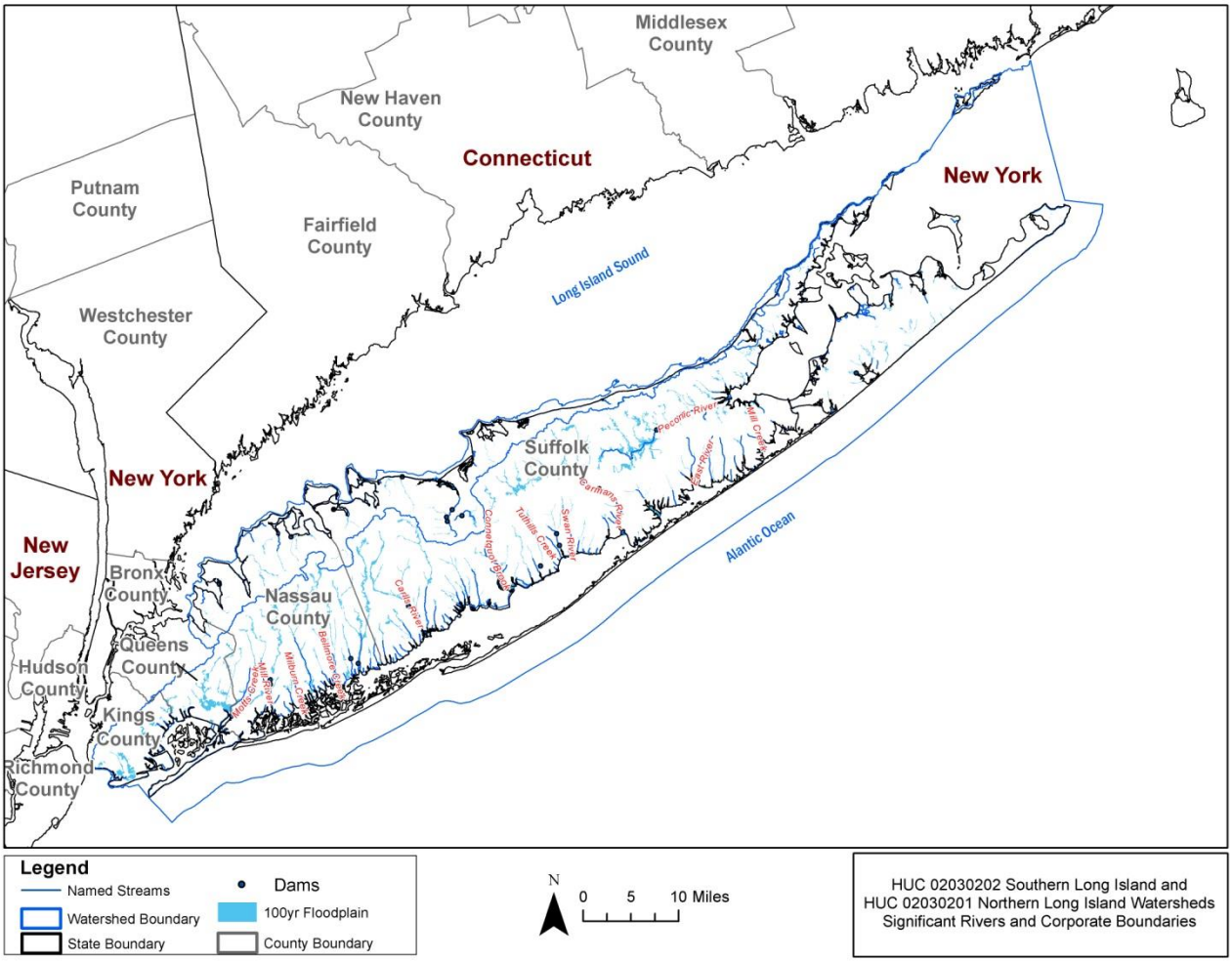

Figure B-2. HUC8s 02030201 Northern Long Island and 02030202 Southern Long Island combined.

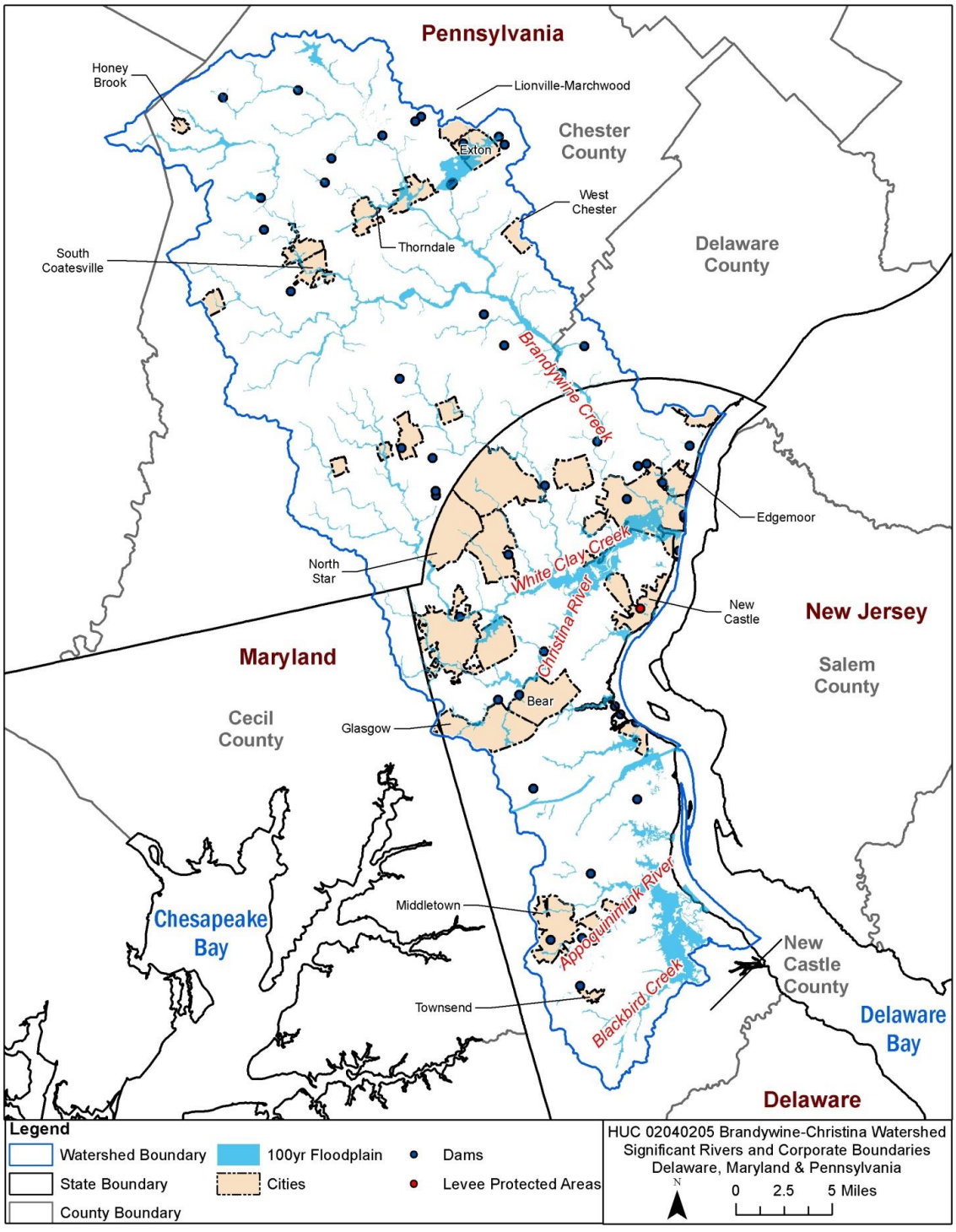

Figure B-3. HUC8 02040205, Brandywine-Christina.

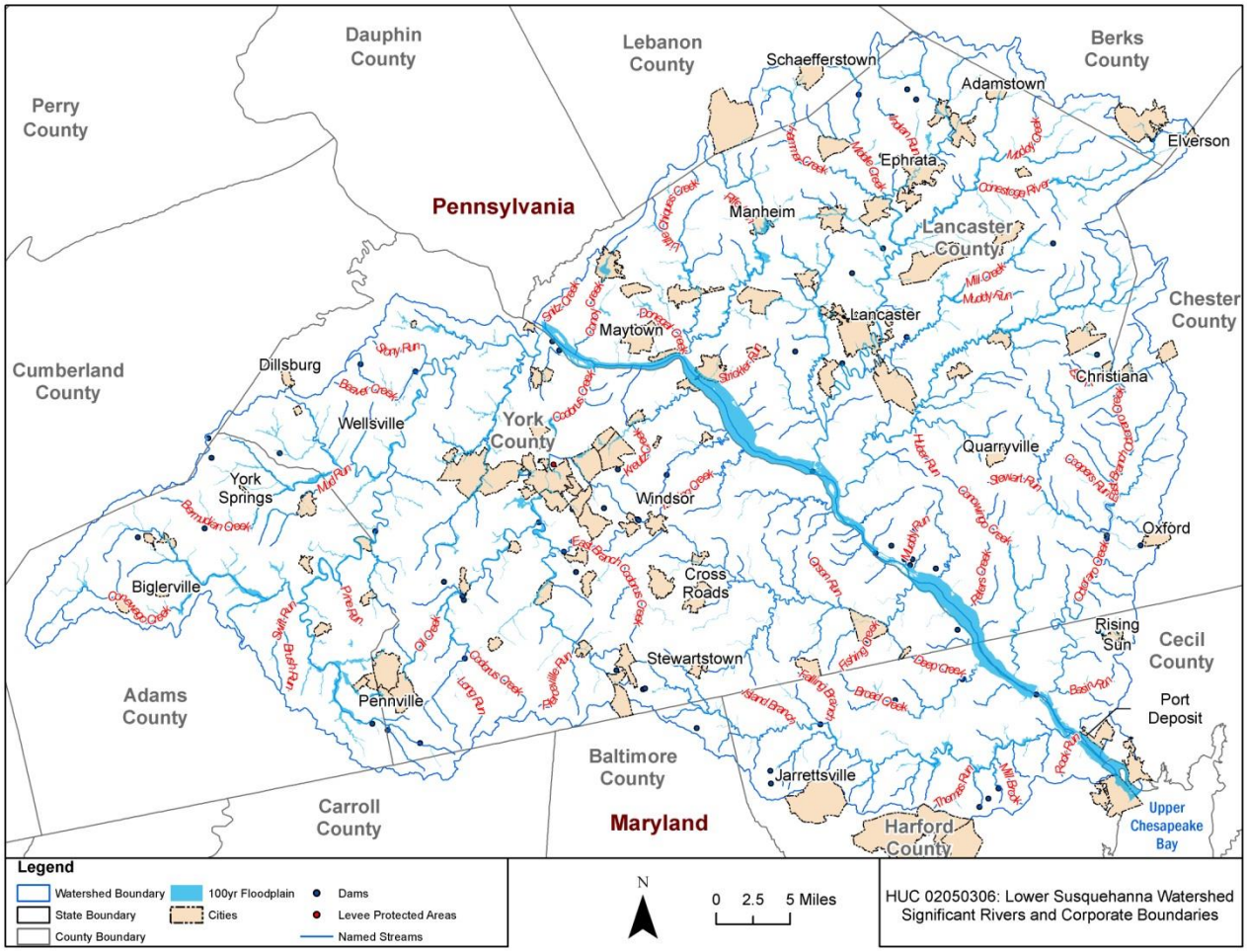

Figure B-4. HUC8 02050306, Lower Susquehanna.

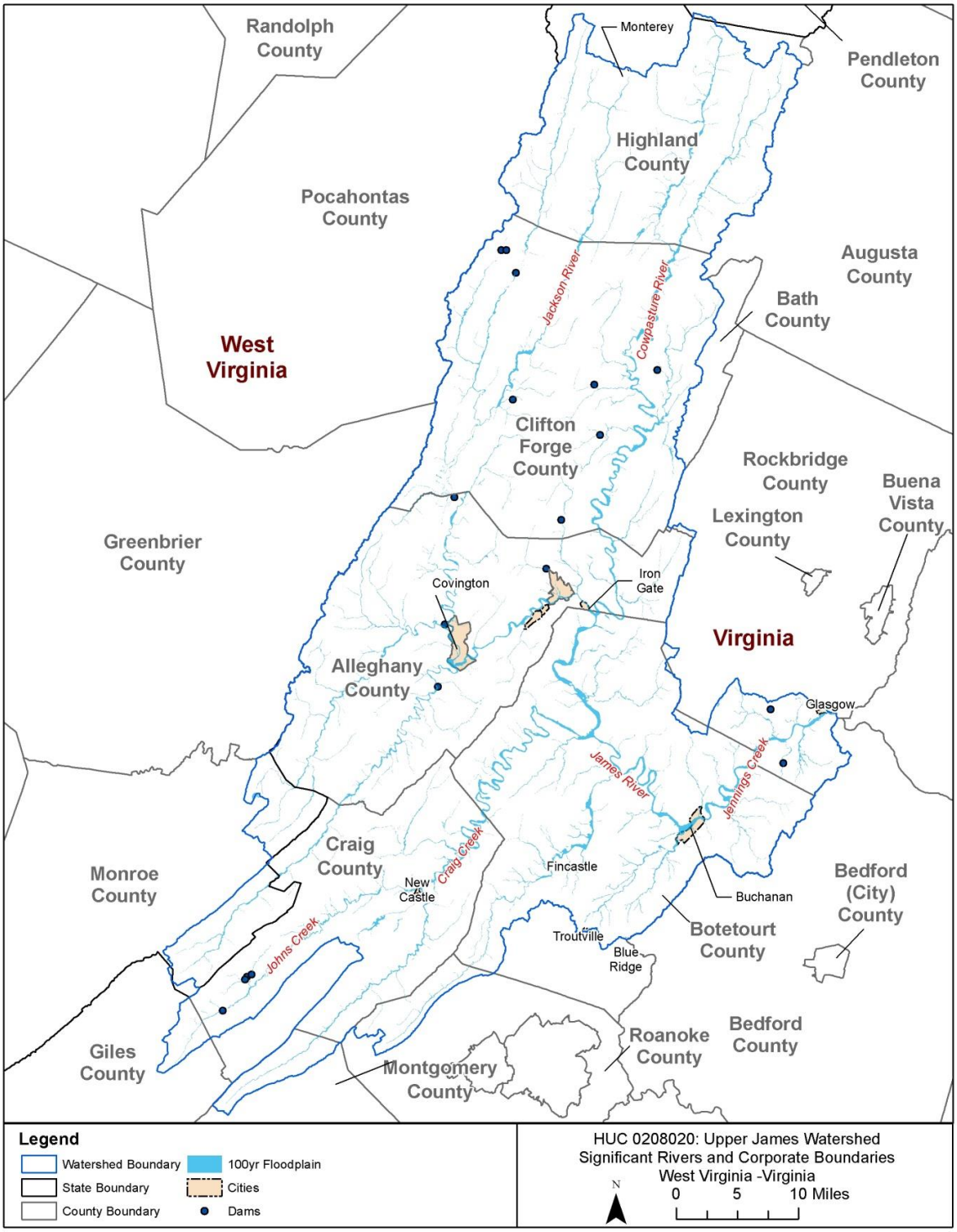

Figure B-5. HUC8 02080201, Upper James.

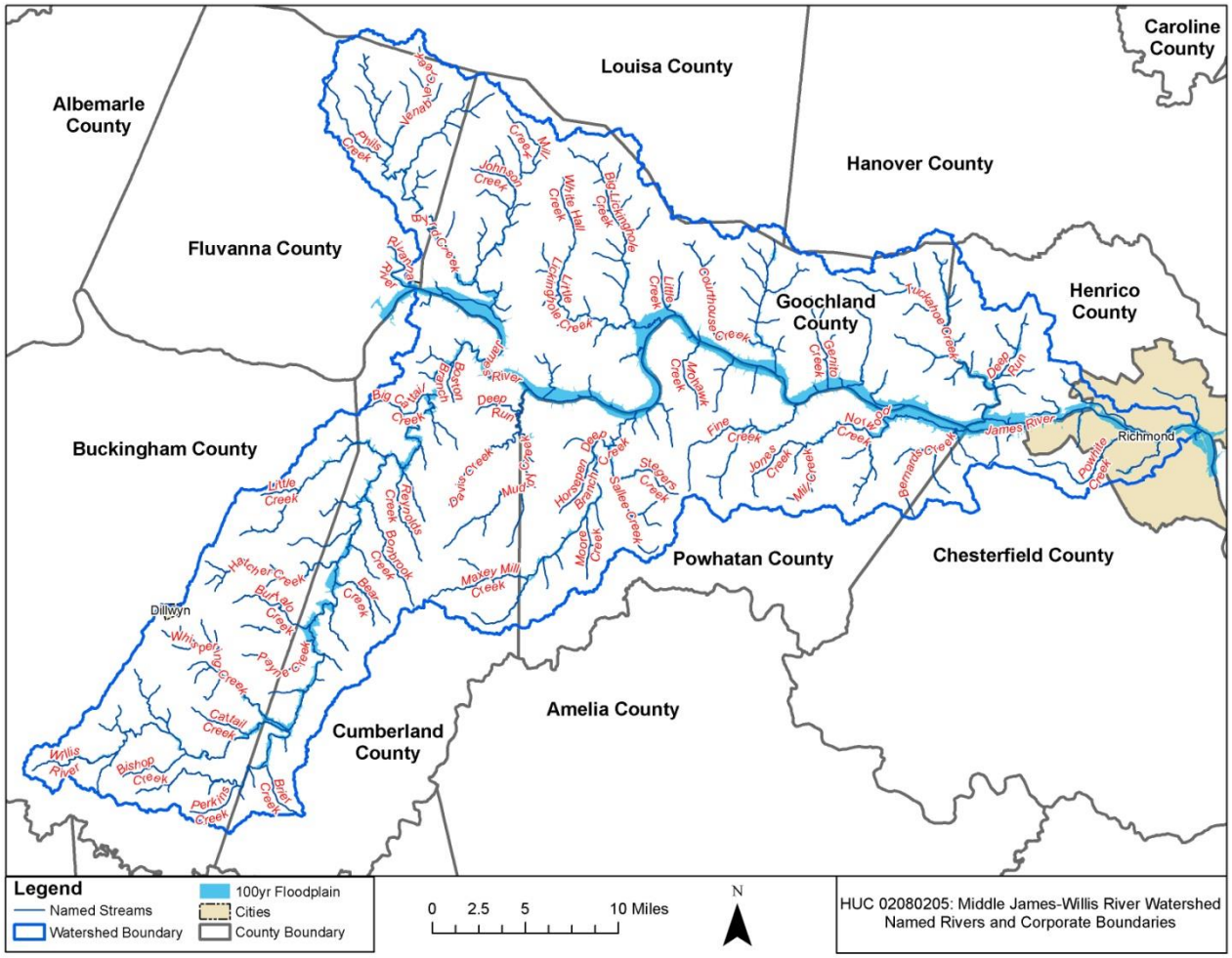

Figure B-6. HUC8 02080205, Middle James.

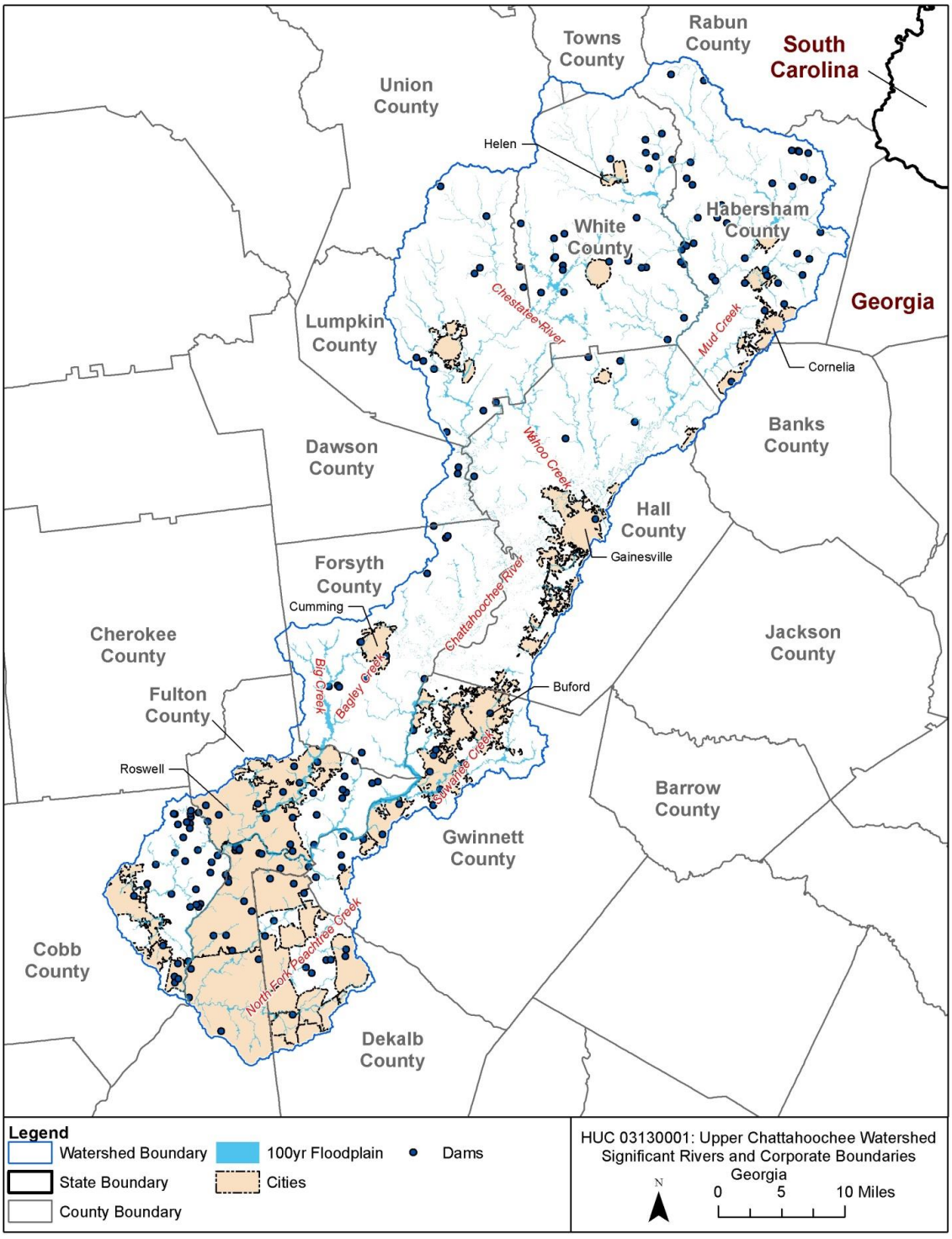

Figure B-7. HUC8 03130001, Upper Chattahoochee.

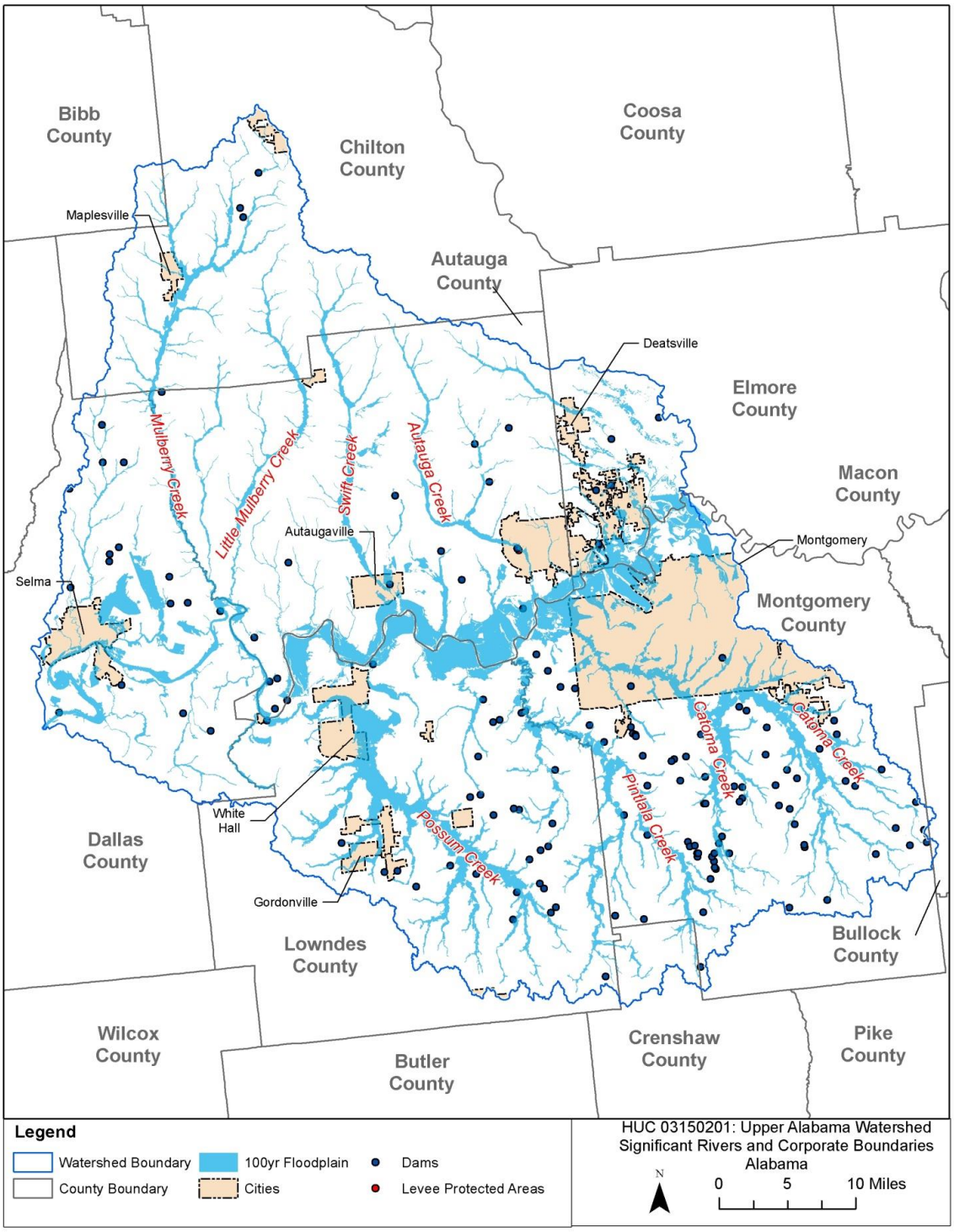

Figure B-8. HUC8 03150201, Upper Alabama.

Figure B-9. HUC8 04080203, Shiawassee.

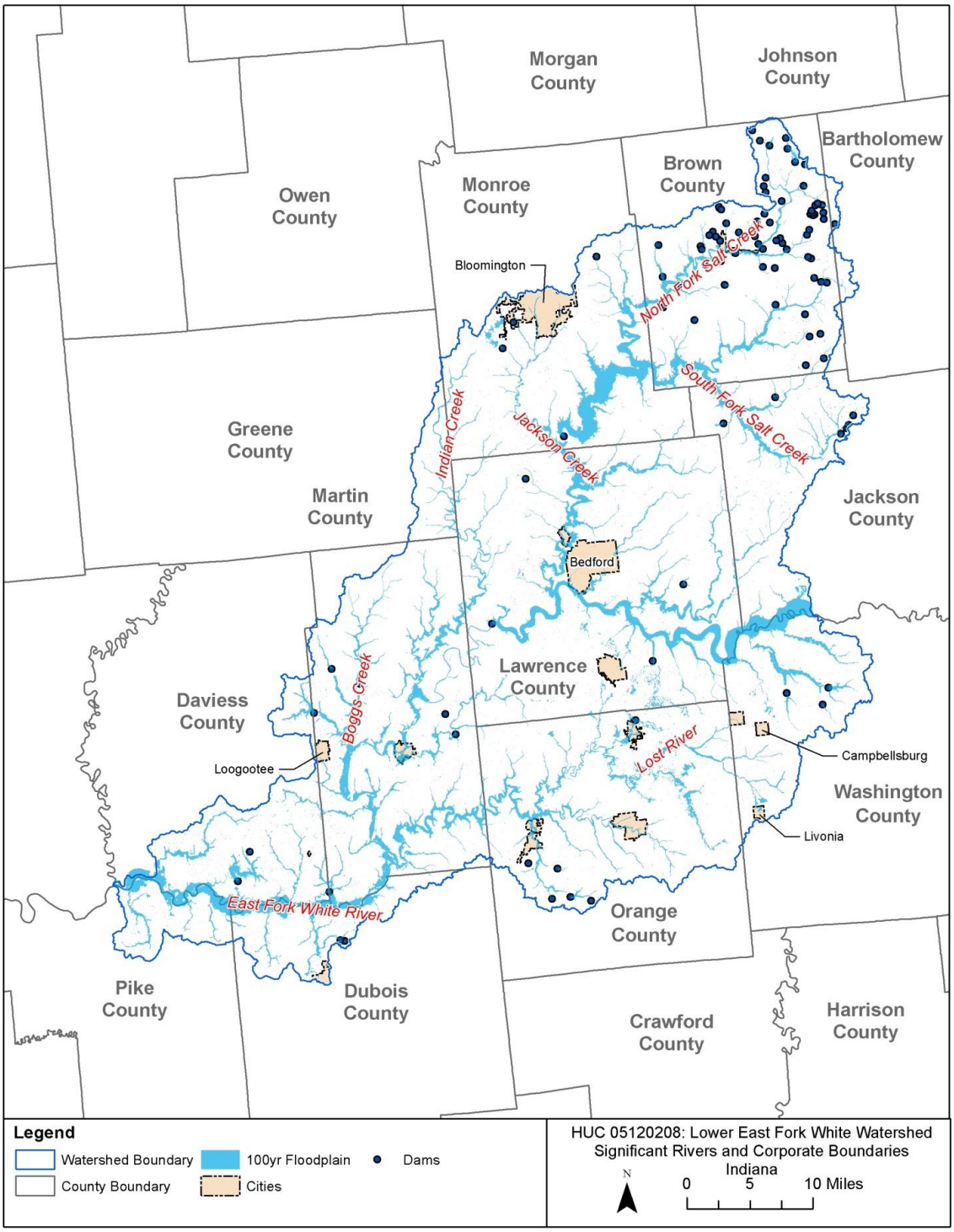

Figure B-10. HUC8 05120208, Lower East Fork White.

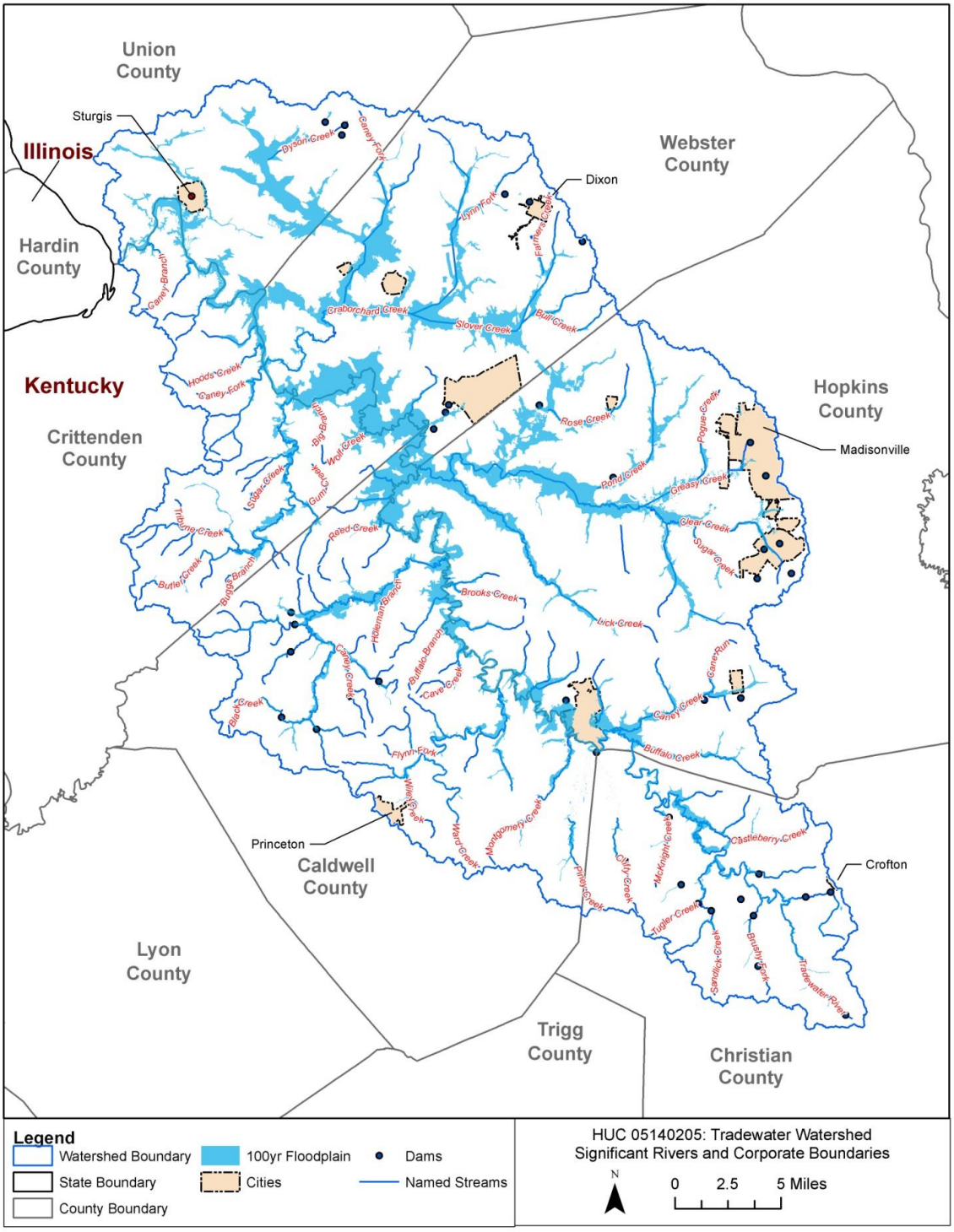

Figure B-11. HUC8 05140205, Tradewater.

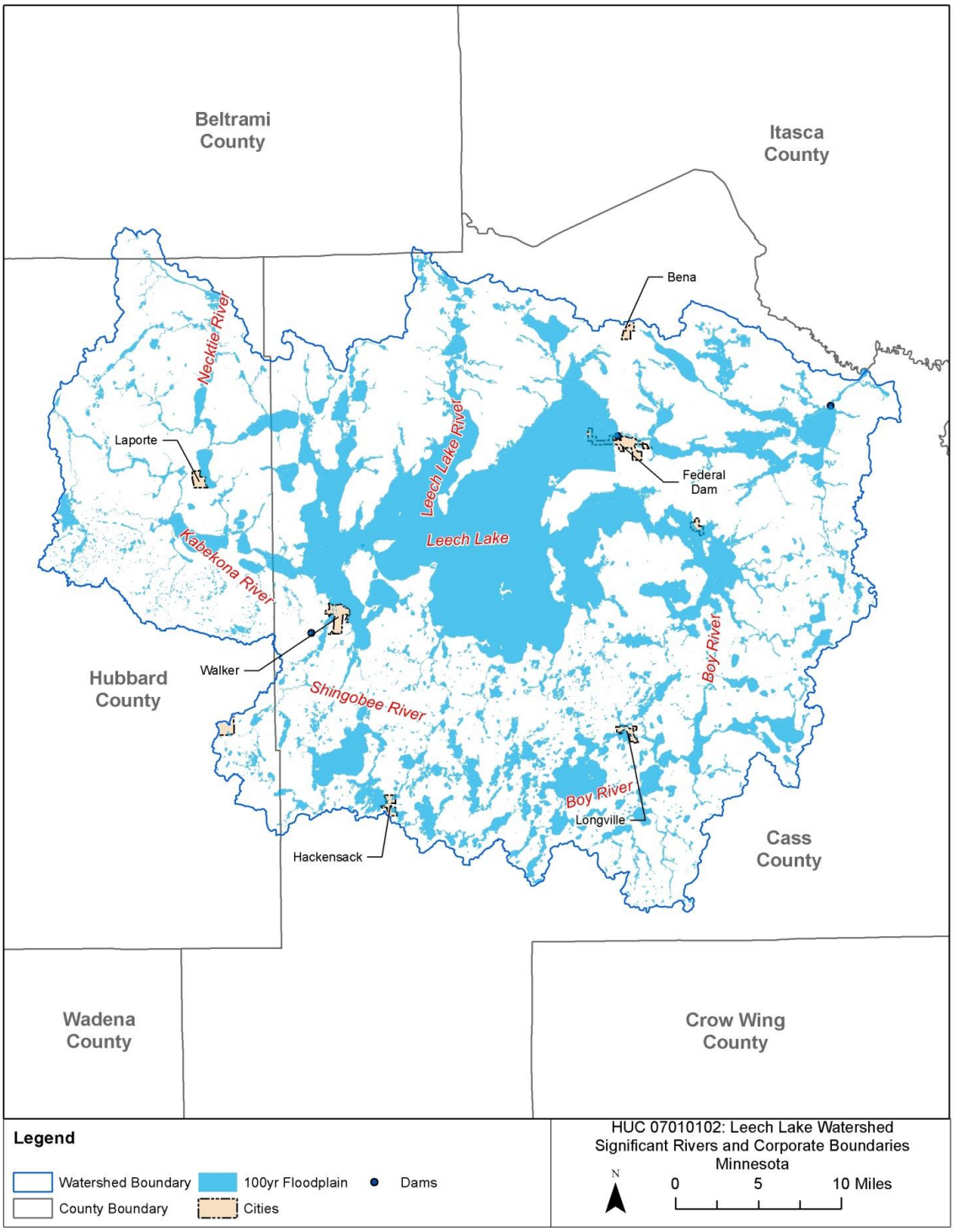

Figure B-12. HUC8 07010102, Leech Lake.

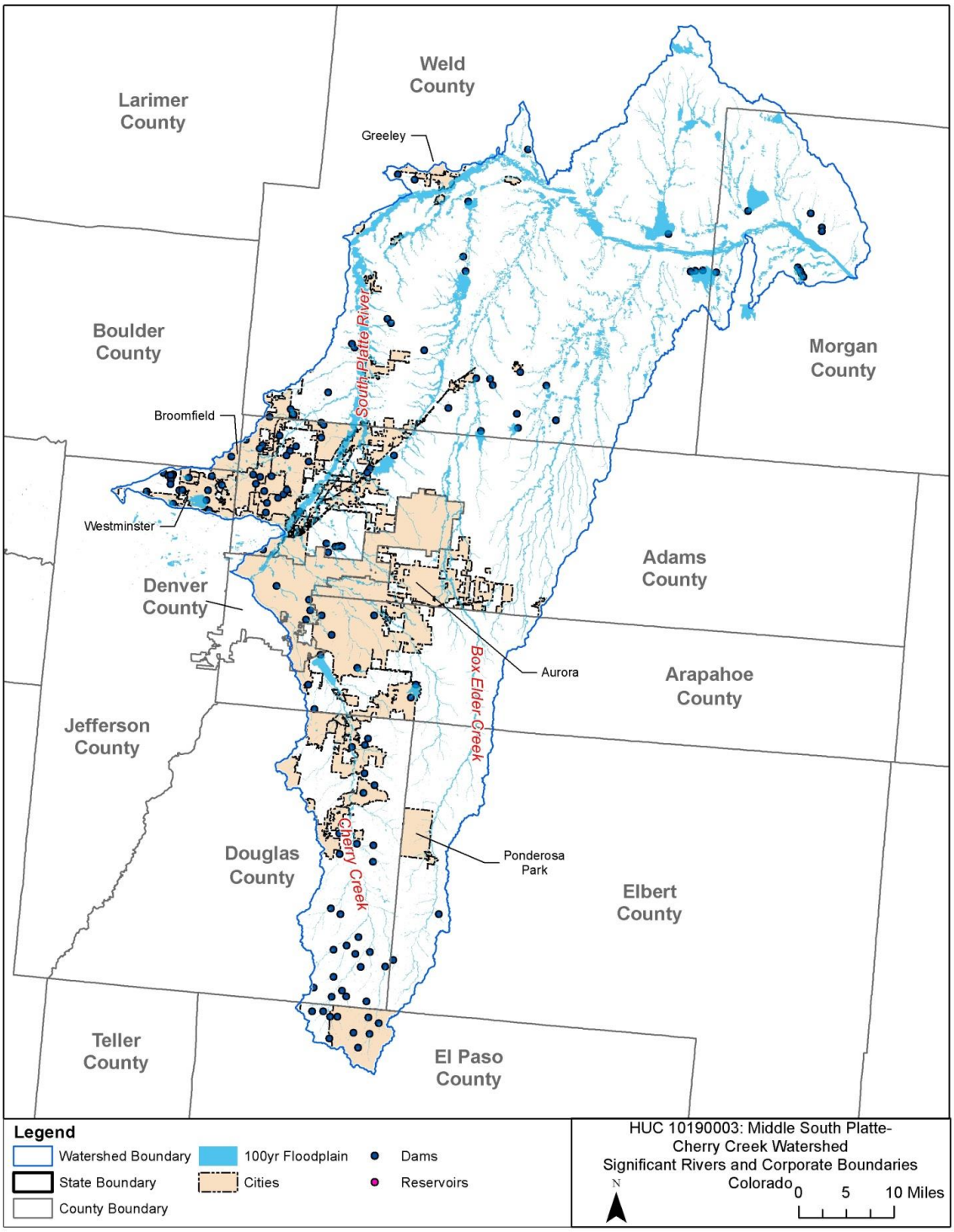

Figure B-13. HUC8 10190003, Middle South Platte-Cherry Creek.

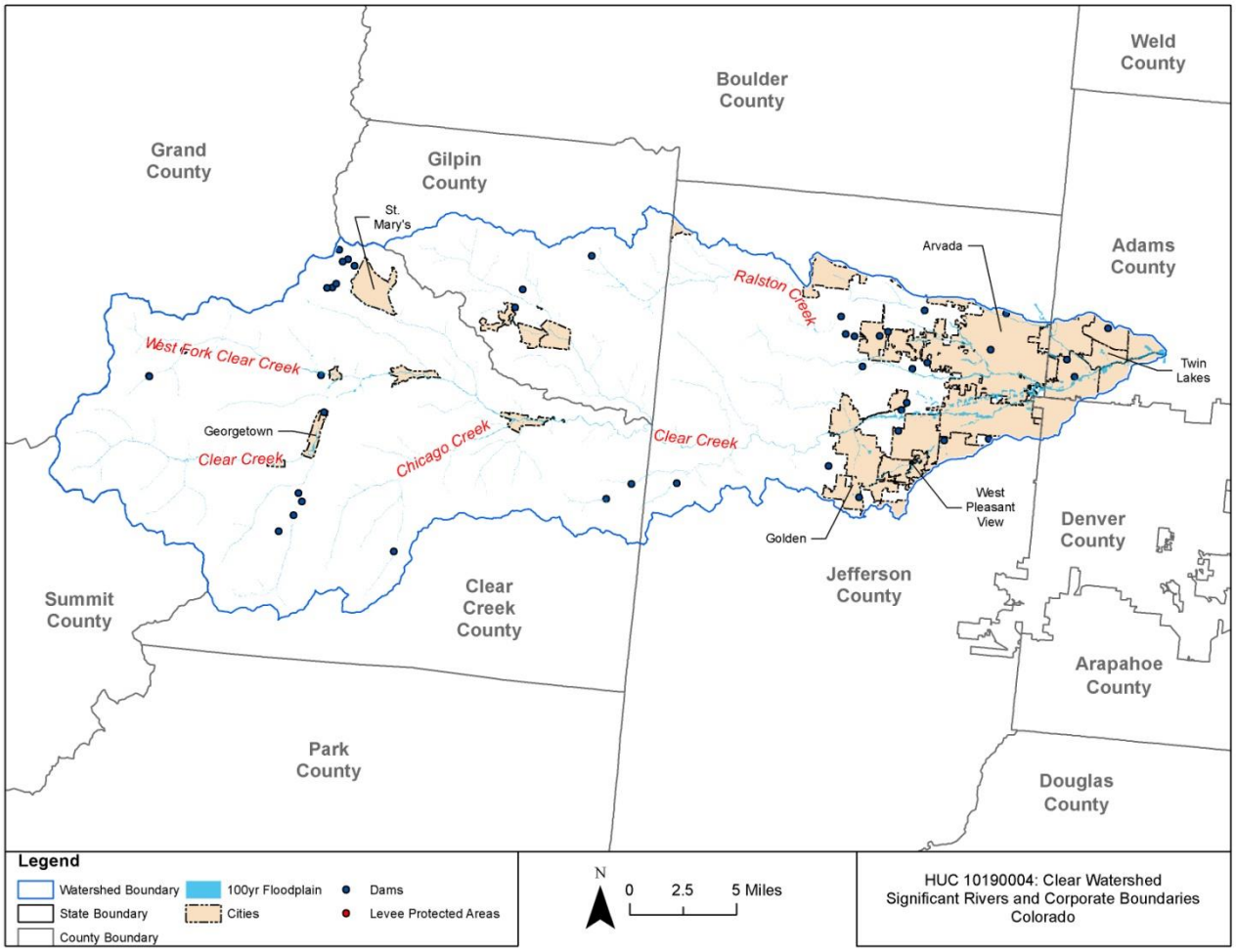

Figure B-14. HUC8 10190004, Clear.

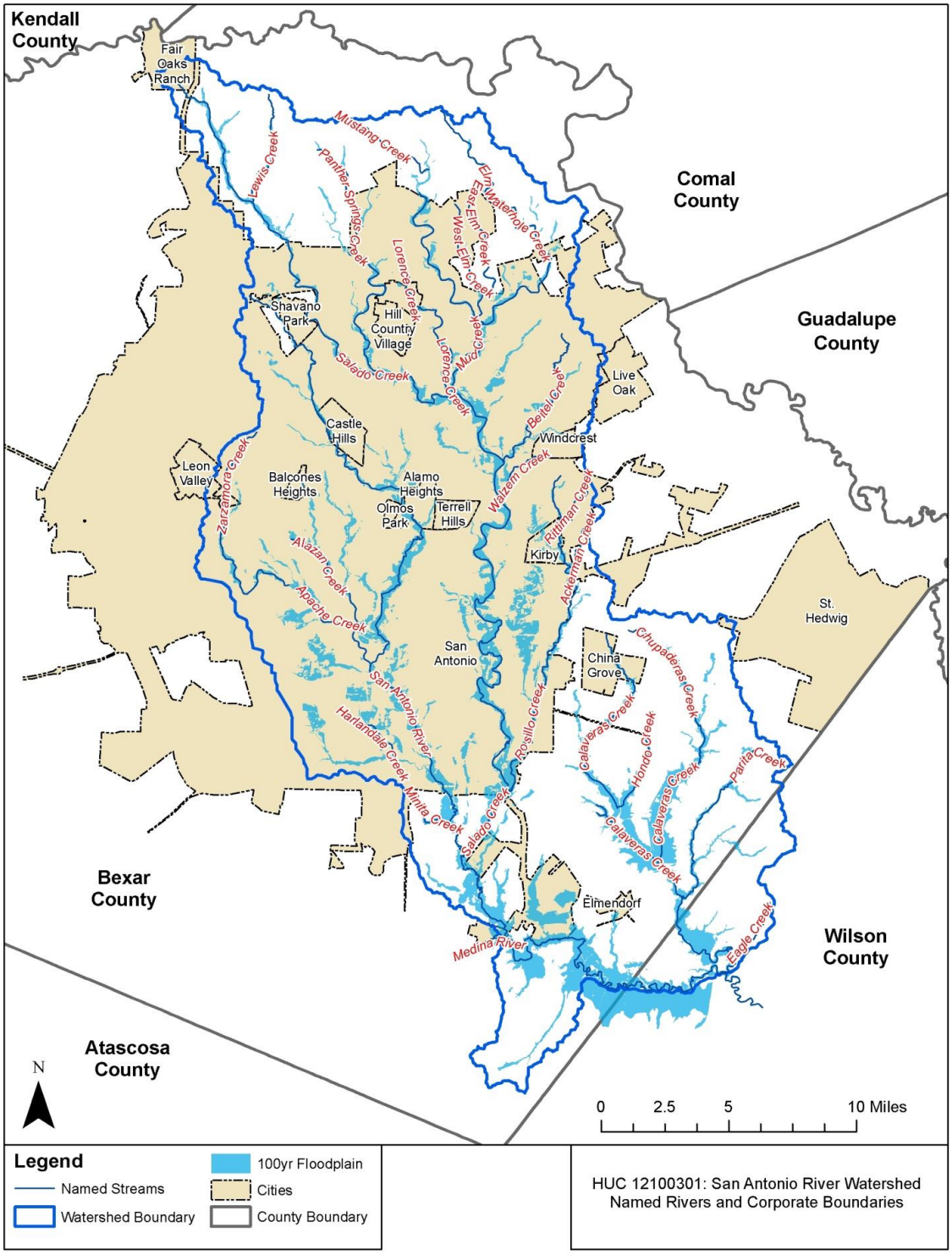

Figure B-15. HUC8 12100301, Upper San Antonio River.

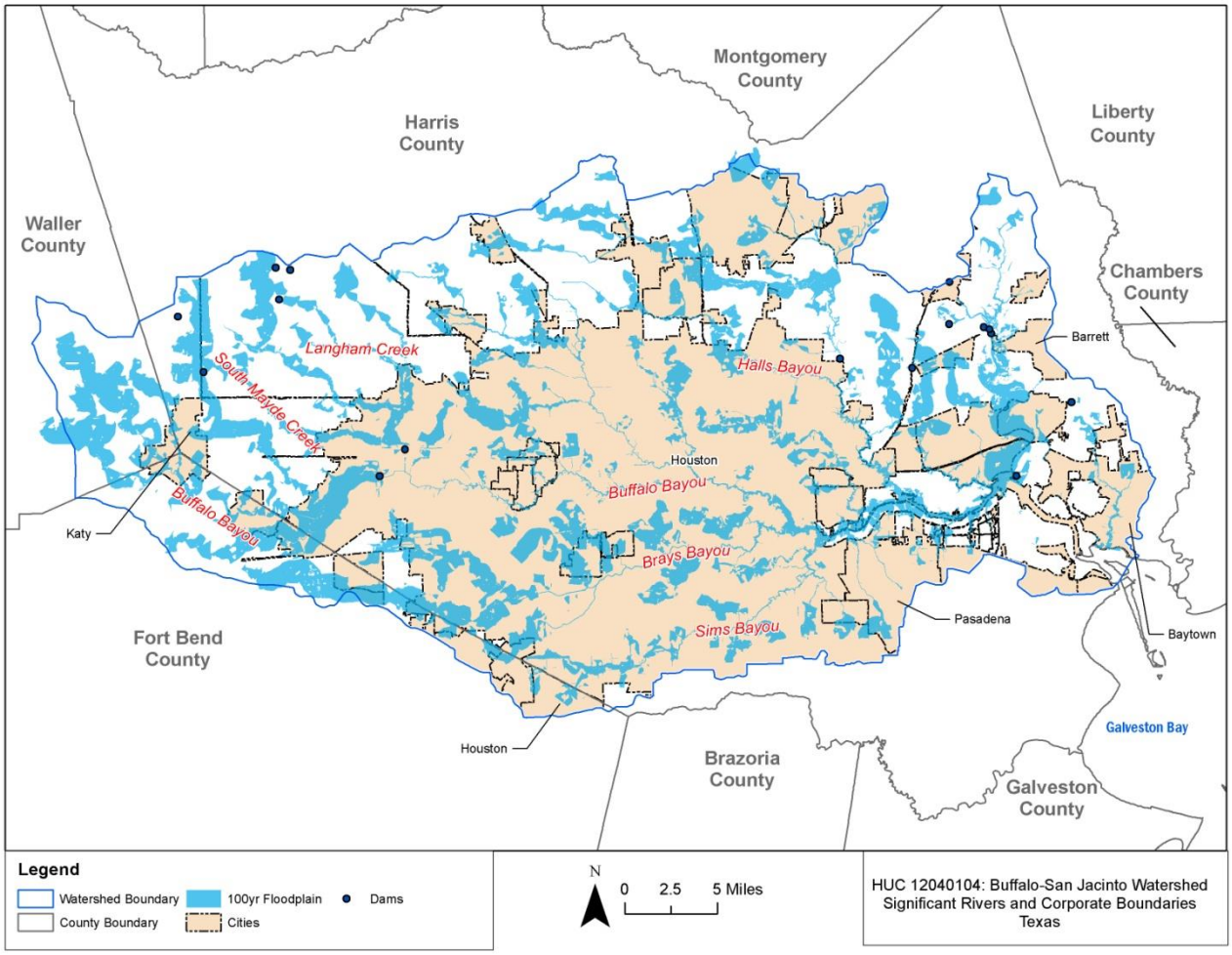

Figure B-16. HUC8 12040104, Buffalo-San Jacinto.

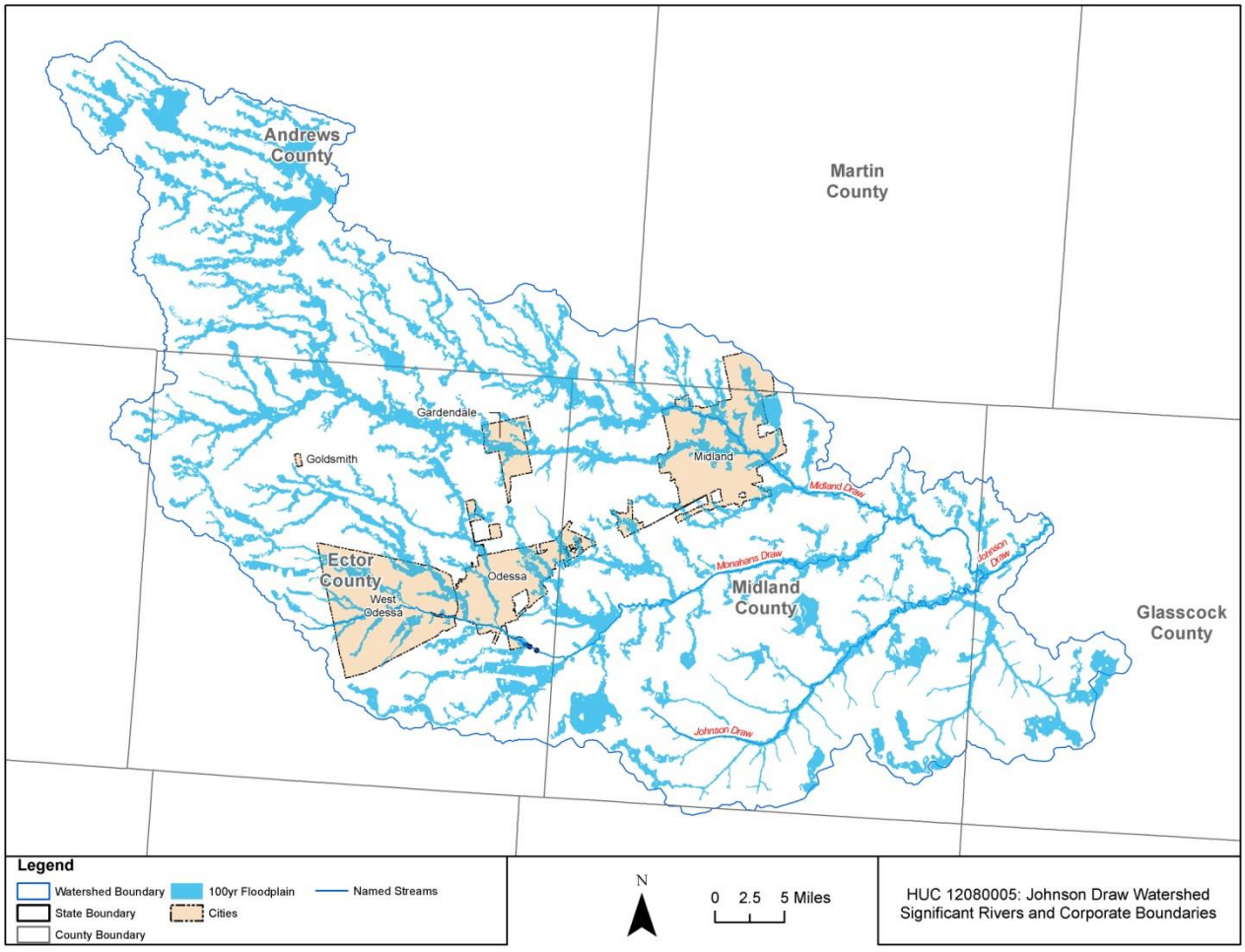

Figure B-17. HUC8 12080005, Johnson Draw.

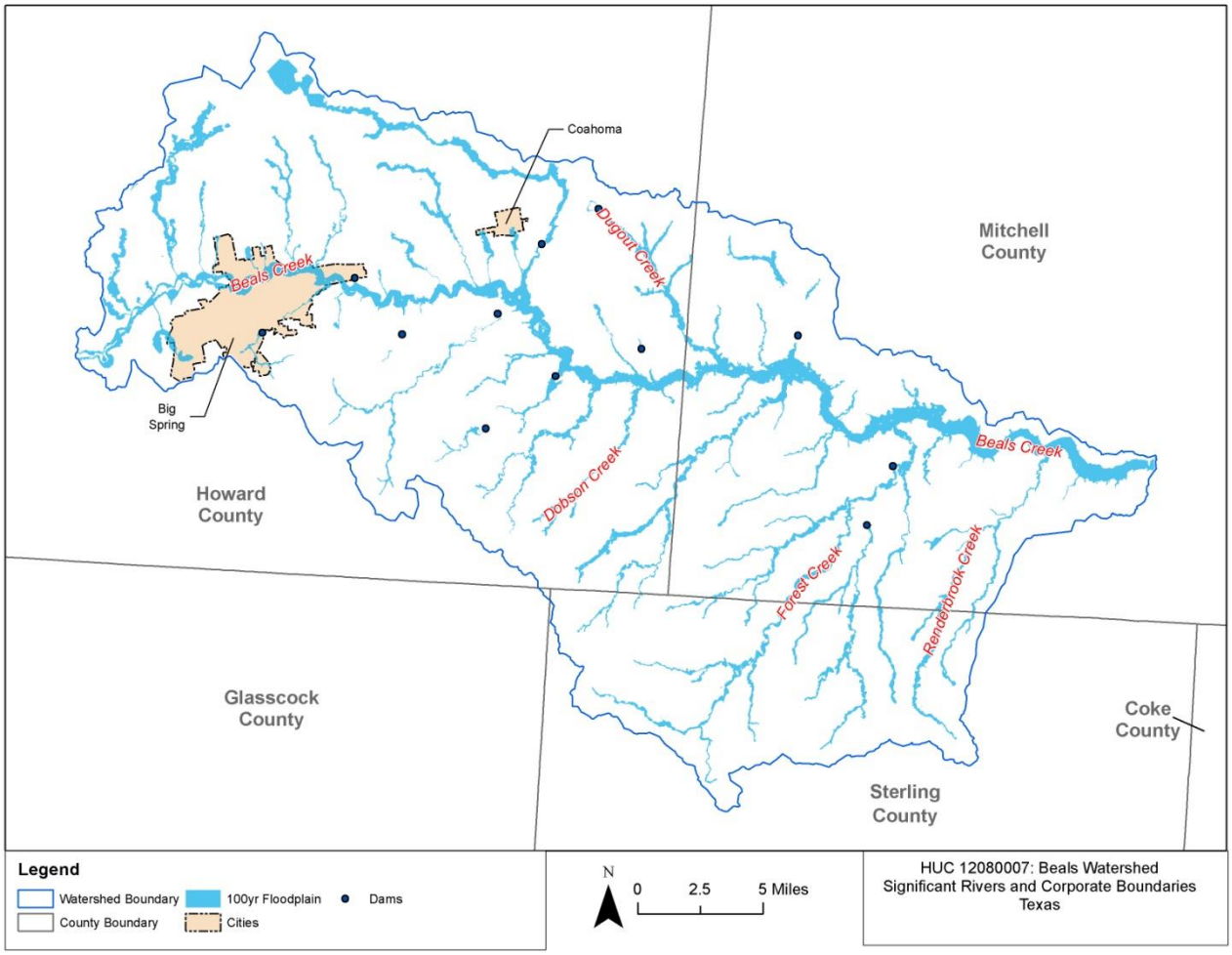

Figure B-18. HUC8 12080007, Beals.

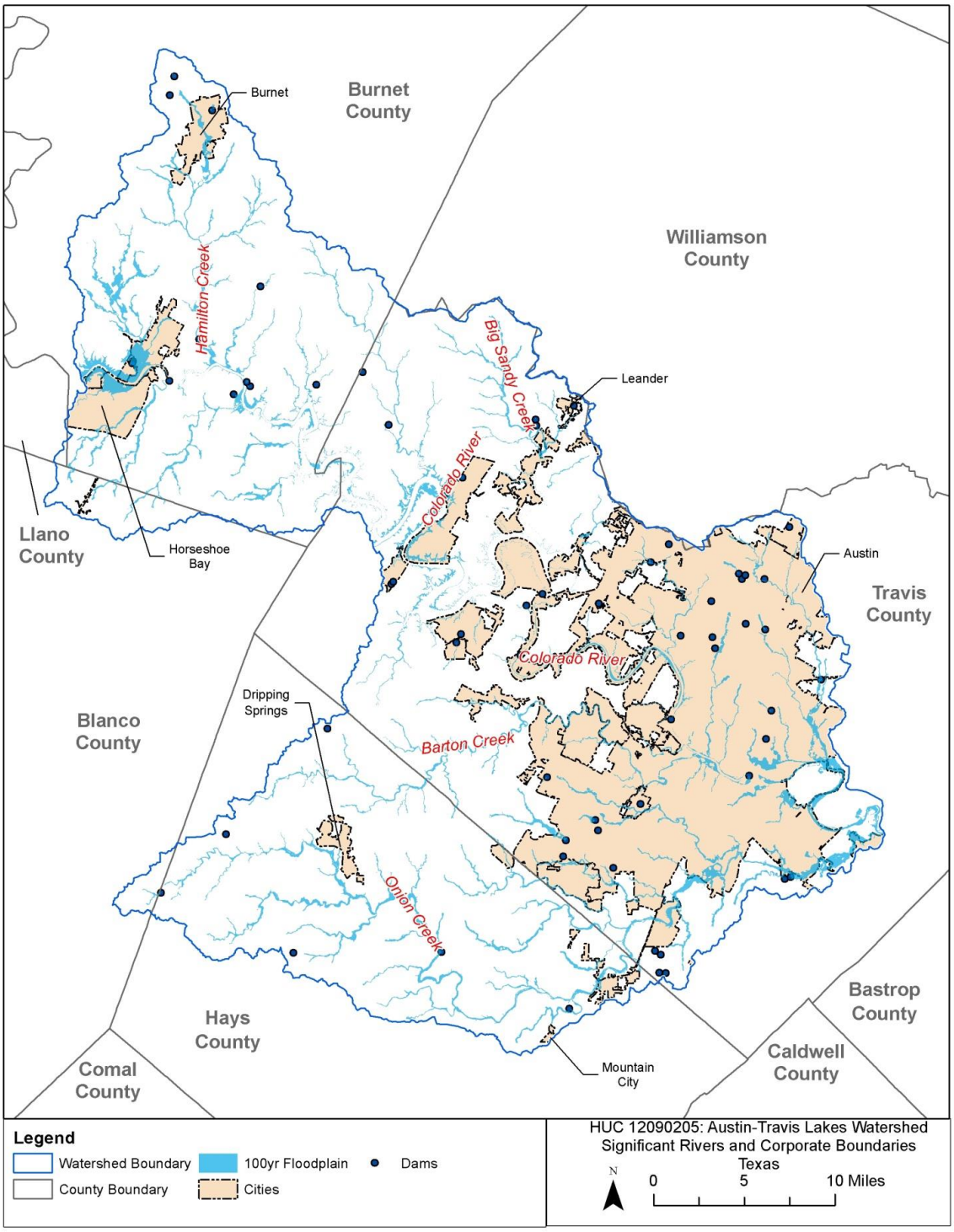

Figure B-19. HUC8 12090205, Austin-Travis Lakes.

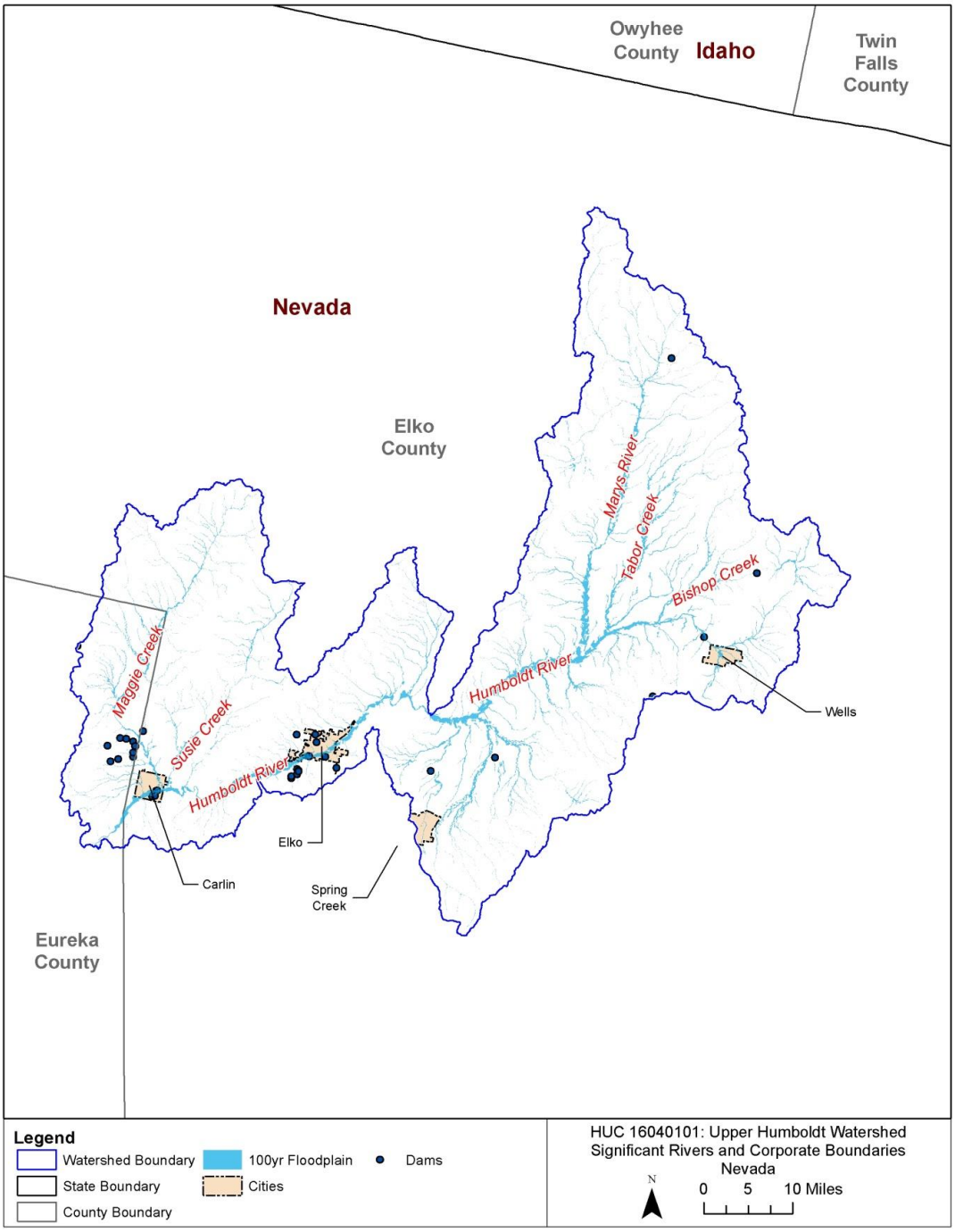

Figure B-20. HUC8 16040101, Upper Humboldt.

Appendix C

Jurisdictions Currently With Retention Standards

State	County	Jurisdiction Name
CA	All	All
MD	All	All
NJ	All	All
NY	All	All
PA	All	All
VT	All	All
WI	All	All
DC	District of Columbia	Washington
MA	Barnstable	Bourne
MA	Barnstable	Brewster
MA	Barnstable	Buzzards Bay
MA	Barnstable	Chatham
MA	Barnstable	Dennis
MA	Barnstable	Dennis Port
MA	Barnstable	East Dennis
MA	Barnstable	East Falmouth
MA	Barnstable	East Harwich
MA	Barnstable	East Sandwich
MA	Barnstable	Falmouth
MA	Barnstable	Forestdale
MA	Barnstable	Harwich Center
MA	Barnstable	Harwich Port
MA	Barnstable	Mashpee Neck
MA	Barnstable	Monomoscoy Island
MA	Barnstable	Monument Beach
MA	Barnstable	New Seabury
MA	Barnstable	North Eastham
MA	Barnstable	North Falmouth
MA	Barnstable	Northwest Harwich
MA	Barnstable	Orleans
MA	Barnstable	Pocasset
MA	Barnstable	Popponesset
MA	Barnstable	Popponesset Island
MA	Barnstable	Sagamore
MA	Barnstable	Sandwich
MA	Barnstable	Seabrook
MA	Barnstable	Seconsett Island
MA	Barnstable	South Dennis
MA	Barnstable	South Yarmouth
MA	Barnstable	Teaticket
MA	Barnstable	West Chatham
MA	Barnstable	West Dennis

State	County	Jurisdiction Name
MA	Barnstable	West Falmouth
MA	Barnstable	West Yarmouth
MA	Barnstable	Woods Hole
MA	Barnstable	Yarmouth Port
MA	Berkshire	Adams
MA	Bristol	Acushnet Center
MA	Bristol	Bliss Corner
MA	Bristol	Mansfield Center
MA	Bristol	North Attleborough Center
MA	Bristol	North Seekonk
MA	Bristol	North Westport
MA	Bristol	Norton Center
MA	Bristol	Ocean Grove
MA	Bristol	Raynham Center
MA	Bristol	Smith Mills
MA	Bristol	Somerset
MA	Essex	Amesbury
MA	Essex	Andover
MA	Essex	Boxford
MA	Essex	Danvers
MA	Essex	Essex
MA	Essex	Ipswich
MA	Essex	Lynnfield
MA	Essex	Marblehead
MA	Essex	Nahant
MA	Essex	Rockport
MA	Essex	Rowley
MA	Essex	Salisbury
MA	Essex	Saugus
MA	Essex	Swampscott
MA	Essex	Topsfield
MA	Hampden	Bondsville
MA	Hampden	Longmeadow
MA	Hampden	Monson Center
MA	Hampden	Palmer
MA	Hampden	Three Rivers
MA	Hampden	West Springfield
MA	Hampden	Wilbraham
MA	Hampshire	Amherst Center
MA	Hampshire	Bondsville
MA	Hampshire	Granby
MA	Hampshire	Hatfield

State	County	Jurisdiction Name
MA	Hampshire	North Amherst
MA	Hampshire	South Amherst
MA	Middlesex	Arlington
MA	Middlesex	Ayer
MA	Middlesex	Belmont
MA	Middlesex	Burlington
MA	Middlesex	Cochituate
MA	Middlesex	East Pepperell
MA	Middlesex	Fort Devens
MA	Middlesex	Framingham
MA	Middlesex	Groton
MA	Middlesex	Hopkinton
MA	Middlesex	Hudson
MA	Middlesex	Lexington
MA	Middlesex	Littleton Common
MA	Middlesex	Maynard
MA	Middlesex	Pepperell
MA	Middlesex	Pinehurst
MA	Middlesex	Reading
MA	Middlesex	Shirley
MA	Middlesex	Stoneham
MA	Middlesex	Townsend
MA	Middlesex	Wakefield
MA	Middlesex	West Concord
MA	Middlesex	Wilmington
MA	Middlesex	Winchester
MA	Norfolk	Bellingham
MA	Norfolk	Braintree
MA	Norfolk	Brookline
MA	Norfolk	Dedham
MA	Norfolk	Dover
MA	Norfolk	Foxborough
MA	Norfolk	Holbrook
MA	Norfolk	Medfield
MA	Norfolk	Millis-Clicquot
MA	Norfolk	Milton
MA	Norfolk	Needham
MA	Norfolk	Norwood
MA	Norfolk	Randolph
MA	Norfolk	Sharon
MA	Norfolk	Walpole
MA	Norfolk	Wellesley

State	County	Jurisdiction Name
MA	Norfolk	Weymouth
MA	Plymouth	Abington
MA	Plymouth	Bridgewater
MA	Plymouth	Duxbury
MA	Plymouth	Green Harbor-Cedar Crest
MA	Plymouth	Hanson
MA	Plymouth	Hingham
MA	Plymouth	Hull
MA	Plymouth	Kingston
MA	Plymouth	Marion Center
MA	Plymouth	Marshfield
MA	Plymouth	Marshfield Hills
MA	Plymouth	Mattapoisett Center
MA	Plymouth	Middleborough Center
MA	Plymouth	North Lakeville
MA	Plymouth	North Pembroke
MA	Plymouth	North Plymouth
MA	Plymouth	North Scituate
MA	Plymouth	Ocean Bluff-Brant Rock
MA	Plymouth	Onset
MA	Plymouth	Plymouth
MA	Plymouth	Scituate
MA	Plymouth	South Duxbury
MA	Plymouth	Wareham Center
MA	Plymouth	West Wareham
MA	Plymouth	Weweantic
MA	Plymouth	White Island Shores
MA	Suffolk	Winthrop
MA	Worcester	Baldwinville
MA	Worcester	Clinton
MA	Worcester	Cordaville
MA	Worcester	East Douglas
MA	Worcester	Fiskdale
MA	Worcester	Fort Devens
MA	Worcester	Hopedale
MA	Worcester	Lunenburg
MA	Worcester	Milford
MA	Worcester	Northborough
MA	Worcester	Oxford
MA	Worcester	Rutland
MA	Worcester	South Ashburnham
MA	Worcester	South Lancaster

State	County	Jurisdiction Name
MA	Worcester	Southbridge
MA	Worcester	Spencer
MA	Worcester	Sturbridge
MA	Worcester	Upton-West Upton
MA	Worcester	Webster
MA	Worcester	Westborough
MA	Worcester	Whitinsville
MA	Worcester	Winchendon
MA	Barnstable	Barnstable Town
MA	Berkshire	North Adams
MA	Berkshire	Pittsfield
MA	Bristol	Attleboro
MA	Bristol	Fall River
MA	Bristol	New Bedford
MA	Bristol	Taunton
MA	Essex	Beverly
MA	Essex	Gloucester
MA	Essex	Haverhill
MA	Essex	Lawrence
MA	Essex	Lynn
MA	Essex	Methuen
MA	Essex	Newburyport
MA	Essex	Peabody
MA	Essex	Salem
MA	Hampden	Agawam
MA	Hampden	Chicopee
MA	Hampden	Holyoke
MA	Hampden	Springfield
MA	Hampden	Westfield
MA	Hampshire	Easthampton
MA	Hampshire	Northampton
MA	Middlesex	Cambridge
MA	Middlesex	Everett
MA	Middlesex	Lowell
MA	Middlesex	Malden
MA	Middlesex	Marlborough
MA	Middlesex	Medford
MA	Middlesex	Melrose
MA	Middlesex	Newton
MA	Middlesex	Somerville
MA	Middlesex	Waltham
MA	Middlesex	Watertown

State	County	Jurisdiction Name
MA	Middlesex	Woburn
MA	Norfolk	Franklin
MA	Norfolk	Quincy
MA	Plymouth	Brockton
MA	Suffolk	Boston
MA	Suffolk	Chelsea
MA	Suffolk	Revere
MA	Worcester	Fitchburg
MA	Worcester	Gardner
MA	Worcester	Leominster
MA	Worcester	Worcester
MA	Barnstable	Barnstable
MA	Berkshire	Berkshire
MA	Bristol	Bristol
MA	Essex	Essex
MA	Hampden	Hampden
MA	Hampshire	Hampshire
MA	Middlesex	Middlesex
MA	Norfolk	Norfolk
MA	Plymouth	Plymouth
MA	Worcester	Worcester
MA	Barnstable	Bourne
MA	Barnstable	Brewster
MA	Barnstable	Chatham
MA	Barnstable	Eastham
MA	Barnstable	Falmouth
MA	Barnstable	Mashpee
MA	Barnstable	Orleans
MA	Barnstable	Sandwich
MA	Barnstable	Yarmouth
MA	Berkshire	Cheshire
MA	Berkshire	Dalton
MA	Berkshire	Hinsdale
MA	Berkshire	Lanesborough
MA	Berkshire	Lenox
MA	Berkshire	Richmond
MA	Bristol	Acushnet
MA	Bristol	Berkley
MA	Bristol	Dartmouth
MA	Bristol	Dighton
MA	Bristol	Easton
MA	Bristol	Fairhaven

State	County	Jurisdiction Name
MA	Bristol	Freetown
MA	Bristol	Mansfield
MA	Bristol	North Attleborough
MA	Bristol	Norton
MA	Bristol	Raynham
MA	Bristol	Rehoboth
MA	Bristol	Seekonk
MA	Bristol	Swansea
MA	Bristol	Westport
MA	Essex	Amesbury
MA	Essex	Andover
MA	Essex	Boxford
MA	Essex	Essex
MA	Essex	Georgetown
MA	Essex	Groveland
MA	Essex	Hamilton
MA	Essex	Ipswich
MA	Essex	Manchester-by-the-Sea
MA	Essex	Merrimac
MA	Essex	Middleton
MA	Essex	Newbury
MA	Essex	North Andover
MA	Essex	Rockport
MA	Essex	Rowley
MA	Essex	Salisbury
MA	Essex	Topsfield
MA	Essex	Wenham
MA	Essex	West Newbury
MA	Hampden	East Longmeadow
MA	Hampden	Hampden
MA	Hampden	Ludlow
MA	Hampden	Monson
MA	Hampden	Palmer
MA	Hampden	Russell
MA	Hampden	Southwick
MA	Hampden	Wilbraham
MA	Hampshire	Belchertown
MA	Hampshire	Granby
MA	Hampshire	Hadley
MA	Hampshire	Hatfield
MA	Hampshire	South Hadley
MA	Hampshire	Southampton

State	County	Jurisdiction Name
MA	Hampshire	Williamsburg
MA	Middlesex	Acton
MA	Middlesex	Ashland
MA	Middlesex	Ayer
MA	Middlesex	Bedford
MA	Middlesex	Billerica
MA	Middlesex	Boxborough
MA	Middlesex	Carlisle
MA	Middlesex	Chelmsford
MA	Middlesex	Concord
MA	Middlesex	Dracut
MA	Middlesex	Dunstable
MA	Middlesex	Groton
MA	Middlesex	Holliston
MA	Middlesex	Hopkinton
MA	Middlesex	Hudson
MA	Middlesex	Lincoln
MA	Middlesex	Littleton
MA	Middlesex	Natick
MA	Middlesex	North Reading
MA	Middlesex	Pepperell
MA	Middlesex	Sherborn
MA	Middlesex	Shirley
MA	Middlesex	Stow
MA	Middlesex	Sudbury
MA	Middlesex	Tewksbury
MA	Middlesex	Townsend
MA	Middlesex	Tyngsborough
MA	Middlesex	Wayland
MA	Middlesex	Westford
MA	Middlesex	Weston
MA	Norfolk	Avon
MA	Norfolk	Bellingham
MA	Norfolk	Braintree
MA	Norfolk	Canton
MA	Norfolk	Cohasset
MA	Norfolk	Dover
MA	Norfolk	Foxborough
MA	Norfolk	Medfield
MA	Norfolk	Medway
MA	Norfolk	Millis
MA	Norfolk	Norfolk

State	County	Jurisdiction Name
MA	Norfolk	Plainville
MA	Norfolk	Sharon
MA	Norfolk	Stoughton
MA	Norfolk	Walpole
MA	Norfolk	Westwood
MA	Norfolk	Wrentham
MA	Plymouth	Bridgewater
MA	Plymouth	Carver
MA	Plymouth	Duxbury
MA	Plymouth	East Bridgewater
MA	Plymouth	Halifax
MA	Plymouth	Hanover
MA	Plymouth	Hanson
MA	Plymouth	Hingham
MA	Plymouth	Kingston
MA	Plymouth	Lakeville
MA	Plymouth	Marion
MA	Plymouth	Marshfield
MA	Plymouth	Mattapoisett
MA	Plymouth	Middleborough
MA	Plymouth	Norwell
MA	Plymouth	Pembroke
MA	Plymouth	Plymouth
MA	Plymouth	Plympton
MA	Plymouth	Rochester
MA	Plymouth	Rockland
MA	Plymouth	Scituate
MA	Plymouth	Wareham
MA	Plymouth	West Bridgewater
MA	Plymouth	Whitman
MA	Worcester	Auburn
MA	Worcester	Berlin
MA	Worcester	Blackstone
MA	Worcester	Bolton
MA	Worcester	Boylston
MA	Worcester	Charlton
MA	Worcester	Clinton
MA	Worcester	Douglas
MA	Worcester	Dudley
MA	Worcester	Grafton
MA	Worcester	Harvard
MA	Worcester	Holden

State	County	Jurisdiction Name
MA	Worcester	Hopedale
MA	Worcester	Lancaster
MA	Worcester	Leicester
MA	Worcester	Lunenburg
MA	Worcester	Mendon
MA	Worcester	Milford
MA	Worcester	Millbury
MA	Worcester	Millville
MA	Worcester	Northborough
MA	Worcester	Northbridge
MA	Worcester	Oxford
MA	Worcester	Paxton
MA	Worcester	Rutland
MA	Worcester	Shrewsbury
MA	Worcester	Southborough
MA	Worcester	Southbridge
MA	Worcester	Spencer
MA	Worcester	Sterling
MA	Worcester	Sturbridge
MA	Worcester	Sutton
MA	Worcester	Templeton
MA	Worcester	Upton
MA	Worcester	Uxbridge
MA	Worcester	Webster
MA	Worcester	West Boylston
MA	Worcester	Westborough
MA	Worcester	Westminster
MA	Worcester	Winchendon
MA	Hampshire	Belchertown
MA	Middlesex	Townsend
MD	Allegany	Allegany
MD	Washington	Washington
MT	Silver Bow	Butte-Silver Bow (balance)
MT	Cascade	Black Eagle
MT	Cascade	Malmstrom AFB
MT	Lewis and Clark	Helena Valley Southeast
MT	Lewis and Clark	Helena Valley West Central
MT	Lewis and Clark	Helena West Side
MT	Missoula	Bonner-West Riverside
MT	Missoula	East Missoula
MT	Missoula	Orchard Homes
MT	Missoula	Wye

State	County	Jurisdiction Name
MT	Yellowstone	Lockwood
MT	Cascade	Great Falls
MT	Flathead	Kalispell
MT	Gallatin	Bozeman
MT	Lewis and Clark	Helena
MT	Missoula	Missoula
MT	Yellowstone	Billings
MT	Cascade	Cascade
MT	Flathead	Flathead
MT	Gallatin	Gallatin
MT	Lewis and Clark	Lewis and Clark
MT	Missoula	Missoula
MT	Yellowstone	Yellowstone
NH	Hillsborough	East Merrimack
NH	Hillsborough	Hudson
NH	Hillsborough	Milford
NH	Hillsborough	Pinardville
NH	Hillsborough	Wilton
NH	Merrimack	Hooksett
NH	Merrimack	South Hooksett
NH	Merrimack	Suncook
NH	Rockingham	Derry
NH	Rockingham	Exeter
NH	Rockingham	Hampton
NH	Rockingham	Londonderry
NH	Rockingham	Newmarket
NH	Rockingham	Raymond
NH	Strafford	Durham
NH	Hillsborough	Manchester
NH	Hillsborough	Nashua
NH	Rockingham	Portsmouth
NH	Strafford	Dover
NH	Strafford	Rochester
NH	Strafford	Somersworth
NH	Hillsborough	Hillsborough
NH	Merrimack	Merrimack
NH	Rockingham	Rockingham
NH	Strafford	Strafford
NH	Hillsborough	Amherst
NH	Hillsborough	Bedford
NH	Hillsborough	Goffstown
NH	Hillsborough	Hollis

State	County	Jurisdiction Name
NH	Hillsborough	Hudson
NH	Hillsborough	Litchfield
NH	Hillsborough	Merrimack
NH	Hillsborough	Milford
NH	Hillsborough	Pelham
NH	Merrimack	Hooksett
NH	Rockingham	Atkinson
NH	Rockingham	Auburn
NH	Rockingham	Brentwood
NH	Rockingham	Chester
NH	Rockingham	Danville
NH	Rockingham	Derry
NH	Rockingham	East Kingston
NH	Rockingham	Exeter
NH	Rockingham	Greenland
NH	Rockingham	Hampstead
NH	Rockingham	Hampton
NH	Rockingham	Hampton Falls
NH	Rockingham	Kingston
NH	Rockingham	Londonderry
NH	Rockingham	New Castle
NH	Rockingham	Newington
NH	Rockingham	Newton
NH	Rockingham	North Hampton
NH	Rockingham	Plaistow
NH	Rockingham	Rye
NH	Rockingham	Salem
NH	Rockingham	Sandown
NH	Rockingham	Seabrook
NH	Rockingham	South Hampton
NH	Rockingham	Windham
NH	Strafford	Durham
NH	Strafford	Madbury
NH	Strafford	Milton
NH	Strafford	Rollinsford
OH	Washington	Belpre
OH	Belmont	Shadyside
OH	Lawrence	South Point
TN	Cheatham	Nashville-Davidson
TN	Davidson	Nashville-Davidson
TN	Robertson	Nashville-Davidson
TN	Blount	Eagleton Village

State	County	Jurisdiction Name
TN	Blount	Seymour
TN	Bradley	East Cleveland
TN	Bradley	Hopewell
TN	Bradley	South Cleveland
TN	Bradley	Wildwood Lake
TN	Carter	Central
TN	Carter	Hunter
TN	Carter	Pine Crest
TN	Hamilton	East Brainerd
TN	Hamilton	Fairmount
TN	Hamilton	Harrison
TN	Hamilton	Middle Valley
TN	Hamilton	Ooltewah
TN	Knox	Mascot
TN	Rutherford	Walterhill
TN	Sevier	Seymour
TN	Sullivan	Bloomingdale
TN	Sullivan	Blountville
TN	Sullivan	Colonial Heights
TN	Sullivan	Spurgeon
TN	Sullivan	Walnut Hill
TN	Washington	Gray
TN	Washington	Midway
TN	Washington	Oak Grove
TN	Washington	Spurgeon
TN	Wilson	Green Hill
TN	Anderson	Clinton
TN	Anderson	Oak Ridge
TN	Bedford	Shelbyville
TN	Blount	Alcoa
TN	Blount	Friendsville
TN	Blount	Louisville
TN	Blount	Maryville
TN	Blount	Rockford
TN	Bradley	Charleston
TN	Bradley	Cleveland
TN	Carter	Elizabethton
TN	Carter	Johnson City
TN	Carter	Watauga
TN	Coffee	Tullahoma
TN	Davidson	Belle Meade
TN	Davidson	Berry Hill

State	County	Jurisdiction Name
TN	Davidson	Forest Hills
TN	Davidson	Goodlettsville
TN	Davidson	Lakewood
TN	Davidson	Oak Hill
TN	Davidson	Ridgetop
TN	Dyer	Dyersburg
TN	Fayette	Piperton
TN	Franklin	Tullahoma
TN	Hamblen	Morristown
TN	Hamilton	Chattanooga
TN	Hamilton	Collegedale
TN	Hamilton	East Ridge
TN	Hamilton	Lakesite
TN	Hamilton	Red Bank
TN	Hamilton	Ridgeside
TN	Hamilton	Soddy-Daisy
TN	Hawkins	Church Hill
TN	Hawkins	Kingsport
TN	Haywood	Brownsville
TN	Jefferson	Jefferson City
TN	Jefferson	Morristown
TN	Knox	Knoxville
TN	Loudon	Lenoir City
TN	Madison	Jackson
TN	Maury	Columbia
TN	Montgomery	Clarksville
TN	Obion	Union City
TN	Putnam	Cookeville
TN	Roane	Oak Ridge
TN	Robertson	Millersville
TN	Robertson	Ridgetop
TN	Robertson	Springfield
TN	Robertson	White House
TN	Rutherford	La Vergne
TN	Rutherford	Murfreesboro
TN	Sevier	Sevierville
TN	Shelby	Bartlett
TN	Shelby	Germantown
TN	Shelby	Lakeland
TN	Shelby	Memphis
TN	Shelby	Millington
TN	Sullivan	Bluff City

State	County	Jurisdiction Name
TN	Sullivan	Bristol
TN	Sullivan	Johnson City
TN	Sullivan	Kingsport
TN	Sumner	Gallatin
TN	Sumner	Goodlettsville
TN	Sumner	Hendersonville
TN	Sumner	Millersville
TN	Sumner	White House
TN	Warren	McMinnville
TN	Washington	Johnson City
TN	Washington	Watauga
TN	Williamson	Brentwood
TN	Williamson	Franklin
TN	Wilson	Mount Juliet
TN	Anderson	Anderson
TN	Bedford	Bedford
TN	Blount	Blount
TN	Bradley	Bradley
TN	Carter	Carter
TN	Davidson	Davidson
TN	Dyer	Dyer
TN	Greene	Greene
TN	Hamblen	Hamblen
TN	Hamilton	Hamilton
TN	Hawkins	Hawkins
TN	Haywood	Haywood
TN	Jefferson	Jefferson
TN	Knox	Knox
TN	Loudon	Loudon
TN	Madison	Madison
TN	Maury	Maury
TN	McMinn	McMinn
TN	Montgomery	Montgomery
TN	Obion	Obion
TN	Putnam	Putnam
TN	Roane	Roane
TN	Robertson	Robertson
TN	Rutherford	Rutherford
TN	Sevier	Sevier
TN	Shelby	Shelby
TN	Sullivan	Sullivan
TN	Sumner	Sumner

State	County	Jurisdiction Name
TN	Warren	Warren
TN	Washington	Washington
TN	Williamson	Williamson
TN	Wilson	Wilson
TN	Anderson	Oliver Springs
TN	Greene	Greeneville
TN	Hamilton	Lookout Mountain
TN	Hamilton	Signal Mountain
TN	Hamilton	Walden
TN	Hawkins	Mount Carmel
TN	Hawkins	Surgoinsville
TN	Jefferson	New Market
TN	Jefferson	White Pine
TN	Knox	Farragut
TN	Loudon	Farragut
TN	Loudon	Loudon
TN	McMinn	Calhoun
TN	Morgan	Oliver Springs
TN	Roane	Oliver Springs
TN	Robertson	Greenbrier
TN	Rutherford	Smyrna
TN	Shelby	Collierville
TN	Sumner	Walnut Grove
TN	Unicoi	Unicoi
TN	Washington	Jonesborough
TN	Williamson	Nolensville
WV	Berkeley	Inwood
WV	Brooke	Hooverson Heights
WV	Cabell	Culloden
WV	Cabell	Pea Ridge
WV	Kanawha	Coal Fork
WV	Kanawha	Cross Lanes
WV	Kanawha	Elkview
WV	Kanawha	Pinch
WV	Kanawha	Tornado
WV	Mineral	Wiley Ford
WV	Monongalia	Brookhaven
WV	Monongalia	Cassville
WV	Monongalia	Cheat Lake
WV	Putnam	Culloden
WV	Putnam	Teays Valley
WV	Raleigh	Beaver

State	County	Jurisdiction Name
WV	Raleigh	Bradley
WV	Raleigh	Crab Orchard
WV	Raleigh	Daniels
WV	Raleigh	MacArthur
WV	Raleigh	Piney View
WV	Raleigh	Prosperity
WV	Raleigh	Shady Spring
WV	Raleigh	Stanaford
WV	Wood	Blennerhassett
WV	Wood	Boaz
WV	Wood	Lubeck
WV	Wood	Mineralwells
WV	Wood	Washington
WV	Berkeley	Martinsburg
WV	Brooke	Follansbee
WV	Brooke	Weirton
WV	Brooke	Wellsburg
WV	Cabell	Huntington
WV	Fayette	Montgomery
WV	Fayette	Mount Hope
WV	Fayette	Oak Hill
WV	Grant	Petersburg
WV	Hancock	Weirton
WV	Harrison	Bridgeport
WV	Harrison	Clarksburg
WV	Kanawha	Charleston
WV	Kanawha	Dunbar
WV	Kanawha	Marmet
WV	Kanawha	Montgomery
WV	Kanawha	Nitro
WV	Kanawha	South Charleston
WV	Kanawha	St. Albans
WV	Marshall	Benwood
WV	Marshall	Glen Dale
WV	Marshall	McMechen
WV	Marshall	Moundsville
WV	Marshall	Wheeling
WV	Mercer	Bluefield
WV	Mineral	Keyser
WV	Monongalia	Morgantown
WV	Monongalia	Star City
WV	Monongalia	Westover

State	County	Jurisdiction Name
WV	Ohio	Wheeling
WV	Putnam	Hurricane
WV	Putnam	Nitro
WV	Raleigh	Beckley
WV	Wayne	Ceredo
WV	Wayne	Huntington
WV	Wayne	Kenova
WV	Wood	Parkersburg
WV	Wood	Vienna
WV	Wood	Williamstown
WV	Berkeley	Berkeley
WV	Brooke	Brooke
WV	Cabell	Cabell
WV	Fayette	Fayette
WV	Hancock	Hancock
WV	Harrison	Harrison
WV	Jefferson	Jefferson
WV	Kanawha	Kanawha
WV	Marshall	Marshall
WV	Mineral	Mineral
WV	Monongalia	Monongalia
WV	Ohio	Ohio
WV	Putnam	Putnam
WV	Raleigh	Raleigh
WV	Wayne	Wayne
WV	Wood	Wood
WV	Berkeley	Hedgesville
WV	Cabell	Milton
WV	Fayette	Fayetteville
WV	Hardy	Moorefield
WV	Kanawha	Belle
WV	Kanawha	Cedar Grove
WV	Kanawha	Chesapeake
WV	Kanawha	Clendenin
WV	Kanawha	East Bank
WV	Kanawha	Glasgow
WV	Kanawha	Jefferson
WV	Mineral	Carpendale
WV	Mineral	Piedmont
WV	Mineral	Ridgeley
WV	Monongalia	Granville
WV	Monongalia	Star City

State	County	Jurisdiction Name
WV	Ohio	Triadelphia
WV	Putnam	Bancroft
WV	Putnam	Eleanor
WV	Putnam	Poca
WV	Putnam	Winfield
WV	Raleigh	Mabscott
WV	Raleigh	Sophia
WV	Wood	North Hills
WV	Cabell	Barboursville
WV	Ohio	Bethlehem
WV	Ohio	Clearview

Appendix D

Methodology to Project Future Development Characteristics and Estimate Future Runoff Volumes and Peak Flows

Overview of Use of EPA's Project Prediction Model for Estimating Future Development Characteristics

EPA prepared future development estimates and provided these estimates to Atkins for use in this study. This section describes the process to arrive at those estimates.

To develop future predictions, EPA combined forecasts of population growth and construction value with distributions of observed project characteristics to estimate a baseline forecast of new development and redevelopment projects covering the period 2016 – 2040. To produce projections that included these factors, a forecasting model referred to as the Project Prediction Model (PPM) was developed. The forecast was made at 5-year increments, predicting individual projects – each with detailed project characteristics – at the Hydrologic Unit Code 12 (HUC12) watershed level. The principal components of the PPM forecasting process include:

- *Estimating the baseline level of development and impervious cover in the year 2010.* The baseline estimate of existing development includes assessments of developed area and impervious surface (IS) cover, and accounts for land area available for future development. The baseline was estimated according to algorithms that integrate:
  1. Population density data obtained from the GIS-based Integrated Climate and Land Use Scenarios model, ICLUS v1.5;
  2. Data on commercial and industrial IS from the National Land Use Cover Database (NLCD);
  3. Ratios of historical industrial and commercial development based on IHS-Global Insight construction value data; and,
  4. Data describing individual project characteristics derived from
     5. RSMeans (Reed Construction), and
     6. State-level Notice of Intent (NOI) databases for Maryland, New York, and California.

  By combining these datasets, an integrated picture of baseline development, including developed area, IS area, population density, and undeveloped land was established for the year 2015 at the HUC12 scale nationwide.
- *Estimating aggregate development value constraints.* The PPM methodology was designed to ensure that the profile of forecasted projects matches future expectations about the quantity, type, and location of development across the United States. These constraints were developed based on estimates of population growth from the US Census Bureau, IHS Global Insight construction value forecasts, and the ratio of new development to redevelopment projects (occurring across construction types and population density categories) estimated from Maryland, New York and California NOI data.
- *Generating a project database for each State-Metropolitan Statistical Area (MSA) region.* The second component of the PPM converts the aforementioned measures of construction activity into individual projects. EPA uses distributions and ratios describing key project characteristics obtained from the RSMeans and the NOI databases. Project level values were randomly drawn,

within constraints, to forecast future construction occurring in State-MSA regions over 5-year increments between 2016 and 2040. Each project was then probabilistically assigned a suitable project size (acres), IS cover (acres) and a dollar value.

- *Spatially allocating forecasted projects to HUC12 watersheds within state and MSA regions.* Project forecasts for a given MSA/Non-MSA region were allocated to HUC12 watershed polygons in that region according to patterns of growth projected by the ICLUS model. If allocation of new projects was not possible (because of insufficient land area available to new development), the fraction of redevelopment projects was increased, projects re-generated, and spatial allocation attempted once again. This process was repeated until either, 1) new projects were successfully assigned, or 2) all construction value was assigned to redevelopment projects.
- *Assigning additional project characteristics.* Once assigned to HUC12s, projects were given additional characteristics appropriate to location, density and construction type, including soil characteristics (according to the US General Soil Map - STATSGO2), state (for MSAs crossing state boundaries), representative climate station, and existing stormwater regulations. Project characteristics assigned into individual HUC12s were tracked such that total IS (and marginal changes to IS occurring with redevelopment) could be calculated through time, while making sure that land available to new construction decreases. Notably, as population densities increase (and available land decreases), the fraction of total construction value occurring in redevelopment projects increases.

Process to Allocate Estimates of Development and IS within the HUC12 Watershed

The PPM was designed to predict projects at the MSA/HUC12 scale for use in EPA applications. This geographic scale was considered to be sufficiently detailed to address climate and demographic patterns relevant for regional and national scale analyses for the other EPA applications, while also being large enough to accommodate the prediction of construction projects that can range in size from one to several hundred acres.

The prediction of individual development projects, rather than developed acres only, was necessary to support the economic and engineering analyses, as these analyses must account for the frequency of occurrence for project level attributes. However, modeling at the HUC12 watershed scale is not sufficiently detailed for estimating the extent to which stormwater retention practices can mitigate flooding damage that may occur during large storm events. Flood damage mitigation analyses are sensitive to the geographic placement of development within the watershed, and are less sensitive to project characteristics such as project type.

To accommodate flood damage mitigation analyses while remaining consistent with the economic and engineering analyses, a methodology was developed to allocate HUC12-scale estimates of development and IS areas to 1-hectare pixels located within the watershed. What follows is an overview of the methodology used to 'push' aggregate development estimates to a finer resolution, first for baseline development, then for future new development and redevelopment.

A basic approach was used to allocate the predicted development area and IS area for each HUC12. First, baseline (i.e., 2015) development and IS estimates were allocated. New development and redevelopment estimates for each of the five subsequent 5-year time steps were then allocated in turn. ICLUS model output and NLCD data were available at the hectare scale, and were used to estimate hectare-scale baseline development and undeveloped land areas. Output from ICLUS provided pixel-level residential IS estimates, while NLCD data provided pixel-level IS estimates for non-residential development. Using ratios of average total developed area to IS from state NOI data, EPA was able to estimate residential land area and non-residential land area.

Baseline Development and Impervious Surface Allocation

For each pixel, the amount of potentially developable land was estimated by subtracting all of the residential development estimated by ICLUS and nonresidential development estimated by NLCD. The ICLUS model removes pixels containing areas considered undevelopable, including water features, parkland, and agricultural zones. No development was allocated to pixels identified as being undevelopable. The developable area is calculated as

Developable Area = Total Area – Residential Area – Commercial/Institutional Area – Industrial Area

Note that ICLUS residential IS output and NLCD non-residential IS data were derived independently of one another. Consequently for this analysis, development area estimates were extrapolated from both of these data sets using average ratios of IS to developed area derived from NOI data. As a result, the sum of residential and nonresidential land exceeded the area (1 hectare) of some pixels. When this occurred this excess developed area was reallocated to other pixels within the same HUC12. Before the excess developed area was reallocated, it was first aggregated across the HUC12 and then divided into smaller units one tenth of a hectare in size. These smaller units were then assigned to pixels with developable space, starting with the pixels with the most developable area. This was done until all of the excess developed area had been reallocated.

Once all developed area was allocated to individual pixels, these pixels were checked for excessive IS. There were cases of pixels with excessive IS because ICLUS/NLCD estimates of IS sometimes exceeded the maximum imperviousness of projects observed in NOI databases. To ensure that the sum of pixel-level estimates of IS were consistent with those used in the project prediction model, reallocation of this excess IS was required. For each pixel, the percent IS was compared against the maximum percent IS observed in the NOI data. For all pixels with IS greater than the maximum, the pixel's IS was capped at the maximum and the excess was aggregated for the HUC12. This process followed the same approach for reallocating excess developed area, where excess IS was divided into 0.1-ha units and reallocated to pixels with developed area below the maximum, with probabilities of reallocation highest in pixels with the lowest percent IS.

New Development and Impervious Surface Allocation

For each time step, each new project greater than one hectare was split into blocks of one hectare. These blocks were then allocated to pixels with developable area equal to one hectare within the same HUC12. Maintaining project integrity (i.e. keeping a divided project on adjacent pixels) was not necessary for the flooding analysis, would have been extremely computationally intensive, and for many HUC12's likely infeasible. Consequently, each block was allocated independently, and there was no effort to allocate blocks to contiguous pixels. These blocks were allocated until either all of the project's blocks were allocated or there were no more pixels with a hectare of developable land remaining in the HUC. When this occurred, the remaining project area was divided into progressively smaller blocks (e.g., 0.5, 0.1, 0.05, 0.01 hectares) and the allocation process was repeated as needed until each project's area had been fully allocated. A check was made to ensure that no pixel contained more than one hectare of development; if any excess development was found, it was aggregated, divided into tenths of a hectare, and reallocated using the same approach as with baseline development above.

Project IS was divided up into the new project blocks equally (i.e., if the initial project had 40% IS, all subsequent blocks were assigned 40% IS). After all project developed area had been allocated, a check was made to ensure that no pixel contains more than the maximum IS observed in the NOI data. If any excess IS was found, it was aggregated and reallocated using the same approach as with baseline IS, described above.

Redevelopment and Impervious Surface Allocation

For a given time step and HUC12, redevelopment projects were allocated after all new development projects. Each redevelopment project was split into blocks and allocated, using a process similar to that used to allocate new development. However, only pixels with existing development were assigned redevelopment projects, and then only to the previously developed area within each pixel.

After all redevelopment projects were allocated, the net change in IS was calculated for each pixel's assigned redevelopment. Similar to the check made with new development IS, net redevelopment IS for each pixel was compared to the maximum IS observed in the NOI data, and all excess IS was reallocated to other pixels containing redevelopment area. Once the redevelopment process was complete, new project area was allocated for the next time step. This process continued until all projects predicted within the analytical time frame and relevant HUC12s were allocated.

Assigning Asset Values to New Development and Redevelopment Areas

The value of future development was also considered for the flood avoidance analysis. Value is one of the project attributes predicted by the PPM and is, in fact, the constraint used to forecast the quantity of future construction (in terms of projects and acres). What follows is an overview of the methodology used to aggregate estimates of construction value:

1. Estimate aggregate construction value to 2025. These values were estimated using IHS Global Insight's U.S. State and Metro Construction Quarterly Briefing.
2. Estimate aggregate construction value through 2040. The analysis used the long-term average annual growth rate (between 1993 and 2025) in constant dollar value of construction by construction category and location to forecast construction spending from 2026 – 2040.
3. Estimate construction values per acre of development. Project level construction values (on a per-acre basis) were obtained using data generated by Reed Construction and the U.S. Census Bureau.
4. Develop project size database. A database of project sizes, densities, and other project characteristics was developed using data from Reed Construction and NOI databases from Maryland, New York, and California.
5. Estimate local construction value constraints by development type. After total spending was established for each state and MSA (step 2, above), it was allocated to new development and redevelopment activities. This split was estimated using an algorithm that used observations from NOI databases to develop relationships between new development and redevelopment project probabilities and construction type (e.g., industrial, commercial, single family, multi-family), and construction density (e.g., rural, exurban, suburban, urban).

Once individual projects (with known construction values) were broken into blocks and allocated to the landscape at the HUC12 scale, their value could then be readily assigned based on each project's size and type. For each HUC12 relevant to the flooding analysis, the project value was aggregated for all new and redeveloped projects predicted to occur between 2016 and 2040. Because the first 8 of the 12 digits within a HUC12 code reflect the underlying HUC8, a database query of forecast projects was conducted to aggregate project values within each HUC8 of interest for the flooding analysis.

Estimation of Future Runoff Volumes

The typical Census block consists of several land uses; some are developed and others are not, and there is often an open water component. New development can take place in some of the undeveloped land uses. Open water and wetlands are not considered developable. Areas already developed can undergo redevelopment in the future. These components are shown generically in Figure D-1. For existing conditions, land use is given by the NLCD and soils by the U.S. General Soil Map (STATSGO2). The equations to calculate runoff volumes are developed based on USDA (1986).

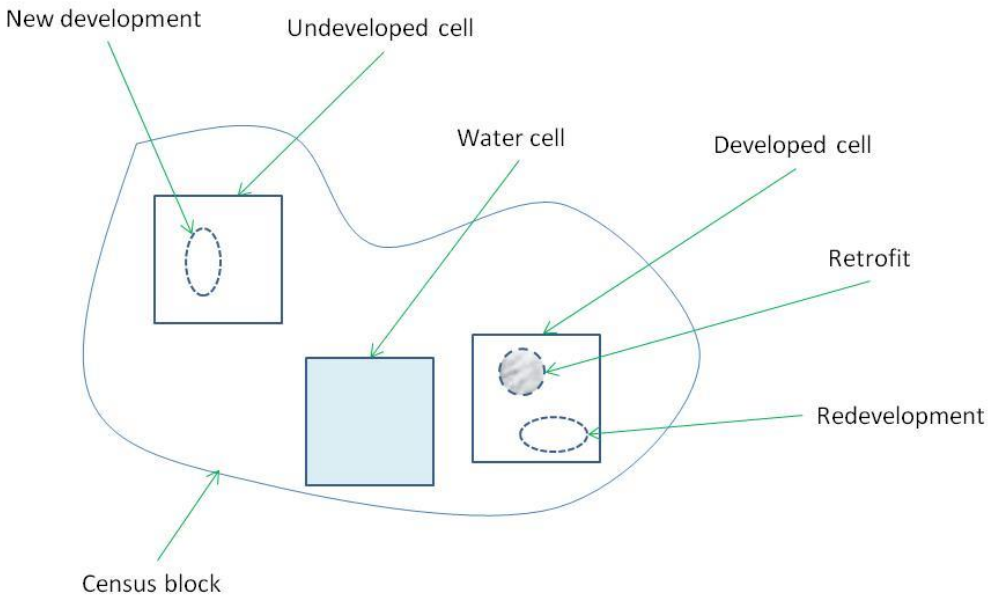

Figure D-1. Generic Census block showing the potential segments available for development.

The methodology described subsequently is based on subdividing the Census block into cells using a uniform grid. Each cell has a homogeneous land use (undeveloped, developed, or water) and soil type.

The following variables are known for each Census block

A = Total area of the Census block (acres)

A_u = Undeveloped area (acres)

i_u = Impervious fraction of undeveloped areas (dimensionless)

A_d = Developed area (acres)

i_d = Impervious fraction of developed areas (dimensionless)

$A_w = A - A_u - A_d$ = Area of open water and wetlands (acres)

A_n = Area slated for future new development (acres)

I_n = Imperviousness added by new development (acres)

A_r = Area slated for future redevelopment (acres)

I_r = Imperviousness added by redevelopment (acres)

Projections for new development and redevelopment were provided by EPA as described earlier in this Appendix. New development can only take place in undeveloped cells. Redevelopment and imperviousness retrofits can occur only in developed cells. Therefore, these land segments must meet the following conditions:

$$I_n < A_n < A_u$$
$$A_r + A_n < A_d$$
$$I_r < A_d$$

Both the undeveloped and developed areas have an impervious and a pervious area. The latter is termed "open space." These open space areas can be estimated from the imperviousness fractions

$$(\boldsymbol{A_u})_{\boldsymbol{open}} = \boldsymbol{A_u}(\mathbf{1} - \boldsymbol{i_u}) \quad \text{(D-1)}$$

$$(A_d)_{open} = A_d(1 - i_d) \quad \text{(D-2)}$$

The following ratios are defined based on these quantities:

$F_n = \frac{A_n}{A_u}$ = ratio of new development to undeveloped areas

$F_r = \frac{A_r}{A_d}$ = ratio of re- development to developed areas

$i_n = \frac{I_n}{A_u}$ = imperviousness introduced by new development

$i_r = \frac{I_r}{A_d}$ = imperviousness introduced by redevelopment

Because no specific projects are assigned to a given Census block, the additional imperviousness introduced by new development is assumed to be distributed uniformly across the undeveloped areas. A similar distribution was done for redevelopment.

Undeveloped Cells

Given an undeveloped cell k with area A^k and imperviousness fraction i^k, the new development area assigned to it is

$$A_n^k = \frac{A_n}{A_u} A^k = F_n A^k \quad \text{(D-3)}$$

The additional imperviousness is similarly distributed, except that it must occupy available open space in the cell. Therefore, the total impervious area (acres) is the sum of the existing and additional impervious areas

$$I_n^k = \frac{I_n}{(A_u)_{open}}(A^k)_{open} + i^k A^k \quad \text{(D-4)}$$

where $(A^k)_{open}$ is the area of open space (acres) in the cell defined by

$$(A^k)_{open} = A^k(1 - i^k) \quad \text{(D-5)}$$

The total impervious fraction after the new imperviousness is added is then

$$i_n^k = \frac{I_n^k}{A^k} = \frac{I_n(1 - i^k)}{A_u(1 - i_u)} + i^k = i_n \frac{1 - i^k}{1 - i_u} + i^k \quad \text{(D-6)}$$

The curve number for the cell is

$$\mathrm{CN}_n^k = \mathrm{CN}_{open}^k(1 - i_n^k) + 98 i_n^k \quad \text{(D-7)}$$

where CN_{open}^k corresponds to the curve number for "open space in good condition" for the soil type in the cell. The runoff depth is

$$V_n^k = \frac{(P - 0.2S_n^k)^2}{P + 0.8S_n^k} \quad \text{(D-8)}$$

where

$$S_n^k = \frac{1000}{\mathrm{CN}_n^k} - 10 \quad \text{(D-9)}$$

and

$$P > 0.2S_n^k \quad \text{(D-10)}$$

The stormwater "medium" scenario will apply only on the new development areas (when considering undeveloped cells); therefore, the runoff generated by those areas will be reduced by an amount equal to the retention scenario. The runoff after GI is applied is then

$$V_{GI}^k = \mathrm{V}_n^k(1 - F_n) + (V_n^k - d_n)F_n \quad \text{(D-11)}$$

where d_n is the 90th percentile retention depth that applies for new development. If $V_n^k < d_n$ then no runoff is produced by the new development.

Developed Cells

Given a developed cell k with area A^k and imperviousness fraction i^k, the redevelopment area assigned to it is

$$A_r^k = \frac{A_r}{A_d} A^k = F_r A^k \tag{D-12}$$

The additional imperviousness is also uniformly distributed on the available open space in the cell. Therefore, the total impervious area (acres) is the sum of the existing and additional impervious areas

$$I_r^k = \frac{I_r}{(A_d)_{open}} (A^k)_{open} + i^k A^k \tag{D-13}$$

where $(A^k)_{open}$ is the area of open space in the cell defined by

$$(A^k)_{open} = A^k(1 - i^k) \tag{D-14}$$

The total impervious fraction after the additional redevelopment imperviousness is placed is then

$$i_r^k = \frac{I_r^k}{A^k} = \frac{I_r(1 - i^k)}{A_d(1 - i_d)} + i^k = i_r \frac{1 - i^k}{1 - i_d} + i^k \tag{D-15}$$

The curve number for the cell is

$$\mathrm{CN}_r^k = \mathrm{CN}_{open}^k (1 - i_r^k) + 98 i_r^k \tag{D-16}$$

Where CN_{open}^k corresponds to the curve number for "open space in good condition" for the soil type in the cell. The runoff depth is

$$V_r^k = \frac{(P - 0.2S_r^k)^2}{P + 0.8S_r^k} \tag{D-17}$$

where

$$S_r^k = \frac{1000}{\mathrm{CN}_r^k} - 10 \quad \text{(D-18)}$$

and

$$P > 0.2S_r^k \quad \text{(D-19)}$$

GI will be applicable only on the redeveloped areas; therefore, the runoff generated by those areas will be decreased by an amount equal to the retention standard for redevelopment. The runoff after GI is applied is then

$$V_{GI}^k = \mathrm{V}_r^k(1 - F_r) + (V_r^k - d_r)F_r \quad \text{(D-20)}$$

where d_r is the 85th percentile retention depth for the "medium" scenario that applies for redevelopment. If $V_r^k < d_r$ then no runoff is produced by the redevelopment areas.

Water Cells

Rain that falls on open water or wetlands cells is considered equal to runoff and is the same with or without GI; therefore

$$V^k = \mathrm{V}_{GI}^k = P \quad \text{(D-21)}$$

Estimation of future peak flows

MMSD (2005) discusses five methods to account for the distributed effect of retention practices on peak flows and runoff hydrographs. Chapter 7 presents a summary of these methods. The current study uses a methodology based on these methods to adjust the peak flows from streamflow records assumed representative of current conditions, to two other conditions: peak flows in 2040 without GI and peak flows in 2040 with GI.

Given the scope of this study and the nature of the available data, the most appropriate method to perform these adjustments in one that takes advantage of the functional relationship between peak flows and runoff volume in the TR-55 method (USDA, 1986):

$$Q = q_u A\, V F_p \quad \text{(D-22)}$$

where:

q_u is the unit peak discharge (cfs/mi²/in)

Q is the peak flow (cfs)

A is the watershed area in (mi^2)

V is the depth of direct runoff (in), and

F_p is the pond-and-swamp adjustment factor

The area of the watershed is constant and the fraction covered by ponds and swamps is assumed not to change in the future. Therefore, in comparing peak flows between two conditions, the runoff volume V and q_u are the variables to consider. The "unit peak discharge" q_u is a function of the time of concentration T_c, the precipitation depth P, and the initial abstraction I_a, which is a function of CN as shown by

$$I_a = 0.2\left(\frac{1000}{\text{CN}} - 10\right) \qquad \text{(D-23)}$$

The subsequent discussion explores the issue of whether q_u can be assumed to remain nearly constant when comparing current conditions with those in 2040, with and without GI. If q_u can be assumed constant, then Eqn. D-8 indicates that the peak flow is directly proportional to the depth of runoff V; therefore, peak flows for the future conditions can be estimated by multiplying times a factor equal to the ratio of the runoff volumes as denoted in Eqn. 4-1.

For the same rainfall depth P, q_u decreases as T_c increases and increases as I_a decreases. Smaller values of the initial abstraction I_a are associated with greater values of CN indicative of high imperviousness.

Behavior for future conditions without GI

T_c affects peak flows noticeably as a watershed becomes increasingly urbanized. A shorter T_c. leads to greater peak flows. However, none of the watersheds in the study are substantially undeveloped and expected to undergo major development in the study period. All exhibit significant development already and future construction is expected to follow current development patterns. Therefore, T_c can be assumed to have been shortened already by the development process and to remain relatively unchanged in the watersheds evaluated.

The addition of impervious surfaces changes the initial abstraction; therefore, as the watersheds develop up to the year 2040, I_a is expected to decrease, which will increase peak flows. In this case q_u could change depending on the additional impervious cover. However, the change is not significant, especially when T_c is long. Figure D-2 summarizes TR-55 computations using various combinations of T_c and I_a /P on a watershed with SCS rainfall distribution Type II. The figure shows that the q_u varies with I_a but that it becomes nearly constant as T_c increases. Given the discussion in the previous paragraph, the changes in 2040 would reduce I_a while T_c stays constant, which means a shift towards the left along a given curve.

The watersheds in the study range in size approximately between 500 and 3,000 square miles, and the length of the main stem of the stream system varies between 350 and 2,300 miles. For these watersheds, the times of concentration are of the order of hours. The most significant deviation from a constant would take place in subwatersheds with T_c values of the order of minutes. Therefore, the assumption is reasonable for areas in the watershed where the time of concentration is of the order of hours.

In summary, q_u does not vary appreciably on the account of T_c and the variation with respect to I_a is such that, within the context of this study, q_u can be assumed constant when adjusting peak flows for 2040 without GI.

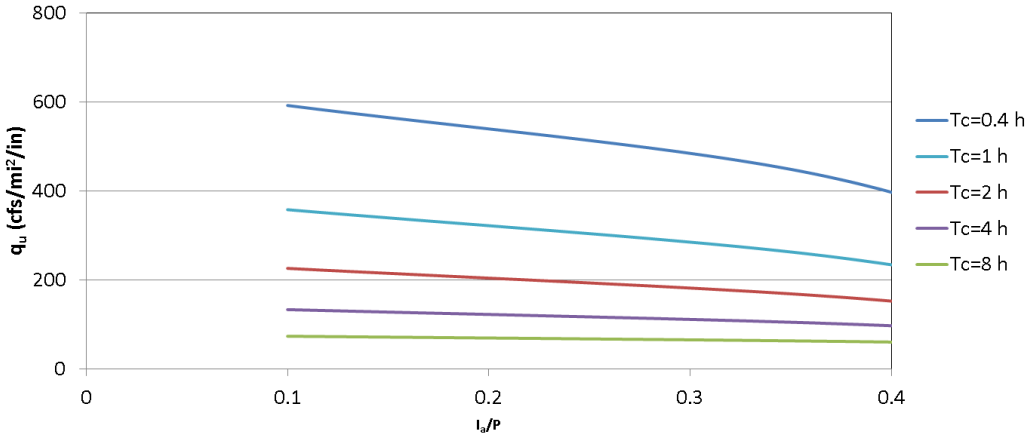

Figure D-2. Typical relationship between q_u, T_c, P and I_a (curve for SCS Type II rainfall distribution; USDA, 1986).

Behavior for Future Conditions with GI

Maintaining or lengthening the time is concentration is often listed as one of the objectives of GI for stormwater management. Therefore, it would be expected that the time of concentration for a watershed with GI would be longer than without GI. However, the lengthening of T_c using GI techniques is not effective in reducing peak flows during flood events because it is the overall drainage capacity of infrastructure that controls the T_c under these circumstances (Zomorodi, 2007). Moreover, the change must lengthen the critical flow path to have an effect on the T_c. The paper concludes that there is some peak flow reduction on more frequent events like the 2-year storm.

The initial abstraction I_a is the amount of rainfall that is intercepted in the early stages of a storm. Some modeling approaches attempt to account for the effect of GI as an increase in the initial abstraction. The rationale is that spatially dispersed GI devices capture water in a similar manner as tree canopies and small depressions on the ground would under natural conditions. The approach in this study is different because it assumes that the GI controls occupy a small fraction of the watershed, too small to change the overall hydrologic properties; therefore, nearly the same amount of runoff is generated with or without GI. The volume of runoff is reduced because the GI controls are engineered devices that capture the

runoff and do not allow it to flow directly to nearby waterways. Therefore, deployment of GI is not expected to increase I_a, if the GI controls are accounted explicitly as engineered devices. In this case q_u would not be expected to change appreciably.

In conclusion, T_c and I_a do not change considerably when GI is deployed; therefore, q_u does not vary appreciably. Within the context of this study, q_u can be assumed constant when adjusting peak flows for 2040 with GI.

Appendix E

Occupancy Classes in Hazus

Hazus Label	Occupancy Class	Standard Industrial Codes (SIC)
	Residential	
RES1	Single Family Dwelling	
RES2	Mobile Home	
RES3A	Multi Family Dwelling - Duplex	
RES3B	Multi Family Dwelling – 3-4 Units	
RES3C	Multi Family Dwelling – 5-9 Units	
RES3D	Multi Family Dwelling – 10-19 Units	
RES3E	Multi Family Dwelling – 20-49 Units	
RES3F	Multi Family Dwelling – 50+ Units	
RES4	Temporary Lodging	70
RES5	Institutional Dormitory	
RES6	Nursing Home	8051, 8052, 8059
	Commercial	
COM1	Retail Trade	52, 53, 54, 55, 56, 57, 59
COM2	Wholesale Trade	42, 50, 51
COM3	Personal and Repair Services	72, 75, 76, 83, 88
COM4	Business/Professional/Technical Services	40, 41, 44, 45, 46, 47, 49, 61, 62, 63, 64, 65, 67, 73, 78 (except 7832), 81, 87, 89
COM5	Depository Institutions	60
COM6	Hospital	8062, 8063, 8069
COM7	Medical Office/Clinic	80 (except 8051, 8052, 8059, 8062, 8063, 8069)
COM8	Entertainment & Recreation	48, 58, 79 (except 7911), 84
COM9	Theaters	7832, 7911
COM10	Parking	
	Industrial	
IND1	Heavy	22, 24, 26, 32, 34, 35 (except 3571, 3572), 37
IND2	Light	23, 25, 27, 30, 31, 36 (except 3671, 3672, 3674), 38, 39
IND3	Food/Drugs/Chemicals	20, 21, 28, 29
IND4	Metals/Minerals Processing	10, 12, 13, 14, 33
IND5	High Technology	3571, 3572, 3671, 3672, 3674
IND6	Construction	15, 16, 17
	Agriculture	
AGR1	Agriculture	01, 02, 07, 08, 09
	Religion/Non-Profit	
REL1	Church/Membership Organizations	86
	Government	
GOV1	General Services	43, 91, 92 (except 9221, 9224), 93, 94, 95, 96, 97
GOV2	Emergency Response	9221, 9224
	Education	
EDU1	Schools/Libraries	82 (except 8221, 8222)
EDU2	Colleges/Universities	8221, 8222

Appendix F

Lookup Tables for Matching Municipal Land Uses to Hazus Occupancy Classes

Salado Creek subwatershed

Municipal land use code	Hazus occupancy class
010 350 STK FEN CPS ASP CPT CON CPT	COM3
135 135 135 135 CON ASP SWP CNP FEN FEN	RES4
135 135 135 CNP ASP CNP	RES4
135 135 135 SWP ASP FEN CON	RES4
140 140 140 200 140 140 140 140 365 CNP ASP CPT SWP CON ASP	RES4
150 150 150 150 150 150 150 150 150 170 SWP WDD CNP ASP FEN	RES6
155 ASP FEN CON RSH	RES6
165 275 CNP 275 275 400 275 275 ASP CON PTO	COM8
170 170 345 350 CON GCR GCR ASP FEN	COM8
200 200 200 200 200 CON ASP CNP CNP EQS FEN CNP	COM1
203 203 FEN ASP ASP CNP	COM1
205 205 ASP CON CNP PTO	COM1
220 200 ASP CON FEN	COM1
234 234 CNP CON FEN CPS ASP STK FEN	COM1
235 CON CPS CWA FEN FEN STK STK STK	COM1
240 240 240 ASP CON CNP LDK FEN	COM1
260 320 RSH CON ASP TPK	COM1
270 CNP ASP CPT CON	COM1
275 ASP CNP CPT LDK LDK CON	COM1
280 280 280 280 CNP ASP CPT FEN EQS	COM1
305 305 400 305 CNP CON FEN	IND2
314 ASP FEN	COM4
315 320 320 400 315 320 325 325 325 400 325 315 320 320 CON	IND1
320	IND1
325 325 320 400 400 400 325 325 350 400 ASP CON CWY FEN CPT	IND1
335 800 400 335 335 335 335 335 335 335 335 FEN CON	IND1
343 315 CNP FEN ASP	IND2
345 350 320 FEN CON ASP CNP RSH GAR RSH FEN FEN	COM4
350 305 400 305 305 LDK OPP CON EQS EQS CON ASP FEN	COM3
352 352 ASP SHI	COM3
353 353 ASP CON	COM3
355 800 355 355 ASP CON SH1 FEN	COM3
363 310 350 363 CON ASP EQS FEN LDK	COM1
400	COM4
410 403 ASP CON	COM7
411 343 CNP ASP EQS	COM7
411 CNP CON ASP	COM7
460 CNP CNP CON ASP ASP	COM6
480 400 400 320 ASP CON CON CON ASP	COM5
481 480 400 400 CON ASP 482 CNP 480 400 400 400 400	COM5
482 482 CNP CON ASP	COM5

Municipal land use code	Hazus occupancy class
485 485 OPP CNP ASP	COM5
500 CNP 500 500 SWP ASP CON	EDU1
525 ASP CON FEN	RES4
525 FEN SWP ASP SWP	RES4
540 CON	COM8
625 625 625 CNP CON ASP	COM8
630 ASP EQS EQS	COM8
700 SWP FEN CON CNP CNP SH4 SPA SH4	RES4
800 800 400 800 800 800 260 EQS SWP ASP OPP SPA FEN	RES3C
ASP	COM10
BHB	AGR1
CAN OPP RSH	RES2
CGH CON FEN CPT	COM1
CNP CON ASP 352	COM4
CON	COM10
CPT	COM3
CWY - MAIN CNP ASP	COM1
DLA1 CON CON GAR CNP FEN	RES1
EQS FEN ASP	COM1
FEN STK	AGR1
GCR	COM8
HPO	AGR1
LA	RES1
MDV	COM8
MRG	RES1
OPP	RES1
RSH	COM3
RSW	COM8
SH1	AGR1
SH4	AGR1
SHI	AGR1
TCT	COM8
TPK	RES2

Big Creek Headwaters watershed

Municipal land use code	Hazus occupancy class
AGRICULTURAL DISTRICT	EDU1
COMMERCIAL BUSINESS DISTRICT	COM1
HIGHWAY BUSINESS DISTRICT	COM1
LAKE RESIDENTIAL DISTRICT	RES1
MULTI-FAMILY RESIDENTIAL DISTRICT	RES3A
OPEN SPACE RESIDENTIAL	RES1
PLANNED UNIT DEVELOPMENT DISTRICT	RES3A
RESTRICTED INDUSTRIAL DISTRICT	IND2
SINGLE FAMILY COMMUNITY RESIDENTIAL DISTRICT	RES1
SINGLE FAMILY RESIDENTIAL DISTRICT	RES1
SINGLE FAMILY RESIDENTIAL RESTRICTED	COM8
SINGLE FAMILY RESIDENTIAL three units per acre DISTRICT	RES1

Appendix G

SAS/STAT Printouts

Multivariate regression model for the 2-year zero-damage threshold

Model for predicting the proportion of losses avoided with no loss in the 2 year floodplain

The REG Procedure
Model: MODEL1
Dependent Variable: LN_PROP_LOSS_AVOIDED_2YR Natural log of proportion of loss avoided, no losses in 2yr floodplain

Number of Observations Read	20
Number of Observations Used	20

Analysis of Variance					
Source	**DF**	**Sum of Squares**	**Mean Square**	**F Value**	**Pr > F**
Model	2	16.43829	8.21915	10.84	0.0009
Error	17	12.88841	0.75814		
Corrected Total	19	29.32670			

Root MSE	0.87071	**R-Square**	0.5605
Dependent Mean	2.13888	**Adj R-Sq**	0.5088
Coeff Var	40.70891		

Parameter Estimates								
Variable	**Label**	**DF**	**Parameter Estimate**	**Standard Error**	**t Value**	**Pr > |t|**	**Tolerance**	**Variance Inflation**
Intercept	Intercept	1	-0.31342	0.65917	-0.48	0.6405	.	0
Storm100yr	One Hundred Year Storm Depth (inches)	1	0.20856	0.09430	2.21	0.0410	0.84054	1.18971
SQRT_PCTNEWREDEV	Square root of the percent of area that is new or redevelopment	1	3.94420	1.37261	2.87	0.0105	0.84054	1.18971

Model for predicting the proportion of losses avoided with no loss in the 2 year floodplain

The REG Procedure
Model: MODEL1
Dependent Variable: LN_PROP_LOSS_AVOIDED_2YR Natural log of proportion of loss avoided, no losses in 2yr floodplain

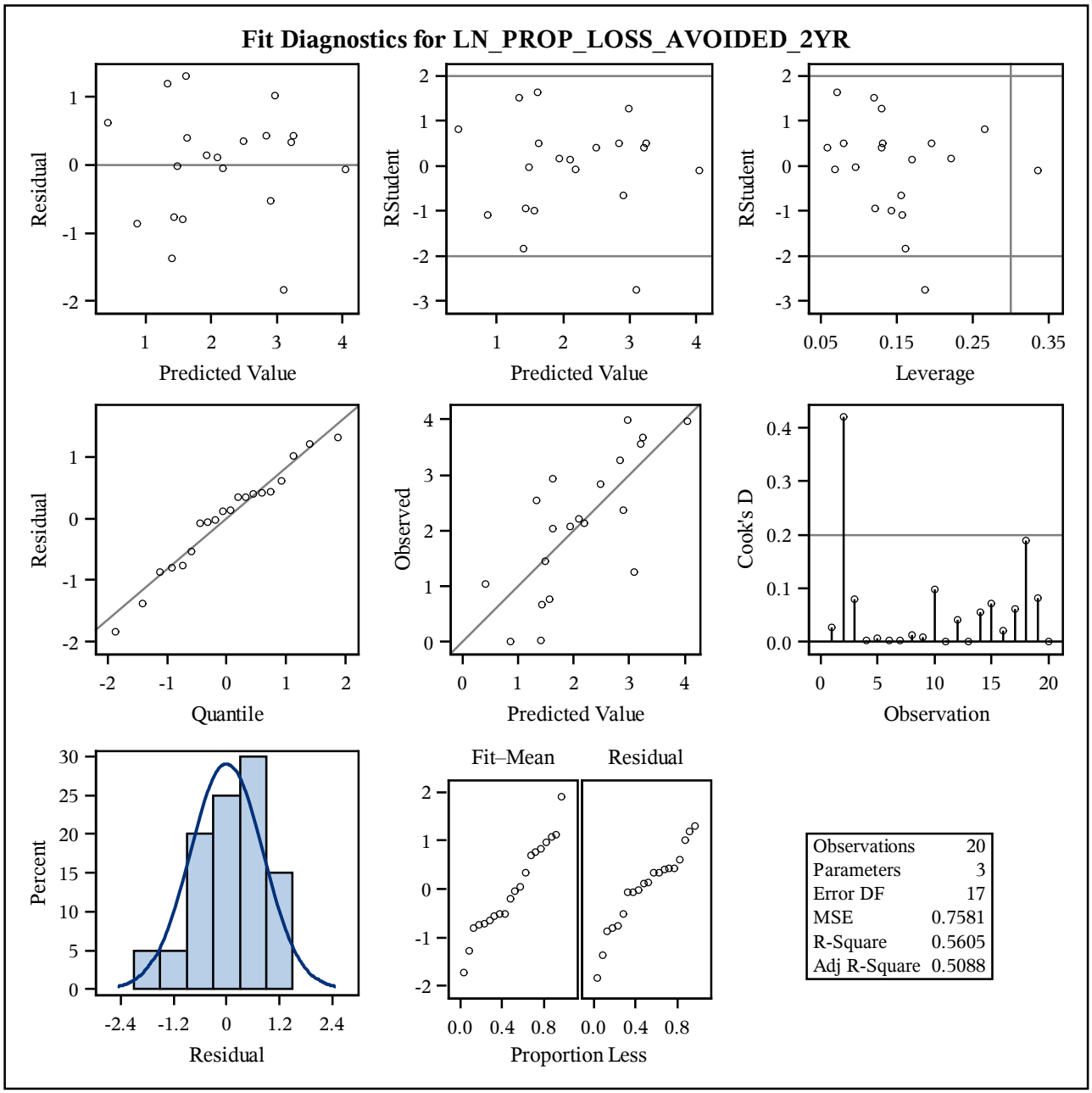

Model for predicting the proportion of losses avoided with no loss in the 2 year floodplain

The REG Procedure
Model: MODEL1
Dependent Variable: LN_PROP_LOSS_AVOIDED_2YR Natural log of proportion of loss avoided, no losses in 2yr floodplain

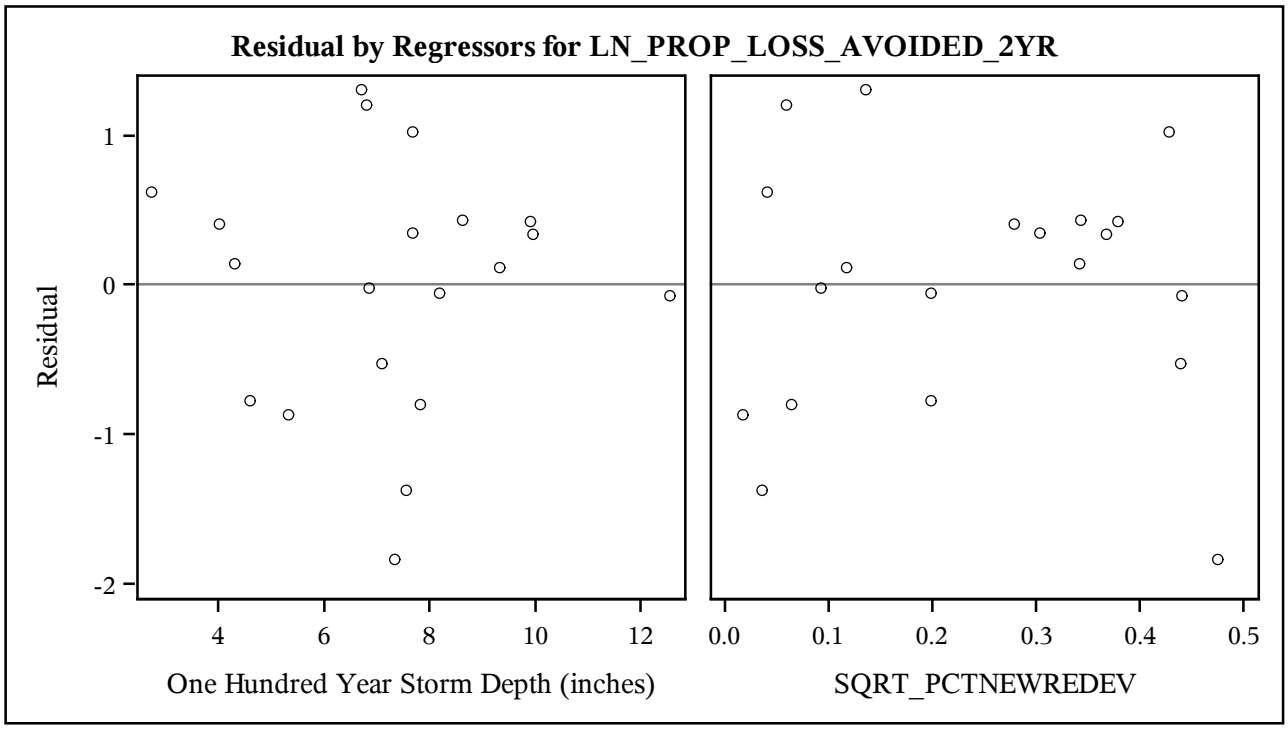

Multivariate regression model for the 5-year zero-damage threshold

Model for predicting the proportion of losses avoided with no loss in the 5 year floodplain

The REG Procedure
Model: MODEL1
Dependent Variable: LN_PROP_LOSS_AVOIDED_5YR Natural log of proportion of loss avoided, no losses in 5yr floodplain

Number of Observations Read	20
Number of Observations Used	20

Analysis of Variance					
Source	**DF**	**Sum of Squares**	**Mean Square**	**F Value**	**Pr > F**
Model	3	11.79390	3.93130	10.11	0.0006
Error	16	6.22137	0.38884		
Corrected Total	19	18.01527			

Root MSE	0.62357	**R-Square**	0.6547
Dependent Mean	1.25061	**Adj R-Sq**	0.5899
Coeff Var	49.86103		

Parameter Estimates								
Variable	**Label**	**DF**	**Parameter Estimate**	**Standard Error**	**t Value**	**Pr > |t|**	**Tolerance**	**Variance Inflation**
Intercept	Intercept	1	-1.43528	0.59846	-2.40	0.0290	.	0
Storm100yr	One Hundred Year Storm Depth (inches)	1	0.18649	0.06770	2.75	0.0141	0.83641	1.19559
SQRT_PCTNEWREDEV	Square root of the percent of area that is new or redevelopment	1	3.12977	0.99892	3.13	0.0064	0.81396	1.22856
RNINT100YR	Ratio of the Hundred Year Storm to Average Annual Rainfall Depth	1	2.62850	1.61059	1.63	0.1222	0.96838	1.03266

Model for predicting the proportion of losses avoided with no loss in the 5 year floodplain

The REG Procedure
Model: MODEL1
Dependent Variable: LN_PROP_LOSS_AVOIDED_5YR Natural log of proportion of loss avoided, no losses in 5yr floodplain

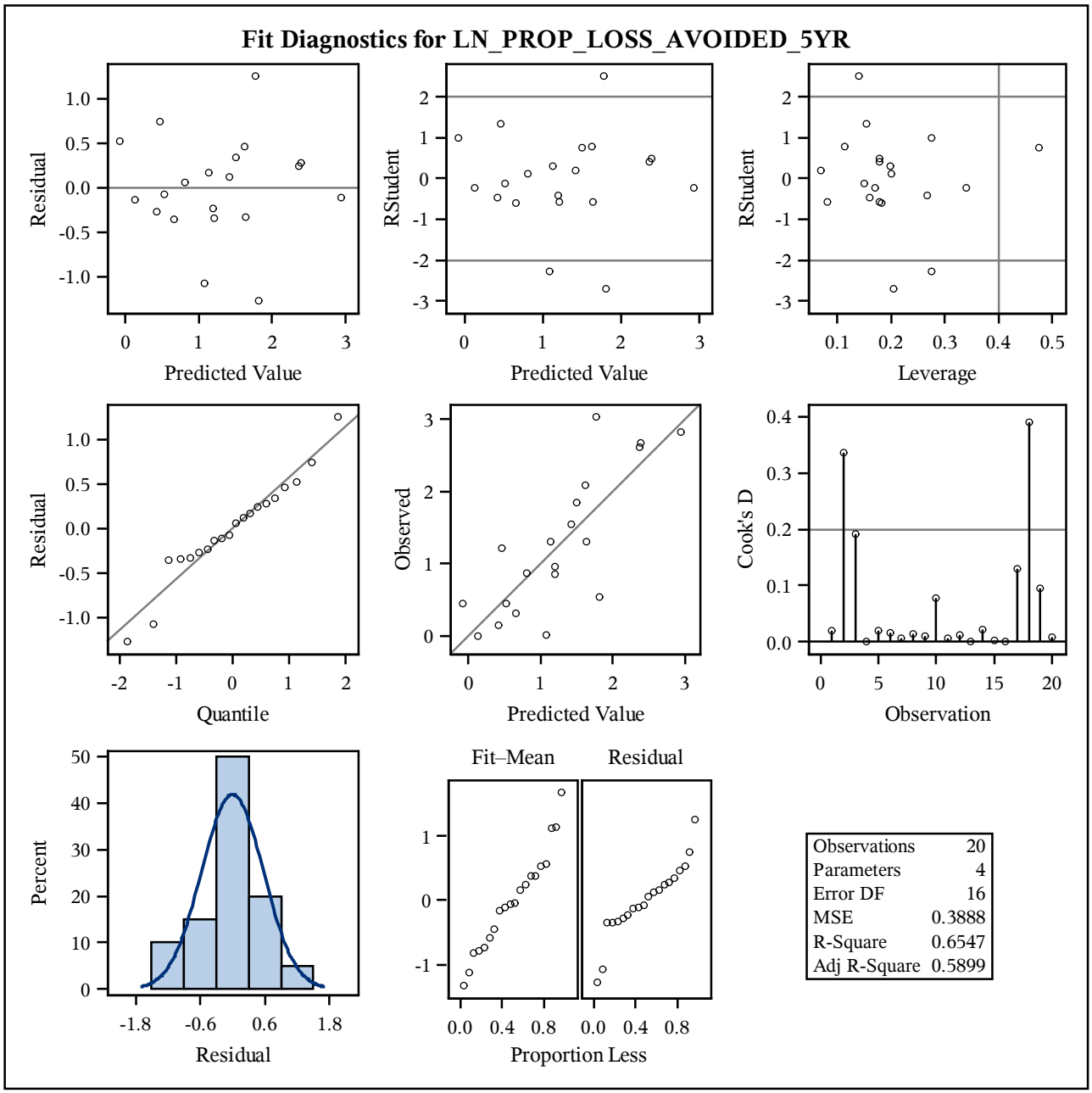

Model for predicting the proportion of losses avoided with no loss in the 5 year floodplain

The REG Procedure
Model: MODEL1
Dependent Variable: LN_PROP_LOSS_AVOIDED_5YR Natural log of proportion of loss avoided, no losses in 5yr floodplain

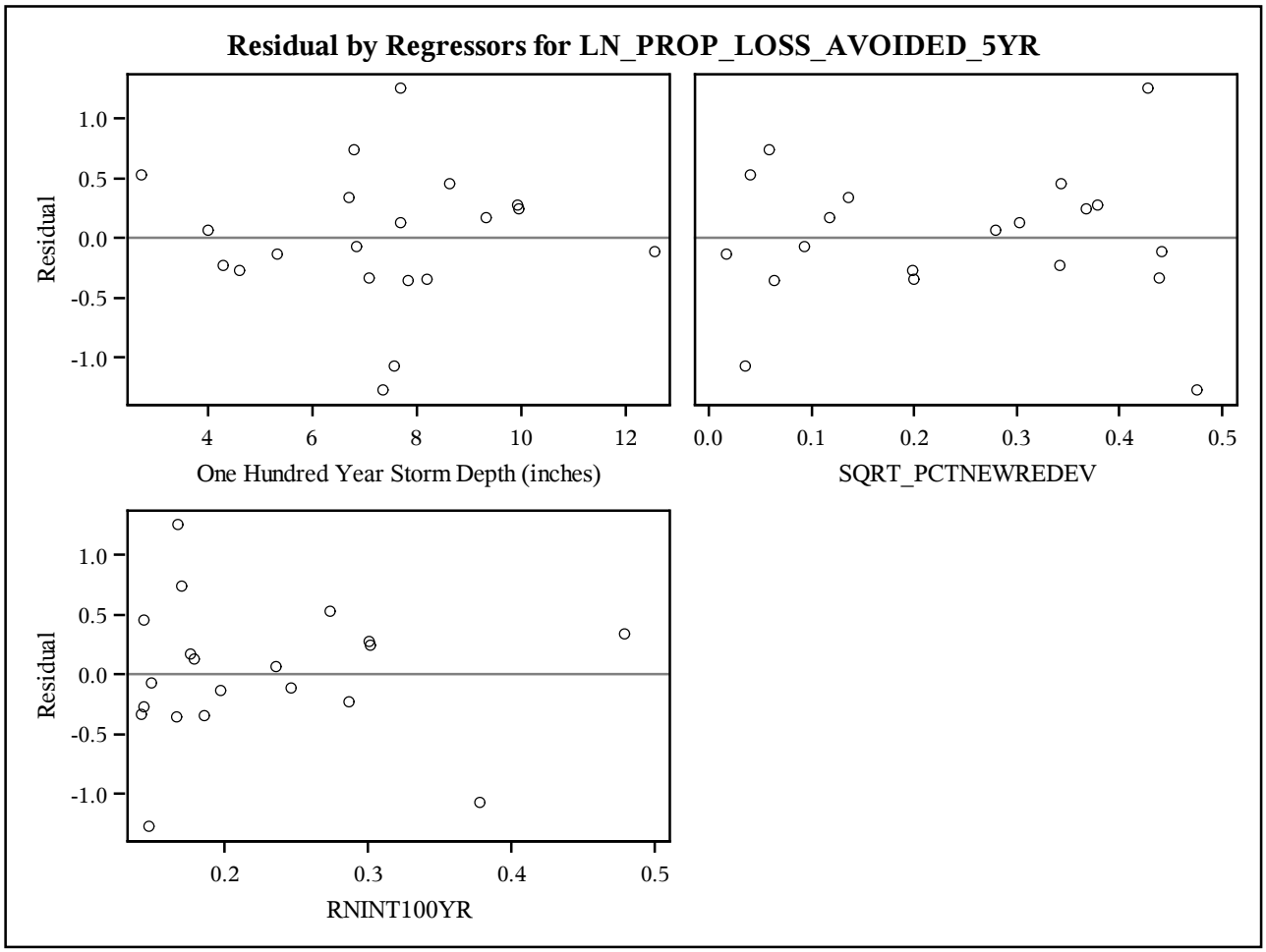

Multivariate regression model for the 10-year zero-damage threshold

Model for predicting the proportion of losses avoided with no loss in the 10 year floodplain

The REG Procedure
Model: MODEL1
Dependent Variable: LN_PROP_LOSS_AVOIDED_10YR Natural log of proportion of loss avoided, no losses in 10yr floodplain

Number of Observations Read	20
Number of Observations Used	20

Analysis of Variance					
Source	**DF**	**Sum of Squares**	**Mean Square**	**F Value**	**Pr > F**
Model	3	6.91483	2.30494	10.44	0.0005
Error	16	3.53391	0.22087		
Corrected Total	19	10.44874			

Root MSE	0.46997	**R-Square**	0.6618
Dependent Mean	0.77462	**Adj R-Sq**	0.5984
Coeff Var	60.67040		

Parameter Estimates								
Variable	**Label**	**DF**	**Parameter Estimate**	**Standard Error**	**t Value**	**Pr > |t|**	**Tolerance**	**Variance Inflation**
Intercept	Intercept	1	-0.74960	0.36013	-2.08	0.0538	.	0
Storm100yr	One Hundred Year Storm Depth (inches)	1	0.23385	0.06252	3.74	0.0018	0.55697	1.79544
SQRT_PCTNEWREDEV	Square root of the percent of area that is new or redevelopment	1	2.09916	0.75039	2.80	0.0129	0.81934	1.22049
ANNUAL_RAINFALL	Average Annual Rainfall Depth (inches)	1	-0.01840	0.00951	-1.93	0.0710	0.57288	1.74556

Model for predicting the proportion of losses avoided with no loss in the 10 year floodplain

The REG Procedure
Model: MODEL1
Dependent Variable: LN_PROP_LOSS_AVOIDED_10YR Natural log of proportion of loss avoided, no losses in 10yr floodplain

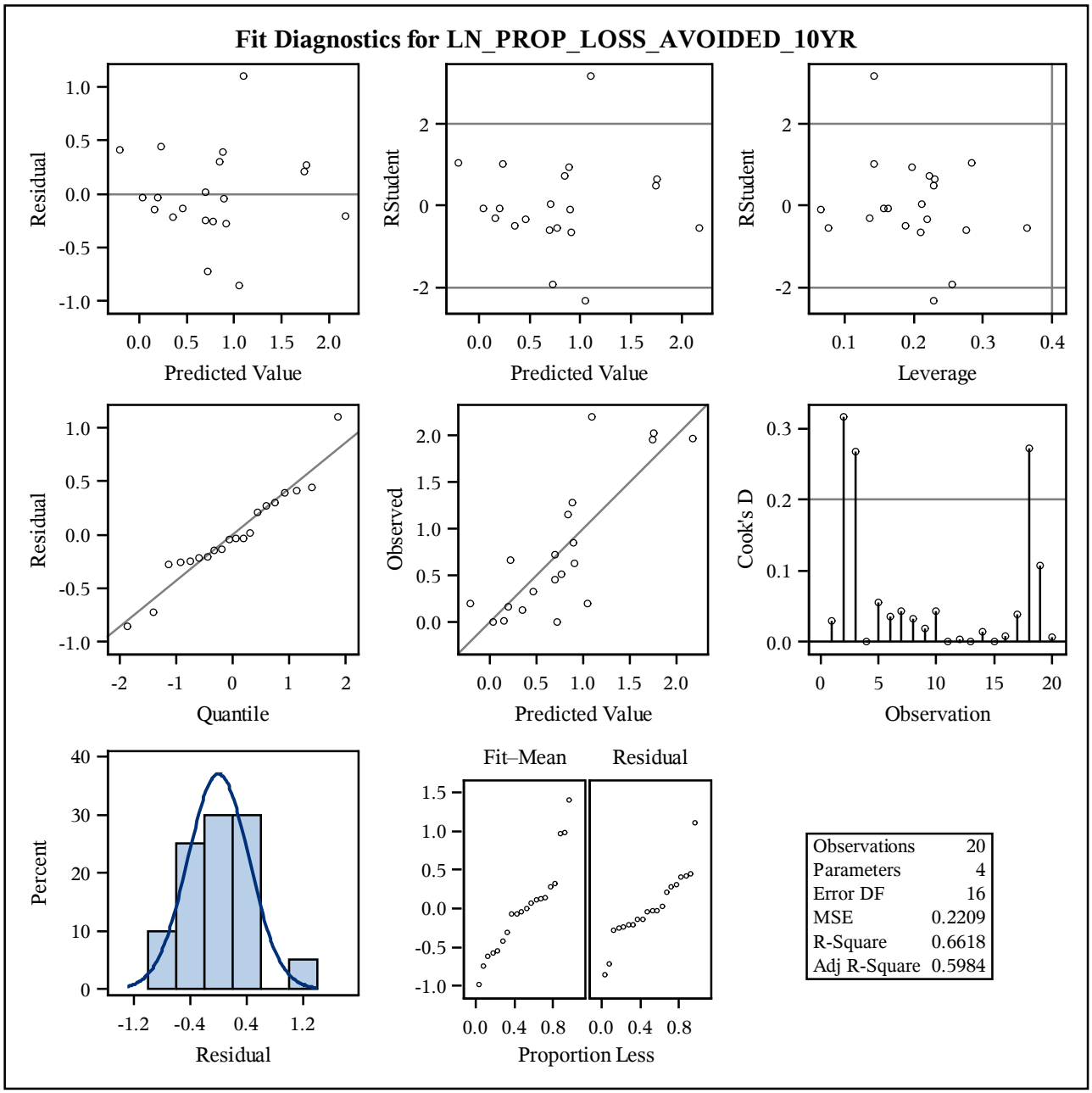

Model for predicting the proportion of losses avoided with no loss in the 10 year floodplain

The REG Procedure
Model: MODEL1
Dependent Variable: LN_PROP_LOSS_AVOIDED_10YR Natural log of proportion of loss avoided, no losses in 10yr floodplain

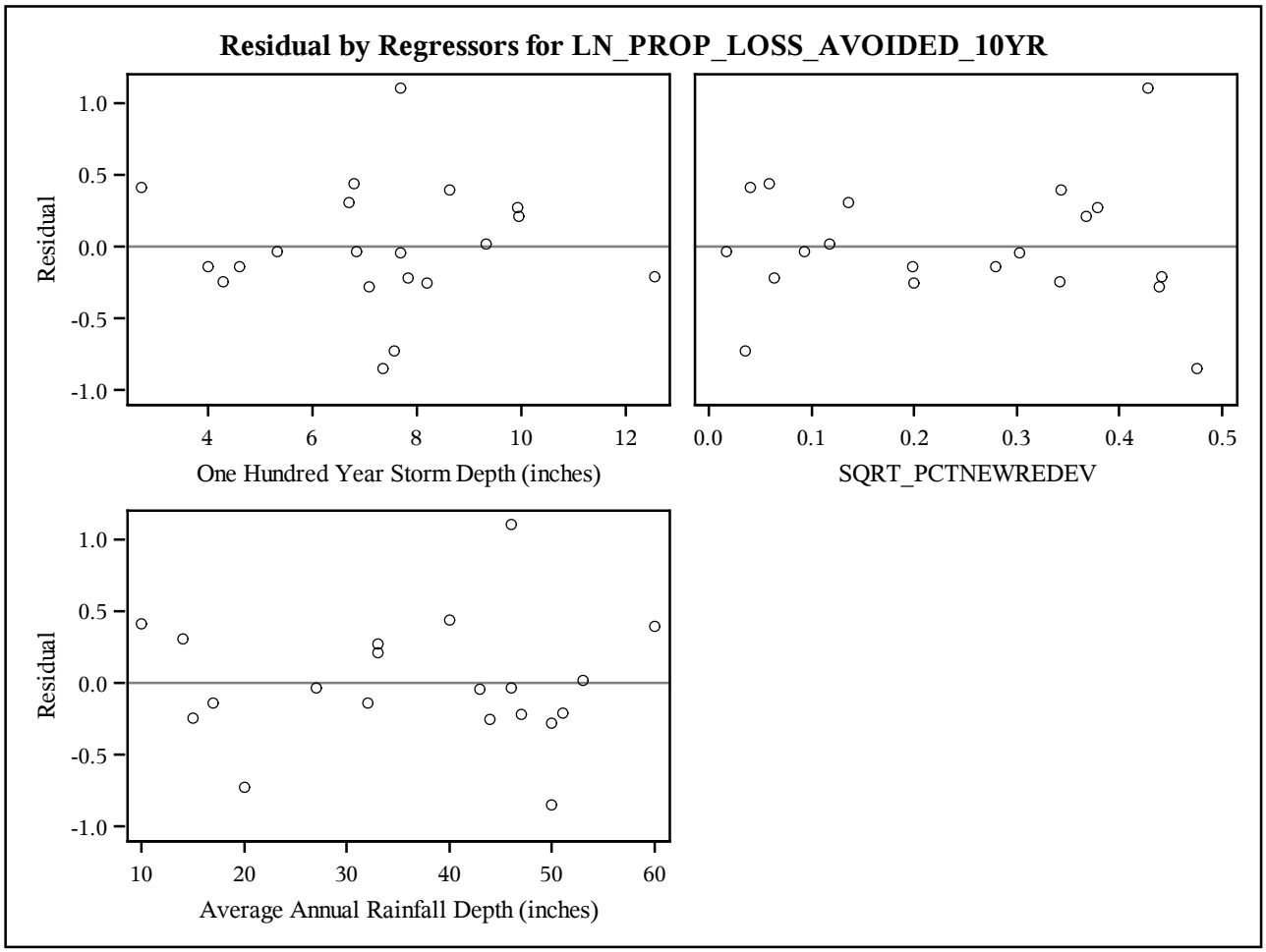

Appendix H

Time Streams of Benefits

Benefits between 2020 and 2040 for the 40 top-growth HUC4 watersheds (2011 dollars)

Year	5-year zero-damage threshold	10-year zero-damage threshold
2020	$0	$0
2021	$4,699,791	$2,214,123
2022	$9,399,583	$4,428,246
2023	$14,099,374	$6,642,369
2024	$18,799,165	$8,856,492
2025	$23,498,957	$11,070,615
2026	$28,198,748	$13,284,738
2027	$32,898,539	$15,498,861
2028	$37,598,331	$17,712,984
2029	$42,298,122	$19,927,107
2030	$46,997,914	$22,141,230
2031	$51,697,705	$24,355,353
2032	$56,397,496	$26,569,476
2033	$61,097,288	$28,783,599
2034	$65,797,079	$30,997,722
2035	$70,496,870	$33,211,845
2036	$75,196,662	$35,425,968
2037	$79,896,453	$37,640,091
2038	$84,596,244	$39,854,214
2039	$89,296,036	$42,068,337
2040	$93,995,827	$44,282,460

Benefits between 2020 and 2040 in the conterminous United States, excluding jurisdictions with a retention standard (2011 dollars).

Year	5-year zero-damage threshold	10-year zero-damage threshold
2020	$0	$0
2021	$6,777,211	$3,125,493
2022	$13,554,421	$6,250,985
2023	$20,331,632	$9,376,478
2024	$27,108,843	$12,501,970
2025	$33,886,053	$15,627,463
2026	$40,663,264	$18,752,955
2027	$47,440,475	$21,878,448
2028	$54,217,685	$25,003,940
2029	$60,994,896	$28,129,433
2030	$67,772,107	$31,254,926
2031	$74,549,318	$34,380,418
2032	$81,326,528	$37,505,911
2033	$88,103,739	$40,631,403
2034	$94,880,950	$43,756,896
2035	$101,658,160	$46,882,388
2036	$108,435,371	$50,007,881
2037	$115,212,582	$53,133,373
2038	$121,989,792	$56,258,866
2039	$128,767,003	$59,384,359
2040	$135,544,214	$62,509,851

Benefits between 2020 and 2040 in the conterminous United States, including jurisdictions with a retention standard (2011 dollars).

Year	5-year zero-damage threshold	10-year zero-damage threshold
2020	$0	$0
2021	$16,449,153	$5,720,028
2022	$32,898,307	$11,440,056
2023	$49,347,460	$17,160,084
2024	$65,796,614	$22,880,112
2025	$82,245,767	$28,600,141
2026	$98,694,921	$34,320,169
2027	$115,144,074	$40,040,197
2028	$131,593,228	$45,760,225
2029	$148,042,381	$51,480,253
2030	$164,491,535	$57,200,281
2031	$180,940,688	$62,920,309
2032	$197,389,842	$68,640,337
2033	$213,838,995	$74,360,366
2034	$230,288,148	$80,080,394
2035	$246,737,302	$85,800,422
2036	$263,186,455	$91,520,450
2037	$279,635,609	$97,240,478
2038	$296,084,762	$102,960,506
2039	$312,533,916	$108,680,534
2040	$328,983,069	$114,400,562